UNIVERSIDADE FEDERAL DE SANTA CATARINA
CENTRO TECNOLÓGICO
PROGRAMA DE PÓS-GRADUAÇÃO EM ENGENHARIA QUÍMICA

Thaíris Karoline Silva Laurintino

SUPERCRITICAL EXTRACTION OF COSTUS SPICATUS LEAFS COMBINED WITH ULTRASOUND PRETREATMENT:
EXPERIMENTATION AND MODELING

Florianópolis
2024

Thaíris Karoline Silva Laurintino

SUPERCRITICAL EXTRACTION OF COSTUS SPICATUS LEAFS COMBINED WITH ULTRASOUND PRETREATMENT:

EXPERIMENTATION AND MODELING

Tese submetida ao Programa de Pós-Graduação em Engenharia Química da Universidade Federal de Santa Catarina como requisito para a obtenção do título de Doutora em Desenvolvimento de Processos Químicos e Biotecnológicos.

Orientador: Prof. Dr. Marintho Bastos Quadri.

Coorientador: Prof. Dr. Ariovaldo Bolzan.

Florianópolis

2024

Ficha catalográfica gerada por meio de sistema automatizado gerenciado pela BU/UFSC.
Dados inseridos pelo próprio autor.

Laurintino, Thaíris Karoline Silva
SUPERCRITICAL EXTRACTION OF COSTUS SPICATUS LEAFS COMBINED WITH ULTRASOUND PRETREATMENT: EXPERIMENTATION AND MODELING / Thaíris Karoline Silva Laurintino ; orientador, Marintho Bastos Quadri, coorientador, Ariovaldo Bolzan, 2024.
210 p.

Tese (doutorado) - Universidade Federal de Santa Catarina, Centro Tecnológico, Programa de Pós-Graduação em Engenharia Química, Florianópolis, 2024.

Inclui referências.

1. Engenharia Química. 2. Costus spicatus. 3. Extração supercrítica. 4. Modelagem matemática. 5. Atividades biológicas. I. Quadri, Marintho Bastos . II. Bolzan, Ariovaldo. III. Universidade Federal de Santa Catarina. Programa de Pós-Graduação em Engenharia Química. IV. Título.

Thaíris Karoline Silva Laurintino

SUPERCRITICAL EXTRACTION OF COSTUS SPICATUS LEAFS COMBINED WITH ULTRASOUND PRETREATMENT:
EXPERIMENTATION AND MODELING

Esta tese de doutorado foi avaliada e aprovada pelos seguintes membros:

Profª. Drª Claudia Sayer
UFSC/PósENQ
Drª Deise Parolo Tramontin
UNESC/LAPLAM/Pós-doutoranda
Drª Thayli Ramires Araújo
UFSC/PósENQ

Certificamos que esta é a versão original e final do trabalho de conclusão que foi julgado adequado para obtenção do título de doutor em Engenharia Química.

Documento assinado digitalmente
Agenor Furigo Junior
Data: 06/12/2024 14:09:45-0300
CPF: ***.789.438-**
Verifique as assinaturas em https://v.ufsc.br

ICP-Edu

_____

Coordenação do Programa de Pós-Graduação

Documento assinado digitalmente
Marintho Bastos Quadri
Data: 06/12/2024 11:07:04-0300
CPF: ***.385.209-**
Verifique as assinaturas em https://v.ufsc.br

ICP-Edu

_____

Prof. Dr. Marintho Bastos Quadri
Orientador

Florianópolis
2024

AGRADECEMENTOS

À Deus, pela proteção e paz interior. Por me encorajar nos momentos em que tudo parecia impossível e colocar pessoas tão especiais no meu caminho.

À toda minha família, a quem devo tudo o que eu sou. Em especial, aos meus pais, Serafim e Veralúcia, e a minha irmã Thuany, por todos amor, dedicação, ensinamento e incentivo.

Aos meus avós, Amauri e Diva, pelo exemplo de amor, serenidade e dedicação. Obrigada por me incentivarem e vibrarem a cada vitória conquistada.

Aos professores Dr. Marintho Bastos Quadri e Dr. Ariovaldo Bolzan, pela orientação, dedicação e incentivo. Obrigada por serem tão prestativos e atenciosos! Vocês são exemplos, não só como excelentes profissionais, mas como pessoas também. Obrigada por todos os conselhos e ensinamentos!

A Thuany, pelo conhecimento compartilhado e incentivo. Obrigada por não medir esforços para ajudar! Obrigada por me acompanhar nos vários experimentos ao longo do dia. Meu muito obrigada por tudo!

Aos membros da banca examinadora, por terem aceitado o convite para contribuírem valiosamente com este trabalho.

Aos amigos do Laboratório de Controle de Processos (LCP) e Laboratório de Sistemas Porosos (LASIPO). Obrigada pela companhia, conversas e ensinamentos compartilhados. Pelo apoio nas horas difíceis, por todo o carinho. A Deise Tramontin pela pelo incentivo e auxílio no entendimento dos fenômenos envolvidos!

À CAPES pelo apoio financeiro.

Enfim, agradeço a todos que torceram, oraram e contribuíram para que este trabalho se tornasse realidade. Meu muito obrigada!

RESUMO

Plantas medicinais, como o *Costus spicatus*, são uma fonte promissora para o isolamento do ácido linolênico, precursor do ômega-3. Esta tese aplica técnicas de extração de baixa pressão (LPE: MAC, UAE, SOX) e alta pressão (SFE, UAE+SFE) para avaliar seu impacto em vários aspectos: rendimento, composição química, propriedades biológicas (como citotoxicidade, redução de óxido nítrico, conteúdo de flavonoides, fenólicos totais, atividade antioxidante, antimicrobiana e antiviral contra HSV-1) e características físico-químicas (incluindo micrografia eletrônica de varredura, estrutura microscópica, estabilidade acelerada e termoestabilidade). Também investiga os efeitos da combinação UAE+SFE no processo de SFE, com o objetivo de otimizar o rendimento e o perfil químico utilizando o Delineamento Composto Central. Para complementar, foram desenvolvidos dois modelos no COMSOL Multiphysics®: I - dinâmico (SFE) e II - batelada (UAE), para investigar os efeitos da pressão (8-20 MPa), temperatura (36-64 °C) e concentração de co-solvente no SFE (0-20% EtOH) e analisar os parâmetros que influenciam na extração os compostos ácido linolênico, ácido palmítico e friedelin. O perfil químico foi determinado por cromatografia gasosa acoplada à espectrometria de massa (GC/MS). Nas extrações foram utilizados como solventes etanol, água e uma mistura de etanol: água (50% v/v). Na UAE, foram avaliadas diferentes condições, como ponteira, amplitude da sonificação, tempo e tipo de solvente, sendo o maior rendimento (8.59%) alcançado com macroponteira, 70% de amplitude e 1 min de extração. A composição química variou conforme o solvente, sendo o EtOH o que revelou mais compostos. A combinação UAE+SFE não apenas aumentou o rendimento (6.97%), mas também a seletividade do ácido linolênico, atingindo 62.52% em 60 °C/11 MPa/5 % EtOH. O extrato UAE+SFE mostrou forte atividade antimicrobiana comparado ao SFE. LPE e UAE+SFE não reduziram a viabilidade celular a 100 $\mu g\ mL^{-1}$. UAE+SFE inibiu o óxido nítrico em mais de 90% nas concentrações de 30 a 300 $\mu g\ mL^{-1}$. O extrato com EtOH mostrou altos níveis de flavonoides (150.38–1328.73 mg GAE g^{-1}), e UAE+SFE melhorou a recuperação desses compostos comparados ao SFE isolado. A atividade antioxidante foi maior com ABTS, e todos os extratos exibiram atividade antibacteriana contra *B. cereus*. UAE+SFE também foi mais eficaz contra HSV-1. A análise MEV mostrou que a amostra tratada com UAE+SFE apresentava microfissuras densas nas estruturas do tecido, e a microscopia confocal confirmou autofluorescência, evidenciando maior eficiência na extração de gotículas lipídicas. O extrato UAE+SFE mostrou estabilidade térmica em análises TG e DTG. Nas simulações, o modelo I indicou que o rendimento, coeficiente de transferência de massa ($h_{D,i}$) e coeficiente de difusão na partícula ($D_{pe,i}$) aumentam com pressão, temperatura e concentração de etanol, enquanto o coeficiente de transferência de massa no fluido ($D_{F,i}$) diminui. O modelo II evidenciou que o tratamento ultrassônico melhorou o rendimento e $k_{D,i}$ para todos os compostos. Assim, a modelagem permite melhor discernir os mecanismos intervenientes na obtenção de compostos bioativos, que são promissores para as indústrias cosmética, farmacêutica e alimentícia.

Palavras-chave: *Costus spicatus*; extração supercrítica; modelagem matemática; transferência de massa compostos bioativos; atividades biológicas

RESUMO EXPANDIDO

Introdução

A planta *Costus spicatus* (Jacq.) Sw., da família Costaceae, nativa de regiões da Mata Atlântica e da Amazônia, é amplamente usada na medicina popular para o tratamento de diversas doenças. Sua composição química confere propriedades analgésicas, antioxidantes, antimicrobianas, antifúngicas e nefroprotetoras. A extração de compostos bioativos de plantas pode ser feita por vários métodos. A extração supercrítica (SFE) tem sido proposta como uma alternativa sustentável e eficiente às técnicas convencionais para obter compostos bioativos de fontes naturais. O CO_2 é um solvente amplamente utilizado, pois é um gás seguro, facilmente disponível, barato, não inflamável e não tóxico. No entanto, a SFE enfrenta desafios econômicos devido aos altos custos de investimento em processos de alta pressão. Para melhorar o desempenho e reduzir custos, combinações de técnicas, como a associação de ultrassom com SFE (UAE + SFE), têm se mostrado promissoras. Não há estudos publicados que explorem a extração de alta eficiência de folhas de *C. spicatus* utilizando UAE + SFE, nem a realização de atividades biológicas e características físico-químicas. Além disso, apesar dos vários modelos de transferência de massa disponíveis, não há dados sobre a cinética de difusão de compostos de *Costus spicatus* com UAE e SFE isolados ou em combinação.

Objetivos

Esta tese tem como objetivo aplicar técnicas de extração de baixa pressão (LPE: MAC, UAE, SOX) e alta pressão (SFE, UAE+SFE) para avaliar o impacto no rendimento, composição química, propriedades biológicas e características físico-químicas. Também investiga os efeitos da combinação UAE+SFE no SFE, visando otimizar o rendimento e o perfil químico com o Delineamento Composto Central. Além disso, foram desenvolvidos dois modelos no COMSOL Multiphysics®: I - dinâmico (SFE) e II - batelada (UAE).

Metodologia

O perfil químico foi analisado por cromatografia gasosa acoplada a espectrômetro de massa (GC/MS), Todas as extrações foram realizadas com solventes como etanol (EtOH), água e etanol: água (50% v/v). Na UAE, diferentes condições foram avaliadas, como ponteira, amplitude, tempo e solvente. As propriedades biológicas dos extratos incluíram citotoxicidade, redução de óxido nítrico, conteúdo de flavonoides, fenólicos totais, atividade antioxidante (DPPH e ABTS), antimicrobiana e antiviral contra HSV-1. Também foram analisadas características físico-químicas e morfológicas, como micrografia eletrônica de varredura (MEV), estrutura microscópica, estabilidade acelerada e termoestabilidade (TGA). Nos modelos desenvolvidos no COMSOL Multiphysics®: I - dinâmico (SFE) e II - batelada (UAE), usaram balanços de massa diferenciais para analisar o fluxo de massa entre o fluido e as partículas, onde foram estudados os efeitos da pressão (8-20 MPa), temperatura (36-64°C) e concentração de co-solvente (0-20% EtOH) no SFE, além dos parâmetros que influenciam o perfil de extração dos compostos ácido linolênico, ácido palmítico e friedelin.

Resultados e discussões

O melhor rendimento foi obtido com etanol: água, registrando valores de 7.25%, 18.74%, 9.29% e 10.12% para MAC, SOX, UAE e UAE+SFE, respectivamente. Na UAE, o maior

rendimento (8.59%) foi alcançado com macroponteira, 70% de amplitude e 1 minuto de extração. A composição química variou conforme o solvente, sendo o EtOH o que revelou mais compostos. A combinação UAE+SFE não apenas aumentou o rendimento (6.97%), mas também a seletividade do ácido linolênico, atingindo 62.52% (60 °C/11 MPa/5 % EtOH), superior às demais técnicas. O extrato UAE+SFE mostrou forte atividade antimicrobiana comparado ao SFE. LPE e UAE+SFE não reduziram a viabilidade celular a 100 μg mL^{-1}, com redução significativa apenas em 300 μg mL^{-1} para o SFE. UAE+SFE inibiu o óxido nítrico em mais de 90% nas concentrações de 30 a 300 μg mL^{-1}. O extrato com EtOH mostrou altos níveis de flavonoides (150.38–1328.73 mg GAE g^{-1}), e UAE+SFE melhorou a recuperação desses compostos comparados ao SFE isolado. A atividade antioxidante foi maior com ABTS, e todos os extratos exibiram atividade antibacteriana contra *B. cereus*. UAE+SFE também foi mais eficaz contra HSV-1. A análise MEV revelou que a amostra tratada com UAE + SFE teve um impacto notável nas estruturas do tecido, com microfissuras densas na superfície. A microscopia confocal confirmou autofluorescência, e UAE+SFE demonstrou maior eficiência na extração de gotículas lipídicas. O extrato UAE+SFE também apresentou estabilidade térmica, conforme análises TG e DTG. Na simulação, os parâmetros ajustados ($D_{F,i}$, $D_{pe,i}$ e o $h_{D,i}$ para o modelo I – SFE-FEM, e $D_{F,i}$ e K_D para o modelo II – UAE-FEM) representaram bem os dados experimentais. O modelo I indicou que o rendimento, $D_{pe,i}$ e $h_{D,i}$ aumentam com pressão, temperatura e concentração de etanol. No modelo II-UAE-FEM, o tratamento ultrassônico melhorou o rendimento, $D_{F,i}$ e K_D para todos os compostos em comparação à extração sem ultrassom. No entanto, apoiados pelos resultados experimentais, evidenciam que o efeito da cavitação produzido pelo ultrassom não foi tão expressivo quanto o poder de extração observado com o fluido supercrítico. Assim, a modelagem atesta que a operação SFE-FEM é quantitativamente mais eficiente para obtenção dos compostos bioativos. Com base nos resultados pioneiros, os compostos bioativos obtidos são promissores e interessantes para aplicação nas indústrias cosmética, farmacêutica e alimentícia.

Considerações finais

Neste estudo, foi desenvolvido com sucesso um processo aprimorado utilizando pré-tratamento ultrassônico combinado com extração supercrítica de CO_2, obtendo compostos bioativos, principalmente ácido linolênico, das folhas de *C. spicatus*. Os resultados mostraram que as técnicas de extração e a escolha do solvente influenciaram diretamente os rendimentos e o teor de metabólitos, impactando as atividades biológicas e as características físico-químicas. O pré-tratamento ultrassônico na SFE aumentou a seletividade do ácido linolênico para 62.52% na condição de 60 °C/11 MPa/5% EtOH. Os parâmetros ajustados representaram bem os dados experimentais. No modelo I (SFE-FEM), o rendimento, $D_{pe,i}$ e $h_{D,i}$ aumentou com a pressão, temperatura e concentração de co-solvente. No modelo II (UAE-FEM), o ultrassom melhorou o rendimento, $K_{D,i}$ e $D_{F,i}$ para todos os compostos, em comparação à extração sem ultrassom. A modelagem demonstrou que o SFE-FEM é mais eficiente para a obtenção de ácido linolênico, ácido palmítico e friedelin. Este estudo fornece uma base sólida para futuras aplicações de *C. spicatus* nas indústrias alimentícia, farmacêutica e cosmética, destacando seu potencial como recurso natural multifuncional.

Palavras-chave: *Costus spicatus*; extração supercrítica; modelagem matemática; transferência de massa compostos bioativos; atividades biológicas

ABSTRACT

Medicinal plants, such as *Costus spicatus*, are a promising source for the isolation of linolenic acid, a precursor of omega-3. This thesis applies low-pressure extraction (LPE: MAC, UAE, SOX) and high-pressure extraction (SFE, UAE+SFE) techniques to evaluate their impact on several aspects: yield, chemical composition, biological properties (such as cytotoxicity, nitric oxide reduction, flavonoid content, total phenolics, antioxidant, antimicrobial and antiviral activity against HSV-1) and physicochemical characteristics (including scanning electron micrograph, microscopic structure, accelerated stability and thermostability). It also investigates the effects of the UAE+SFE combination on the SFE process, aiming to optimize the yield and chemical profile using the Central Composite Design. To complement, two models were developed in COMSOL Multiphysics®: I - dynamic (SFE) and II - batch (UAE), to investigate the effects of pressure (8-20 MPa), temperature (36-64 °C) and co-solvent concentration on the SFE (0-20% EtOH) and to analyze the parameters that influence the extraction of the compounds linolenic acid, palmitic acid and friedelin. The chemical profile was determined by gas chromatography coupled to mass spectrometry (GC/MS). Ethanol, water, and ethanol: water mixture (50% v/v) were used as solvents in the extractions. In UAE, different conditions were evaluated, such as tip, sonication amplitude, time, and solvent type, with the highest yield (8.59%) being achieved with macrotip, 70% amplitude, and 1 min of extraction. The chemical composition varied according to the solvent, with EtOH revealing more compounds. The UAE+SFE combination increased the yield (6.97%) and the selectivity of linolenic acid, reaching 62.52% at 60 °C/11 MPa/5% EtOH. The UAE+SFE extract showed strong antimicrobial activity compared to SFE. LPE and UAE+SFE did not reduce cell viability at 100 μg mL^{-1}. UAE+SFE inhibited nitric oxide by more than 90% at 30 to 300 μg mL^{-1} concentrations. The EtOH extract showed high levels of flavonoids (150.38–1328.73 mg GAE g^{-1}), and UAE+SFE improved the recovery of these compounds compared to SFE alone. Antioxidant activity was higher with ABTS, and all extracts exhibited antibacterial activity against *B. cereus*. UAE+SFE was also more effective against HSV-1. SEM analysis showed that the sample treated with UAE+SFE presented dense microcracks in the tissue structures, and confocal microscopy confirmed autofluorescence, evidencing greater efficiency in the extraction of lipid droplets. The UAE+SFE extract showed thermal stability in TG and DTG analyses. In the simulations, model I indicated that the yield, mass transfer coefficient ($h_{D,i}$), and particle diffusion coefficient ($D_{pe,i}$) increase with pressure, temperature, and ethanol concentration while the fluid mass transfer coefficient ($D_{F,i}$) decreases. Model II showed that ultrasonic treatment improved the yield and $k_{D,i}$ for all compounds. Thus, the modeling allows better discernment of the mechanisms involved in the production of bioactive compounds, which are promising for the cosmetic, pharmaceutical, and food industries.

Keywords: *Costus spicatus*; supercritical extraction; mathematical modeling; mass transfer; bioactive compounds; biological activities

LIST OF FIGURES

Figure 1. Illustration of the Soxhlet apparatus..... 34
Figure 2. Collapse of the solid matrix due to cavitation bubbles. 36
Figure 3. Diagram for supercritical extraction of solid matrices..... 38
Figure 4. Phase diagram for a substance. 38
Figure 5. The typical supercritical CO_2 extraction curve has three stages: constant extraction rate (CER), decreasing extraction rate (FER), and diffusional rate (DC). 41
Figure 6. Pre-processing, processing and post-processing steps in COMSOL. 46
Figure 7. (A) Apparatus used for extraction via Soxhlet e (B) Experiments performed on tip ultrasound. 60
Figure 8. Schematic diagram of ultrasound pretreatment of *C. spicatus* leafs. 62
Figure 9. Kinetics by ultrasound technique. 74
Figure 10. Comparison of the chemical profiles of *C. spicatus* leaf extracts obtained by macrotip (70 and 30%), microtip (30%) and UAE+SFE. 83
Figure 11. Schematic diagram of ultrasound pretreatment of C. *spicatus* leafs. 109
Figure 12. Response surfaces for the global yield derived from UAE + SFE for leaves of C. *spicatus*. (a) Global yield response surface as a function of temperature and cosolvent concentration. (b) Global yield response surface as a function of pressure and cosolvent concentration. (c) Global yield response surface as a function of temperature and pressure. 118
Figure 13. Scanning Electron Microscopy images of C. *spicatus* leaves (zoom 500 and 2000 times). (a-e). Untreated sheet. (b-f). Leaves treated with UAE (ultrasound extraction). (c-g). Leaves treated with SFE (supercritical CO_2 extraction). (d-h). Leaves treated with UAE + SFE (ultrasonic pretreatment in supercritical CO_2 extraction). ... 121
Figure 14. Cytotoxicity of *C. spicatus* extracts determined by colorimetric MTT in L929 cells. All treatments were tested at 30, 100, and 300 μg mL^{-1}. 153
Figure 15. Evaluation of NO inhibition through the application of *C. spicatus* leaf extracts. All treatments were tested at 30, 100 and 300 μg mL^{-1}. 155
Figure 16. Confocal laser scanning microscopy images. (a) Untreated sheet without Nile Red dye. (b) Leaves treated with UAE. (c) Leaves treated with SFE*. (d) Leaves treated with UAE+SFE*. 160
Figure 17. Instability index of C. *spicatus* leaf extracts. 162
Figure 18. Thermogravimetric analysis of *C. spicatus* extracts. 163

Figure 19. Model I fitted to the experimental data of the extracted mass of the compounds as a function of time. Columns: Same compound studied, left side (linolenic acid), center (palmitic acid) and right side (friedelin); Rows: Same extraction condition*. 188
Figure 20. Model II fitted to the experimental data of the extracted mass of the compounds as a function of time. Columns: Same compound studied, left side (linolenic acid), center (palmitic acid) and right side (friedelin); Rows: Same extraction condition*. 198

LIST OF TABLES

Table 1. Biological activity from *Costus spicatus*. 31
Table 2. Applications of supercritical extraction combined with ultrasound for the extraction of bioactive compounds. 42
Table 3. The overall yield of extracts obtained by low and high-pressure techniques.. 64
Table 4. Main compounds obtained by Maceration (HEX, EtOH, and EtOH:H_2O) and Soxhlet (EtOH, H_2O, and EtOH:H_2O) 67
Table 5. Phytochemical constituents of the major compounds obtained by maceration and Soxhlet in different solvents. 71
Table 6. Extractions performed using the ultrasound technique. 72
Table 7. Area percentage of compounds identified in the macrotip at amplitudes of 70 and 30% and microtip at amplitude of 30%. 77
Table 8. Area percentage of compounds identified in UAE+SFE. 81
Table 9. Independent variables and level coding for experimental design. 111
Table 10. Comparison of the yields of C.*spicatus* leaf extract obtained by ultrasound extraction (UAE) and supercritical CO_2 extraction (SFE) combined with and without ultrasound pretreatment (UAE + SFE). 116
Table 11. Regression coefficients (RC) of the adjusted model for global UAE + SFE yield. 119
Table 12. Chemical profile of C. *spicatus* leaf extract obtained by ultrasound extraction (UAE) and supercritical CO_2 extraction (SFE) combined with and without ultrasound pretreatment (UAE + SFE). 123
Table 13. The total phenolic and flavonoid contents and antioxidant capacities (DPPH and ABTS) of C. *spicatus* leaf extracts were obtained with ultrasound (UAE), supercritical CO_2 extraction (SFE), and ultrasound pretreatment in supercritical CO_2 extraction (UAE + SFE). 126
Table 14. Minimal inhibitory concentration MIC (mg mL^{-1}) obtained for C. *spicatus* extracts for specific fungi and bacteria. 129
Table 15. The total flavonoid content and antioxidant capacities (DPPH and ABTS) of C. spicatus leaf extracts were obtained with maceration (MAC), ultrasound (UAE), Soxhlet (SOX), supercritical CO_2 extraction (SFE), and ultrasound pretreatment in supercritical CO_2 extraction (UAE + SFE). 156

Table 16. Diameter of inhibition halos formed by different extraction conditions from *C. spicatus* leaves. 158
Table 17. Cytotoxicity on Vero cells and antiviral activity against HSV-1 in *C. spicatus* extracts. 159
Table 18. Assumptions adopted for SFE-FEM and UAE-FEM mathematical modeling. 177
Table 19. Characterization of particles and fluid properties. 184
Table 20. Yield and mass percentagem by extraction component. 184
Table 21. Kinetic parameters of model I (SFE-FEM). 192
Table 22. Kinetic parameters of model II (UAE-FEM). 199

LIST OF ABBREVIATIONS AND ACRONYMS

AOAC –Association of Official Analytical Chemists

CER – Constant Extraction rate

CGE – Global extraction curve

CO_2 – Carbon dioxide

DC – Diffusion Controlled

SFE – Supercritical extraction

Ethanol: water – 50% aqueous ethanol

SFE-CO_2 – Supercritical extraction with carbon dioxide as solvent

FER – Falling Extraction Rate

FR – Friedelin

GC/MS – Gas chromatography coupled to mass spectrum

H_2O – Water

HPLC-SC – Supercritical extraction unit

GUI – Graphical User Interface

LA – Linolenic acid

LCP – Polymerization process and control laboratory

LC-PUFA omega-3 – Long-chain polyunsaturated fatty acid omega-3

LPE – Low-pressure Extraction

MAC – Maceration

MEF – Finite element method

PA – Palmitic acid

Pc – Critical pressure

RENISUS – National List of Medicinal Plants of Interest to the Unified Health System

RT – Retention Time

SARS-CoV-2 – Coronavirus 2

SDRA – Acute respiratory distress syndrome

SOX – Soxhlet

Tc – Critical temperature

TGA – Thermostability analysis

UAE – Ultrasound-assisted extraction

UAE + SFE – Ultrasonic pretreatment in supercritical CO_2 extraction

UTI – Intensive care unit

LIST OF SYMBOLS

Symbol	Description	Unit
$\mathbf{Humidity_{(bs)}}$	Moisture content in relation to dry solid mass	%
$\mathbf{m_{sample}}$	Sample mass on dry basis	g
$\mathbf{m_i}$	Moisture free sample mass	g
$\mathbf{Y_i}$	Overall performance	%
$\boldsymbol{Mass_{tot}}$	Total mass of sample	Kg
$\boldsymbol{\rho_a}$	Apparent density of the bed	Kg m^{-3}
$\boldsymbol{\rho_r}$	Real density	Kg m^{-3}
$\boldsymbol{\rho_{pe}}$	Specific mass of the particle	Kg m^{-3}
$\mathbf{V_{ext}}$	Capsule volume	cm^3
$\boldsymbol{V_{pe}}$	Particle volume	cm^3
$\boldsymbol{\varepsilon}$	Bed porosity	-
$\boldsymbol{\varepsilon_{pe}}$	Particle porosity	-
$\mathbf{M_{extrato}}$	Extract mass	g
$\mathbf{M_{vegetal}}$	Mass of plant material	g
$\mathbf{C_i}$	Interparticle concentration of species i	mol m^{-3}
$\mathbf{C_{pe,i}}$	Concentration of component i in the particle	mol m^{-3}
$\boldsymbol{\overline{C}_{pe,i}}$	Average particle concentration	mol m^{-3}
T	Time	s
$\boldsymbol{D_{b,i}}$	Effective diffusion coefficient	m^2 s^{-1}
$\boldsymbol{D_{pe,i}}$	Effective diffusion coefficient in the particle	m^2 s^{-1}
$\boldsymbol{\tau}$	Tortuosity	-
U	Speed	m s^{-1}
μ	Dynamic viscosity of the mixture	Pa s
$\boldsymbol{N_{i,inward}}$	Molar flux in the free fluid inside the particle	mol m^{-2} s^{-1}
$\mathbf{h_{D,i}}$	Mass transfer coefficient	m s^{-1}
$\mathbf{S_b}$	Surface area exposed to free fluid flow in the particle bed	m^2 m^{-3}
r	Radial coordinate that goes from 0 to 1	-
$\mathbf{r_{pe}}$	Particle radius	m
Sh	Sherwood number	-

L	Length	m
$\mathbf{D_{F,i}}$	Fluid diffusion coefficient	$m^2\ s^{-1}$
$\boldsymbol{k_{c,i}}$	Convective mass transfer coefficient	$m\ s^{-1}$

SUMMARY

CHAPTER I - INTRODUCTION 25

1.1 OBJECTIVES 27

1.1.1 General objective 27

1.1.2 Specific objectives 27

1.1.3 Structure of the thesis 28

CHAPTER II - LITERATURE REVIEW 29

2.1 ESSENTIAL OILS AND NATURAL EXTRACTS 29

2.2 COSTUS SPICATUS 30

2.2.1 Phytochemical properties of Costus spicatus 30

2.2.2 Linolenic acid 32

2.3 EXTRACTION METHODS 34

2.3.1 Low pressure extraction methods 34

2.3.1.1 Soxhlet Extraction (SOX) 34

2.3.1.2 Extraction by Maceration (MAC) 35

2.3.1.3 Ultrasonic Extraction (UAE) 35

2.3.2 High pressure extraction methods 37

2.3.2.1 Supercritical Extraction (SFE) 37

2.3.2.2 Supercritical fluid 38

2.3.2.2.1 Carbon dioxide (CO_2) 39

2.3.2.2.2 Solubility 39

2.3.2.2.3 Extraction curves 40

2.3.2.3 Ultrasonic pretreatment in supercritical extraction 41

2.4 MATHEMATICAL MODELING 43

2.4.1 Dynamic extraction of the SFE process 43

2.3.2 COMSOL Multiphysics® 44

2.5 REFERENCES 47

CHAPTER III - EVALUATION OF THE YIELD AND CHEMICAL COMPOSITION OF LOW AND HIGH-PRESSURE EXTRACTS OF *COSTUS SPICATUS* LEAVES. 56

ABSTRACT 57

3.1 INTRODUCTION 58

3.2 MATERIAL AND METHODS 59
3.2.1 Raw material preparation 59
3.2.2 Extractions 59
3.2.2.1 Low-pressure Extraction (LPE) **59**
3.2.2.2 Supercritical Fluid Extraction (SFE) **61**
3.2.2.3 Ultrasound pretreatment (UAE + SFE) **61**
3.2.3 Post-processing of extracts 62
3.2.4 Extract characterization 62
3.2.4.1 Chemical profile of C. *spicatus* extracts **62**
3.2.5 Statistical analysis 63
3.3 RESULTS AND DISCUSSION 63
3.3.1 Yield of extractions obtained by different extraction techniques (MAC, SOX, UAE, SFE, and UAE+SFE) 63
3.3.2 Determination of chemical composition (Maceration and Soxhlet) 67
3.3.3 Ultrasonic pretreatment 72
3.3.3.1 Yield **72**
3.3.3.1.1 Influence of the ultrasound tip **72**
3.3.3.1.2 Influence of amplitude **73**
3.3.3.1.3 Influence of solvent **73**
3.3.3.1.4 Influence of time **74**
3.3.3.2 Chemical composition **75**
3.3.3.2.1 Macrotip (70 e 30%) and microtip (30%) **75**
3.3.4 Combination of ultrasound technique and supercritical extraction 81
3.4 CONCLUSIONS 84
3.5 REFERENCES 85

CHAPTER IV - ULTRASOUND PRETREATMENT COMBINED WITH SUPERCRITICAL CO_2 EXTRACTION OF *COSTUS SPICATUS* LEAF EXTRACT 104

ABSTRACT 105
4.1 INTRODUCTION 106
4.2 MATERIAL AND METHODS 107
4.2.1 Plant material 107
4.2.2 Ultrasound-assisted extractions (UAE) 108

4.2.3 Ultrasound pretreatment (UAE + SFE) 109
4.2.4 Supercritical Fluid Extraction (SFE) 110
4.2.4.1 Response Surface Methodology (RSM) **110**
4.2.5 Extract characterization 111
4.2.5.1 Chemical profile of *Costus spicatus* extracts **112**
4.2.5.2 Total phenolic content (TPC) **112**
4.2.5.3 Total flavonoid content (TFC) **113**
4.2.5.4 Antioxidant capacity **113**
4.2.5.4.1 DPPH free radical scavenging activity (DPPH) **113**
4.2.5.4.2 $ABTS^{+}$ free radical scavenging activity **114**
4.2.6 Determination of antibacterial and antifungal activity 114
4.2.6.1 Microorganisms and media **114**
4.2.6.2 Determination of minimum inhibitory concentration (MIC) 115
4.2.7 Scanning electron micrograph (SEM) 115
4.2.8 Statistical analysis 115
4.3 RESULTS AND DISCUSSION 116
4.3.1 Global yield (X_0) 116
4.3.2 Effect of operating conditions 118
4.3.3 Scanning Electron Microscopy of C. *spicatus* leaves 120
4.3.4 Chemical profile of C. *spicatus* extracts 122
4.3.5 Phenolic and flavonoid content wich the antioxidante activity 125
4.3.6 Antimicrobial activity 128
4.4 CONCLUSIONS 131
4.5 REFERENCES 132

CHAPTER V - EVALUATION OF BIOLOGICAL ACTIVITY, PHYSICOCHEMICAL AND MORPHOLOGICAL CHARACTERISTICS OF LOW AND HIGH PRESSURE EXTRACTS OF *COSTUS SPICATUS* LEAVES. 141

ABSTRACT 142
5.1 INTRODUCTION **143**
5.2 MATERIAL AND METHODS 144
5.2.1 Raw material and sample preparation 144
5.2.2 Extractions 144

5.2.2.1 Low-pressure Extraction (LPE) **144**
5.2.2.2 Supercritical Fluid Extraction (SFE) **145**
5.2.2.3 Ultrasound pretreatment (UAE + SFE) **145**
5.2.3 Post-processing of extracts **146**
5.2.4 Cell viability **146**
5.2.4.1 Cell culture **146**
5.2.4.2 Cell viability assay **147**
5.2.5 Nitric oxide inhibitory activity **147**
5.2.5.1 Cell cultures and treatment **147**
5.2.5.2 Griess assay **147**
5.2.6 Total flavonoid contente (TFC) **148**
5.2.7 Antioxidant capacity **148**
5.2.7.1 DPPH free radical scavenging activity (DPPH) **148**
5.2.7.2 ABTS+ free radical scavenging activity **149**
5.2.8 Determination of antibacterial activity **149**
5.2.8.1 Microorganisms and media **149**
5.2.9 Viability of VERO cells and antiviral activity against HSV-1 virus **150**
5.2.9.1 Cytotoxicity Assay **150**
5.2.9.2 Antiviral Assay **151**
5.2.10 Confocal laser scanning microscopy **151**
5.2.11 Accelerated stability analysis **152**
5.2.12 Thermogravimetric analysis (TGA and DTG) **152**
5.2.13 Statistical analysis **152**
5.3 RESULTS AND DISCUSSION 152
5.3.1 Cell viability **153**
5.3.2 Nitric oxide (NO) inhibitory activity **154**
5.3.3 Flavonoid content wich the antioxidante activity **155**
5.3.4 Antibacterial activity **157**
5.3.5 Cytotoxicity and antiviral activity against HSV-1. ..... **159**
5.3.6 Confocal microscopy **160**
5.3.7 Accelerated stability analysis **161**
5.3.8 Thermogravimetric analysis (TGA and DTG) **162**
5.4 CONCLUSIONS 163
5.5 REFERENCES 164

CHAPTER VI - MATHEMATICAL MODELING OF THE EXTRACTION OF BIOACTIVE COMPOUNDS FROM *COSTUS SPICATUS* WITH SUPERCRITICAL CO_2 AND ULTRASOUND 170

ABSTRACT 171

6.1 INTRODUCTION 172

6.2 MATERIAL AND METHODS 173

6.2.1 Sample preparation and characterization 173

6.2.2 Supercritical Fluid Extraction (SFE) 174

6.2.3 Ultrasound-assisted extractions (UAE) 175

6.2.4 Conventional extraction in a water bath with manual agitation 175

6.2.5 Post processing of extracts 175

6.2.6 Extract characterization 176

6.2.6.1 Global yield of compounds 176

6.2.6.2. Quantification of the compounds of interest by GC/MS **176**

6.2.7 Finite element method (FEM) model 176

6.2.7.1 Hypotheses (SFE-FEM and UAE – FEM) **177**

6.2.7.2 Mass transfer (Model I – SFE-FEM) **178**

6.2.7.2.1. Initial and boundary condition (Model I – SFE-FEM) **180**

6.2.7.2.2 Mathematical modeling strategy (Model I – SFE-FEM) **180**

6.2.7.3 Mass transfer (Model II – UAE-FEM) **181**

6.2.7.3.1. Initial and boundary condition (Model II – UAE-FEM) **181**

6.2.7.3.2. Mathematical modeling strategy (Model II – UAE-FEM) **182**

6.2.7.4 Model parametes **183**

6.2.7.5 Mesh study for numerical simulation **183**

6.2.8 Statistical analysis 183

6.3 RESULTS AND DISCUSSION 183

6.3.1 Characterization of particles and properties fluid 183

6.3.2 Yield of component extraction 184

6.3.3 Finite element method (FEM) method 186

6.3.3.1 Mesh study for numerical simulation **186**

6.3.3.2 Model fit to experimental data (Model I – SFE-FEM) **187**

6.3.3.2.1 Effect of pressure **194**

6.3.3.2.2. Effect of temperature **195**

6.3.3.2.3 Effect of cosolvent **196**
6.3.3.3. Model fit to experimental data (Modelo II – UAE-FEM)..... **197**
6.3.3.4 Comparison between model I and II **199**
6.4 CONCLUSIONS 200
6.5 REFERENCES 200
CHAPTER VII - FINAL CONSIDERATIONS AND FUTURE STUDIES 209

CONCEPTUAL DIAGRAM OF WORK

Because?

i. The “cana do brejo” (*Costus spicatus*) is a medicinal plant little known in academia. However, it has stood out with its highly relevant bioactive compounds;
ii. Ultrasound, considered with green technology, enhances bioactive compounds' performance when used as a pre-treatment;
iii. Disseminate a natural source that can potentially prevent infectious diseases due to its bioactive compounds.

Who has done?

i. There aren’t works on the extraction of bioactive compounds from the leaves of the "cana do brejo" using a combination of extraction techniques in the literature;
ii. Scarcity of studies that present antioxidant and biological activity to *Costus spicatus*;
iii. The simulation of supercritical extraction and ultrasound for “cana do brejo” has not been carried out to date.

What is the hypothesis?

i. Is it possible for the pretreatment technique with the supercritical fluid extraction (SFE) to recover bioactive compounds from the leaves of the “cana do brejo”?
ii. Could combining processes increase the production of multiple compounds of interest, such as linolenic acid?
iii. Do extracts from *Costus spicatus* leaves have biological activities?
iv. Can the simulation demonstrate the effect of supercritical extraction and ultrasound? How to make?

How to make?

i. Analyze pretreatment conditions to optimize operating conditions;
ii. Observe the combination of ultrasound pretreatment with SFE;
iii. Evaluate cytotoxicity, nitric oxide reduction, flavonoid content, total phenolics, antioxidant, antimicrobial, and antiviral activity against HSV-1, scanning electron micrograph, microscopic structure, accelerated stability, and thermostability;
iv. Study the behavior of the dynamic extraction curves obtained from SFE and UAE using a computational tool for modeling and simulation.

THESIS METHODOLOGICAL SEQUENCE FLOWCHART

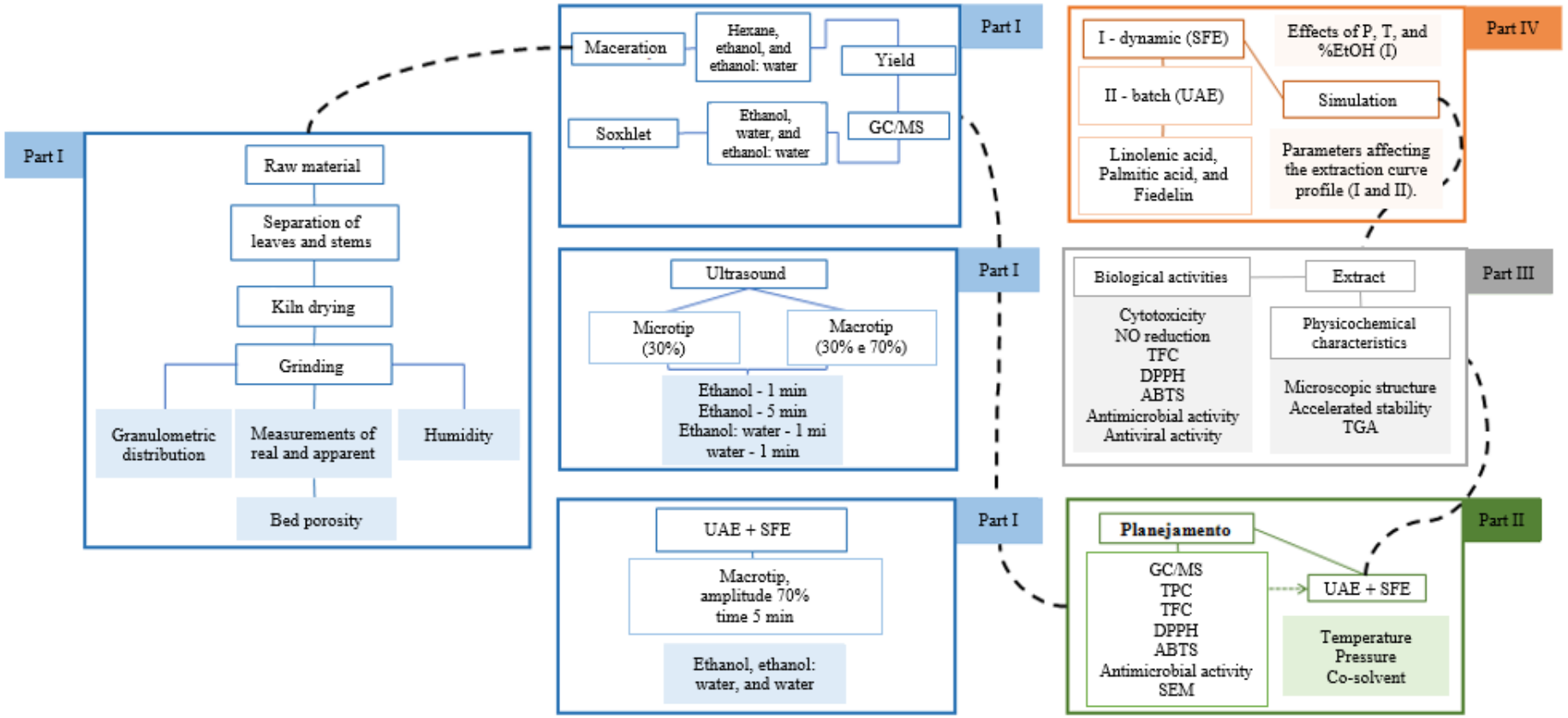

CHAPTER I - INTRODUCTION

The negative impact of infectious diseases, such as COVID-19, has generated concern among the general population, as it presents complicated symptoms with severe lung damage, called acute respiratory distress syndrome (ARDS), which is usually lethal, leading to systemic inflammation and multiple organ failure. Researchers have shown that diets rich in linolenic acid (ALA), a precursor of omega-3, can be useful in preventing these infectious diseases, as it has an anti-inflammatory effect and acts on the immune system (GUO *et al.*, 2020; CALDER *et al.*, 2018).

In this context, demonstrating the usefulness of linolenic acid, which functions as a kind of "barrier" against a future pandemic, sustainable and technological alternative sources coming from medicinal plants, such as the *Costus spicatus* species, become an alternative natural source for the isolation of this essential fatty acid.

Costus spicatus, a medicinal plant of the Costaceae family, is widely distributed throughout most of Brazil, especially in the Atlantic Forest and Amazon region. It is commonly known as "cana do brejo", "canela de macaco", "cana do mato", etc. This plant species has been widely used as a folk remedy to treat colds, sore throat, diarrhea, kidney stones, and diuretic action. In addition, they are used for ornamental purposes, such as in gardens and cutting flowers. Currently, biological research on the aerial parts of *Costus spicatus* has been reported, which contain compounds with antifungal and anti-inflammatory properties (AZEVEDO *et al.*, 2014; BITENCOURT and ALMEIDA, 2014; BORGES, 2016).

The natural extract is a complex mixture of secondary metabolites that protect the plant against biotic and abiotic stresses. Its main components are of terpenic origin, such as monoterpenes and sesquiterpenes, but aromatic compounds are also found in the extracts. The content and type of these components differ substantially based on the separation method applied, subsequently affecting the medicinal and nutritional application (BAJPAI *et al.*, 2012; BAKKALI *et al.*, 2008).

For the isolation of the plant extract, low-pressure techniques, such as ultrasound (UAE), microwave, maceration (MAC), hydrodistillation, and Soxhlet (SOX), or high-pressure techniques, such as supercritical extraction (SFE) and pressurized liquid extraction, can be used. Low-pressure methods consume a lot of time and energy, and those that apply high temperatures for a prolonged period cause variations in the composition. SFE was developed to overcome these limitations as it is environmentally

friendly, selective, and provides solvent-free extract. The fluid normally used is CO_2, which is safe, non-toxic, and non-flammable (CHEN *et al*, 2020; DIAS *et al.,* 2021).

The application of raw material pretreatment techniques has been used to obtain superior performance compared to isolated techniques. UAE can be highlighted among the techniques used to carry out this preliminary treatment (DA PORTO *et al.*, 2015). Scaling the process promotes increased extraction efficiency and cost reduction due to lower energy expenditure resulting from the shorter time spent in extraction (LIMA, 2020).

The ultrasound technique produces high-frequency ultrasonic waves that can promote cavitation phenomena and increase energy and mass transfer in liquid media, thus causing the rupture of plant cell walls and promoting solvent penetration. This technique presents non-selectivity to the target compounds and generates a large amount of residue. However, the combination of UAE with SFE provides an advantageous complementarity in the phytotherapeutic material to be extracted, being able to increase the yield, the content of certain constituents in the extraction, and the obtaining of extracts with desirable properties (VIDOVIC *et al.*, 2014; LIU *et al.*, 2020).

The use of computational numerical simulation tools, mainly in the field of engineering, has been receiving attention in recent years. These tools offer several benefits, including virtual prototyping, cost avoidance, and reduced design time. Furthermore, they can also handle severe operating conditions (SANTANA *et al.*, 2020; LIMA, 2020).

No studies have been reported on ultrasound pretreatment followed by SFE of active constituents from the leaves of the "cana do brejo" (*Costus spicatus*). This study fills this gap and represents the sequential use of the effectiveness of ultrasound-assisted pretreatment for extracting compounds, mainly linolenic acid, to observe the influence on yield, composition, and biological activities. In addition to the experimental study, modeling, and simulation of the experimental data obtained from SFE will be applied in the COMSOL Multiphysics® software to evaluate the phenomena involved and the behavior of the extraction curves.

1.1 OBJECTIVES

1.1.1 General objective

Obtain natural extracts from *Costus spicatus* leaves using ultrasound as pretreatment when applying supercritical technology (a combination of environmentally friendly techniques) and perform modeling and simulation of the supercritical extraction and ultrasound processes separately.

1.1.2 Specific objectives

In line with the general objective, the following specific objectives were established:

1. Characterize the extracts from the leaves of the "cana do brejo" (*Costus spicatus*);
2. Obtain extracts from the leaves of *Costus spicatus* using the maceration and Soxhlet techniques in different solvents and evaluate the chemical composition;
3. Obtain extracts using the ultrasound technique and evaluate the inference in yield and chemical composition under the following operating conditions: macrotip, microtip, amplitude, solvent, and time;
4. Ultrasound pretreatment applied to supercritical extraction;
    a) Obtain extracts by supercritical extraction of ultrasound residue;
    b) Evaluate the yield and chemical composition;
    c) Assess whether pretreatment is an efficient operation for extracting value-added compounds, mainly linolenic acid;
    d) Check whether an experimental design can identify the significant operational conditions (temperature, pressure, and cosolvent with supercritical CO_2) based on pretreatment with ultrasound;
    e) Perform dynamic curves of the extraction process;
5. Analyze biological activities: cytotoxicity, nitric oxide reduction, flavonoid content, total phenolics, antioxidant, antimicrobial, and antiviral activity against HSV-1;
6. Evaluate physical-chemical and morphological characteristics: scanning electron micrograph, microscopic structure, accelerated stability, and thermostability;
7. Model and mathematically simulate dynamic extraction curves of compounds of interest, for a better understanding of the phenomena involved;
8. Perform model validation against experimental data.

1.1.3 Structure of the thesis

This thesis is divided into chapters, which present the development of this work. Chapter I comprises the introduction, general objective, and specific objectives developed in carrying out the thesis and its structure.

Chapter II presents a literature review, addressing relevant aspects of essential oils and natural extracts, the medicinal plant “cana do brejo” (*Costus spicatus*), and low and high-pressure techniques, emphasizing combining UAE with SFE and mathematical modeling.

Chapters III, IV, V, and VI describe the methodology applied and the study's results in evaluating the yield and chemical composition of *Costus spicatus* leaf extracts using low and high-pressure techniques. They include the pre-treatment by ultrasound combined with supercritical CO_2 extraction, the evaluation of the biological activity and the physicochemical and morphological characteristics of the extracts, in addition to the simulation of two models: I - dynamic (SFE) and II - batch (UAE), through the COMSOL Multiphysics® software.

Chapter VII presents the conclusions of the work.

CHAPTER II - LITERATURE REVIEW

This chapter aims to address aspects found in the literature and contextualize the work's main interests and relevance. Next, a brief bibliographic review will be presented, addressing essential oils and natural extracts and highlighting aspects related to the main characteristics of “cana do brejo” (*Costus spicatus*). Next, the low and high-pressure extraction techniques used in this study will be reported, emphasizing the UAE pretreatment with SFE and, finally, the mathematical modeling.

2.1 ESSENTIAL OILS AND NATURAL EXTRACTS

Considering the increasing global demand for bioactive compounds, an important natural resource resource, researchers and industry are focusing on finding sustainable and technological alternative sources to isolate these compounds. Medicinal plants are used in large quantities to obtain these compounds. Therefore, the valorization of these medicinal plants is of fundamental importance due to the increasing consumer concern about health in terms of the negative impact of the use of artificial substances (DIAS *et al.*, 2021; BRUNING, MOSEGUI, and VIANNA, 2012).

In developing countries such as Brazil, it is estimated that around 85% of the population uses traditional medicine (BRAZIL, 2016). This percentage reflects the importance of conducting an in-depth study of medicinal plants with highly relevant active ingredients.

Medicinal plants have active principles (bioactive substances), components that constitute essential oils and natural extracts. These are produced during their secondary metabolism and protect the plant against biotic and abiotic stresses. Flavonoids, phenols, glycosides, essential oils, vitamins, and alkaloids, among others, are responsible for the therapeutic action in plants (SOUZA and RODRIGUES, 2016; OLIVEIRA, 2012).

Essential oils are a mixture of natural compounds with low molecular weight organic structures, while natural extracts contain low and high molecular weight compounds. They are obtained from various plant sources, such as leaves, herbs, roots, bark, and seeds. Characterized by their odors and oily appearance, oils and extracts may have different chemical compositions, physical-chemical characteristics, and odors when extracted from different parts of the same plant. In addition, variations in climate and soil conditions, harvesting times and seasons, type of extraction, and other factors influence the synthesis of these compounds (SIMÕES and SPITZER, 2003).

2.2 COSTUS SPICATUS

Costus spicatus (Jacq.) Sw. is a medicinal plant commonly known as "cana do brejo", "cana de macaco", "cana do mato", etc. It is a species belonging to the order Zingiberales, whose family and genus are Costaceae and Costus, respectively. Furthermore, it is widely distributed throughout almost all of Brazil, especially in the Atlantic Forest and Amazon region (AZEVEDO *et al.*, 2014; BITENCOURT and ALMEIDA, 2014; BORGES, 2016). The genus Costus was even indicated in the National List of Medicinal Plants of Interest to the Unified Health System (RENISUS), justified by the widespread ethnopharmacological use of these species in Brazil (AMORIM *et al.*, 2022).

Due to its vigorous and floriferous nature, *Costus spicatus* is used for ornamental purposes, in gardens, and to produce cut flowers. It has also been widely used as a folk remedy, where its leaves, stems, and rhizomes are used for medicinal purposes, to treat colds, sore throats, and diarrhea. In addition, it helps in the treatment of kidney stones and various diseases, such as urinary infections, thanks to its diuretic properties (AZEVEDO *et al.*, 2014; PEDROSA, 2017; PAES, MEDONÇA and CASAS, 2013).

It is characterized by a long life cycle (perennial), rhizomatous (underground stems), caespitose, erect, and unbranched plant species. As an adult, it can reach 2 m in height. It has 25 - 40 cm long membranous leaves with red bracts and yellow flowers. It can be propagated by seeds and rhizomes (LORENZI and MATOS, 2002).

According to Boorhem *et al.* (1999), they report that the decoction of the vegetative parts of *Costus spicatus* helps in the treatment of ulcers and vaginal irritations. As described by Albuquerque (1989) and Borrás (2003), fresh stem juice has properties that treat syphilis, insect bites, diabetes, and bladder problems. Pinna *et al.* (2008) describe that the *Costus spicatus* tea is effective in treating Herpes Zoster. Finally, Manfred (1947) reports that the rhizome of this plant is used to expel kidney stones.

2.2.1 Phytochemical properties of *Costus spicatus*

Phytochemical investigations on extracts of *Costus spicatus* revealed the presence of alkaloids, triterpenes, flavonoids, saponins, and tannins (AZEVEDO *et al.*, 2014; DEVENDRAN and SIVAMANI, 2015; PAES *et al.*, 2013). Bitencourt and Almeida (2014), De Souza *et al.* (2004), and Silva *et al.* (2008) subjected the aerial parts

of this plant species to ethanolic extraction, resulting in the presence of alkaloids, phenols, and tannins.

Laurintino (2020) applied the supercritical extraction technique with CO_2, with the addition of cosolvent, to extract bioactive compounds from the leaves and stems of *Costus spicatus* under different experimental conditions. Active phytotherapeutic compounds with anti-inflammatory activity were found in the leaves (linolenic acid, friedelin, palmitic acid, and linoleic acid). In the stems, the compounds sitosterol, stigmasterol, and linolenic acid present mechanisms of action to improve glycemic control in diseases with diabetes, that is, conferring antidiabetic properties.

Scientific records carried out with *Costus spicatus* demonstrate the existence of important secondary metabolites in its chemical composition, with proven pharmacological activities, as seen in Table 1.

Table 1. Biological activity from *Costus spicatus*.

Biological activity	*Reference*
Anti-inflammatory	Silva *et al.,* 2000; Picanço *et al.,* 2016; Quintans júnior *et al.*, 2010;
Analgesics	Picanço *et al.,* 2016; Quintans júnior *et al.,* 2010;
Antidiabetics	Madhavan *et al.,* 2019;
Antifungal	Silva *et al.*, 2008; Souza *et al.*, 2012;
Antimicrobial	Silva *et al.*, 2008; Souza *et al.*, 2012;
Nephroprotective	Moreno *et al.,* 2021;
Antioxidant	Azevedo *et al.*, 2014, Pedrosa, 2017; Uliana, Silva e Fronza, 2015.

Source: Developed by the author, 2022.

The bioactive substances present in the extracts have a wide variety of biological activities, corroborating the use of *Costus spicatus*, widely used as a remedy in folk medicine. Thus, due to the existence of important secondary metabolites in its chemical composition, it represents a vast reservoir of promising properties with high added value of interesting biological activities.

The species *Costus spicatus* has demonstrated potential protective effects in several pathologies, including kidney disorders. These kidney diseases are a public health problem and are the leading cause of death and disability worldwide (AMORIM *et al.*, 2022). According to the ethnobotanical study carried out in the Grande Dourado region (MS) by Coelho *et al.* (2019), *Costus spicatus* (Jacq.) Sw. was among the three species

most cited by people who use this plant medicinally in the region for the treatment of urinary tract diseases.

Among kidney diseases, the incidence of nephrolithiasis consists of the formation of kidney stones that originate from the precipitation of poorly soluble salts in concentrated urine; that is, insoluble components are formed by the combination of components in the urine, generating the formation of crystals, which when they grow and adhere, promote the development of kidney stones. They can cause some complications, whether mild or of fatal potential. This kidney disease affects 10 to 12% of men and 5 to 6% of women (MOE, 2006).

The treatment of nephrolithiasis is expensive due to pharmacological expenses, hospitalization, dialysis, and surgery. Numerous studies have sought new alternatives for the treatment and prevention of this kidney disease, as well as for the treatment of crises, using anti-inflammatories that improve the patient's pain with their analgesic effect. Therefore, *Costus spicatus* becomes an alternative because it presents this property (EDVARDSSON *et al.*, 2013; MORENO *et al.*, 2021).

Therefore, the determination of active compounds present in the *Costus spicatus* extract must be carefully analyzed to provide data that support the traditional use of this medicinal species for the treatment of kidney diseases.

2.2.2 Linolenic acid

Among the unsaturated fatty acids, there are two polyunsaturated ones, called linoleic acid (C18:2ω6) and linolenic acid (C18:3ω3), considered essential from a nutritional point of view, as they cannot be synthesized by the human body, but can be acquired through diet or other supplements (SANTESTEVAN, 2011). In addition, they belong to the omega-6 and omega-3 families of fatty acids, respectively. In most plant tissues, linolenic acid is the one that exists in the greatest quantity, with more than 80% of the acyl group of chloroplast membrane lipids (BATISTA *et al.*, 2002).

In this context, an adequate supply of nutrients, such as omega-3 long-chain polyunsaturated fatty acid (omega-3 LC-PUFA), whose precursor is linolenic acid (ALA) and the long-chain derivatives, eicosapentaenoic acid (EPA) and docosahexaenoic acid (DHA), have benefits for the control of chronic and acute inflammation, as well as for the immune system (CALDER *et al.*, 2020). Therefore, its supplementation in the diet or as a pharmacological nutrient could reduce the impact of inflammation caused by viral

infectious diseases, such as COVID-19, caused by the coronavirus 2 (SARS-CoV-2) strain, which recently emerged in late 2019 (Weill *et al.*, 2020).

According to GUO *et al.* (2020), patients with COVID-19 cases are at high risk of developing acute respiratory distress syndrome (ARDS), which can lead to intensive care unit (ICU) admission, which is often fatal. This ARDS appears 7 to 15 days after the onset of symptoms and promotes the uncontrolled overproduction of immune cells and cytokines, leading to systemic inflammation and multiple organ failure. In addition, Covid not only affected people with severe disease (hospitalized) but also those with mild symptoms, who after infection, are prone to neuropsychiatric complications, such as anxiety, depression, post-traumatic stress disorder, and unrestored sleep (YANG *et al.*, 2022).

Countries with high intakes of omega-3 LC-PUFA (ALA, EPA, and DHA) had a very low number of victims of COVID-19 (Weill *et al.*, 2020). This can be attributed to the anti-inflammatory and immunomodulating effect of omega-3 LC-PUFA. Human studies have reported that enteral (where liquid food processed by the gastrointestinal tract is received) and parenteral (intravenous) nutrition of fish oil, rich in omega-3 LC-PUFA, reduced the infection rate and length of hospital stay in clinical and surgical patients admitted to the ICU (CALDER *et al.*, 2018). Furthermore, animal studies have observed that omega-3 LC-PUFA supplementation increased tissue omega-3, mainly in lung tissues (ZHONG *et al.*, 2018). In other studies with animals, where they were exposed to microbial infections, the animals' diet enriched with omega-3 promoted a beneficial impact against acute pneumonia (SHARMA *et al.*, 2013).

Therefore, a diet rich in omega-3 LC-PUFA (ALA, EPA, and DHA) may increase their overall storage in tissues, improving the severity of COVID-19 disease by controlling cytokine cells and promoting positive outcomes in infected patients, especially in viral entry and replication (Weill *et al.*, 2020). Interestingly, another study revealed that ALA and EPA block the entry of SARS-CoV-2 (GOC *et al.*, 2021). In addition, studies are reporting the demonstrated efficacy of omega-3 LC-PUFA as a supplement for neuropsychiatric complications associated with COVID-19 (YANG *et al.*, 2022).

In connection with these interesting results, linolenic acid, a precursor of omega-3, is present in the plant species *Costus spicatus* (LAURINTINO, 2020). Thus, the investigation of the popular medicinal use of the species *Costus spicatus*, as well as its chemical constituents and biological activities, can provide new therapeutic options for

the treatment of kidney diseases, as well as for infectious diseases, such as COVID-19, since the increase in the level of omega-3 intake can function as a kind of "barrier" against a future pandemic, as it has an anti-inflammatory effect and acts on the immune system.

2.3 EXTRACTION METHODS

2.3.1 Low pressure extraction methods

Several extraction methods can be found in the literature and are classified into low-pressure techniques, such as Soxhlet, ultrasound, microwave, maceration, and hydrodistillation, or high-pressure techniques, such as supercritical extraction and pressurized liquid extraction, can be used (CHEN *et al.*, 2020; DIAS *et al.*, 2021).

Theoretical aspects of the extraction techniques used in this work are presented below.

2.3.1.1 Soxhlet Extraction (SOX)

The Soxhlet extraction methodology was carried out in 1989 by the German chemist Ritter Von Soxhlet, based on determining the lipid fraction in beds. This technique is used as a form of comparison with unconventional methods in terms of yield and quality of extracts obtained due to the simplicity of operation combined with the use of high temperatures that decrease the viscosity of the solvent and increase the extraction rate, thus providing the detachment of the extract from the matrix (LUQUE DE CASTRO; PRIEGO-CAPOTE, 2010; FERRO, 2019).

The apparatus consists of a condenser, extractor with a siphon, collecting flask, and a heating blanket, as shown in Figure 1.

Figure 1. Illustration of the Soxhlet apparatus.

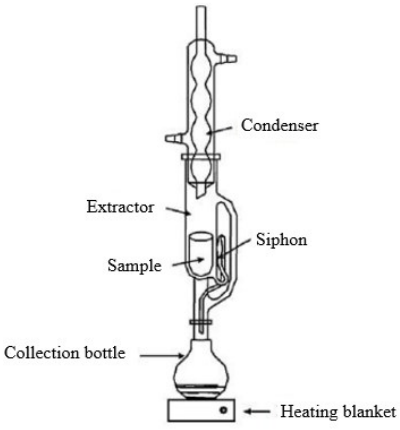

Source: Luque de Castro; Priego-Capote (2010).

The Soxhlet technique is part of one of the methods considered conventional. The process involves placing the plant material in cartridges attached to the extractor, which is gradually filled with the condensed solvent. As the liquid reaches a certain level inside the extractor, it is sucked up by a siphon and then discharged into the collection bottle. This operation is repeated until all the solute has been extracted (LUQUE DE CASTRO; PRIEGO-CAPOTE, 2010; SARTOR, 2009).

Among the advantages of Soxhlet extraction, the most important are the low cost of acquiring the apparatus, simplicity of operation, and obtaining a high extraction yield resulting from the combination of the use of solvent and the employment of high temperatures. On the other hand, it has the following disadvantages: long operating time, a large volume of solvent, and the high temperature employed, which promotes the degradation of thermolabile compounds of interest. In addition, the use of organic solvents generates the need for solvent evaporation steps and the possibility of causing undesirable changes in the extract (BIMAKR *et al.*, 2011; BENELLI, 2010; WANG and WELLER, 2006).

2.3.1.2 Extraction by Maceration (MAC)

Maceration consists of direct contact between the solvent and the plant matrix in a closed container at room temperature for a long period (hours or days) with occasional or constant agitation. At the end of the process, the mixture is filtered to separate the plant matrix from the solvent (AZMIR *et al.*, 2013).

This technique is a non-selective process applied when the compounds are soluble at room temperature and can be altered by heat. However, it has the disadvantage of not completely depleting the plant compound due to the saturation of the solvent or the equilibrium between the interior of the cell and the solvent (LEITE, 2009; TRAMONTIN, 2020).

2.3.1.3 Ultrasonic Extraction (UAE)

The ultrasound-assisted extraction technique has increased recently, as it effectively extracts compounds from solid samples. In addition, it has low cost, simple equipment, fast extraction, and uses a low volume of solvent. Its efficiency can be affected by several variables, such as ultrasound amplitude, sonication time, solvent-solid ratio,

and temperature, in addition to the particle size, moisture content, and solvent used (CARRERA *et al.*, 2012; ANDRADE, 2011; AZMIR *et al.*, 2013).

In ultrasound equipment, transducers convert electrical or mechanical energy into inaudible sound energy (frequency above 16 kHz). The use of ultrasound in fluids can cause physical effects, such as turbulence, rupture of biological cells, and agglomeration of particles, as well as chemical effects (formation of free radicals). These effects arise mainly from cavitation (BALACHANDRAN *et al.*, 2006; SOUZA, 2016).

Cavitation (Figure 2) is a phenomenon that results in the formation, growth, and violent collapse of microbubbles in a sonication liquid due to pressure fluctuations from acoustic waves. Implosion also generates turbulence. When these microbubbles collapse violently (cavitation), microjets are formed, which can result in the rupture of the cell wall, providing penetration of the solvent into the cells, thus promoting the transfer of mass from the solutes to the solvent (LEIGHTON, 1994; MCQUEEN, 1990; DASSOFF e LI, 2019; CHEMAT *et al.*, 2017).

Figure 2. Collapse of the solid matrix due to cavitation bubbles.

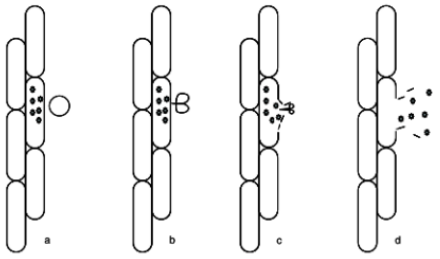

Source: CHEMAT *et al.*, 2017.

Ultrasonic waves can accelerate plant mass transfer processes without altering their main quality characteristics (SOUZA, 2016). These high-power ultrasonic waves are generally applied using two types of devices: ultrasonic baths or ultrasonic probes. The ultrasonic bath provides low-cost temperature control and operates at a frequency of approximately 40 KHz. Its advantage is that it offers the possibility of treating several samples simultaneously; however, compared to the probe, it offers low reproducibility and low power delivered directly to the sample (CHEMAT *et al.*, 2017; DIAS, 2017).

The ultrasonic probe offers greater extraction power because the probe is immersed directly in the solution, thus providing minimal loss of ultrasonic energy and up to 100 times greater power than the bath, reducing extraction time (RUDKE, 2019; PICÓ, 2013). However, it can cause the degradation of thermolabile compounds because

direct sonication causes an increase in temperature. In addition, they present a lack of uniformity in energy distribution and the need for filtration after extraction (ANDRADE, 2011; VIERA, 2016).

2.3.2 High pressure extraction methods

2.3.2.1 Supercritical Extraction (SFE)

Supercritical extraction uses fluids as extraction agents and is a viable alternative to traditional techniques. In addition, it has been attracting great interest for several decades in the food, pharmaceutical, and cosmetic sectors, as it has an environmentally friendly extraction approach, generates greater selectivity of compounds, shorter extraction time, and does not use toxic organic solvents (SERRA *et al.*, 2010; LIU *et al.*, 2020).

The supercritical extraction process consists of two processes: the extraction itself (a) and the separation of the solute/solvent mixture (b). Figure 3 shows a simplified diagram of the supercritical extraction process (BRUNNER, 1994; SUFLUX, 2018; CRUZ, 2019).

a) In the first process, the supercritical fluid (CO_2) leaves the pump at a pressure above 7.4 MPa and is heated to above 31ºC, reaching the supercritical state. It then flows through a fixed bed consisting of a solid matrix (raw material) stored in the extractor, solubilizing the components present in the solid. As the solvent flows through the plant material, the mass of the solute is transferred from the solid phase to the liquid phase until equilibrium is reached.
b) In the second part of the process occurs the mixture of compounds (solute) and the supercritical solvent is separated by reducing the pressure to atmospheric pressure, vaporizing the solvent, and precipitating the extracted compounds.

Figure 3. Diagram for supercritical extraction of solid matrices.

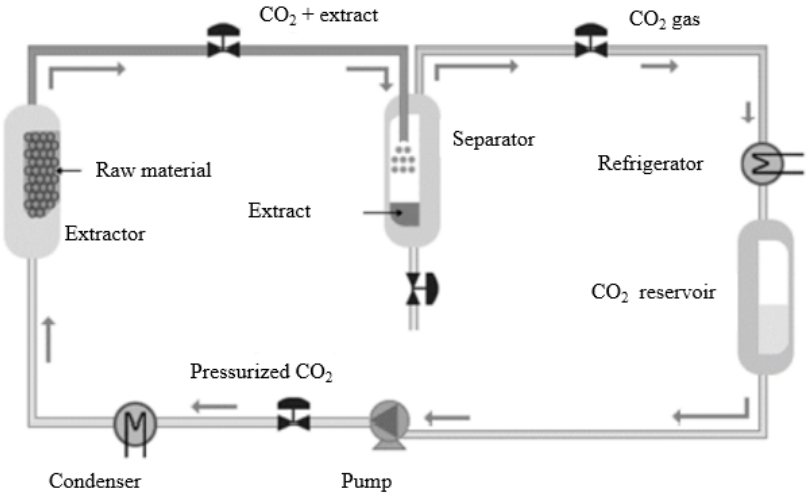

Source: Suflux, 2018.

2.3.2.2 Supercritical fluid

The supercritical fluid used in extraction is defined as any substance that is above its critical temperature (Tc) (considered as the maximum temperature at which gas can be converted into liquid by an increase in pressure) and critical pressure (Pc) (corresponds to the highest pressure at which a liquid can be converted into vapor by an increase in temperature). When this substance is above Tc and Pc, it passes into a condition called the "Supercritical Fluid State", possessing very peculiar properties and adopting the behavior of gases and liquids simultaneously (BRUNNER, 2005). Figure 4 presents a phase diagram with the gas, liquid, solid, and supercritical fluid regions.

Figure 4. Phase diagram for a substance.

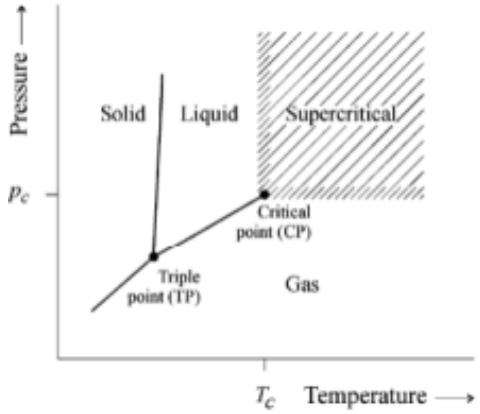

Source: BRUNNER, 2005.

2.3.2.2.1 Carbon dioxide (CO_2)

CO_2 is a widely used solvent in techniques involving supercritical fluids. This supercritical solvent is ideal because it has moderate critical constants ($T_{critical}$, 31ºC; $P_{critical}$, 7.4 MPa), which can protect thermosensitive compounds against degradation. Furthermore, it is a safe and inexpensive gas that is non-toxic, non-flammable, non-explosive, and easily eliminated in the decompression stage, obtaining solvent-free extracts (ARA *et al.*, 2014; YANG, WAN, and WEI, 2019).

The combination of liquid-like dissolution and gas-like dispersion capacity gives supercritical CO_2 excellent transport properties, allowing easy access to porous matrices' interiors, thus generating better extraction productivity. It is worth noting that, through changes in temperature, pressure, and co-solvent conditions, the properties of CO_2 can vary, generating greater solvation power and high selectivity in the target compounds (YANG and WEI, 2016; RAHMANIAN *et al.*, 2015; YANG WAN and WEI, 2019).

Despite all the benefits of supercritical CO_2 (a nonpolar solvent), its main disadvantage is its low ability to extract polar compounds, even under high-density conditions. However, this deficiency can be overcome by using polar substances, such as water and ethanol, which can improve the solubility of the compounds and/or increase extraction selectivity. Generally, ethanol is the most widely used co-solvent, as it meets the legal requirements for the use of organic solvents in inputs for the food industry (MOYLER, 1993; BISCAIA, 2007; PIES, 2017).

2.3.2.2.2 Solubility

According to Huang, Shi, and Jiang (2012), two main factors affect the development of SFE-CO_2 extraction technologies: the rate of mass transfer of the solute out of the plant matrix and the solubility of the solute in the supercritical fluid, the latter being directly related to its solvent density (a) and the vapor pressure of the solute (b).

(a) With an increase in pressure at a given temperature, the solubility of the solute increases due to the increase in the solvent's density (greater mass of fluid per unit volume), generating a higher extraction yield and lower selectivity (BRUNNER, 1994).

(b) As the temperature increases at a given pressure, the density of supercritical CO_2 reduces, and consequently, its solubility decreases; at the same time, the vapor pressure of the compounds to be extracted increases. The extraction rate will be

influenced by whether the solute is volatile or non-volatile (LAURINTINO, 2017; ANDRADE, 2011).

- Non-volatile solute: increasing the temperature reduces the solubility of supercritical CO_2, resulting in a lower extraction rate;
- Volatile solute: the extraction rate will depend on the factor that intervenes more strongly. This factor could be the solubility of supercritical CO_2, which decreases with increasing temperature, or the volatility, which increases as the temperature increases. The competition between these two effects (solvent density and solute vapor pressure) promotes the crossing of the isotherms, generating the phenomenon known as retrogradation.

2.3.2.2.3 Extraction curves

In the extraction process with supercritical fluids, it is possible to construct a kinetic curve or global extraction curve (GEC). This curve is normally presented as a graph of accumulated extract mass as a function of total extraction time, with data collected at predetermined time intervals. The representation of the curve provides fundamental information on the mass transfer phenomenon over the plant matrix under study and enables the obtaining of other process parameters, such as time and characterization of the supercritical extraction stages (BRUNNER, 1994; ANDRADE, 2011).

According to Brunner (1994), different mass transfer mechanisms control the extraction process, allowing three distinct stages to be attributed to the kinetic curve, as described below and illustrated in Figure 5.

I) Constant Extraction Rate (CER) stage:

The particle contains an external surface covered by extract, and as the solvent flows, the easily accessible material is extracted until its maximum concentration at saturation (equilibrium solubility) is reached. The extraction rate is constant. In many cases, the extraction is completed at this CER stage since approximately 50 to 90% of the extract is obtained at this stage, except in cases where the compound of interest is located in a cellular structure that is difficult to access by the solvent or has low solubility in the solvent. The main mass transfer mechanism is convection (BRUNNER, 1994; PEREIRA and MEIRELES, 2010).

II) Falling Extraction Rate (FER) stage:

The solute is transferred from the outer layer of the particle and from part of the inside of the particles, with a drop in the extraction rate. The extraction rate is determined by two effects that occur simultaneously, convective in the fluid phase and diffusional in the solid phase.

III) Diffusion stage (DC – Diffusion Controlled):

When the solute is exhausted on the outside of the particle, mass transfer occurs only in the solute inside the particles, so that diffusion becomes the predominant mechanism.

Figure 5. The typical supercritical CO_2 extraction curve has three stages: constant extraction rate (CER), decreasing extraction rate (FER), and diffusional rate (DC).

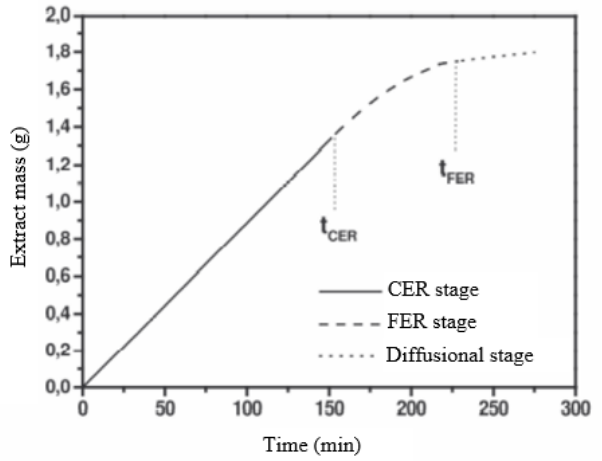

Source: Andrade, 2011.

Despite the few shortcomings of supercritical extraction, such as high equipment cost and low extraction rate, due to the high-pressure characteristics that make mechanical agitation difficult, there is the feasibility of combining SFE - CO_2 with another extraction technique to obtain higher yields in shorter extraction times or greater economic efficiency (DE MELO, SILVESTRE and SILVA, 2014; YANG, WANG and WEI, 2019).

2.3.2.3 Ultrasonic pretreatment in supercritical extraction

Ultrasound-assisted extraction and supercritical fluid extraction are some techniques that have attracted interest in recent years and are classified as emerging, innovative, and unconventional technologies as they meet the requirements of the green process concept. This concept aims to reduce extraction time, energy consumption, and

process temperature, thus preserving the integrity of thermosensitive compounds. In addition, it intensifies mass transfer and extraction yields and seeks to minimize/avoid the use of toxic organic solvents (DIAS *et al.*, 2021; BARBA *et al.*, 2019; KOUBA *et al.*, 2018).

Generally, in an SFE unit, the temperature, pressure, co-solvent, extraction bed size, and solvent flow rate, among other factors, can be changed to maximize a specific compound's extraction rate and yield. The SFE process capacity can be improved by using combined extraction techniques, such as ultrasonic waves (SANTOS, 2015; LIU *et al.*, 2020).

Combining high-pressure extraction processes with the propagation of ultrasound waves is an efficient way to intensify them. Due to the numerous advantages of this application before and during ultrasound-assisted extraction, a compilation of some works in the literature on the application of UAE+SFE for the extraction of compounds was carried out and presented in Table 2.

Table 2. Applications of supercritical extraction combined with ultrasound for the extraction of bioactive compounds.

Plant matrix	***Raw material***	***Extract***	***Advantages***	***Ref.***
Iberis amara	Seed	Monounsaturated fatty acids	Ultrasound improved oil yield and quality	Liu *et al.*, 2020
Salvia offiibalis L.	Aerial parts	Diterpenes, sesquiterpenes, and triterpenes	5% increase in diterpenes, 45% in sesquiterpenes, and 3.6 times higher triterpenes	Glisib *et al.*, 2011
Vitis vinifera L.	Bagasse	Polyphenols	High yield as well as antioxidant activity	Da Porto, Natolino, and Decorti, 2015
Scutellaria barbata D. Don	Plant	Flavonoids	Higher flavonoid yield under milder conditions	Yang, Wang, and Wei, 2019
Iberis amara	Seed	Cucurbitacin E.	Improved performance by 26.1%, as well as reduced operating time and amount of CO_2 consumed	Liu *et al.*, 2020
Passiflora edulis sp.	Seed and pulp	Fatty acids, tocopherol, and tocotrienol	Increased performance by up to 29% when compared to ESC without ultrasound	Barrales *et al.*, 2015
Zingiber Officinale Roscoe	Rhizomes	Gingerols	Yield of up to 30% at the end of extraction	Balachandran *et al.*, 2006

Source: Developed by the author, 2022.

As observed in Table 2, several studies in the literature present the use of the combination of UAE with SFE. The explanation for this is related to the effect of ultrasonic waves on the plant material, causing the rupture of cells and allowing the release of their contents into the extraction medium. The ease of access of the solvent to the interior of the plant cell provides intensification of mass transfer and better penetration of the solvent into the plant tissue (GLISIB *et al.*, 2011).

2.4 MATHEMATICAL MODELING

Mathematical models link theory with practice, leading to an understanding of the phenomena involved and the observed mechanism. In addition, they become an important tool, as they allow the evaluation of the system's performance in various operating conditions without having to perform them experimentally. This reduces the number of experiments and allows the prediction of the system's response in conditions that are difficult to reproduce (WEBER and SMITH, 1987).

2.4.1 Dynamic extraction of the SFE process

Mathematical models are considered powerful and useful tools in the design of supercritical fluid extraction processes. In this sense, several mathematical models have been proposed and developed in the literature to model of mass transfer for SFE from a solid matrix. These models describe the phenomena involved in the process and vary according to the particularities, assumptions, and adaptations of each one (LEILA, RATIBA, and MARZOUQI, 2022).

Most of the kinetic models used to represent the global extraction curve cited in the literature are classified into three types: empirical models, which have limited viability because they do not have physical meanings for the materials and processes studied; models based on balances in analogies with heat transfer; and differential mass balances. The latter is the most valuable model for representing the packed bed of solid substrates (HUANG, SHI, and JIANG, 2012; MELO, SILVESTRE, and SILVA, 2014).

The mass balance models proposed to characterize the mass transfer kinetics were developed based on the concept first introduced by Sovová (1994). All models consider that the particles are conditioned inside an extraction column (OLIVEIRA, SILVESTRE, and SILVA, 2011).

Most authors use simplifying assumptions in SFE modeling, such as isothermal operation, bed porosity, and negligible pressure drop in the extractor. Each author adopts

such assumptions to reduce the number of equations needed to describe the process and generate models with different mathematical expressions according to the assumptions adopted (OLIVEIRA, SILVESTRE, and SILVA, 2011). Some examples of mathematical models to describe ESC are described below.

Sovová (1994) developed the broken and intact cell (BIC) model, which involves grinding pre-treatment plant material to reduce particle size and partially disrupt cells. This process reduces the resistance to mass transfer for solute extraction, facilitating solute release and solvent flow through the packed bed. As a result, higher extraction rates and yields are obtained. In the BIC model, mass transfer in broken cells is carried out by convection, while in the inner core, it occurs by molecular diffusion.

Glueckauf (1955) simplified the general mass balance for a solid particle, obtaining the linear driving force model. In this model, the proposed assumption presents the mass transfer flux as proportional to the difference between the particle's average solute concentration and the solute concentration at equilibrium in the fluid phase.

The shrunken core model assumes that there is a boundary between the extracted and unextracted parts of the particle. When the solute is extracted, the boundary recedes until it reaches the center of the particle. Thus, the model describes a situation of irreversible desorption, followed by diffusion in the porous solid (OLIVEIRA, SILVESTRE, and SILVA, 2011; GOTO, ROY, and HIROSE, 1996).

Reverchon and Marrone (2001) implemented a model in which broken and intact cells transfer solute to the fluid with a parallel resistance mechanism. In addition, they determined the value of the fraction of broken cells by scanning electron microscopy.

Fiori et al (2009) proposed a combined model between the BIC model and the shrunken core model. In this model, it was assumed that a particle exists in N concentric layers, where, according to the BIC, the milling process breaks the cells, and each layer is depleted continuously, from the outer layer to the center of the particle, as described by the retractable core.

Despite the great achievements of models representing the extraction of solutes with supercritical fluid from plant matrices, efforts are still needed to develop modeling and scaling up of SFE-CO_2 extraction processes for various plant matrices.

2.3.2 COMSOL Multiphysics®

The Finite Element Method (FEM) can be used to solve the equations related to the model considered. The FEM is a numerical technique that allows obtaining

approximate solutions for differential equations that model related problems the engineering and physics. In this technique, the problem is defined by a geometry, which is subsequently subdivided into small regions (mesh). From each finite element, the unknown variables are approximated using known functions, which can be linear or of high polynomial orders (LIN, 2006).

There are several implementations of finite element (FE) in commercial software packages, for example, ABQUS, ANSYS, and COMSOL. These commercial packages offer several benefits, such as the availability of highly optimized standard libraries, visualization toolboxes, and an online community for problem-solving (SARKA, SINGH, and MISHRA, 2022).

Among the commercial FE implementation software available, COMSOL Multiphysics® is used to solve mathematical and engineering problems, as it offers simplifications and computational efficiency. In addition, it is easy to understand due to the following reasons (SARKA, SINGH, and MISHRA, 2022; SOLANKI, BARUAH, and TIWARI, 2022):

- COMSOL is used because of its highly intuitive and versatile user interface;
- It is computationally efficient and capable of solving large-scale complex problems with minimal computational resources;
- Allows the user to couple different physics involved in a given process;
- Many of the available customizations are useful for advanced users who want to implement new models;
- The graphical user interface (GUI) based implementation in COMSOL eliminates the requirement of coding skill for the user, i.e., no need to write codes, unlike other commercial software like ABAQUS and ANSYS;
- Solution-dependent variables can be defined and tracked using the GUI.

The implementation in COMSOL follows a procedure that involves three steps: pre-processing, processing, and post-processing. In pre-processing, the problem and domain are defined. In the second step (processing), finite elements are applied to solve the problem. Finally, in post-processing, the resolution of the results and graphical visualization are presented (ULIANA, 2016). As shown in Figure 6, these tasks are highlighted in the Model Builder in several sections, where different activities are performed in each task.

Figure 6. Pre-processing, processing and post-processing steps in COMSOL.

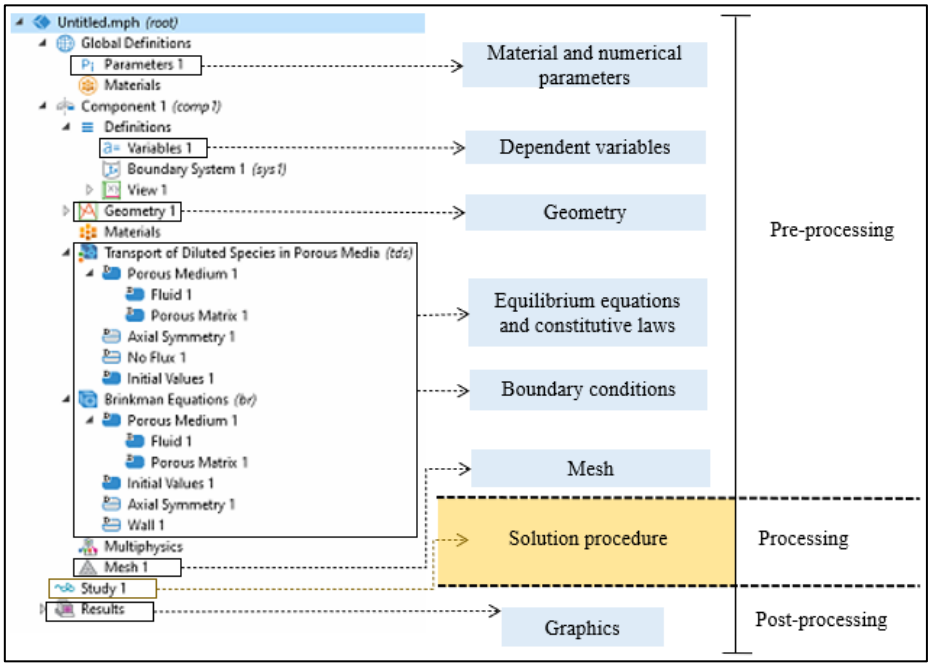

Source: Developed by the author, 2022.

As seen in Figure 6, in Model Builder, the following important points are (LIN, 2006; ANDERSON *et al.*, 2019):

- In COMSOL implementation, there is minimal user involvement in processing and post-processing tasks, saving time and effort;
- The general mathematical model is subdivided into non-overlapping components of simple “elements”, where these elements are connected by nodes;
- Allows you to solve several differential equations that describe the physics that act on the object through discretization of the object and numerical integration;
- Defining initial and boundary conditions is capable of resolving unknown variables at the nodes.

For a given number of elements in the mesh, the solutions are obtained approximately. The greater the number of elements, the more accurate the calculations will be; however, it requires greater computational demand to solve the equations involved in the model. In addition to requiring greater computational effort, it generates longer simulation time. Therefore, coarse meshes are faster to compute. At the same time, fine meshes present better approximations and high computing time costs (TRAMONTIN, 2020; ULIANE, 2016).

2.5 REFERENCES

ALBUQUERQUE, J.N. Plantas medicinais de uso popular. Brasília: ABEAS, p. 100, 1989.

AMORIM, J.M.; SOUZA, L.C.; SOUZA, R.A.L.; FILHA, R.S.; SILVA, J.O.; ARAÚJO, S.A.; TAGLITI, C.A; SIMÕES, A.C.; CASTILHO, R.O. Costus spiralis extract restores kidney function in cisplatin-induced nephrotoxicity model: Ethnopharmacological use, chemical and toxicological investigation. Journal of Ethnopharmacology, v.299, nº 5, 115510, 2022.

ANDERSON, E.; SOTTILDUPRAT, S.; SCHESKE, C. Design of an Improved Pyrolyzer to Support Biochar Research on MacDonald Campus, 2019.

ANDRADE, K. S. Avaliação das técnicas de extração e do potencial antioxidante dos extratos obtidos a partir de casca e de borra de café (*Coffea arábica* L.). Dissertação (Mestre em Engenharia de Alimentos). Departamento de Engenharia Química e Engenharia de Alimentos. Universidade Federal de Santa Catarina, Florianópolis - SC, 2011.

ARA, K.M.; KARAMI, M., RAOFIE, F. Application of response surface methodology for the optimization of supercritical carbon dioxide extraction and ultrasound-assisted extraction of *Capparis spinosa* seed oil**.** J. Supercrit. Fluids, nº 85, p. 173-182, 2014.

AZMIR, J.; ZAIDUL, I.S.M.; RAHMAN, M.M.; SHARIF, K.M.; MOHAMED, A.; SAHENA, F.; JAHURUL, M.H.A.; GHAFOOR, K.; NORULAINI, N.A.N.; OMAR, A.K.M. Techniques for extraction of bioactive compounds from plant materials: a review. Journal of Food Engineering, v. 117, nº 4, p. 426–436, 2013.

AZEVEDO, L.F.P.; FARIA, T.S.A.; PESSANHA, F.F.; ARAUJO, M.F.; LEMOS, G.C.S. Triagem fitoquímica e atividade antioxidante de Costus spicatus (Jacq.) S.w. Rev. Bras. PI. Med., Campinas, v.16, nº 2, p. 209-215, 2014.

BAJPAI, V.K., BAEK, K.H., KANG, S.C. Control of Salmonella in foods by using essential oils: a review. Food Res. Int. 45, p. 722–734, 2012.

BALACHANDRAN, S.; KENTISH, S.E.; MAWSON, R.; ASHOKKUMAR, M. Ultrasonic enhancement of the supercritical extraction from ginger, v. 13, nº 6, p. 471-479, 2006.

BATISTA, R. B. *et al.* Caracterização bioquímica e cinética de lipoxigenases de plantas de soja submetidas à aplicação de ácidos graxos poliinsaturados. Pesq. agropec. bras., Brasília, v. 37, nº 11, p. 1517-1524, 2002.

BAKKALI, F., AVERBECK, S., AVERBECK, D., IDAOMAR, M. Biological effects of essential oils – a review. Food Chem. Toxicol. n. 46, p. 446–475, 2008.

BARBA F.J., ROSELLÓ-SOTO E., MARSZAŁEK K., BURSAĆKOVAČEVIĆ D., REŽEKJAMBRAK A., LORENZO J.M., CHEMAT F., PUTNIK P. Green food processing: concepts, strategies, and tools. Green Food Process. Tech. p. 1–21, 2019.

BARRALES, F.M.; REZENDE, C.A.; MARTÍNEZ. J. Supercritical CO_2 extraction of passion fruit (Passiflora edulis sp.) seed oil assisted by ultrasound, J. Supercrit. Fluids, v. 104, p. 183-192, 2015.

BENELLI, P. Agregação de valor ao bagaço de laranja (Citrussinensis L. Osbeck) mediante obtenção de extratos bioativos através de diferentes técnicas de extração. Dissertação (mestrado), Centro Tecnológico. Programa de Pós-Graduação em Engenharia de Alimentos, Universidade Federal de Santa Catarina, Florianópolis – SC, 2010.

BIMAKR, M. *et al.* Comparison of different extraction methods for the extraction of major bioactive flavonoid compounds from spearmint (*Mentha spicata* L.) leaves. Food and Bioproducts Processing**,** n. 1, v. 89, p. 67–72, 2011.

BISCAIA, D. Comparação entre tecnologia supercrítica e técnicas convencionais de extração para obtenção de extratos de própolis avaliados através de suas atividades biológicas. Dissertação (Mestrado em Engenharia de Alimentos), Departamento de Engenharia Química e Engenharia de Alimentos, Universidade Federal de Santa Catarina, Florianópolis – SC, 2007.

BITENCOURT, A. P. R., ALMEIDA, S. S. M. S. Estudo fitoquímico, toxicológico e microbiológico das folhas de Costus spicatus Jacq. Biota Amazônia, nº 4, v. 4, p. 75-79, 2014.

BOORHEM, R.L. *et al.* Segredos e virtudes das plantas medicinais. Rio de Janeiro: Reader'sDigest Brasil Ltda, p.416, 1999.

BORRÁS, M.R.L. Plantas da Amazônia: medicinais ou mágicas - Plantas comercializadas no mercado Adolpho Lisboa. Manaus: Valer, p. 322, 2003.

BORGES, P. M. O. Avaliação da atividade tóxica e do perfil fitoquímico de Costusspicatus e Jatrophamultifica. Trabalho de conclusão do curso (Licenciatura em Química), Coordenação de Química, Instituto Federal de Educação, Ciência e Tecnologia de Goiás, Anápolis, 2016.

Brazil. Ministry of Health. Secretariat of Science, Technology and Strategic Inputs. Department of Pharmaceutical Assistance and Strategic Inputs. National Policy of Medicinal Plants and Herbal Medicines, v. 189, Ministry of Health, Brasilia, 2016.

BRUNNER, G. Gas extraction: An introduction to fundamentals supercritical fluid sand the application to separation processes. New York: Springer, 1994.

BRUNNER, G. Supercritical fluids: technology and application to food processing. Journal of Food Engineering, v. 67, p. 21-33, 2005.

BRUNING, M. C. R.; MOSEGUI, G. B. G. VIANNA, C. M. de M. A utilização da fitoterapia e de plantas medicinais em unidades básicas de saúde nos municípios de Cascavel e Foz do Iguaçu – Paraná: a visão dos profissionais de saúde. Revista Ciência e Saúde Coletiva – OPINIÃO, p. 2675 – 2685, 2012.

CARRERA, C. *et al.* Analytica Chimica Acta Ultrasound assisted extraction of phenolic compounds from grapes. Analytica Chimica Acta**,** v. 732, p. 100–104, 2012.

CALDER, P.C.; CARR, A.C.; GOMBART, A.F.; EGGERSDORFER, M. Optimal nutritional status for a well-functioning immune system is an important factor to protect against viral infections. Nutrients, v.12, p. 1181, 2020.

CALDER, P.C.; ADOLPH, M.; DEUTZ, N.E.; GRAU, T.; INNES, J.K.; KLEK, S.; LEV, S.; MAYER, K.; MICHAEL-TITUS, A.T.; PRADELLI, L.; PUDER, M.; VLAARDINGERBROEK, H.; SINGER, P. Lipids in the intensive care unit: recommendations from the ESPEN expert group. Clin. Nutr, v. 37, p. 1-18, 2018.

CHEMAT, F. *et al.* Ultrasound assisted extraction of food and natural products. Mechanisms, techniques, combinations, protocols and applications. A review. Ultrasonics Sonochemistry, v. 34, p. 540–560, 2017.

CHEN, F. YANG, X. MA, Y. WANG, X. LUO, D. YANG, L. YANG, Y. Synthesis and application of novel silver magnetic amino silicone adhesive particles for preparation of high purity α-linolenic acid from tree peony seed oil under applied magnetic field. Journal of Chromatography A, v.1610, p.460-540, 2020.

COELHO, F.C.; TIRLONI, C.A.S.; MARQUES, A.A.M.; GASPAROTTO, F.M.; LÍVERO, F.A.R.; A. Gasparotto Junior. Traditional plants used by remaining healers from the region of Grande Dourados, Mato Grosso do Sul, Brazil. J. Relig. Health, nº 58, p. 572-588, 2019.

CRUZ, P. N. Extração e encapsulação supercrítica de extratos de folhas e flores de yacon (*Smallanthus sonchifolius*). Tese (Doutorado em Engenharia de Alimentos), Pós graduação em Engenharia de Alimentos, Universidade Federal do Paraná, Curitiba, 2019.

DA PORTO, C.; NATOLINO, A.; DECORTI, D. The combined extraction of polyphenols from grape marc: Ultrasound assisted extraction followed by supercritical CO_2 extraction of ultrasound-raffinate. LWT - Food Science and Technology, v. 61, nº 1, p. 98-104, 2015.

DASSOFF, E.; LI, Y. Mechanisms and effects of ultrasound-assisted supercritical CO_2 extraction. Trends in Food Science & Technology, v. 86, p. 492-501, 2019.

DE MELO, M.M.R.; SILVESTRE, A.J.D.; SILVA, C.M. Supercritical fluid extraction of vegetable matrices: applications, trends and future perspectives of a convincing green technology**.** J. Supercrit. Fluids, nº 92, p. 115-176, 2014.

DE SOUZA, A.M.; LARA, L.D.; PREVIATO, J.O.; LOPES, A.G.; CARUSO-NEVES, C.; DA SILVA, B.P.; PARENTE, J.P. Modulation of sodium pumps by steroidal saponins. Zeitschrift Fur Naturforschung C - A Journal of Biosciences, v.59, p.432-436, 2004.

DEVENDRAN, G.; SIVAMANI, G. Phytochemical analysis of leaf extract of plant *Costus spicatus* by gcms method. J. Drug Deliv. Therapeut., v. 5, nº 4, p. 24-26, 2015.

DIAS, A.L.B.; AGUIAR, A.C.; ROSTAGNO, M.A. Extraction of natural products using supercritical fluids and pressurized liquids assisted by ultrasound: Current status and trends. Ultrasonics sono chermistry, 105584, 2021.

DIAS, J.L. Extração supercrítica e técnicas convencionais de extração na obtenção de compostos bioativos da semente de umbu (*Spondias tuberosa*). Dissertação (Mestre em Engenharia Química). Programa de pós-graduação em Engenharia Química, Universidade Federal de Santa Catarina, Florianópolis, 2017.

EDVARDSSON, V.O.; INDRIDASON, O.S.; HARALDSSON, G.; KJARTANSSON, O.; PALSSON, R. Temporal trends in the incidence of kidney stone disease. Kidney Int., 83, p. 146-152, 2013.

FERRO, D.M.; MAZZUTTI, S.; CARMEN, L.V.; MULLER, M.O.; FERREIRA, S.R.S. Integrated extraction approach to increase the recovery of antioxidant compounds from Sida rhombifolia leaves. The Journal of Supercritical Fluids, v. 149, p. 10-19, 2019.

FIORI, L.; BASSO, D.; COSTA, P. Supercritical extraction kinetics of seed oil: a new model bridging the "broken and intact cells" and the "shrinking-core" models. J. Supercrit. Fluids, nº 48, p. 131-138, 2009.

GLUECKAUF. E. Theory of chromatography. Part 10. Formulae for diffusion into spheres and their application to chromatography. Trans. Faraday Soc., nº 51, p. 1540-1551, 1955.

GLISIB, S.B.; RISTIC, M.; SKALA, D.U. The combined extraction of sage (*Salvia officinalis* L.): Ultrasound followed by supercritical CO_2 extraction. Ultrasonics Sonochemistry, v.18, nº1, p. 318-326, 2011.

GOC, A.; NIEDZWIECKI, A.; RATH, M. Polyunsaturated omega-3 fatty acids inhibit ACE2-controlled SARS-CoV-2 binding and cellular entry. Sci. Rep., v.11, p. 5207, 2021.

GOTO, M.; ROY, B.C.; HIROSE, T. J. Supercrit. Fluids, nº 9, p. 128, 1996.

GUO, Y.R.; CAO, Q.D.; HONG, Z.S.; TAN, Y.Y.; CHEN, S.D.; JIN, H.J.; SEN TAN, K.; WANG, D.Y.; YAN, Y. The origin, transmission and clinical therapies on coronavirus disease 2019 (COVID-19) outbreak- A n update on the status. Mil. Med. Res., v. 7, p. 1-10, 2020.

HUANG, Z.; SHI, X.H.; JIANG, W.J. Theoretical models for supercritical fluid extraction. Journal of Chromatography A, v. 1250, p. 2-26, 2012.

KOUBA, A. M., MHEMDI, H., FAGES, J. Recovery of valuable component sandin activating microorganisms in the agro-food industry with ultrasound-assisted supercritical fluid technology. J. Supercrit. Fluids. v.134, p.71–79, 2018.

LAURININO, T. N. S. Avaliação do potencial do extrato e do óleo essencial de Palo santo (*Bursera graveolens*) para aplicação em produtos inseticidas. Dissertação (mestrado), Programa de Pós-Graduação em Engenharia Química, Universidade Federal de Santa Catarina, Florianópolis - SC, 2017.

LAURININO, T. K. S. Avaliação de compostos bioativos e potencial antioxidante da folha e caule da cana do brejo (*Costus spicatus*) diferentes métodos de extração. Dissertação (mestrado), Programa de Pós-Graduação em Engenharia Química, Universidade Federal de Santa Catarina, Florianópolis - SC, 2020.

LEIGHTON.T. Acoustic Bubble. Academic Press, London, 1994.

LEILA, M.; RATIBA, D.; MARZOUQI, A. Experimental and mathematical modelling data of green process of essential oil extraction: Supercritical CO_2 extraction. Materials today: proceedings. v.49, p. 1023-1029, 2022.

LEITE, J. P. V. Fitoterapia: Bases científicas e tecnológicas. São Paulo: Atheneu, p. 328, 2009.

LIMA, S.V.M. Simulação numérica do escoamento reativo no reator fluhelik: investigação da degradação fotocatalítica da oxitetraciclina. Dissertação (mestrado), Centro Tecnológico. Programa de Pós-Graduação em Engenharia Química, Universidade Federal de Santa Catarina, Florianópolis – SC, 2020.

LIN, L. Introduction to the Finite Element Method. Berkeley University. Berkeley, 2006. U.S, >. Retrieved from: https://lwlin.me.berkeley.edu/me128/FEMNotes.pdf

LIU, X.; OU, H.; XIANG, Z.; GREGERSEN, H. Ultrasound pretreatment combined with supercritical CO_2 extraction of Iberis amara seed oil. Journal of Applied Research on Medicinal and Aromatic Plants, v. 18, 100265, 2020.

LORENZI, H.; MATOS, F. J. A. Plantas Medicinais no Brasil: nativas e exóticas. Nova Odessa, SP: Instituto Plantarum, Edição 2, p. 222. 2002.

LUQUE DE CASTRO, M. D.; PRIEGO-CAPOTE, F. Soxhlet extraction: Pastand presente panacea. Journal of Chromatography A**,** v. 1217, n. 16, p. 2383–2389, 16 abr. 2010.

MADHAVAN, S.A.; SENTHILKUMAR, S.; ANDREWS, S.; GANESAN, S. Anti-diabetic effect of ethanol extract of *Costus spicatus* jacq. In rhizome extract in streptozotocin-induced diabetic rats –histological study. J. Drug Deliv. Therapeut., v. 9, nº 4, p. 483-487, 2019.

MANFRED, L. 7000 Recetas Botnicas a Base de 1,300 Plamtas Medicinales Americanas. Buenos Aires: Editorial Kier, 1947.

MCQUEEN, DH. Ultrasonics, nº 28, p. 422, 1990.

MELO, M. M. R.; SILVESTRE, A. J. D.; SILVA, C. M. Supercritical fluid extraction of vegetable matrices: Applications, trends and future perspectives of a convincing green technology. The Journal of Supercritical Fluids, v. 92, p. 115–176, 2014.

MOE, O.W. Kidney stones: pathophysiology and medical management. Lancet, 367, p. 333-344, 2006.

MORENO, K. G. T., JUNIOR, A. G., DOS SANTOS, A. C., PALOZI, R. A. C., GUARNIER, L. P., MARQUES, A. A. M., & DE BARROS, M. E. Nephroprotective and antilithiatic activities of Costus spicatus (Jacq.) Sw.: Ethnopharmacological investigation of a species from the Dourados region, Mato Grosso do Sul State, Brazil. Journal of Ethnopharmacology, v. 266, 113409, 2021.

MOYLER, D. A. Extraction of essential oils with carbon dioxide. Flavour and fragrance journal, v. 8, p. 235-247, 1993.

OLIVEIRA, G. C. Plantas medicinais utilizadas em comunidades rurais do município de Alagoa Nova – PB. Trabalho de conclusão de curso (graduação em biologia), Universidade Estadual da Paraíba, Centro de Ciências Biológicas e da Saúde, Campina Grande, 2012.

OLIVEIRA, E.L.G.; SILVESTRE, A.J.D.; SILVA, C.M. Review of kinetic models for supercritical fluid extraction. Chemical Engineering Research and Design, v. 89, nº 7, p. 1104-1117, 2011.

PAES, L.S.; MEDONÇA, M.S.; CASAS, L.L. Aspectos Estruturais e Fitoquímicos de partes vegetativas de Costus spicatus (Jacq.) Sw. (Costaceae). Rev. bras. Plantas med, v. 15, nº 3, 2013.

PEDROSA, D. M. Análise de perfil químico e investigação dos potenciais antioxidantes, antibacteriano e citotóxico in vitro de extratos obtidos do caule de Costus spicatusSwartz (Costaceae). Trabalho de conclusão de curso (grau de Farmacêutico), Faculdade de Farmácia da Universidade Federal de Juiz de Fora, Juiz de Fora, 2017.

PEREIRA, C. G.; MEIRELES, M. A. A. Supercritical Fluid Extraction of Bioactive Compounds: Fundamentals, Applications and Economic Perspectives. Food and Bioprocess Technology, v. 3, n. 3, p. 340–372, 2010.

PICANÇO, L.C.S.; BITTENCOURT, J.A.H.M.; HENRIQUES, S.V.C.; SILVA, J.S.; OLIVEIRA, J.M.S.; RIBEIRO, J.R.; SANJAY, A.-B.; CARVALHO, J.C.T.; STIEN, D.; SILVA, J.O. Pharmacological activity of *Costus spicatus* in experimental Bothrops atrox envenomation. Pharm. Biol., 54, p. 2103-2110, 2016.

PICÓ, Y. Ultrasound-assisted extraction for food and environmental samples. TrAC - Trends in Analytical Chemistry, v. 43, p. 84–99, 2013.

PIES, G. Tecnologia supercrítica aplicada à obtenção de extratos ricos em compostos fenólicos a partir de casca de jabuticaba Pliniatrunci flora (O. Berg) Kausel. Dissertação (Mestre em Engenharia de alimentos), Programa de pós-graduação em Engenharia de Alimentos, Universidade Federal de Santa Catarina, Florianópolis-SC, 2017.

PINNA, F.L. *et al.* Prospecção fitoquímica e avaliação da atividade cicatrizante do spray a base de *Costus spicatus* Jacq. In: Reunião anual da sociedade brasileira de química, v.31, 2008.

QUINTANS JÚNIOR, L.J; SANTANA, M.T.; MELO, M.S.; SOUSA, D.P.I.; SANTOS, S.; SIQUEIRA, R.S.; LIMA, T.C.; SILVEIRA, G.O.; ANTONIOLLI, A.R.; RIBEIRO, L.A.A.; SANTOS, M.R.V. Antinociceptive and anti-inflammatory effects of *Costus spicatus* in experimental animals**.** Pharm. Biol., 48, p. 1097-1102, 2010.

RAHMANIAN, N.; JAFARI, S.M.; WANI, T.A. Bioactive profile, dehydration, extraction and application of the bioactive components of olive leaves. Trends Food Sci. Technol., nº 42, p. 150-172, 2015.

REVERCHON, E.; MARRONE, C. Modeling and simulation of the supercritical CO_2 extraction of vegetable oils. J. Supercrit. Fluids, nº 19, p. 161-175, 2001.

RUDKE, A.R. Obtenção de extratos de resíduos de buriti (*Mauritia Flexuosa* L.*)* por diferentes técnicas de extração e avaliação do seu potencial antioxidante. Dissertação (Mestre em Engenharia de Alimentos). Programa de pós-graduação em Engenharia de Alimentos, Universidade Federal de Santa Catarina, Florianópolis, 2019.

SANTANA, H. S. *et al.* Computational methodology for the development of microdevices and microreactors with ANSYS CFX. Methods X, v. 7, p. 82–103, 2020.

SANTESTEVAN, V. A. Desenvolvimento de metodologia para a análise de óleo de arroz. Dissertação (Mestre em Química), Programa de Pós-Graduação em Química, Universidade Federal do Rio Grande do Sul, Porto Alegre, 2011.

SANTOS, P.; AGUIAR, A.C.; BARBERO, G.F.; REZENDE, A.A.; MARTÍNEZ, J. Supercritical carbon dioxide extraction of capsaicinoids from malagueta pepper (*Capsicum frutescens* L.) assisted by ultrasound. Ultrasonics Sonochemistry, v.22, p. 78-88, 2015.

SARTOR, R. B. Modelagem, Simulação e Otimização de uma Unidade Industrial de Extração de Óleos Essenciais por Arraste a Vapor. Dissertação (Mestrado em Pesquisa e Desenvolvimento de Processos). Escola de Engenharia, Universidade Federal do Rio Grande do Sul. Porto Alegre, 2009.

SARKAR, S.; SINGH, I.V.; MISHRA, B.K. A simple and efficient implementation of localizing gradient damage method in COMSOL for fracture simulation. Engineering Fracture Mechanics, v. 269, 108552, 2022.

SERRA, A. T. *et al.* Processing cherries (*Prunus avium*) using supercritical fluid technology. Part 1: Recovery of extract fractions rich in bioactive compounds. The Journal of Supercritical Fluids, v. 55, n. 1, p. 184–191, 2010.

SHARMA, S.; CHHIBBER, S.; MOHAN, H.; SHARMA, S. Dietary supplementation with omega-3 polyunsaturated fatty acids ameliorates acute pneumonia induced by Klebsiella pneumoniae in BALB/c mice. Can. J. Microbiol., v. 59, p. 503-510, 2013.

SILVA, D. N.; GONÇALVES, M.J.; AMORAL, M.T.; BATISTA, M.T. Antifungal activity of a flavonoid-rich fraction from *Costus spicatus* leaves against dermatophytes. Planta Medica, v.74, n.9, p.961-961, 2008.

SILVA, B.P. *et al.* Flavonol glycosides from *Costus spicatus.* Phytochemistry, v.53, nº1, p.87-92, 2000.

SIMÕES, C. M. O.; SPITZER, V. Óleos voláteis. In: SIMÕES, C.M.O *et al.* Farmacognosia: da planta ao medicamento. 5. ed. Porto Alegre/Florianópolis: Editora UFRGS/ Editora UFSC, 2003.

SOLANKI, S.; BARUAH, B.; TIWARI, P. Modeling and simulation of wood pyrolysis process using COMSOL Multiphysics. Bioresource Technology Reports, v. 17, 100941, 2022.

SOUZA, D.R; RODRIGUES, E. C. A. M. S. Plantas medicinais: indicação de raizeiros para o tratamento de feridas. Revista Brasileira em Promoção da Saúde, v. 29, nº 2, p. 198-203, Fortaleza, 2016.

SOUZA, S.P.; PEREIRA, L.L.S.; SOUZA, A.A.; SANTOS, C.D. Seleção de extratos brutos de plantas com atividade antiobesidade. Rev. Bras. Plantas Med., 14, p. 643-648, 2012.

SOVOVÁ, H. Rate of the vegetable oil extraction with supercritical CO_2. I. Modelling of extraction curves. Chem. Eng. Sci., nº 49, p. 409-414, 1994.

SUFLUX. Supercritical plant. Disponível em:http://www.suflux.com. Acesso em: 12 agosto. 2021.

TRAMONTIN, D.P. Extração de compostos bioativos de sementes de *Artocarpus heterophyllus*: experimentação e modelagem matemática. Tese (Doutorado em Engenharia Química). Programa de pós-graduação em Engenharia Química, Universidade Federal de Santa Catarina, Florianópolis, 2020.

ULIANA, N. R. Polimento de biodiesel mediante contato com particulados ativos. Tese (doutorado), Programa de Pós-Graduação em Engenharia Química, Universidade Federal de Santa Catarina, Florianópolis - SC, 2016.

ULIANA, M. P.; DA SILVA, A. G.; FRONZA, M. SCHDRER, R. In vitro antioxidant and antimicrobial activities of Costus spicatus swartz usede in folk medicine for urinary tract infection in Brazil. Latin American Journal of Pharmacy, v. 34, n.4, p. 766-72, 2015.

VIDOVIC, S.; ZEKOVIC, Z.; MAROSANOVIC, B.; TODOROVIC, J.V. Influence of pre-treatments on yield, chemical composition and antioxidant activity of Satureja montana extracts obtained by supercritical carbon dioxide. The jornal of supercritical fluids, v. 95, p. 468-473, 2014.

VIERA, V. B. Compostos bioativos, atividade antoxidante e antimicrobiana na casca de cebola roxa (Allium cepa L.) submetidos a diferentes métodos de extração. Tese de doutorado. Programa de pós-graduação em ciência e tecnologia dos alimentos, Universidade Federal de Santa Maria, 2016.

WANG, L.; WELLER, C. L. Recentadvances in extraction of nutraceuticals from plants. Trends in Food Science & Technology, v. 17, n. 6, p. 300–312, 2006.

WEBER, JR., W. J., SMITH, E.H. Simulation and design models for adsorption processes. Environmental Science & Technology, v. 21, p. 1050- 1096, 1987.

WEILL, P.; PLISSONNEAU, C.; LEGRAND, P.; RIOUX, V.; THIBAULT, R. May omega-3 fatty acid dietary supplementation help reduce severe complications in Covid-19 patients? J. Biochi., v. 179, p. 275-280, 2020.

YANG, Y. C.; WAN, C.S.; WEI, M.C. Kinetics and mass transfer considerations for an ultrasound-assisted supercritical CO_2 procedure to produce extracts enriched in flavonoids from Scutellaria barbata. Journal of CO_2 Utilization, v. 32, p. 219-231, 2019.

YANG, Y.C.; WEI, M.C. A combined procedure of ultrasound-assisted and supercritical carbon dioxide for extraction and quantitation olean oil candursolic acids from *Hedyotis corymbosa*. Ind. Crops Prod., nº 79, p. 7-17, 2016.

YANG, C.P.; CHANG, C.M.; YANG, C.C.; PARIANTE, C.M.; SU, K.P. Long COVID and long chain fatty acids (LCFAs): Psychoneuroimmunity implication of omega-3 LCFAs in delayed consequences of COVID-19. Brain, Behavior, and Immunity, v.103, p.19-27, 2022.

ZHONG, Y.; CATHELINE, D.; HOUEIJEH, A.; SHARMA, D.; DU, L.; BESENGEZ, C.; DERUELLE, P.; LEGRAND, P.; STORME, L. Maternal omega-3 PUFA supplementation prevents hyperoxia-induced pulmonary hypertension in the offspring. Am. J. Physiol. Cell. Mol. Physiol., v. 315, p. 116-132, 2018.

CHAPTER III - EVALUATION OF THE YIELD AND CHEMICAL COMPOSITION OF LOW AND HIGH-PRESSURE EXTRACTS OF *COSTUS SPICATUS* LEAVES.

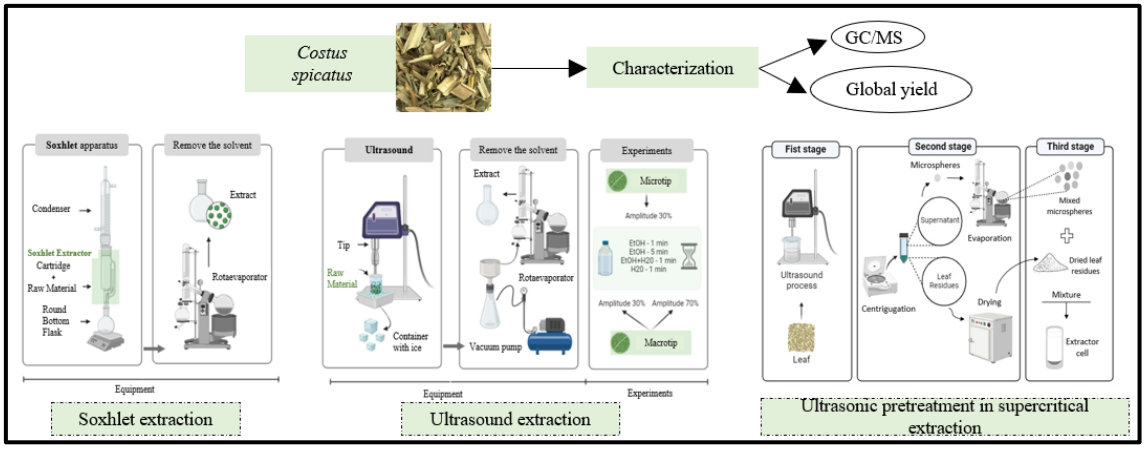

ABSTRACT

The negative impact of infectious diseases, such as COVID-19, has raised concerns in the general population due to the severe symptoms that can lead to systemic inflammation and multiple organ failure. Researchers suggest that diets rich in linolenic acid (ALA), a precursor of omega-3, can help prevent these diseases. In this context, the plant *Costus spicatus* is a natural source of this essential fatty acid. The study aimed to extract bioactive compounds from the leaves of *C. spicatus* using different methods: maceration (MAC), Soxhlet (SOX), ultrasound (UAE), supercritical extraction (SFE), and the UAE+SFE combination, to evaluate the yield and chemical profile by gas chromatography coupled to a mass spectrometer (GC/MS). The extractions were performed with solvents such as ethanol, water, and ethanol: water (50% v/v). In UAE, different conditions were evaluated, involving variations in parameters such as tip, amplitude, time, and solvent. The best yield was obtained with ethanol: water, with values of 7.25%, 18.74%, 9.29%, and 10.12% for MAC, SOX, UAE, and UAE+SFE, respectively. In UAE, the highest yield was 8.59% under macro tip conditions, 70% amplitude, and 1 min extraction. The chemical composition varied according to the solvent, with ethanol revealing more identified compounds. The UAE+SFE combination increased the yield and the selectivity of ALA, reaching 29.34% compared to other techniques. Thus, ALA extracted from *C. spicatus* by these techniques may be a potential candidate for preventing infectious diseases, such as COVID-19.

Keywords

Costus spicatus; Supercritical extraction; Ultrasound; Bioactive compounds; COVID-19; Supercritical carbon dioxide

3.1 INTRODUCTION

The negative impact of infectious diseases, such as COVID-19, has raised concerns among the general population, as it presents complicated symptoms that lead to systematic inflammation and multiple organ failure. Researchers have shown that diets rich in linolenic acid (ALA), a precursor of omega-3, can be useful in preventing these infectious diseases, as it has an anti-inflammatory effect and acts on the immune system (GUO *et al.*, 2020; CALDER *et al.*, 2018). In this context, medicinal plants, such as *Costus spicatus*, become an alternative natural source for isolating this essential fatty acid, which a wide variety of techniques can obtain.

Costus spicatus, from the Costaceae family, is widely found in Brazil, especially in the Atlantic Forest and the Amazon region. Known as cana do brejo, cana de macaco, and cana do mato, it is used in folk medicine to treat colds, sore throats, diarrhea, and kidney stones. In addition, it is used in gardening and producing cut flowers. Studies on the aerial parts of this plant have revealed that its extracts contain compounds with antifungal and anti-inflammatory properties (AZEVEDO *et al.*, 2014; BITENCOURT and ALMEIDA, 2014; BORGES, 2016).

The natural extract is a complex mixture of secondary metabolites protecting plants against biotic and abiotic stresses. Its main components are of terpenic origin, such as monoterpenes and sesquiterpenes, but aromatic compounds are also found in the extracts. The content and type of these components differ substantially based on the separation method applied, subsequently affecting the medicinal and nutritional application (BAJPAI *et al.*, 2012; BAKKALI *et al.*, 2018).

To isolate plant extracts, low-pressure techniques such as ultrasound (UAE), microwave, maceration (MAC), hydrodistillation, and Soxhlet (SOX), or high-pressure techniques such as supercritical extraction (SFE) and pressurized liquid extraction can be used. Low-pressure methods consume more time and energy, while those using high temperatures can alter the chemical composition of the extracts. SFE overcomes these limitations by being environmentally friendly and selective and producing solvent-free extracts. The fluid typically used is CO_2, which is safe, non-toxic, and non-flammable (CHEN *et al.*, 2020; DIAS *et al.*, 2021).

Applying pretreatment techniques, such as ultrasound-assisted extraction, can improve performance compared to isolated techniques. UAE, which uses ultrasonic waves to promote cavitation and facilitate solvent penetration, can be an effective

preliminary treatment for processes such as supercritical fluid extraction (DA PORTO *et al.*, 2015). Combining UAE with SFE extraction offers significant advantages, increasing the yield and content of desirable compounds in the extracts (VIDOVIC *et al.*, 2014; LIU *et al.*, 2020).

No research has been reported on ultrasound pretreatment followed by SFE of active constituents from leaves of cana do brejo (*C. spicatus*). This study fills this gap and represents the sequential use of the efficacy of ultrasound-assisted pretreatment for the extraction of compounds, mainly linolenic acid, in order to observe the influence on yield and chemical composition.

3.2 MATERIAL AND METHODS

3.2.1 Raw material preparation

The leaves and stems of *C. spicatus* were purchased from Comercial Charoma (Piraquara, PR, Brazil). The leaves were manually separated from the stems and dried in an oven with forced air circulation (CE 220/2016, Cienlab, Campinas, SP, Brazil) at 35 °C for 24 h. They were then ground in a coffee grinder (MDR302, Cadence, Balneário Piçarras, SC, Brazil). Particle characterization was performed by granulometric classification in a Tyler Standard sieve (A bronzinox, São Paulo, SP, Brazil) using a 45-mesh sieve (355 µm), according to preliminary tests by Laurintino (2020). To preserve the stability of the bioactive compounds, the sample was packaged and stored in a freezer at -18 °C (BRM39, Brastemp, São Bernardo do Campo, SP, Brazil) until extraction.

3.2.2 Extractions

3.2.2.1 Low-pressure Extraction (LPE)

Maceration extraction (MAC) was performed according Mazzutti *et al.* (2012), using a sample:solvent ratio of 1:4 w/v for 168 h with daily manual stirring at room temperature (25 °C).

Soxhlet extraction (SOX) was performed according to method 920.39 of AOAC Official Methods (2005). Figure 7A shows the apparatus used for Soxhlet extraction. The procedure involved recycling 150 mL of solvent in 5 g of raw material in a Soxhlet apparatus. The system was heated to the solvent's boiling point, and reflux was

maintained for 5 h. After extraction, the extracts were rotary evaporated to eliminate the solvent present in the balloons and determine the yield of the extract obtained.

Figure 7. (A) Apparatus used for extraction via Soxhlet e (B) Experiments performed on tip ultrasound.

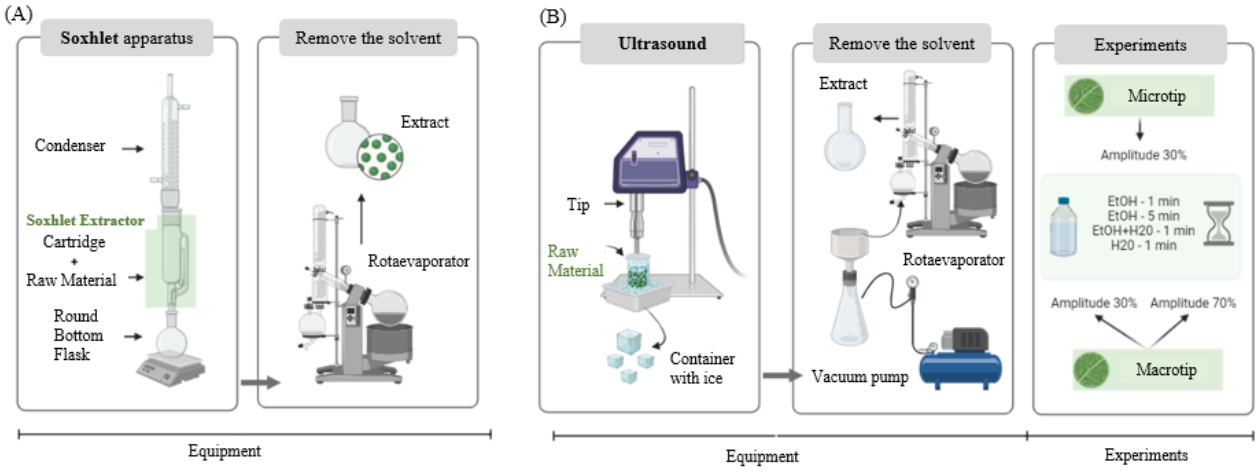

Source: Developed by the author, 2022.

As shown in Figure 7B, the ultrasound-assisted extractions (UAE) experiments were performed according to the method adapted from Luque-García and Luque De Castro (2003). Approximately 1 g of the sample was mixed with 30 mL of solvent and subjected to an ultrasonic probe (DES5000, Unique, São Paulo, SP, Brazil) for 5 minutes at a frequency of 20 kHz. Both the macrotip, with amplitudes of 30% and 70% (maximum power of 500 W), and the microtip, with amplitude of 30%, were used. The sample was vacuum-filtered and subjected to rotary evaporation to eliminate the solvent. The extraction kinetics were performed under macrotip conditions, amplitude of 70% and ethanol solvent, varying the extraction time from 0.5, 1, 2, 3 and 4 min to study the effect of this parameter on the extraction process.

The MAC extraction used the solvents hexane (HEX), ethanol (EtOH), and a mixture of ethanol: water (EtOH: H_2O) in a proportion of 50% v/v. For the SOX and UAE methods, ethanol (EtOH), ethanol: water (EtOH: H_2O) (50% v/v), and water (H_2O) were used, with solvent polarity indices of 5.2, 7.1, and 9.0, respectively. The solvent polarity index for aqueous solution was calculated by (IA/100 x PA) + (IB/100 x PB), where IA and IB are polarity indices of solvent A and B, respectively, PA and PB are the percentages of solvents A and B, respectively (RITCHIE, 2000; MAZZUTI *et al.*, 2017).

3.2.2.2 Supercritical Fluid Extraction (SFE)

High-pressure extraction was performed in a supercritical chromatography and extraction unit (LC 2000, Jasco, Hachioji, Tokyo, Japan). The extraction conditions were kept constant, including pressure, temperature, and volumetric flow rate of solvent (CO_2) and cosolvent (EtOH). CO_2 from a cylinder passed through a cooling system at −10 °C (FL-1201, Julabo, Seelbach, Baden-Württemberg, Germany) and was pressurized by an HPLC pump (PU-2087/2087 Plus, Jasco, Hachioji, Tokyo, Japan) at a constant flow rate. The cosolvent ethanol (EtOH) was added in mass fractions relative to CO_2, pumped by a positive displacement HPLC pump (PU-2087/2087 Plus, Jasco, Hachioji, Tokyo, Japan), and mixed with the supercritical CO_2 before entering the extraction cell.

Due to the low apparent density of the raw material and the small volume of the extraction column, approximately 1.4 g of leaves were added to the column (127.5 mm in length x 10 mm in diameter and internal volume of 10 cm^3), forming a fixed bed, with an extraction time of 120 min. The volumetric flow rate of CO_2 was kept constant at 3 mL/min. CO_2 (99.99%, White Martins, Florianópolis, SC, Brazil) was the solvent, while ethanol (99.99%, Metaquímica, Jaraguá do Sul, SC, Brazil) acted as the cosolvent. The SFE operating conditions were established based on preliminary experiments by Laurintino *et al.* (2020), which indicated that the condition of 50 °C/14 MPa/10% EtOH favored the extraction of the major compound. The extracts were collected in an offline collection system, or "trapping", where the solute precipitation occurred by depressurization to atmospheric pressure (Taylor, 1996). The extract was filtered and stored in a freezer at -18 °C (BRM39, Brastemp, São Bernardo do Campo, SP, Brazil) until analysis.

3.2.2.3 Ultrasound pretreatment (UAE + SFE)

UAE+SFE extraction was performed as described by Liu *et al.* (2020). As shown in Figure 8, the process consisted of three steps: in the first, ultrasound-assisted extractions (UAE) followed the method adapted from Luque-García and Luque De Castro (2003). After ultrasonic treatment, the phases were separated by centrifugation at 3,000 rpm for 5 min in the second step. The leaf residue was dried at 40 °C for 24 h. The supernatant, containing 2 g of hollow glass microspheres (VS5500, 3M, Minnesota, USA), was evaporated in a rotary vacuum evaporator (RE100-Pro, Scilogex, USA),

resulting in microspheres coated with the crude extract. Finally, in the third step, the dried residue and microspheres were mixed and placed in the SFE chamber for re-extraction.

Figure 8. Schematic diagram of ultrasound pretreatment of *C. spicatus* leafs.

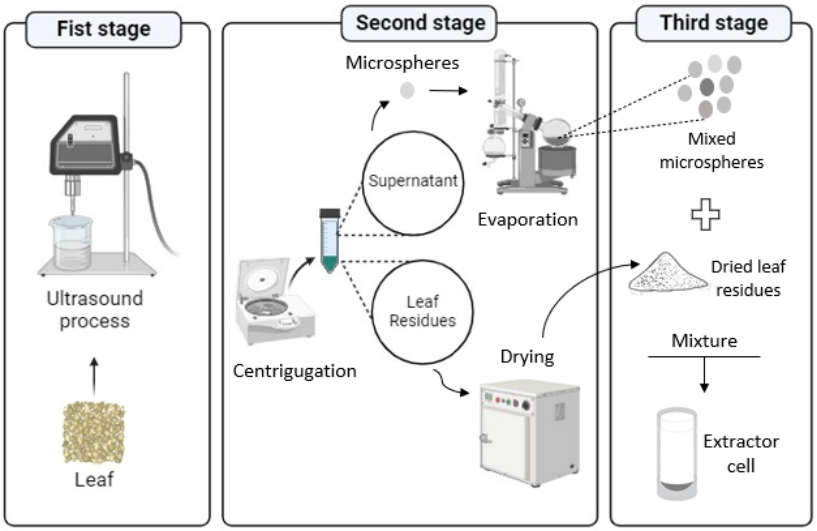

Source: Developed by the author, 2022.

The UAE + SFE was performed using the solvents ethanol (EtOH), ethanol: water (EtOH: H_2O) (50% v/v), and water. The evaluated condition was 50 ºC/14 MPa/10 % EtOH. Previous studies by Laurintino (2020) confirmed that this operating condition favored the extraction of the majority of compounds. Therefore, it was decided that all experiments should be carried out under this condition.

3.2.3 Post-processing of extracts

A rotary evaporator (R-100, BUCHI, Flawil, St. Gallen, Switzerland) was used for LPE, SFE, and UAE+SFE to separate the solvent at the end of extractions.

3.2.4 Extract characterization

For LPE, SFE, and UAE + SFE, the global yield (X_0) was calculated as the ratio between the mass of the extract and the mass of the dry solid used.

3.2.4.1 Chemical profile of C. *spicatus* extracts

GC/MS analyses of the extracts were performed on an Agilent GC instrument (7890 A, Agilent, Santa Clara, CA, USA) coupled to an MS detector (5975 C MS,

Agilent, Santa Clara, CA, USA). A fused silica capillary column (HP-5 ms, Agilent, Santa Clara, CA, USA) (30 m long × 250 µm internal diameter × 0.25 µm film thickness, composed of 5 % phenyl and 95 % methylpolysiloxane) was connected to a quadrupole detector operating in EI (electron impact ionization) mode at 70 eV. Helium was adopted as the carrier gas at a 0.8 mL min^{-1} flow rate. The input and interface (G6502B, Agilent, Santa Clara, CA, USA) have a temperature of 280 °C with a split ratio of 1:5. The injected sample volume was 1 µL. The oven temperature program consisted of maintaining the oven at 80 °C for 1 min, increasing it at a rate of 10 °C min^{-1} until it reached 190 °C and then reducing the heating rate to 5 °C min^{-1} until it reached 300 ºC and keep it there for 15 min. Compounds were identified by comparing their mass spectra with those provided by the National Institute of Standards and Technology (2018). The SFE extracts were diluted in EtOH (99.8 % Vetec, Duque de Caxias, RJ, Brazil) at an average concentration of 5.0 mg mL^{-1}.

3.2.5 Statistical analysis

The assays were performed in duplicate. Data are expressed as mean ± standard deviation. To evaluate significant differences ($p < 0.05$) between the results obtained, the Tukey test was applied to the yield results of SFE extractions. All statistical analyses were evaluated using Statistica for Windows 7.0 software (Statsoft Inc., Tulsa, OK, USA).

3.3 RESULTS AND DISCUSSION

3.3.1 Yield of extractions obtained by different extraction techniques (MAC, SOX, UAE, SFE, and UAE+SFE)

Table 3 contains the average mass yield of the extract from *C. spicatus* leaves for the different techniques: MAC, SOX, UAE, SFE, and the combination of UAE with supercritical extraction, varying the solvent (hexane, ethanol, and ethanol: water). The overall yield is defined as the amount of solute extractable by the solvent under the established extraction conditions and indicates, quantitatively, the effectiveness of the process. The results showed that the percentage of extractable yield varied according to the techniques and solvents studied.

Table 3. The overall yield of extracts obtained by low and high-pressure techniques.

Extraction procedure	Raw material (g)	Solvent (mL)	Time (min)	Solvent	Polarity index	Molecular weight (g mol^{-1})	X_o[3] (%)
MAC	10	40	10080	Hexane	0	86.18	4.13 ^{i,C} ± 0.22
				Ethanol	5.2	46.07	5.42 ^{h,B} ± 0.68
				Ethanol: water [2]	7.1	-	7. 25 ^{f,A} ± 0.45
SOX	5	150	300	Ethanol	5.2	46.07	6.41 ^{g,C} ± 0.27
				Water	9	18.01	16.72 ^{b,B} ± 0.58
				Ethanol: water [2]	7.1	-	18.74 ^{a,A} ± 0.41
UAE	1	30	4	Ethanol	5.2	46.07	1.07 ^{k,C} ± 0.13
				Water	9	18.01	8.94 ^{e,B} ± 0.25
				Ethanol: water [2]	7.1	-	9.29 ^{d,A} ± 0.14
SFE[1]	1.4	36	120	CO_2/EtOH	-	-	1.38 ^{j} ± 0.17
UAE + SFE[1]	1.3	36	120	Ethanol	5.2	46.07	1.44 ^{j,C} ± 0.21
				Water	9	18.01	9.24 ^{d,B} ± 0.58
				Ethanol: water [2]	7.1	-	10.12 ^{c,A} ± 0.41

Abbreviations: MAC, maceration extraction; SOX, Soxhlet extraction; UAE, ultrasound extraction; SFE, supercritical CO_2 extraction; UAE + SFE, Ultrasonic pretreatment in supercritical CO_2 extraction;

[1] Extraction condition: Pressure, 14 MPa; temperature, 50ºC and ethanol as co-solvent, 10% W.

[2] Ethanol: water: 50% (v/v).

[3] Mean ± standard deviation; the same lowercase letters indicate no significant difference ($p < 0.05$) for all extraction techniques simultaneously; the same uppercase letters indicate no significant difference ($p < 0.05$) for the same extraction technique (MAC, SOX, UAE and UAE+SFE).

As observed in Table 3, the yield obtained by MAC has increased in the following solvent order: hexane < ethanol < ethanol/water (50% v/v). This result can be explained by the increase in polarity and reduction in viscosity of the solvent that contributes to the solubility of phytochemicals. The higher the molecular weight of the solvent, the lower its polarity, thus allowing the extraction of other compounds with approximately the same molecular weight. Hexane, as the least polar solvent, obtained the lowest yield, followed by ethanol and ethanol/water, which has a higher viscosity than water (KADERIDES *et al.*, 2015).

These results corroborate Pedrosa (2017), who, when using the maceration technique in solvents of increasing polarity in the stem of the Cana do brejo, obtained higher yields in polar solvents - hexane extract - 1.13%, ethyl acetate - 6.76%, and ethanolic - 5.18%, where the solvents present the following polarity indexes: 0, 4.2, and 5.2, respectively. It is worth noting that the yield obtained in the ethanolic extract by the author was similar to the present work, with 5.42%.

The highest yield was obtained when using the ethanol: water solvent, where MAC, SOX, UAE, and UAE+SFE presented values of 7.25, 18.74, 9.29, and 10.12%, respectively. This can be considered a characteristic of this matrix since the compounds

presented greater affinity for this solvent. This mixture behaves as an amphiphilic solvent and extracts substances of polar character and medium polarity (SANTOS, 2008).

The use of solvent mixtures, such as ethanol and water, can favor extraction efficiency since one solvent improves the solubility of the analyte and the other increases dissolution. In this context, water would help to break the matrix and matrix-analyte (hydrogen) bond, resulting in a higher extraction yield (MUSTAFA and TURNER, 2011).

In work developed by Hormaza *et al.* (2020), the extraction of leaves and epicarp of *Garcinia madruno* was performed using the high-intensity ultrasound technique, where a series of solvents with decreasing polarity with mixtures of water and ethanol (0% to 85% ethanol) were tested. Among the mixtures, ethanol: water (50% v/v) was selected as the most selective solvent due to its ability to diffuse into plant tissues, solubilize and extract the compounds. Kalpana *et al.* (2008) also observed that 50% aqueous ethanol was more efficient than the pure or aqueous forms of methanol and 50% acetone for extracting phenolics from aerial parts of *Potentilla atrosanguinea*.

Two factors can directly influence the extraction yield: the polarity of the solvent and the temperature used in the process. Among the techniques and solvents used, the highest efficiency was obtained by Soxhlet extraction (18.74%), using the ethanol: water mixture. This is due to the high temperature, which reduces the viscosity and surface tension of the solvent, in addition to breaking the interactions between the analyte and the matrix caused by van der Waals forces, hydrogen bonds, and dipolar attractions. This process facilitates access to the plant matrix's active sites and solubilizes the present solutes. In addition, extending the extraction time and recycling the solvent increase the overall yield (TRAMONTIN *et al.*, 2019; FERRO *et al.*, 2019; MUSTAFA and TURNER, 2011).

When comparing the Soxhlet and maceration techniques involving the aqueous ethanol solvent (50% v/v), a higher yield percentage was observed in Soxhlet. Susanna, Balakrishnan, and Ettiyappan (2022) also observed this behavior, where the yield of N. *foetida* leaf extracts was higher with the Soxhlet technique (10.03%) in ethanol: water (80% v/v) than in relation to maceration, with 7.56%.

Although the Soxhlet technique is widely used and well established, providing higher yields with the solvents tested, thermal degradation of the compounds is a concern since the solvent is kept close to its boiling point for long periods. In addition, the process requires a long extraction time, which results in high energy consumption. This impact is

even greater due to the need for subsequent procedures, such as evaporation and/or concentration, since the technique uses large volumes of solvent (ALVES *et al.*, 2022).

The effect of ultrasound pretreatment on supercritical extraction significantly impacted the extraction yield. When comparing the yield obtained by SFE from *C. spicatus* leaves that did not undergo pretreatment, an increase in yield was observed after applying SFE in all solvent combinations studied. However, the difference between the yield of supercritical SFE extraction (1.38%) and the combination of two techniques UAE+SFE (1.44%), using ethanol as solvent, was not statistically significant.

Among the solvents tested in UAE+SFE, the highest extraction yield was achieved in the plant material pretreated with ethanol: water, with 10.12%. This can be explained by the positive impact of solvent polarity and the effect of cavitation bubbles, which played an important role in increasing the extractable constituents of the plant material (VIDOVIC *et al.*, 2014). Furthermore, when comparing the UAE and UAE+SFE yields, it is observed that there was no significant difference in yield when the solvents ethanol: water (9.29%) and water (9.24%) were used.

The results published in the literature for the combination of UAE+SFE applied to other vegetable plants also obtained good performance. Liu *et al.* (2020) presented the best yield and quality of *Iberis amara* seed oil when they applied UAE pretreatment to SFE. For De Souza *et al.* (2020), the extraction yield improved by 12.54% by pretreatment of grape seeds with ultrasound. Meanwhile, Vidovic *et al.* (2014) recovered oil from the species *Satureja montana* and obtained a 25% increase in carvacrol content after pretreatment with ultrasound. These results indicate that compounds with different polarities can be extracted in different proportions, depending on the type of solvent and the extraction method used. Thus, these factors directly influence the properties of the extract, such as its chemical composition, due to the selectivity aspects involved in the process (TRAMONTIN *et al.*, 2019; FERRO *et al.*, 2019).

3.3.2 Determination of chemical composition (Maceration and Soxhlet)

The extracts obtained from the leaves of *C. spicatus* were characterized by GC/MS, through two distinct procedures: Maceration and Soxhlet, as shown in Table 4.

Table 4. Main compounds obtained by Maceration (HEX, EtOH, and EtOH: H_2O) and Soxhlet (EtOH, H_2O, and EtOH: H_2O).

		Percentage area (%)					
	RT	Maceration			Soxhlet		
Compounds	(min)	HEX	EtOH	EtOH: H_2O	EtOH	H_2O	EtOH: H_2O
Glycerin	3.40	ND	12.15	10.44	20.83	20.23	15.97
dl-Treitol	3.52	ND	0.20	ND	ND	ND	ND
2,3-Dihydro-3,5-dihydroxy-6-methyl-4h-pyran-4-one	5.53	ND	ND	ND	ND	2.34	ND
Coumaran	6.47	ND	ND	ND	5.31	14.52	9.78
Tetrahydro-2H-pyran-4-ol	6.79	ND	ND	ND	ND	0.89	ND
2-Methoxy-4-vinylphenol	7.78	ND	ND	ND	5.62	5.32	2.55
3-Hydroxy-4-methoxybenzaldehyde	8.88	ND	ND	ND	ND	3.29	ND
α-curcumene	9.92	ND	0.68	ND	2.66	ND	ND
2,6-Di-tert-butyl-4-methylphenol	10.25	1.69	ND	ND	ND	ND	ND
Myristicin	10.40	ND	1.53	ND	ND	ND	ND
Dihydroactinidiolide	10.56	ND	0.60	0.61	2.39	1.91	0.50
2,5-Dimethoxy-4-methylbenzaldehyde	10.87	ND	ND	ND	ND	2.50	2.76
Spatulenol	11.12	ND	1.43	ND	1.70	ND	ND
Dodecanoic acid, ethyl ester	11.15	ND	ND	0.90	ND	ND	ND
Decanoic acid	11.83	ND	ND	1.03	ND	ND	ND
4-(3-Hydroxy-2-methoxyphenyl)butan-2-one	11.84	ND	ND	ND	ND	4.50	ND
3,5-Dimethoxy-4-hydroxybenzaldehyde	11.99	ND	ND	ND	ND	1.78	ND
Benzyl benzoate	13.25	ND	3.88	1.76	ND	ND	ND
Octadecanoic acid, ethyl ester	13.45	ND	ND	ND	ND	ND	ND
Ethyl coumarate	13.86	ND	ND	5.42	ND	ND	ND
Hexadecanal	14.01	ND	ND	ND	ND	ND	3.53
1,19-Eicosadiene	14.02	ND	ND	1.49	ND	ND	ND
6,10,14-Trimethylpentadecan-2-one	14.10	ND	1.13	0.67	ND	ND	ND
1,2-Epoxyoctadecane	14.26	ND	ND	ND	4.46	ND	3.16
Diisobutyl phthalate	14.42	ND	ND	0.40	ND	ND	ND
Ethyl 9-hexadecenoate	15.95	ND	ND	0.75	ND	ND	ND
Palmitic acid	16.02	3.33	3.85	3.45	5.11	4.92	4.91
Heptadecanoic acid, ethyl ester	17.43	ND	ND	0.35	ND	ND	ND
Phytol	17.72	ND	4.99	2.69	ND	ND	3.03
Linoleic acid	18.41	4.06	3.34	ND	ND	1.53	2.61
Linoleic acid, ethyl ester	18.43	ND	3.21	11.18	3.14	ND	ND
Linolenic acid	18.51	10.86	9.52	13.36	6.97	5.26	5.65
cis-vaccenic acid	18.59	ND	ND	0.35	ND	ND	ND
Octadecanoic acid, ethyl ester	18.88	ND	ND	1.68	ND	ND	ND

Hexadecane	18.95	1.06	ND	ND	ND	ND	ND
Heptadecane	20.42	1.60	ND	ND	ND	ND	ND
Tetracosane	20.95	6.62	ND	ND	ND	ND	ND
Oleic acid	21.24	ND	ND	ND	ND	ND	ND
Palmitic acid	22.11	ND	ND	0.51	ND	ND	ND
Eicosane	22.40	9.74	9.81	10.01	ND	ND	ND
Oleic acid	22.63	ND	ND	0.66	ND	ND	ND
1-(4-bromobutyl)-2-piperidone	24.02	0.85	ND	ND	ND	ND	ND
1-Hexacosene	24.09	3.06	ND	ND	ND	ND	ND
Hexacosane	24.67	0.97	ND	ND	ND	ND	ND
Heneicosan	25.26	7.62	ND	ND	ND	ND	ND
Tricosane	25.61	2.83	ND	ND	ND	ND	ND
Octatriacontyl pentafluoropropionate	26.51	5.46	ND	ND	ND	ND	ND
1,1,3,3,5,5,7,7,9,9,11,11,13,13-Tetradecamethylheptasiloxane	27.06	ND	ND	1.17	ND	ND	ND
Octacosane	28.89	4.19	ND	ND	ND	ND	ND
Octadecane	29.23	ND	ND	ND	3.43	ND	3.22
Vitamin E	31.89	3.07	ND	ND	ND	ND	1.48
Cyclotrisiloxane, hexamethyl-	33.03	ND	7.16	5.02	ND	ND	2.19
Stigmasterol	33.41	2.25	ND	ND	ND	ND	ND
Gamma-Sitosterol	34.11	3.97	ND	ND	ND	ND	ND
Octasiloxane, 1,1,3,3,5,5,7,7,9,9,11,11,13,13,15,15-hexadecamethyl-	34.12	ND	10.17	4.45	4.53	0.96	12.59
Friedelin	37.04	4.33	ND	ND	8.75	ND	ND
TR	-	22.45	26.34	21.67	25.10	30.04	26.07

Abbreviations: HEX, hexane; EtOH, ethanol and EtOH: H_2O, ethanol: water (50% v/v); RT, Retention time; ND, not detected; TR, trace compound.

Table 4 lists the constituents extracted by the maceration technique in different solvents. The EtOH: H_2O extract (50% v/v) leads with 23 compounds, followed by hexane (19 compounds) and ethanol (16 compounds). Although the three extracts (hexane, ethanol, and ethanol: water) contained the same components, such as palmitic acid, linolenic acid, and eicosane, the proportions varied according to the solvent, as did the most abundant component isolated.

During maceration, linolenic acid was the dominant compound in the EtOH: H_2O extract (13.36%) and the HEX solvent (10.86%). However, glycerin (12.15%) became the major compound when EtOH was used as the solvent. Thus, it is possible to verify that the extraction method influenced the selection of the major compound. Furthermore, combining the extraction technique and the type of solvent used also increased the proportion of some compounds in isolation. For example, in HEX: 2,6-di-tert-butyl-4-methylphenol, hexadecane, and heptadecane; in EtOH: dl-threitol, α-curcumene and myristicin; and in EtOH: H_2O: dodecanoic acid, ethyl ester, decanoic acid

and ethyl 9-hexadecenoate. This can be explained by the interaction of the solvent with the compound.

Given the results, it is clear that the extracts of *C. spicatus* are rich in secondary metabolites in their chemical composition, corroborating with the data presented in the literature. Bitencourt and Almeida (2014) subjected the leaves of *C. spicatus* to extraction by maceration in EtOH for 3 days. They obtained the presence of the following classes of compounds: alkaloids, phenols, and tannins. While Azevedo *et al.* (2014), when using different parts of the Cana do brejo (stems, leaves, and flowers), observed the presence of triterpenes, steroids, flavonoids, saponins, alkaloids, and tannins when subjected to liquid-liquid extraction, varying the solvent hexane, ethyl acetate, and butanol.

Several factors can influence the synthesis of secondary metabolites, such as seasonality, water availability, temperature, ultraviolet radiation, nutrients, altitude, atmospheric pollution, and others, altering plant tissue constituents (SILVA, 2013).

As shown in Table 4, only 13 and 14 compounds were detected in the Soxhlet extraction using EtOH and H_2O as solvents, respectively. The EtOH: H_2O mixture (50% v/v) presented a greater quantity of bioactives, with 15 compounds, compared to the other solvents. This better performance in the diversity of compounds solubilized by the mixture reduces selectivity but promotes greater interaction between the target compound and the solvent since the low viscosity of the EtOH: H_2O solution facilitates the penetration of the solvent into the plant matrix, favoring the extraction process (MUSTAFA and TURNER, 2011).

Glycerin, identified as the major compound (Table 4), was found in all solvents used - EtOH, H_2O, and EtOH: H_2O (50% v/v) - in the Soxhlet extraction, with concentrations of 20.83%, 20.23%, and 15.97%, respectively. Due to its humectant and moisturizing properties, glycerin has wide commercial applications in cosmetics and pharmaceutical products (BHALLA *et al.*, 2021).

The results showed that the Soxhlet method extracted fewer compounds compared to maceration, possibly due to the degradation of thermolabile substances and irreversible structural modifications (OLIVEIRA *et al.*, 2016). Despite this decreased number of extracted compounds, the Soxhlet method effectively isolated specific compounds, such as glycerin and coumaran. Oliveira *et al.* (2016) corroborates this result. The authors report that, among several techniques applied to the extraction of *Dicksonia sellowiana*, Soxhlet resulted in the lowest concentrations of metabolites in ethanol and 70% hydroalcoholic solution.

Ganesan and Sivamani (2015) performed a phytochemical analysis of the ethanolic extract of *C. spicatus* leaves using the Soxhlet technique for 48 hours. Fourteen compounds were identified by the GC-MS method, with the main major compounds being eremantine and isolongifolene,4,5-dehydro-. Although the authors used the same plant species as in the present study, there was a variation in the composition, probably caused by climatic and regional factors. In addition, the authors used a different extraction time, 9.6 times longer when compared to that used in this study.

By observing the previous tables, the major compounds of the extract of *C. spicatus* leaves obtained by the maceration and Soxhlet technique in different solvents were verified. Table 5 was constructed from this, containing the two major compounds and their respective properties in the literature.

Table 5. Phytochemical constituents of the major compounds obtained by maceration and Soxhlet in different solvents.

Technique	Solvent	Major compounds *		Application	Reference
Maceration	Hexane	I	Linolenic acid	Reduce complications in patients with Covid-19 and neuroprotective properties	Weill *et al.,* 2020; Blondeau *et al.,* 2015
		II	Eicosane	Antitumor activity against human gastric SGC-7901 cell line	Sivasubramanian e Brindha, 2013
	Ethanol	I	Glycerin	Used as a humectant, moisturizer with application in cosmetics and medicines	Sagiv *et al.*, 2001
		II	Octasiloxane, 1,1,3,3,5,5,7,7,9,9,11,11,13,13,15,15-hexadecamethyl-	Antimicrobial and insecticidal activity	Ahmed *et al.*, 2020; Abdullah, 2019
	Ethanol: water	I	Linolenic acid	Reduce complications in patients with Covid-19 and neuroprotective properties	Weill *et al.,* 2020; Blondeau *et al.,* 2015
		II	Linoleic acid	Anti-inflammatory, hypocholesterolemic, cancer prevention, hepatoprotective, antihistamine, anti-acne, 5-α-reductase inhibitor, antiandrogenic, antiarthritic and antifungal activity	Chhouk *et al.*, (2018)
Soxhlet	Ethanol	I	Glycerin	Used as a humectant, moisturizer with application in cosmetics and medicines	Sagiv *et al.*, 2001
		II	Friedelin	Anti-inflammatory, hepatoprotective, antibacterial, antidiarrheal, antitumor, antiproliferative, antipyretic, antiulcerogenic and antimicrobial	Odeh *et al.* (2016); Mariot e Barbieri (2007); Silva *et al.,* (2014)
	Water	I	Glycerin	Used as a humectant, moisturizer with application in cosmetics and medicines	Sagiv *et al.*, 2001
		II	Coumaran		
	Ethanol: water	I	Linolenic acid	Reduce complications in patients with Covid-19 and neuroprotective Properties	Weill *et al.,* 2020; Blondeau *et al.,* 2015
		II	Octasiloxane, 1,1,3,3,5,5,7,7,9,9,11,11,13,13,15,15-hexadecamethyl-	Antimicrobial and insecticidal activity	Ahmed *et al.*, 2020; Abdullah, 2019

* First (I) and second (II) majority compound.

3.3.3 Ultrasonic pretreatment

Ultrasound pretreatment to obtain extracts via SFE was investigated in *C. spicatus* leaves under different conditions: tip types (macrotip and microtip), amplitude (30% and 70%), time (1 and 5 minutes), and solvent (ethanol, ethanol: water and water), with the aim of evaluating both the extraction yield and the chemical composition of the extracts.

3.3.3.1 Yield

Table 6 shows the average yield of the extractions performed under different process conditions. Extractions from the leaf with the microtip at 70% amplitude were not performed, as they presented a low yield in the preliminary tests.

Table 6. Extractions performed using the ultrasound technique.

Tip	Amplitude	Solvent [1]	Time (min)	X_0 (%)[2]
Microtip	30%	Ethanol	1	0,48 ^{i,D} ± 0,35
			5	1,15 ^{g,C} ± 0,21
		Ethanol: water	1	6,66 ^{d,A} ± 0,15
		Water		5,82 ^{e,B} ± 0,14
Macrotip	30%	Ethanol	1	0,53 ^{i,C} ± 0,25
			5	1,21 ^{g,B} ± 0,20
		Ethanol: water	1	7,34 ^{c,A} ± 0,17
		Water		7,29 ^{c,A} ± 0,18
	70%	Ethanol	1	0,83 ^{h,D} ± 0,22
			5	1,43 ^{f,C} ± 0,13
		Ethanol: water	1	8,59 ^{a,A} ± 0,18
		Water		8,35 ^{b,B}± 0,34

(1) Ethanol: water (50% v/v);

(2) Mean ± standard deviation; the same lowercase letters indicate no significant difference (p< 0.05) considering all experiments simultaneously; the same uppercase letters on the same tip and amplitude indicate a significant difference (p < 0,05).

3.3.3.1.1 Influence of the ultrasound tip

Initially, extractions were performed using two types of ultrasound tips (macrotip and the microtip), maintaining the mass-volume ratio, amplitude (30% and 70%), solvent (ethanol, ethanol: water and water), and time (1 and 5 min), to evaluate the effect of the probe tip diameter.

As observed in Table 6, the yields obtained with the 13 mm probe tip (macrotip) were higher than the 3 mm probe (microtip), considering the same amplitude, solvent and time conditions. The only exception was the extraction of *C. spicatus* leaves with an

amplitude of 30%, using ethanol as a solvent for 1 and 5 minutes, where the yields were not significantly different.

The increase in yield with the use of the macrotip can be explained by the fact that its tip has a larger diameter, which results in more intense sonication. This increases the permeability of the cell wall, facilitating the penetration of the solvent into the plant cells and promoting more efficient extraction. In addition, the macrotip allows the processing of larger sample volumes compared to the microtip (POTDAR *et al.,* 2022).

3.3.3.1.2 Influence of amplitude

Table 6 also shows the impact of amplitude on the extract yield of *C. spicatus*. The extract yield increased significantly when using amplitude from 30 to 70%, when the process variables were kept constant: tip (macrotip), solvent and time.

The improvement in yield at increasing amplitudes is caused by cavitation and the mechanical effect of ultrasound, which expands the contact area between solid and liquid surfaces, promoting greater solvent penetration into the plant matrix. The size of the resonant bubbles is directly proportional to the amplitude of the ultrasonic wave, which generates high temperatures and pressures inside the bubbles. The violent collapse of the bubbles, in a short period of time, causes a significant mechanical impact, facilitating the diffusion of the solvent in the cellular tissues and accelerating the release of the solute into the solvent by rupturing the cell walls (DASH, PATHAK and PRADHAN, 2021; SUSLICK and PRICE, 1999).

In agreement with this study's results, other studies that used ultrasound-assisted extraction also reported better extraction yields when employing high amplitudes (GOULA, 2013; KADERIDES *et al.,* 2015; RAKSHIT *et al.,* 2020; HORMAZA *et al.,* 2020).

3.3.3.1.3 Influence of solvent

The ultrasound extraction technique revealed the polar nature of the compounds from the leaves of *C. spicatus* since the use of pure polar solvents, such as ethanol, water, and especially the ethanol-water mixture, resulted in statistically higher yields. Despite presenting an intermediate polarity index (7.1) about ethanol (5.2) and water (9.0), the ethanol: water solvent presented slightly higher efficiency in terms of overall yield when compared to the other solvents.

The yield increased in the following solvent order: ethanol < water < ethanol: water (50% v/v). The combination of ethanol and water favored the extraction efficiency since, while one solvent improves the solubility of the analyte, the other increases the dissolution (MUSTAFA and TURNER, 2011). However, when using the macrotip with an amplitude of 30% for 1 minute, there was no significant difference between the ethanol: water and water solvents, resulting in 7.34% and 7.29% yields, respectively.

Corroborating this work, Santos *et al.* (2019) identified higher extraction yields from Feijoa (*Psidium guajava L.*) peel obtained by UAE when ethanol: water (50% v/v) was used compared with pure water and pure ethanol. Mazzuti *et al.* (2017) also observed this trend when they obtained extracts by different extraction methods from the plant species P. *major* e P. *lanceolata*.

3.3.3.1.4 Influence of time

The extraction kinetics were performed as illustrated in Figure 9. It is possible to observe that the extraction rate by UAE increases by up to 4 minutes. This can be explained by the high initial extraction rate, which is characterized by a fast speed, resulting from the greater difference in concentration since the compounds are easily accessible on the external surface of the particles (VETAL, LADE e RATHOD, 2013).

Figure 9. Kinetics by ultrasound technique.

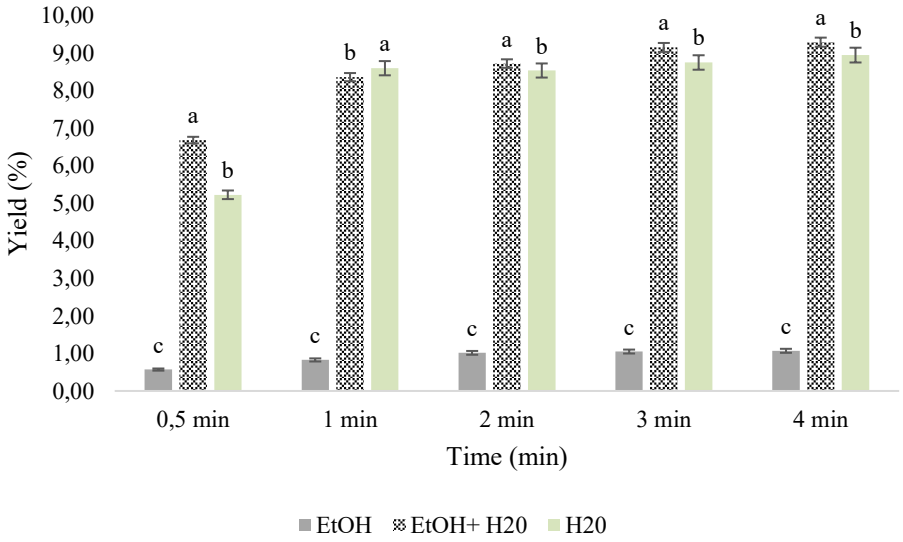

Abbreviations: EtOH, ethanol; EtOH:H_2O, ethanol: water (50% v/v); water, H_2O. The same lowercase letters indicate no significant difference ($p < 0.05$) considering the same extraction time.

The higher extraction yields in the initial stages can be explained by Fick's second law, which states that the extraction rate increases until the equilibrium state is reached, that is, when the concentration in the plant material and solvent reaches equilibrium (RAJ and DASH, 2020).

According to Zhang *et al.* (2008), when studying the process variables, such as the time taken to extract oil from *Terminalia chebula*, they observed that the higher oil content on the surface of the material was caused by the effect of ultrasonication over the course of the time process, since the fragmentation of the cell wall occurs, leading to an improvement in the contact area between the solvent and the solid interface.

Vetal, Lade, and Rathod (2013) and Naik *et al.* (2022) also found trends similar to this work. When studying the extraction kinetics, they noticed a gradual increase in extraction with time variation and constant process conditions. For Kaderides *et al.* (2015), in all their experiments applying pomegranate peel, the extraction yield increased when using ultrasonic times of 2 to 10 min.

3.3.3.2 Chemical composition

By previous results, the extracts of *C. spicatus* leaves obtained by UAE had a higher yield in solvents with high (water) and medium (ethanol: water) polarity index, with 9.0 and 7.1, respectively. When comparing with the yield, the chemical composition presented different behavior. The detection of compounds with the solvent with the lowest polarity index (5.2), ethanol, identified a greater quantity of extracted compounds with great commercial interest. Furthermore, regardless of the tip application and amplitude used, the ethanolic extracts presented a higher percentage of relative area in the identified compounds.

3.3.3.2.1 Macrotip (70 e 30%) and microtip (30%)

The compounds' chemical composition and percentage area varied according to the solvent used. For the macrotip at amplitudes of 70% and 30%, as well as for the microtip at an amplitude of 30%, the number of compounds followed the following increasing order: ethanol (5 min) > ethanol (1 min) > ethanol: water (1 min) > water (1 min).

Table 7 presents the chemical compositions of the extracts obtained by macrotip with amplitudes of 70 and 30% and microtip with amplitude of 30%, varying the solvent

and pre-established time. The maximum number of identified compounds was obtained when using the macrotip (amplitude of 70%, ethanol and 5 min) and the microtip (amplitude of 30%, ethanol and 5 min), with values of 36 and 34 compounds, respectively.

Table 7. Area percentage of compounds identified in the macrotip at amplitudes of 70 and 30% and microtip at amplitude of 30%.

		Percentage area (%)											
		Macrotip (amplitude of 70%)				Macrotip (amplitude of 30%)				Microtip (amplitude of 30%)			
	RT*	Ethanol	Ethanol	Ethanol: water	Water	Ethanol	Ethanol	Ethanol: water	Water	Ethanol	Ethanol	Ethanol: water	Water
Compounds	(min)	1 min	5 min	1 min	1 min	1 min	5 min	1 min	1 min	1 min	5 min	1 min	1 min
Glycerin	3.43	0.81	1.84	7.43	ND	0.61	1.54	5.43	ND	0.52	1.04	4.99	ND
Erythritol	3.46	ND	ND	ND	ND	ND	ND	8.22	ND	ND	ND	ND	ND
D-Limonene	3.99	ND	ND	ND	ND	ND	ND	ND	2.50	ND	ND	ND	2.13
Mequinol	4.73	ND	ND	ND	ND	ND	ND	ND	1.32	ND	ND	ND	ND
α-Terpineol	6.12	0.15	0.17	ND	ND	0.09	0.13	ND	ND	0.09	0.12	ND	ND
Coumaran	6.49	ND	ND	10.25	3.74	ND	ND	7.46	3.31	ND	ND	ND	ND
D-Carvone	6.83	0.09	ND	ND	ND	5.83	5.98	ND	ND	ND	ND	5.15	6.15
2-Methoxy-4-vinylphenol	7.60	ND	ND	5.89	13.61	ND	ND	5.57	12.47	ND	ND	11.47	10.48
Phenol, 2,6-dimethoxy-	8.06	ND	ND	3.07	5.64	ND	ND	1.98	3.66	ND	ND	ND	ND
D-Allose	9.66	ND	ND	ND	3.74	ND	ND	ND	0.15	ND	ND	ND	ND
Levoglucosan	9.68	ND	ND	ND	8.70	ND	ND	ND	5.48	ND	ND	ND	5.66
α-curcumene	9.86	0.18	0.20	ND	ND	ND	ND	1.19	5.30	0.22	0.28	8.47	10.52
Dihydroactinidiolide	10.49	ND	ND	0.65	ND	ND	ND	0.52	ND	ND	ND	ND	ND
Lauric acid	10.71	0.33	0.54	0.41	ND	ND	ND	ND	ND	0.35	0.43	0.82	2.68
2,5-Dimethoxy-4-methylbenzaldehyde	10.81	ND	0.28	3.46	ND	ND	0.10	5.58	9.22	ND	ND	ND	ND
Fumaric acid, cyclobutyl ethyl ester	10.86	ND	ND	ND	ND	ND	ND	ND	ND	ND	ND	1.55	1.42
4-(3-Hydroxy-2-methoxyphenyl)butan-2-one	11.68	ND	ND	ND	3.84	ND	ND	ND	ND	ND	ND	ND	ND
Zingerone	11.67	ND	ND	ND	1.43	ND	ND	1.87	ND	ND	ND	ND	ND
Phytol acetate	13.90	ND	ND	ND	ND	ND	5.01	ND	ND	ND	0.77	ND	ND
Tetradecanoic acid	12.96	0.33	0.41	ND	ND	ND	ND	ND	ND	0.19	0.27	ND	ND
3,7,11,15-Tetramethyl-2-hexadecene	13.98	ND	ND	ND	ND	ND	0.63	ND	ND	ND	ND	ND	ND
Benzyl benzoate	13.14	5.22	5.33	ND	ND	2.06	2.68	ND	ND	0.63	0.73	ND	ND
Methyl (2E,4E)-2,4-heptadienoate	13.16	ND	ND	2.22	ND	ND	ND	ND	ND	ND	ND	ND	ND
2-Tetradecene	13.38	ND	0.04	ND	ND	ND	ND	ND	ND	ND	ND	ND	ND
Pentadecanal	13.95	ND	0.73	ND	ND	ND	ND	ND	ND	ND	ND	ND	ND
6,10,14-Trimethylpentadecan-2-one	14.02	5.98	6.23	0.44	ND	ND	ND	ND	ND	0.30	0.77	ND	ND

Ethyl 15-methylhexadecanoate	14.12	ND	ND	ND	ND	ND	ND	ND	1.71	ND	ND	ND	ND
Pentadecanoic acid	14.17	0.25	0.33	ND	ND	ND	ND	ND	ND	0.18	0.37	ND	ND
Diisobutyl phthalate	14.34	0.12	ND	ND	ND	ND	ND	ND	ND	0.18	ND	3.95	5.67
1,4-Eicosadiene	14.49	4.51	ND	0.68	ND	ND	ND	ND	ND	ND	0.19	ND	ND
3-Eicosine	14.49	ND	ND	ND	ND	ND	ND	ND	ND	ND	ND	0.97	2.44
Pentadecanoic acid, 14-methyl-, methyl ester	14.89	ND	ND	ND	ND	ND	ND	ND	3.91	ND	ND	ND	ND
cis-vaccenic acid	15.81	ND	ND	ND	ND	0.20	ND	ND	ND	0.28	ND	ND	ND
Ethyl E-11-hexadecenoate	15.86	ND	ND	ND	ND	ND	ND	ND	ND	ND	0.35	ND	ND
Ethyl 9-hexadecenoate	15.86	0.28	0.31	ND	ND	ND	0.27	ND	ND	ND	ND	ND	ND
Palmitic acid	15.95	10.27	10.78	11.42	ND	6.75	6.97	7.31	ND	0.22	0.53	2.01	ND
Heptadecanoic acid	16.86	0.21	0.29	ND	ND	ND	ND	ND	ND	ND	0.55	Na	ND
Phytol	17.63	2.71	2.97	1.10	ND	2.09	2.79	1.92	ND	2.03	2.43	1.50	ND
1,2-Epoxyoctadecane	17.71	ND	ND	ND	ND	ND	0.51	ND	ND	ND	ND	ND	ND
Linoleic acid	18.01	2.13	3.71	5.15	ND	ND	ND	ND	ND	1.32	1.57	2.43	ND
Linolenic acid	18.12	14.03	14.67	13.72	ND	12.01	13.62	11.24	ND	9.41	10.13	8.52	ND
Linoleic acid, ethyl ester	18.32	ND	ND	5.05	ND	5.67	ND	3.25	ND	ND	ND	5.73	4.65
Octadecanoic acid, ethyl ester	18.79	1.42	1.53	0.56	ND	1.12	1.22	0.44	ND	0.49	0.53	ND	4.40
2-Pentadecanone	20.45	ND	ND	ND	ND	ND	ND	ND	ND	0.45	ND	ND	ND
1,19-Eicosadiene	20.68	ND	ND	ND	ND	ND	0.34	ND	ND	ND	ND	ND	ND
Oleic acid	21.08	ND	ND	ND	ND	ND	0.23	0.45	ND	ND	0.53	ND	ND
4,8,12,16-Tetramethylpentadecane-4-olinde	21.13	ND	ND	ND	ND	ND	ND	ND	ND	0.20	ND	ND	ND
2-Methyl-Z,Z-3,13-octadecadienol	21.24	ND	ND	ND	ND	ND	ND	ND	ND	ND	0.20	ND	ND
Eicosanoic acid	21.25	0.18	0.26	ND	ND	ND	ND	ND	ND	ND	ND	ND	ND
1,5,9,13-Tetradecatetraene	21.67	ND	ND	ND	ND	ND	ND	ND	ND	0.26	ND	ND	ND
Heptadecanoic acid, ethyl ester	21.68	ND	ND	ND	ND	0.19	ND	ND	ND	ND	ND	ND	ND
Nonadecanoic acid, ethyl ester	21.72	ND	0.17	ND	ND	ND	ND	ND	ND	ND	ND	ND	ND
Ethyl E-11-hexadecenoate	21.73	ND	ND	ND	ND	ND	0.33	ND	ND	ND	ND	ND	ND
(Z)-9-Hexadecenal	21.78	0.24	ND	ND	ND	ND	ND	ND	ND	ND	ND	ND	ND
1-Octadecene	23.18	0.15	ND	ND	ND	ND	ND	ND	ND	0.35	ND	ND	ND
Heptadecane	23.24	0.11	ND	ND	ND	ND	ND	ND	ND	ND	ND	ND	ND
Glyceryl palmitate	23.34	ND	ND	0.69	ND	ND	ND	ND	ND	ND	ND	ND	ND
2-Palmitoylglycerol	23.34	ND	ND	ND	ND	ND	ND	ND	ND	0.47	ND	ND	ND

17-Pentatriaconten	24.61	ND	0.25	ND	ND	ND	ND	ND	ND	ND	ND	ND	ND
Methyl 17-methyl octadecenoate	24.61	ND	ND	ND	ND	ND	ND	ND	ND	ND	0.25	ND	ND
1-Heptacosanol	26.01	ND	ND	ND	ND	ND	ND	ND	ND	ND	0.23	ND	ND
(Z)-9-Tricosene	26.01	ND	0.22	ND	ND	ND	ND	ND	ND	ND	ND	ND	ND
Hexadecane	26.07	ND	ND	ND	ND	ND	ND	ND	ND	ND	0.36	ND	ND
Eicosane	26.08	0.76	0.81	ND	ND	ND	0.35	ND	ND	1.13	0.36	ND	ND
9-Nonadecene	27.39	ND	0.48	ND	ND	ND	ND	ND	ND	ND	ND	ND	ND
Squalene	27.84	0.36	0.39	ND	ND	ND	ND	ND	ND	ND	0.28	ND	ND
(5E)-6,10-dimethyl undec-5,9-dien-2-one	27.84	ND	ND	ND	ND	ND	ND	ND	ND	0.23	ND	ND	ND
Gamma-Tocopherol	30.74	ND	ND	ND	ND	ND	0.58	ND	ND	ND	ND	ND	ND
Vitamin E	31.77	0.98	1.39	ND	ND	0.81	1.26	ND	ND	0.73	1.12	ND	ND
Campesterol	32.88	1.66	1.67	ND	ND	1.37	1.46	ND	ND	1.23	1.43	ND	ND
Octasiloxane, 1,1,3,3,5,5,7,7,9,9,11,11,13,13,15,15-hexadecamethyl-	33.12	ND	ND	ND	11.60	ND	ND	ND	10.73	ND	ND	ND	ND
Stigmasterol	33.29	4.95	5.11	2.39	ND	3.19	3.54	1.12	ND	6.03	7.74	ND	ND
Gamma-Sitosterol	33.99	1.54	2.35	3.08	ND	15.32	15.74	ND	ND	14.19	16.97	ND	ND
β-amirenol	34.09	ND	1.71	ND	ND	ND	ND	ND	ND	ND	1.37	ND	ND
Cyclotrisiloxane, hexamethyl-	34.18	2.83	2.85	3.92	13.81	1.31	2.34	4.12	12.47	1.65	2.63	ND	ND
Bis(trimethylsilyl)diethylsilicate	34.66	2.26	2.74	ND	ND	ND	ND	ND	ND	ND	ND	ND	ND
1,1,1,3,5,5,5-Heptamethyltrisiloxane	34.91	1.09	ND	ND	ND	ND	ND	ND	ND	1.03	2.96	ND	ND
4,22-Stigmatidene-3-one	34.91	ND	0.82	ND	ND	ND	ND	ND	ND	ND	ND	ND	ND
Sitostenone	35.72	2.08	2.31	ND	ND	3.45	3.73	ND	ND	2.71	2.98	ND	ND
Friedelin	36.89	8.01	8.32	7.27	ND	7.23	7.74	6.15	ND	7.05	7.14	6.04	ND
1-ethenoxyhexadecane	37.79	1.60	ND	ND	ND	ND	ND	ND	ND	ND	ND	ND	ND
Tiglyceric acid	37.79	ND	1.81	ND	ND	ND	ND	ND	ND	ND	ND	ND	ND
TR	-	22.19	15.98	11.16	33.89	30.68	20.91	23.70	27.77	42.54	28.60	31.98	43.80

Abbreviations: RT, retention time; ND, not detected; TR, trace compound.

From Table 7, it is possible to see that the extractions performed on the leaves of *C. spicatus*, under the operational conditions of macro tip, amplitude of 70%, ethanol solvent, and time of 5 min, produced the major compounds linolenic acid (14.67%), palmitic acid (10.78%), friedelin (8.32%), and 6,10,14-trimethylpentadecan-2-one (6.23%).

The extracts obtained with the macrotip at 30% amplitude showed a reduction in compounds' quantity and percentage content compared to the macrotip at 70% amplitude. In the ethanol solvent (5 min), 25 compounds were identified, while using water resulted in a smaller quantity, with 13 compounds. Linoleic acid was not detected in any solvent using the macrotip (30% amplitude). Compounds such as palmitic acid, linolenic acid, stigmasterol, and friedelin showed a reduction in the percentage content, regardless of the solvent, be it ethanol (1 to 5 min) or ethanol: water. On the other hand, the macrotip (30% amplitude) favored the extraction of other compounds, such as gamma-sitosterol in the ethanol solvent (1-5 min) and cyclotrisiloxane, hexamethyl-, in the ethanol: water and water solvents, with percentage contents of 15.32%, 15.74%, 4.12%, and 12.47%, respectively.

The chemical compositions of the extracts of *C. spicatus* leave obtained with the microtip at an amplitude of 30% showed a significant reduction in the quantity of compounds, especially when compared to the extracts obtained with the macrotip at amplitudes of 70% and 30%. In the ethanol: water and water solvents, 15 and 11 compounds were identified, respectively. In addition, the target compounds, such as palmitic acid, linoleic acid, linolenic acid, and friedelin, showed an even more pronounced reduction in the percent area in the ethanol (1-5 min), ethanol: water and water solvents, compared with the results obtained with the macrotip.

It is important to highlight that, in some experimental conditions (varying tip type, amplitude, solvent, and time), a low quantity of the compounds identified in the leaves of *C. spicatus* was observed. This may be related to the presence of high molecular weight waxes in the extract, which may not have been identified by the chromatographic column or not detected due to their longer retention time, outside the analyzed range. This behavior was also observed by Corrêa (2016) when extracting compounds from inflorescences of *Musa paradisíaca L.* using supercritical CO_2 and propane as solvents.

Finally, based on the results of the multivariate optimization, it can be suggested that the application of the macrotip, with an amplitude of 70%, during 5 min of sonication

and the solvent ethanol, can be recommended for the ultrasound-assisted extraction of *C. spicatus* leaves.

3.3.4 Combination of ultrasound technique and supercritical extraction

GC/MS analysis was performed to identify and quantify several bioactive compounds present in the extract obtained by the combination of UAE+SFE, as shown in Table 8. Values of 30, 25, and 41 compounds were observed for the solvents ethanol, water, and ethanol: water, respectively. Compared to the isolated extraction process, the percentage area was increased for the main compounds: palmitic acid, linoleic acid, linolenic acid, and friedelin.

Table 8. Area percentage of compounds identified in UAE+SFE.

				Percentage area (%)		
	RT[1] (min)	Molecular formula	MM[2] g mol^{-1}	Solvents		
Compounds				Ethanol	Water	Ethanol: water
Coumaran	7.57	C_8H_8O	120	0.43	1.21	1.60
Salicylic acid	8.65	$C_7H_6O_3$	138	0.10	ND	ND
2-Methoxy-4-vinylphenol	8.92	$C_9H_{10}O_2$	150	ND	0.39	0.26
Decanoic acid, ethyl ester	9.95	$C_{12}H_{24}O_2$	200	0.20	0.24	0.54
Myristicin	11.58	$C_{11}H_{12}O_3$	192	0.47	0.23	0.18
Dihydroactinidiolide	11.83	$C_{11}H_{16}O_2$	180	0.10	ND	0.15
Lauric acid	11.89	$C_{12}H_{24}O_2$	200	1.23	1.25	1.31
2,5-Dimethoxy-4-methylbenzaldehyde	11.99	$C_{10}H_{12}O_3$	180	ND	ND	0.17
Ciclododecano	12.25	$C_{12}H_{24}$	168	0.07	ND	ND
Hexadecane	12.27	$C_{16}H_{34}$	226	ND	ND	0.34
Tetradecanoic acid	14.28	$C_{14}H_{28}O_2$	228	ND	0.19	0.26
Benzyl benzoate	14.65	$C_{14}H_{12}O_2$	212	0.08	0.12	0.12
Nonadecanoic acid, ethyl ester	14.77	$C_{21}H_{42}O_2$	326	0.42	ND	ND
Octadecane	14.83	$C_{18}H_{38}$	254	0.22	ND	0.41
4-Hydroxy-3,5,6-trimethyl-4-(3-oxobut-1-enyl)-cyclohex-2-en-1-on	14.91	$C_{13}H_{18}O_3$	222	ND	ND	0.11
Ethyl coumarate	15.30	$C_{11}H_{12}O_3$	192	ND	ND	0.33
6,10,14-Trimethylpentadecan-2-one	15.49	$C_{18}H_{36}O$	268	0.74	0.79	0.56
Pentadecanoic acid	15.62	$C_{15}H_{30}O_2$	242	ND	ND	0.35
1,4-Eicosadiene	15.74	$C_{20}H_{38}$	278	1.32	ND	ND
Diisobutyl phthalate	15.92	$C_{16}H_{22}O_4$	278	0.30	ND	ND
Butyl octyl phthalate	15.92	$C_{20}H_{30}O_4$	334	ND	0.32	ND
Ethyl 13-methyltetradecanoate	16.14	$C_{17}H_{34}O_2$	270	0.13	0.37	ND
Palmitoleic acid	16.81	$C_{16}H_{30}O_2$	254	ND	ND	0.17
Palmitic acid	17.10	$C_{16}H_{32}O_2$	256	19.90	20.17	22.14
cis-vaccenic acid	17.31	$C_{18}H_{34}O_2$	282	0.82	ND	0.12
Heptadecanoic acid	18.58	$C_{17}H_{34}O_2$	270	ND	ND	0.36
(z)-9,17-octadecadienal	19.26	$C_{18}H_{32}O$	264	0.21	ND	ND

Phytol	19.46	$C_{20}H_{40}O$	296	ND	ND	0.39
Methyl stearate	19.61	$C_{19}H_{38}O_2$	298	0.15	ND	0.19
Linoleic acid	19.73	$C_{18}H_{32}O_2$	280	4.57	13.81	9.19
Linolenic acid	19.85	$C_{18}H_{30}O_2$	278	29.34	27.12	28.95
Linoleic acid, ethyl ester	20.18	$C_{20}H_{36}O_2$	308	7.97	ND	6.70
Octadecanoic acid, ethyl ester	20.64	$C_{20}H_{40}O_2$	312	ND	ND	1.19
Eicosane	22.23	$C_{20}H_{42}$	282	1.88	2.14	0.20
2-Pentacosanone	22.41	$C_{25}H_{50}O$	366	ND	0.42	0.46
5-Eicosene	23.17	$C_{20}H_{40}$	280	ND	ND	0.18
Eicosanoic acid	23.23	$C_{20}H_{40}O_2$	312	0.17	0.15	0.61
Heptadecanoic acid, ethyl ester	23.71	$C_{19}H_{38}O_2$	298	0.36	0.24	ND
Ethyl 9-hexadecenoate	24.41	$C_{18}H_{34}O_2$	282	ND	0.17	ND
Docosanoic acid	26.23	$C_{22}H_{44}O_2$	340	ND	ND	0.09
Heptadecane	28.14	$C_{17}H_{36}$	240	ND	ND	0.56
Ethyl tetracosanoate	29.50	$C_{26}H_{52}O_2$	396	ND	ND	0.67
Octadecanoic acid, ethyl ester	29.51	$C_{20}H_{40}O_2$	312	1.25	0.62	ND
Squalene	30.01	$C_{30}H_{50}$	410	ND	ND	0.97
Heneicosan	30.88	$C_{21}H_{44}$	296	ND	ND	0.97
Vitamin E	34.06	$C_{29}H_{50}O_2$	430	ND	ND	0.58
Campesterol	35.43	$C_{28}H_{48}O$	400	ND	2.21	0.90
Stigmasterol	35.91	$C_{29}H_{48}O$	412	3.76	5.71	2.77
Gamma-Sitosterol	36.82	$C_{29}H_{50}O$	414	5.80	7.32	2.97
Ciclotrissiloxano, hexametil-	37.08	$C_6H_{18}O_3Si_3$	222	ND	0.03	ND
1,1,1,3,5,5,5-Heptamethyltrisiloxane	37.08	$C_7H_{21}O_2Si_3$	221	1.60	ND	ND
4,22-Stigmatidene-3-one	38.15	$C_{29}H_{46}O$	410	ND	ND	0.50
Bis(trimethylsilyl)diethylsilicate	39.27	$C_{10}H_{28}O_4Si_3$	296	0.94	1.08	ND
Sitostenone	39.29	$C_{29}H_{48}O$	412	ND	ND	0.81
Friedelin	41.03	$C_{30}H_{50}O$	426	13.72	12.40	9.10
TR	-	-	-	1.76	1.32	1.58

Abbreviations: RT, retention time (min); ND, not detected; TR, trace compound; MM, molecular weight.

Thus, this increase in compounds and/or percentage area suggests that plant cells were disrupted on the surface of the solute substrate, and/or the extraction of cells from the internal substrate was intensified with ultrasound (PEREIRA *et al.*, 2021). Other studies, such as Liu *et al.* (2020), De Souza *et al.* (2020), and Vidovic *et al.* (2014), found that the mechanical effects involved in ultrasound can accelerate internal and external diffusion, increasing mass transfer.

Table 8 shows that although the ethanol solvent presented a smaller quantity of compounds, it offered linolenic acid (29.34%) and friedelin (13.72%) with a higher percentage area than the other solvents used in the ultrasound-assisted extraction with supercritical extraction. When using the ethanol: water (50% v/v) solvent and water, a greater variety of compounds was obtained, where the major compounds were palmitic acid (22.14%) and linoleic acid (13.81%), respectively.

The four major compounds — linolenic acid, palmitic acid, linoleic acid, and friedelin — share a relevant biological activity: a potent anti-inflammatory effect (CORRÊA, 2018; ODEH *et al.*, 2016; CHHOUK *et al.*, 2018). This finding suggests that the extract of *C. spicatus* leaves may offer significant therapeutic benefits for symptom relief in individuals with inflammatory conditions.

It is important to highlight that there are no records in the literature on the use of the combined ultrasound extraction technique with supercritical fluids in the species *C. spicatus*, which makes this study pioneering in providing unprecedented information on the leaves of this plant. Thus, the results can be evaluated from different perspectives.

The influence of ultrasound pretreatment on supercritical extraction, in terms of chemical composition, was accentuated and can be seen in Figure 10. The enhanced percentage area of the compounds, linolenic acid, palmitic acid, linoleic acid, and friedelin, in UAE+SFE, with ethanol, ethanol: water, and water solvents, can be described by acoustic cavitation, originating from ultrasonication in the plant matrix. The decreasing order in terms of percentage area was UAE+SFE > macrotip (amplitude of 70% and 30%) > microtip (amplitude of 30%).

Figure 10. Comparison of the chemical profiles of *C. spicatus* leaf extracts obtained by macrotip (70 and 30%), microtip (30%) and UAE+SFE.

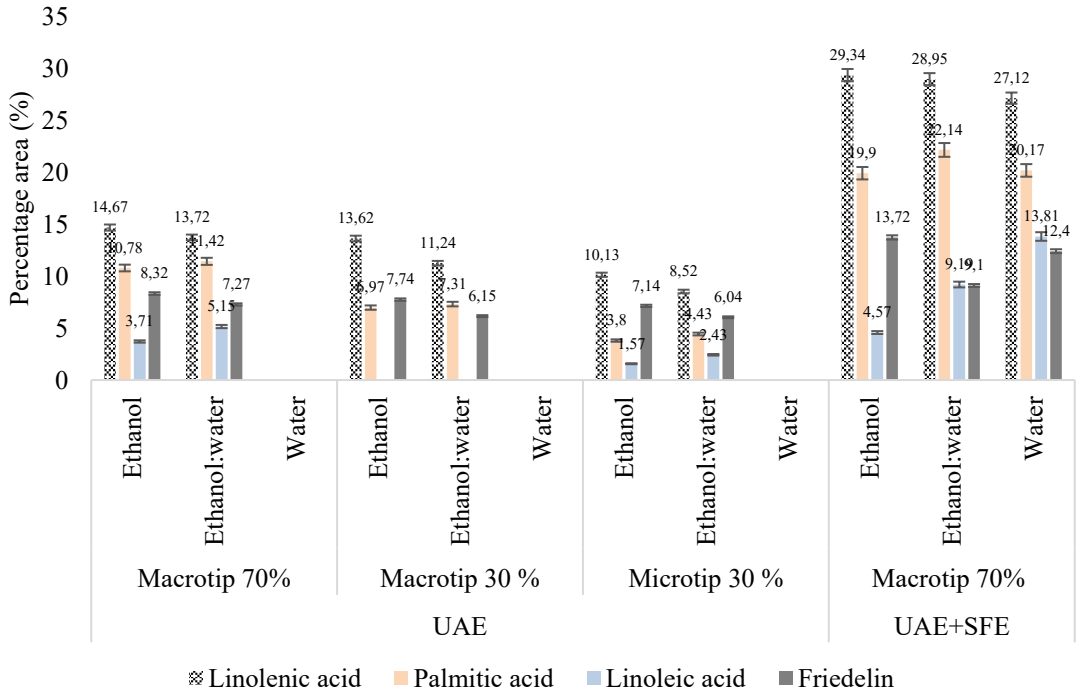

Abbreviations: UAE, ultrasound extraction; UAE + SFE, Ultrasonic pretreatment in supercritical CO_2 extraction; Extraction condition: UAE+SFE, all solvents in 5 min time; UAE with ethanol: 5min; UAE with ethanol: water and water, 1min time.

Comparing the results obtained in the previous Table, linolenic acid and friedelin presented the highest percentage area in the solvent with the lowest polarity index, ethanol, regardless of the technique applied, ultrasound or UAE+SFE. Palmitic acid presented the best result with the solvent ethanol: water (50% v/v) in all methodologies studied. However, linoleic acid was favored by the medium to high polarity solvent in ultrasound with ethanol: water (50% v/v) and in UAE+SFE with water.

The combination of UAE+SFE techniques offers several benefits, mainly due to its high capacity to disrupt cellular structures, which increases the accessibility of the solvent to the internal layers of the plant matrix. This improves intraparticle diffusivity and, consequently, enhances the extracts' quality. In addition, this combination can significantly increase extraction efficiency and reduce processing time, factors that are essential for the viability of the process (SORIA and VILLAMIEL, 2010).

As shown in Figure 10, the major compound in the UAE+SFE combination was linolenic acid, with 29.34%. Ultrasound pretreatment was beneficial in increasing the percentage area of this target compound when compared to the result obtained with the isolated techniques, ultrasound (macrotip, 70% amplitude, and ethanol) with 14.67% and SFE with 12.33% (LAURINTINO, 2020). GUO *et al.* (2020) and CALDER *et al.* (2018) found that linolenic acid has an anti-inflammatory effect and can act on the immune system, providing a positive impact on infectious diseases, such as COVID-19. Thus, the result presented in the present work demonstrates a very relevant application for the extract of the medicinal plant *C. spicatus*.

3.4 CONCLUSIONS

In this study, an improved process using ultrasonic pretreatment combined with supercritical CO_2 extraction was successfully performed, obtaining important bioactive compounds from Cana do brejo (*C. spicatus*) leaves, such as linolenic acid. The results showed that the extraction techniques and the nature of the solvent directly affected the extractive yields and the content of the metabolites present, which may infer biological and pharmacological activities.

The extract obtained with the solvent with a polarity index of 7.1, ethanol: water, favored the yield in all extraction techniques, MAC, SOX, UAE, and UAE+SFE, with

7.25, 18.74, 9.29, and 10.12%, respectively. It was also possible to observe that the organic solvents influenced the percentage of the major constituents, where the MAC technique (ethanol: water) obtained linolenic acid with 13.36% and SOX with glycerin (20.83%).

In the analysis of the ultrasound tests, it was found that using the macrotip at 70% amplitude in the ethanol: water solvent and for a time of 5 minutes increased the extract yield. However, under the same conditions, using ethanol, a solvent with a lower polarity index (5.2), resulted in the extraction of a greater quantity of compounds of commercial interest. Furthermore, with ethanol, regardless of the tip used (macrotip or microtip) and the amplitude applied (70% or 30%), the highest percentage of the relative area of the compounds was detected.

Combining the ultrasound technique with supercritical CO_2 provided a higher yield when compared to traditional UAE and SFE. In addition, UAE+SFE also improved the selectivity of the linolenic acid compound, with 29.34%, when compared to other extraction techniques, such as maceration (ethanol: water), Soxhlet (ethanol) and ultrasound (macrotip, amplitude 70%, ethanol, and 5 min) which obtained the following percentage areas, 13.36%, 6.97%, and 14.67%, respectively.

Consequently, UAE+SFE can be considered an efficient and environmentally friendly alternative to obtaining a high-quality extract from the leaves of Cana do brejo (*C. spicatus*). This combination of techniques provides an extract rich in linolenic acid, which can benefit human health in preventing infectious diseases such as COVID-19.

3.5 REFERENCES

ABDULLAH, R.R. Insecticidal Activity of Secondary Metabolites of Locally Isolated Fungal Strains against some Cotton Insect Pests. J. Plant Prot. Path., v. 10, nº 12, p. 647-653, 2019.

ADAMS, R. P. Identification of essential oil components by gas chromatography/ mass spectrometry, 4th Edition. Allured Publ., Carol Stream, IL Is out of print, 2007.

ALBUQUERQUE, J.N. Plantas medicinais de uso popular. Brasília: ABEAS, p. 100, 1989.

ALVES, T.P; TRIQUES, C.C.; PALSIKOWSHI, P.A.; SILVA, C.; FIORESE, M.L; SILVA, E.A.; KLEN, M.R.F. Improved extraction of bioactive compounds from

Monteverdi aquifolia leaves by pressurized-liquid and ultrasound-assisted extraction: Yield and Chemical composition. J. Supercrit. Fluids, v. 181, 105468, 2022.

AOAC. Association of official analytical chemist, official methods of analysis, 18, a. AOAC International, Maryland, 2005.

AMORIM, J.M.; SOUZA, L.C.; SOUZA, R.A.L.; FILHA, R.S.; SILVA, J.O.; ARAÚJO, S.A.; TAGLITI, C.A; SIMÕES, A.C.; CASTILHO, R.O. Costus spiralis extract restores kidney function in cisplatin-induced nephrotoxicity model: Ethnopharmacological use, chemical and toxicological investigation. Journal of Ethnopharmacology, v.299, nº 5, 115510, 2022.

ANDERSON, E.; SOTTILDUPRAT, S.; SCHESKE, C. Design of an Improved Pyrolyzer to Support Biochar Research on MacDonald Campus.2019.

ANDRADE, K. S. Avaliação das técnicas de extração e do potencial antioxidante dos extratos obtidos a partir de casca e de borra de café (*Coffea arábica* L.). Dissertação (Mestre em Engenharia de Alimentos). Departamento de Engenharia Química e Engenharia de Alimentos. Universidade Federal de Santa Catarina, Florianópolis - SC, 2011.

AHMED, M.; PEIWEN, Q.; GU, Z.; LI, Y.; SIKANDAR, A.; HUSSAIN, D. *ET AL.* Insecticidal activity and biochemical composition of *Citrullus colocynthis*, Cannabis indica and *Artemisia argyi* extracts against cabbage aphid (*Brevicoryne brassicae* L.). Sci. Rep., v. 10, p. 522, 2020.

ARA, K.M.; KARAMI, M., RAOFIE, F. Application of response surface methodology for the optimization of supercritical carbon dioxide extraction and ultrasound-assisted extraction of *Capparis spinosa* seed oil**.** J. Supercrit. Fluids, nº 85, p. 173-182, 2014.

AZMIR, J.; ZAIDUL, I.S.M.; RAHMAN, M.M.; SHARIF, K.M.; MOHAMED, A.; SAHENA, F.; JAHURUL, M.H.A.; GHAFOOR, K.; NORULAINI, N.A.N.; OMAR, A.K.M. Techniques for extraction of bioactive compounds from plant materials: a review. Journal of Food Engineering, v. 117, nº 4, p. 426–436, 2013.

AZEVEDO, L.F.P.; FARIA, T.S.A.; PESSANHA, F.F.; ARAUJO, M.F.; LEMOS, G.C.S. Triagem fitoquímica e atividade antioxidante de Costus spicatus (Jacq.) S.w. Rev. Bras. PI. Med., Campinas, v.16, nº 2, p. 209-215, 2014.

BAJPAI, V.K., BAEK, K.H., KANG, S.C. Control of Salmonella in foods by using essential oils: a review. Food Res. Int. 45, p. 722–734, 2012.

BALACHANDRAN, S.; KENTISH, S.E.; MAWSON, R.; ASHOKKUMAR, M. Ultrasonic enhancement of the supercritical extraction from ginger, v. 13, nº 6, p. 471-479, 2006.

BATISTA, R. B. *et al.* Caracterização bioquímica e cinética de lipoxigenases de plantas de soja submetidas à aplicação de ácidos graxos poliinsaturados. Pesq. agropec. bras., Brasília, v. 37, nº 11, p. 1517-1524, 2002.

BAKKALI, F., AVERBECK, S., AVERBECK, D., IDAOMAR, M. Biological effects of essential oils – a review. Food Chem. Toxicol. n. 46, p. 446–475, 2008.

BARBA F.J., ROSELLÓ-SOTO E., MARSZAŁEK K., BURSAĆKOVAČEVIĆ D., REŽEKJAMBRAK A., LORENZO J.M., CHEMAT F., PUTNIK P. Green food processing: concepts, strategies, and tools. Green Food Process. Tech. p. 1–21, 2019.

BARRALES, F.M.; REZENDE, C.A.; MARTÍNEZ. J. Supercritical CO_2 extraction of passion fruit (Passiflora edulis sp.) seed oil assisted by ultrasound, J. Supercrit. Fluids, v. 104, p. 183-192, 2015.

BHALLA, N.; INGLE, N.; PATRI, S.; HARANATH, D. Phytochemical analysis of Moringa Oleifera leaves extracts by GC-MS and free radical scavenging potency for industrial applications. Saudi Journal of Biological Sciences, v. 28, nº 12, p. 6915-6928, 2021.

BENELLI, P. Agregação de valor ao bagaço de laranja (Citrussinensis L. Osbeck) mediante obtenção de extratos bioativos através de diferentes técnicas de extração. Dissertação (mestrado), Centro Tecnológico. Programa de Pós-Graduação em Engenharia de Alimentos, Universidade Federal de Santa Catarina, Florianópolis – SC, 2010.

BELWAL, T.; EZZAT, S. M.; RASTRELLI, L.; BHATT, I. D.; DAGLIA, M.; BALDI, A.; DEVKOTA, H. P.; ORHAN, I. E.; PATRA, J. K.; DAS, G.; ANANDHARAMAKRISHNAN, C.; GOMEZ-GOMEZ, L.; NABAVI, S. F.; NABAVI, S. M.; ATANASOV, A. G. A critical analysis of extraction techniques used for botanicals: Trends, priorities, industrial uses and optimization strategies. TrAC - Trends in Analytical Chemistry, v. 100, p. 82–102, 2018.

BIMAKR, M. *et al.* Comparison of different extraction methods for the extraction of major bioactive flavonoid compounds from spearmint (*Mentha spicata* L.) leaves. Food and Bioproducts Processing**,** n. 1, v. 89, p. 67–72, 2011.

BISCAIA, D. Comparação entre tecnologia supercrítica e técnicas convencionais de extração para obtenção de extratos de própolis avaliados através de suas atividades biológicas. Dissertação (Mestrado em Engenharia de Alimentos), Departamento de Engenharia Química e Engenharia de Alimentos, Universidade Federal de Santa Catarina, Florianópolis – SC, 2007.

BITENCOURT, A. P. R., ALMEIDA, S. S. M. S. Estudo fitoquímico, toxicológico e microbiológico das folhas de Costus spicatus Jacq. Biota Amazônia, nº 4, v. 4, p. 75-79, 2014.

BLONDEAU, N., LIPSKY, R.H., BOUROUROU, M., DUNCAN, M.W., PHILIP, 2015. Alpha-Linolenic Acid: An Omega-3 Fatty Acid with Neuroprotective Properties—Ready for Use in the Stroke Clinic? https://doi.org/10.1155/2015/519830.

BOORHEM, R.L. *et al.* Segredos e virtudes das plantas medicinais. Rio de Janeiro: Reader'sDigest Brasil Ltda, p.416, 1999.

BORRÁS, M.R.L. Plantas da Amazônia: medicinais ou mágicas - Plantas comercializadas no mercado Adolpho Lisboa. Manaus: Valer, p. 322, 2003.

BORGES, P. M. O. Avaliação da atividade tóxica e do perfil fitoquímico de Costusspicatus e Jatrophamultifica. Trabalho de conclusão do curso (Licenciatura em Química), Coordenação de Química, Instituto Federal de Educação, Ciência e Tecnologia de Goiás, Anápolis, 2016.

Brazil. Ministry of Health. Secretariat of Science, Technology and Strategic Inputs. Department of Pharmaceutical Assistance and Strategic Inputs. National Policy of Medicinal Plants and Herbal Medicines, v. 189, Ministry of Health, Brasilia, 2016.

BRUNNER, G. Gas extraction: An introduction to fundamentals supercritical fluid sand the application to separation processes. New York: Springer, 1994.

BRUNNER, G. Supercritical fluids: technology and application to food processing. Journal of Food Engineering, v. 67, p. 21-33, 2005.

BRUNING, M. C. R.; MOSEGUI, G. B. G. VIANNA, C. M. de M. A utilização da fitoterapia e de plantas medicinais em unidades básicas de saúde nos municípios de Cascavel e Foz do Iguaçu – Paraná: a visão dos profissionais de saúde. Revista Ciência e Saúde Coletiva – OPINIÃO, p. 2675 – 2685, 2012.

CARRERA, C. *et al.* Analytica Chimica Acta Ultrasound assisted extraction of phenolic compounds from grapes. Analytica Chimica Acta**,** v. 732, p. 100–104, 2012.

CALDER, P.C.; CARR, A.C.; GOMBART, A.F.; EGGERSDORFER, M. Optimal nutritional status for a well-functioning immune system is an important factor to protect against viral infections. Nutrients, v.12, p. 1181, 2020.

CALDER, P.C.; ADOLPH, M.; DEUTZ, N.E.; GRAU, T.; INNES, J.K.; KLEK, S.; LEV, S.; MAYER, K.; MICHAEL-TITUS, A.T.; PRADELLI, L.; PUDER, M.; VLAARDINGERBROEK, H.; SINGER, P. Lipids in the intensive care unit: recommendations from the ESPEN expert group. Clin. Nutr, v. 37, p. 1-18, 2018.

CHHOUK, K.; WAHYUDIONO.; KANDA, H.; GOTO, M. Efficacy of supercritical carbon dioxide integrated hydrothermal extraction of Khmer medicinal plants with potential pharmaceutical activity. Journal of Environmental Chemical Engineering, v.6, p. 2944–2956, 2018.

CHEMAT, F. *et al.* Ultrasound assisted extraction of food and natural products. Mechanisms, techniques, combinations, protocols and applications. A review. Ultrasonics Sonochemistry, v. 34, p. 540–560, 2017.

CHEN, F. YANG, X. MA, Y. WANG, X. LUO, D. YANG, L. YANG, Y. Synthesis and application of novel silver magnetic amino silicone adhesive particles for preparation of high purity α-linolenic acid from tree peony seed oil under applied magnetic field. Journal of Chromatography A, v.1610, p.460-540, 2020.

CHHOUK, K.; WAHYUDIONO.; KANDA, H.; GOTO, M. Efficacy of supercritical carbon dioxide integrated hydrothermal extraction of Khmer medicinal plants with potential pharmaceutical activity. Journal of Environmental Chemical Engineering, v.6, p. 2944–2956, 2018.

COELHO, F.C.; TIRLONI, C.A.S.; MARQUES, A.A.M.; GASPAROTTO, F.M.; LÍVERO, F.A.R.; A. Gasparotto Junior. Traditional plants used by remaining healers from the region of Grande Dourados, Mato Grosso do Sul, Brazil. J. Relig. Health, nº 58, p. 572-588, 2019.

CORRÊA, A. J. C. Contribuição do conhecimento popular para a descoberta de novos antimicrobianos. Tese (Doutor em Ciências Farmacêuticas), Universidade Federal de Pernambuco, Recife – PE, 2018.

CORREA, M. S. Extração de inflorêscencia da bababeira (*Musa paradisíaca* L.) utilizando CO_2 supercrítico e propano comprimido. Dissertação (Mestre em Engenharia de Alimentos), Curso de Pós-Graduação em Engenharia de Alimentos, Universidade Federal do Paraná, Curitiba, 2016.

CRUZ, P. N. Extração e encapsulação supercrítica de extratos de folhas e flores de yacon (*Smallanthus sonchifolius*). Tese (Doutorado em Engenharia de Alimentos), Pós graduação em Engenharia de Alimentos, Universidade Federal do Paraná, Curitiba, 2019.

DA PORTO, C.; NATOLINO, A.; DECORTI, D. The combined extraction of polyphenols from grape marc: Ultrasound assisted extraction followed by supercritical CO_2 extraction of ultrasound-raffinate. LWT - Food Science and Technology, v. 61, nº 1, p. 98-104, 2015.

DASSOFF, E.; LI, Y. 2019. Mechanisms and effects of ultrasound-assisted supercritical CO_2 extraction. Trends in Food Science & Technology, v. 86, p. 492-501, 2019.

DASH, D.R.; PATHAK, S.S.; PRADHAN, R.C. Extraction of oil from Terminalia chebula kernel by using ultrasound technology: Influence of process parameters on extraction kinetics. Industrial Crops and Products, v. 171, 113893, 2021.

DE MELO, M.M.R.; SILVESTRE, A.J.D.; SILVA, C.M. Supercritical fluid extraction of vegetable matrices: applications, trends and future perspectives of a convincing green technology**.** J. Supercrit. Fluids, nº 92, p. 115-176, 2014.

DE SOUZA, A.M.; LARA, L.D.; PREVIATO, J.O.; LOPES, A.G.; CARUSO-NEVES, C.; DA SILVA, B.P.; PARENTE, J.P. Modulation of sodium pumps by steroidal saponins. Zeitschrift Fur Naturforschung C - A Journal of Biosciences, v.59, p.432-436, 2004.

DE SOUZA, R.D.; MACHADO, B.A.S.; BARRETO, G.D.; LEAL, I.L.; DOS ANJOS, J.P.; UMSZA-GUEZ, M.A. Effect of experimental parameters on the extraction of grape seed oil obtained by low pressure and supercritical fluid extraction. Molecules, v. 25, p. 1634, 2020.

DEVENDRAN, G.; SIVAMANI, G. Phytochemical analysis of leaf extract of plant *Costus spicatus* by gcms method. J. Drug Deliv. Therapeut., v. 5, nº 4, p. 24-26, 2015.

DIAS, A.L.B.; AGUIAR, A.C.; ROSTAGNO, M.A. Extraction of natural products using supercritical fluids and pressurized liquids assisted by ultrasound: Current status and trends. Ultrasonics sono chermistry, 105584, 2021.

DIAS, J.L. Extração supercrítica e técnicas convencionais de extração na obtenção de compostos bioativos da semente de umbu (*Spondias tuberosa*). Dissertação (Mestre em Engenharia Química). Programa de pós-graduação em Engenharia Química, Universidade Federal de Santa Catarina, Florianópolis, 2017.

EDVARDSSON, V.O.; INDRIDASON, O.S.; HARALDSSON, G.; KJARTANSSON, O.; PALSSON, R. Temporal trends in the incidence of kidney stone disease. Kidney Int., 83, p. 146-152, 2013.

FERRO, D.M. Guanxuma (*Sida rhombifolia*L.): Obtenção de extratos com potencial antioxidante por métodos à alta pressão e encapsulação via *spray-drying.* Tese (Doutor

em Engenharia de Alimentos). Programa de pós-graduação em Engenharia de Alimentos, Universidade Federal de Santa Catarina, Florianópolis, 2019.

FERRO, D.M.; MAZZUTTI, S.; CARMEN, L.V.; MULLER, M.O.; FERREIRA, S.R.S. Integrated extraction approach to increase the recovery of antioxidant compounds from Sida rhombifolia leaves. The Journal of Supercritical Fluids, v. 149, p. 10-19, 2019.

FIORI, L.; BASSO, D.; COSTA, P. Supercritical extraction kinetics of seed oil: a new model bridging the "broken and intact cells" and the "shrinking-core" models. J. Supercrit. Fluids, nº 48, p. 131-138, 2009.

GANESAN, D.; SIVAMANI, G. Phytochemical analysis of leaf extract of plant Costus spicatus by GCMS method. Journal of Drug Delivery & Therapeutics. nº 5, p. 24-26, 2015.

GLUECKAUF. E. Theory of chromatography. Part 10. Formulae for diffusion into spheres and their application to chromatography. Trans. Faraday Soc., nº 51, p. 1540-1551, 1955.

GLISIB, S.B.; RISTIC, M.; SKALA, D.U. The combined extraction of sage (*Salvia officinalis* L.): Ultrasound followed by supercritical CO_2 extraction. Ultrasonics Sonochemistry, v.18, nº1, p. 318-326, 2011.

GOC, A.; NIEDZWIECKI, A.; RATH, M. Polyunsaturated omega-3 fatty acids inhibit ACE2-controlled SARS-CoV-2 binding and cellular entry. Sci. Rep., v.11, p. 5207, 2021.
GOMIDE, R. Operações unitárias – operações com sistemas sólidos granulares. Edição do Autor. São Paulo: Reynaldo Gomide, v. 3, p. 289, 1983.

GOULA, A.M. Ultrasound-assisted extraction of pomegranate seed oil – Kinetic modeling. Journal of Food Engineering, v.117, p. 492 – 498, 2013.
GOTO, M.; ROY, B.C.; HIROSE, T. J. Supercrit. Fluids, nº 9, p. 128, 1996.

GUO, Y.R.; CAO, Q.D.; HONG, Z.S.; TAN, Y.Y.; CHEN, S.D.; JIN, H.J.; SEN TAN, K.; WANG, D.Y.; YAN, Y. The origin, transmission and clinical therapies on coronavirus disease 2019 (COVID-19) outbreak- A n update on the status. Mil. Med. Res., v. 7, p. 1-10, 2020.

HORMAZA, L. C.; DUQUE, L.; PARRA, S.L.; OSÓRIO, E. High-intensity ultrasound-assisted extraction of Garcinia madruno biflavonoids: Mechanism, kinetics, and productivity. Biochemical Engineering Journal, v. 161, 107676, 2020.

HUANG, Z.; SHI, X.H.; JIANG, W.J. Theoretical models for supercritical fluid extraction. Journal of Chromatography A, v. 1250, p. 2-26, 2012.

KADERIDES, K.; GOULA, A.M.; ADAMOPOULOS, K.G. A process for turning pomegranate peels into a valuable food ingredient using ultrasound-assisted extraction and encapsulation. Innovative Food Science & Emerging Technologies, v. 31, p. 204-215, 2015.

KALPANA, K.; KAPIL, S.; HARSH, P.S.; BIKRAM, S. Effects of extraction methods on phenolic contents and antioxidant activity in aerial parts of *Potentilla atrosanguinea* Lodd. and quantification of its phenolic constituents by RP-HPLC. Journal of Agricultural and Food Chemistry, v. 56, p. 10129-10134, 2008.

KOUBA, A. M., MHEMDI, H., FAGES, J. Recovery of valuable component sandin activating microorganisms in the agro-food industry with ultrasound-assisted supercritical fluid technology. J. Supercrit. Fluids. v.134, p.71–79, 2018.

LAURININO, T. N. S. Avaliação do potencial do extrato e do óleo essencial de Palo santo (*Bursera graveolens*) para aplicação em produtos inseticidas. Dissertação (mestrado), Programa de Pós-Graduação em Engenharia Química, Universidade Federal de Santa Catarina, Florianópolis - SC, 2017.

LAURININO, T. K. S. Avaliação de compostos bioativos e potencial antioxidante da folha e caule da cana do brejo (*Costus spicatus*) diferentes métodos de extração. Dissertação (mestrado), Programa de Pós-Graduação em Engenharia Química, Universidade Federal de Santa Catarina, Florianópolis - SC, 2020.

LEIGHTON.T. Acoustic Bubble. Academic Press, London, 1994.

LEILA, M.; RATIBA, D.; MARZOUQI, A. Experimental and mathematical modelling data of green process of essential oil extraction: Supercritical CO_2 extraction. Materials today: proceedings. v.49, p. 1023-1029, 2022.

LEITE, J. P. V. Fitoterapia: Bases científicas e tecnológicas. São Paulo: Atheneu, p. 328, 2009.

LIMA, S.V.M. Simulação numérica do escoamento reativo no reator fluhelik: investigação da degradação fotocatalítica da oxitetraciclina. Dissertação (mestrado), Centro Tecnológico. Programa de Pós-Graduação em Engenharia Química, Universidade Federal de Santa Catarina, Florianópolis – SC, 2020.

LIN, L. Introduction to the Finite Element Method. Berkeley University. Berkeley, 2006. U.S, >. Retrieved from: https://lwlin.me.berkeley.edu/me128/FEMNotes.pdf

LIU, X.; OU, H.; XIANG, Z.; GREGERSEN, H. Ultrasound pretreatment combined with supercritical CO_2 extraction of Iberis amara seed oil. Journal of Applied Research on Medicinal and Aromatic Plants, v. 18, 100265, 2020.

LORENZI, H.; MATOS, F. J. A. Plantas Medicinais no Brasil: nativas e exóticas. Nova Odessa, SP: Instituto Plantarum, Edição 2, p. 222. 2002.

LUQUE DE CASTRO, M. D.; PRIEGO-CAPOTE, F. Soxhlet extraction: Pastand presente panacea. Journal of Chromatography A**,** v. 1217, n. 16, p. 2383–2389, 16 abr. 2010.

LUQUE-GARCÍA, J. L.; CASTRO, M. D. L. Ultrasound: a powerful tool for leaching. Trends in Analytical Chemistry, v. 22, n. 1, p. 41-47, 2003.

MADHAVAN, S.A.; SENTHILKUMAR, S.; ANDREWS, S.; GANESAN, S. Anti-diabetic effect of ethanol extract of *Costus spicatus* jacq. In rhizome extract in streptozotocin-induced diabetic rats –histological study. J. Drug Deliv. Therapeut., v. 9, nº 4, p. 483-487, 2019.

MANFRED, L. 7000 Recetas Botnicas a Base de 1,300 Plamtas Medicinales Americanas. Buenos Aires: Editorial Kier, 1947.

MARIOT, M. P.; BARBIERI, R. L. Metabolitos secundários e propriedades medicinais de espinheira-santa (*Maytenus ilicifolia* Mart. Ex Reiss. E *M. aquifolium* Mart.). Rev. Bras. Pl. Med., Botucatu, v.9, n.3, p.89-99, 2007.

MARSOUL, A.; LJJAALI, M.; OUMOUS, I.; BERNNANI, B.; BOUKIR, A. Determination of polyphenol contents in Papaver rhoeas L. flowers extracts (soxhlet, maceration), antioxidant and antibacterial evaluation. Material stoday: proceedings, v. 31, p. 183-189, 2020.

MAZZUTTI, S.; FERREIRA, S.R.S.; RIEHL, C.A.S.; SMANIA Jr, A; SMANIAC, F.A.; MARTÍNEZ, J. Supercritical fluid extraction of *Agaricus brasiliensis*: antioxidant and antimicrobial activities. The Journal of Supercritical Fluids, v. 70, p. 48–56, 2012.

MAZZUTI, S.; RIEHL, C.A.S, IBAÑEZ, E.; FERREIRA, S.R.S. Green-based methods to obtain bioactive extracts from Plantago major and Plantago lanceolata. The Journal of Supercritical Fluids, v. 119 p. 211–220, 2017.

MCQUEEN, DH. Ultrasonics, nº 28, p. 422, 1990.

MELO, M. M. R.; SILVESTRE, A. J. D.; SILVA, C. M. Supercritical fluid extraction of vegetable matrices: Applications, trends and future perspectives of a convincing green technology. The Journal of Supercritical Fluids, v. 92, p. 115–176, 2014.

MOE, O.W. Kidney stones: pathophysiology and medical management. Lancet, 367, p. 333-344, 2006.

MORENO, K. G. T., JUNIOR, A. G., DOS SANTOS, A. C., PALOZI, R. A. C., GUARNIER, L. P., MARQUES, A. A. M., & DE BARROS, M. E. Nephroprotective and antilithiatic activities of Costus spicatus (Jacq.) Sw.: Ethnopharmacological investigation of a species from the Dourados region, Mato Grosso do Sul State, Brazil. Journal of Ethnopharmacology, v. 266, 113409, 2021.

MOYLER, D. A. Extraction of essential oils with carbon dioxide. Flavour and fragrance journal, v. 8, p. 235-247, 1993.

MUSTAFA, A.; TURNER, C. Pressurized liquid extraction as a green approach in food and herbal plants extraction: A review. Analytica Chimica Acta, v. 703, n. 1, p. 8–18, 2011.

NAIK, M.; NATARAJAN, V.; MODUPALLI, N.; THANGARAJ, S.; RAWSON, A. Pulsed ultrasound assisted extraction of protein from defatted Bitter melon seeds

(Momardica charantia L.) meal: Kinetics and quality measurements. LWT, v. 155, 112997, 2022.

NIST. Webbook, Instituto Nacional de Normas e Tecnologia – NIST, 2018.

ODEH, I. C.; TOR-ANYIIN, T. A.; IGOLI, J. O.; ANYAM, J. V. In vitro antimicrobial properties of friedelan-3-one from PterrocarpussantalinoidesL‟‟Herit, ex Dc. African Journal of Biotechnology, v.15, p. 531-538, 2016.

OLIVEIRA, G. C. Plantas medicinais utilizadas em comunidades rurais do município de Alagoa Nova – PB. Trabalho de conclusão de curso (graduação em biologia), Universidade Estadual da Paraíba, Centro de Ciências Biológicas e da Saúde, Campina Grande, 2012.

OLIVEIRA, V.B.1.; ZUCHETTO, M.; OLIVEIRA, C.F.; PAULA, C.S.; DUARTE, A.F.S.; MIGUEL, M.D.; MIGUEL, O.G. Efeito de diferentes técnicas extrativas no rendimento, atividade antioxidante, doseamentos totais e no perfil por clae-dad de dicksoniasellowiana (presl.). Hook, dicksoniaceae. Rev. Bras. Pl. Med., Campinas, v.18, nº 1, p.230-239, 2016.

OLIVEIRA, E.L.G.; SILVESTRE, A.J.D.; SILVA, C.M. Review of kinetic models for supercritical fluid extraction. Chemical Engineering Research and Design, v. 89, nº 7, p. 1104-1117, 2011.

PAES, L.S.; MEDONÇA, M.S.; CASAS, L.L. Aspectos Estruturais e Fitoquímicos de partes vegetativas de Costus spicatus (Jacq.) Sw. (Costaceae). Rev. bras. Plantas med, v. 15, nº 3, 2013.

PEDROSA, D. M. Análise de perfil químico e investigação dos potenciais antioxidantes, antibacteriano e citotóxico in vitro de extratos obtidos do caule de Costus spicatusSwartz (Costaceae). Trabalho de conclusão de curso (grau de Farmacêutico), Faculdade de Farmácia da Universidade Federal de Juiz de Fora, Juiz de Fora, 2017.

PEREIRA, C. G.; MEIRELES, M. A. A. Supercritical Fluid Extraction of Bioactive Compounds: Fundamentals, Applications and Economic Perspectives. Food and Bioprocess Technology, v. 3, n. 3, p. 340–372, 2010.

PEREIRA, D.T.V.; ZABOT, G.L.; REYES, F.G.R.; MARTÍNEZ, J. Integration of pressurized liquids and ultrasound in the extraction of bioactive compounds from passion fruit rinds: Impact on phenolic yield, extraction kinetics and technical-economic evaluation. Innovative Food Science & Emerging Technologies, v. 67, 102549, 2021.

PICANÇO, L.C.S.; BITTENCOURT, J.A.H.M.; HENRIQUES, S.V.C.; SILVA, J.S.; OLIVEIRA, J.M.S.; RIBEIRO, J.R.; SANJAY, A.-B.; CARVALHO, J.C.T.; STIEN, D.; SILVA, J.O. Pharmacological activity of *Costus spicatus* in experimental Bothrops atrox envenomation. Pharm. Biol., 54, p. 2103-2110, 2016.

PICÓ, Y. Ultrasound-assisted extraction for food and environmental samples. TrAC - Trends in Analytical Chemistry, v. 43, p. 84–99, 2013.

PIES, G. Tecnologia supercrítica aplicada à obtenção de extratos ricos em compostos fenólicos a partir de casca de jabuticaba Pliniatrunci flora (O. Berg) Kausel. Dissertação (Mestre em Engenharia de alimentos), Programa de pós-graduação em Engenharia de Alimentos, Universidade Federal de Santa Catarina, Florianópolis-SC, 2017.

PINNA, F.L. *et al.* Prospecção fitoquímica e avaliação da atividade cicatrizante do spray a base de *Costus spicatus* Jacq. In: Reunião anual da sociedade brasileira de química, v.31, 2008.

POURMORTAZAVI, S. M.; HAJIMIRSADEGHI, S. S. Supercritical fluid extraction in plant essential and volatile oil analysis. Journal of Chromatography A, v. 1163, n. 1-2, p. 2–24, 2007.

POTDAR, S.; BAGALE, U. POTOROKO, I.; HAKKE, V.S.; MARALLA, Y.; SIVAKUMAR, M.; SONAWANE, S. Sonochemical approach for the synthesis of safflower oil based low fat emulsion: Effectof ultrasonic parameters. Material stoday: proceedings, v. 57, p. 1619-1625, 2022.

QUINTANS JÚNIOR, L.J; SANTANA, M.T.; MELO, M.S.; SOUSA, D.P.I.; SANTOS, S.; SIQUEIRA, R.S.; LIMA, T.C.; SILVEIRA, G.O.; ANTONIOLLI, A.R.; RIBEIRO, L.A.A.; SANTOS, M.R.V. Antinociceptive and anti-inflammatory effects of *Costus spicatus* in experimental animals**.** Pharm. Biol., 48, p. 1097-1102, 2010.

RAHMANIAN, N.; JAFARI, S.M.; WANI, T.A. Bioactive profile, dehydration, extraction and application of the bioactive components of olive leaves. Trends Food Sci. Technol., nº 42, p. 150-172, 2015.

RAJ, G.V.S.B.; DASH, K. K. Ultrasound-assisted extraction of phytocompounds from dragon fruit peel: Optimization, kinetics and thermodynamic studies. Ultrasonics Sonochemistry, v. 68, 105180, 2020.

RAKSHIT, M. SRIVASTAV, P.P.; BHUNIA, K. Kinetic modeling of ultrasonic-assisted extraction of punicalagin from pomegranate peel. Journal of Food Process Engineering, v. 43, 2020.

REVERCHON, E.; MARRONE, C. Modeling and simulation of the supercritical CO_2 extraction of vegetable oils. J. Supercrit. Fluids, nº 19, p. 161-175, 2001.

RITCHIE, M. QTL mapping; a user's guide, 2000.

RUDKE, A.R. Obtenção de extratos de resíduos de buriti (*Mauritia Flexuosa* L.*)* por diferentes técnicas de extração e avaliação do seu potencial antioxidante. Dissertação (Mestre em Engenharia de Alimentos). Programa de pós-graduação em Engenharia de Alimentos, Universidade Federal de Santa Catarina, Florianópolis, 2019.

SAGIV A.E., DIKSTEIN S., INGBER A. The efficiency of humectants as skin moisturizers in the presence of oil. PubMed, S.R&T, v. 7, nº 1, p.32-5, 2001.

SANTANA, H. S. *et al.* Computational methodology for the development of microdevices and microreactors with ANSYS CFX. Methods X, v. 7, p. 82–103, 2020.

SANTESTEVAN, V. A. Desenvolvimento de metodologia para a análise de óleo de arroz. Dissertação (Mestre em Química), Programa de Pós-Graduação em Química, Universidade Federal do Rio Grande do Sul, Porto Alegre, 2011.

SANTOS, P.; AGUIAR, A.C.; BARBERO, G.F.; REZENDE, A.A.; MARTÍNEZ, J. Supercritical carbon dioxide extraction of capsaicinoids from malagueta pepper (*Capsicum frutescens* L.) assisted by ultrasound. Ultrasonics Sonochemistry, v.22, p. 78-88, 2015.

SANTOS, T.A. Avaliação de diferentes métodos e solventes de extração sobre a composição fenólica e centesimal, atividade antimicrobiana e citotóxica de extratos dos frutos da Momordica charantia L. Trabalho de conclusão de curso, departamento de farmácia, Universidade Federal de Sergipe, Lagarto, 2008.

SANTOS, P.H.; RIBEIRO, D.H.B.; MICKE, G.A.; VITALI, L.; HENSE, H. Extraction of bioactive compounds from feijoa (Acca sellowiana (O. Berg) Burret) peel by lowand high-pressure techniques. Supercrit. Fluids, v. 145, p. 219-227, 2019.

SARTOR, R. B. Modelagem, Simulação e Otimização de uma Unidade Industrial de Extração de Óleos Essenciais por Arraste a Vapor. Dissertação (Mestrado em Pesquisa e Desenvolvimento de Processos). Escola de Engenharia, Universidade Federal do Rio Grande do Sul. Porto Alegre, 2009.

SARKAR, S.; SINGH, I.V.; MISHRA, B.K. A simple and efficient implementation of localizing gradient damage method in COMSOL for fracture simulation. Engineering Fracture Mechanics, v. 269, 108552, 2022.

SERRA, A. T. *et al.* Processing cherries (Prunus avium) using supercritical fluid technology. Part 1: Recovery of extract fractions rich in bioactive compounds. The Journal of Supercritical Fluids, v. 55, n. 1, p. 184–191, 2010.

SHARMA, S.; CHHIBBER, S.; MOHAN, H.; SHARMA, S. Dietary supplementation with omega-3 polyunsaturated fatty acids ameliorates acute pneumonia induced by Klebsiella pneumoniae in BALB/c mice. Can. J. Microbiol., v. 59, p. 503-510, 2013.

SILVA, D. N.; GONÇALVES, M.J.; AMORAL, M.T.; BATISTA, M.T. Antifungal activity of a flavonoid-rich fraction from *Costus spicatus* leaves against dermatophytes. Planta Medica, v.74, n.9, p.961-961, 2008.

SILVA, C. M. A. Metabólitos secundários de plantas dos semi-árido de Pernambuco – uma inovação no controle de fitopatógenos. Dissertação de mestrado (mestre) – Título de mestre em Bioquímica e Fisiologia Universidade Federal de Pernambuco, Recife, 2013.

SILVA, B.P. *et al.* Flavonol glycosides from *Costus spicatus.* Phytochemistry, v.53, nº1, p.87-92, 2000.

SILVA, F. C.; DUARTE, L.P.; VIEIRA FILHO, S. A. Celastráceas: fontes de triterpenos pentacíclicos com potencial atividade biológica. Revista virtual química, v.6, n. 5, p. 1205-1220, 2014.

SIQUEIRA, S.; SILVA, V.S.F.; AGRA, M.F.; DARIVA, C.; JÚNIOR, J.P.S.; FONSECA, M.J.V. Biological activities of Solanum paludosum Moric. extracts obtained by maceration and supercritical fluid extraction. The Journal of Supercritical Fluids, v. 58, n. 3, p. 391–397, 2011.

SIVASUBRAMANIAN, R., BRINDHA, P. In-vitro cytotoxic, antioxidant and GC-MS studies on Centratherum punctatum Cass. Int. J. Pharm. Pharm. Sci, v. 5, nº 3, p. 364-367, 2013.

SIMÕES, C. M. O.; SPITZER, V. Óleos voláteis. In: SIMÕES, C.M.O *et al.* Farmacognosia: da planta ao medicamento. 5. ed. Porto Alegre/Florianópolis: Editora UFRGS/ Editora UFSC, 2003.

SOLANKI, S.; BARUAH, B.; TIWARI, P. Modeling and simulation of wood pyrolysis process using COMSOL Multiphysics. Bioresource Technology Reports, v. 17, 100941, 2022. (BARUAH e TIWARI, 2022).

SORIA, A.C.; VILLAMIEL, M. Effect of ultrasound on the technological properties and bioactivity of food: a review. Trends in Food Science & Technology, v. 21, nº 7, p.323-331, 2010.

SOUZA, D.R; RODRIGUES, E. C. A. M. S. Plantas medicinais: indicação de raizeiros para o tratamento de feridas. Revista Brasileira em Promoção da Saúde, v. 29, nº 2, p. 198-203, Fortaleza, 2016.

SOUZA, S.P.; PEREIRA, L.L.S.; SOUZA, A.A.; SANTOS, C.D. Seleção de extratos brutos de plantas com atividade antiobesidade. Rev. Bras. Plantas Med., 14, p. 643-648, 2012.

SOVOVÁ, H. Rate of the vegetable oil extraction with supercritical CO_2. I. Modelling of extraction curves. Chem. Eng. Sci., nº 49, p. 409-414, 1994.

SUSLICK, K.S.; PRICE, G.J. Applications of ultrasound to materials chemistry. Annu. Rev. Mater. Sci., v. 29, p. 295-326, 1999.

SUFLUX. Supercritical plant. Disponível em:http://www.suflux.com. Acesso em: 12 agosto. 2021.

SUSANNA, D.; BALAKRISHNAN, R.M.; ETTIYAPPAN, J.P. Comprehensive insight into the extract optimization, phytochemical profiling, and biological evaluation of the medicinal plant Nothapodytes foetida. Biocatalysis and Agricultural Biotechnology, v. 42, 102365, 2022.

TAYLOR, L.T. Supercritical Fluid Extraction, Wiley Interscience, New York, 1996. https://doi.org/10.1007/BF01242421.

TRAMONTIN, D.P. Extração de compostos bioativos de sementes de *Artocarpus heterophyllus*: experimentação e modelagem matemática. Tese (Doutorado em Engenharia Química). Programa de pós-graduação em Engenharia Química, Universidade Federal de Santa Catarina, Florianópolis, 2020.

TRAMONTIN, D.P.; CARRERA, S.E.C.; BELLA-CRUZ, A.; BELLA CRUZ, C.C.; BOLZAN, A.; QUADRI, M.B. Biological activity and chemical profile of Brazilian jackfruit seed extracts obtained by supercritical CO_2 and low pressure techniques. The Journal of Supercritical Fluids, v. 152, 104551, 2019.

ULIANA, N. R. Polimento de biodiesel mediante contato com particulados ativos. Tese (doutorado), Programa de Pós-Graduação em Engenharia Química, Universidade Federal de Santa Catarina, Florianópolis - SC, 2016.

ULIANA, M. P.; DA SILVA, A. G.; FRONZA, M. SCHDRER, R. In vitro antioxidant and antimicrobial activities of Costus spicatus swartz usede in folk medicine for urinary tract infection in Brazil. Latin American Journal of Pharmacy, v. 34, n.4, p. 766-72, 2015.

VETAL, M.D.; LADE, V.G.; RATHOD, V.K. Extraction of ursolic acid from Ocimum sanctum by ultrasound: Process intensification and kinetic studies. Chemical Engineering and Processing: Process Intensification, v. 69, p.24-30, 2013.

VIDOVIC, S.; ZEKOVIC, Z.; MAROSANOVIC, B.; TODOROVIC, J.V. Influence of pre-treatments on yield, chemical composition and antioxidant activity of Satureja montana extracts obtained by supercritical carbon dioxide. The jornal of supercritical fluids, v. 95, p. 468-473, 2014.

VIERA, V. B. Compostos bioativos, atividade antoxidante e antimicrobiana na casca de cebola roxa (Allium cepa L.) submetidos a diferentes métodos de extração. Tese de doutorado. Programa de pós-graduação em ciência e tecnologia dos alimentos, Universidade Federal de Santa Maria, 2016.

WANG, L.; WELLER, C. L. Recentadvances in extraction of nutraceuticals from plants. Trends in Food Science & Technology, v. 17, n. 6, p. 300–312, 2006.

WEBER, JR., W. J., SMITH, E.H. Simulation and design models for adsorption processes. Environmental Science & Technology, v. 21, p. 1050- 1096, 1987.

WEILL, P.; PLISSONNEAU, C.; LEGRAND, P.; RIOUX, V.; THIBAULT, R. May omega-3 fatty acid dietary supplementation help reduce severe complications in Covid-19 patients? J. Biochi., v. 179, p. 275-280, 2020.

YANG, Y. C.; WAN, C.S.; WEI, M.C. Kinetics and mass transfer considerations for an ultrasound-assisted supercritical CO_2 procedure to produce extracts enriched in flavonoids from *Scutellaria barbata*. Journal of CO_2 Utilization, v. 32, p. 219-231, 2019.

YANG, Y.C.; WEI, M.C. A combined procedure of ultrasound-assisted and supercritical carbon dioxide for extraction and quantitation olean oil candursolic acids from *Hedyotis corymbosa*. Ind. Crops Prod., nº 79, p. 7-17, 2016.

YANG, C.P.; CHANG, C.M.; YANG, C.C.; PARIANTE, C.M.; SU, K.P. Long COVID and long chain fatty acids (LCFAs): Psychoneuroimmunity implication of omega-3 LCFAs in delayed consequences of COVID-19. Brain, Behavior, and Immunity, v.103, p.19-27, 2022.

ZHONG, Y.; CATHELINE, D.; HOUEIJEH, A.; SHARMA, D.; DU, L.; BESENGEZ, C.; DERUELLE, P.; LEGRAND, P.; STORME, L. Maternal omega-3 PUFA supplementation prevents hyperoxia-induced pulmonary hypertension in the offspring. Am. J. Physiol. Cell. Mol. Physiol., v. 315, p. 116-132, 2018.

ZHANG, Z. S.; WANG, L.J.; LI, D.; JIAO, S.S.; CHEN, X.D.; MAO, Z.H. Ultrasound-assisted extraction of oil from flaxseed. Sep. Purif. Technol, v.62, p. 192-198, 2008.

ZIBETTI, A.W. Desenvolvimento de um processo de separação de compostos bioativos de Rosmarinus officinalis. Tese (Doutorado em Engenharia Química). Programa de pós-graduação em Engenharia Química, Universidade Federal de Santa Catarina, Florianópolis, 2012.

CHAPTER IV - ULTRASOUND PRETREATMENT COMBINED WITH SUPERCRITICAL CO_2 EXTRACTION OF *COSTUS SPICATUS* LEAF EXTRACT

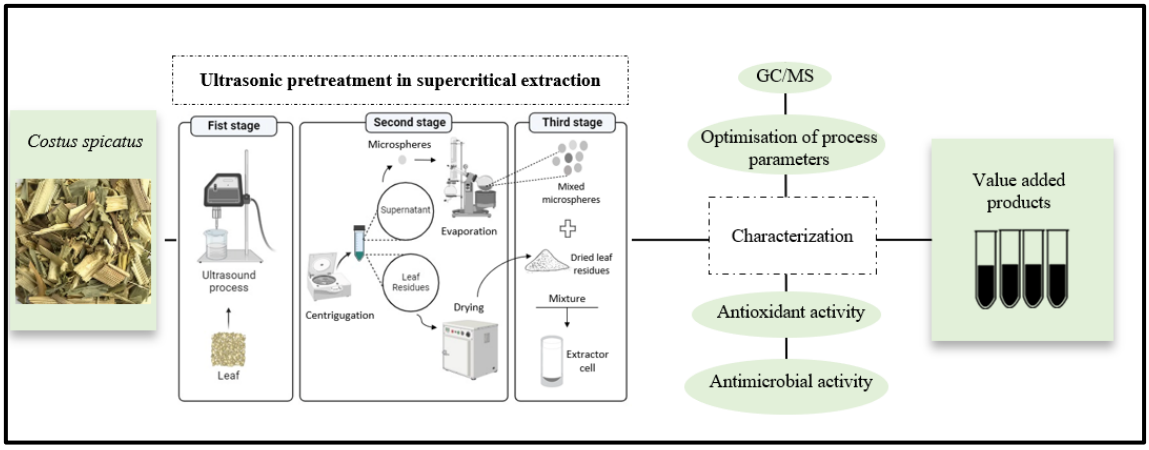

ABSTRACT

This work aimed to obtain extracts from *Costus spicatus* leaves through ultrasonic pretreatment in supercritical CO_2 extraction (UAE+SFE). A central composite design was used to evaluate the influence of temperature (36–64 °C), pressure (8–20 MPa), and cosolvent (0-20 %w) in terms of overall yield and chemical composition. Morphology using scanning electron micrograph (SEM), total phenolic content, content of total flavonoid, antioxidant (DPPH and ABTS), and antibacterial activities were evaluated. UAE+SFE showed a more notable overall yield, with 6.97%. In the SEM, the sample treated with UAE+SFE significantly impacted tissue structures, improving the selectivity of SFE regarding linolenic acid, leading to a maximum composition value of 62.5% area according to GC-MS. Furthermore, the UAE+SFE extract exhibited strong antimicrobial activity compared to the extract obtained by the SFE technique. Based on the pioneering results, the bioactives obtained are promising and interesting for application in the cosmetic, pharmaceutical, and food industries.

Keywords

Costus spicatus; Fractionation; Ultrasound; Supercritical extraction; Response surface methodology; Bioactive compounds

4.1 INTRODUCTION

Costus spicatus (Jacq.) Sw., belonging to the Costaceae family, is native to regions of the Atlantic Forest and the Amazon [1]. It is cultivated for ornamental purposes and is widely used as a popular medicine to treat kidney pain, back pain, thick and dark urine, hepatitis, kidney problems, and urinary problems [2,3,4]. Due to its important chemical composition, C. *spicatus* has a series of activities, including analgesic, antioxidant, antimicrobial, antifungal, and nephroprotective, which are attributed to the presence of triterpenes, sterols, flavonoids, saponins, alkaloids and tannins [5,6].

Several extraction techniques can be used to obtain bioactive compounds from natural sources. Conventional techniques, such as hydrodistillation and maceration, are commonly applied for compound recovery, as they present simple execution and do not require specialized training. However, prolonged extraction time, the use of large amounts of solvent, high energy consumption, solvent contamination, and the need for purification after the extraction stage are some challenges these techniques face [7, 8]. Thus, unconventional extraction techniques, such as pressurized liquid extraction (PLE), ultrasound-assisted extraction (UAE), and supercritical fluid extraction (SFE), emerge as an alternative to overcome these limitations, besides involving the principles established by Green Chemistry, its are considered environmentally friendly, require a short extraction time, low energy consumption, and less solvent, yielding a safe and high-quality final extract [7, 9].

Supercritical extraction (SFE) has been proposed as a more sustainable and efficient alternative to conventional techniques. This is due to using green solvents at high pressure to increase the solubility and desorption of bioactive compounds in the plant matrix and reduce extraction time. CO_2 is the most widely used solvent, as it is a safe, easily available, cheap, non-flammable, and non-toxic gas. Furthermore, it has a high solubility and mass transfer rate due to low viscosity and high diffusivity.

However, SFE has an economic constraint due to the high investment cost inherent to high-pressure processes [10, 11]. Among the countless variables involved, pressure is the one that most influence supercritical extraction, being the main one responsible for establishing answers to the technical and economic aspects of the process [12]. The increase in pressure may be associated not only with an increase in energy consumption but also with an increase in the amount of solvent required for the extraction process [13]. Nevertheless, applying techniques to pre-treat raw materials before SFE can

optimize the use of natural resources and save operational costs [14]. Therefore, additional studies must be carried out to evaluate the economic viability of the process involving high pressures in conjunction with pretreatments.

Extraction technique combinations are tested to perform better in obtaining the compounds of interest and reduce production costs, providing maximum economic efficiency. This technique is based on the formation of high-frequency ultrasonic waves, which are capable of causing cavitation due to expansion and contraction cycles when the material is subjected to ultrasound waves. It can lead to the rupture of the cell walls of the plant matrix, favoring solvent penetration and mass transfer, thus increasing the extraction rate and yield [15]. However, this tecnique is not selective for the target compound, and the extract contains considerable organic residue.

Some studies demonstrate that ultrasound-assisted SFE (UAE+SFE) can significantly improve the acquisition of the target bioactive compound. Liu *et al.* [16] reported that the yield of cucurbitacin E., present in *Iberis amara* seeds, increased by 26.1% after introducing ultrasound into the SFE. Barreles and Rezende [17] reported that the introduction of ultrasound in the SFE achieved a 29% improvement in the yield of passion fruit seed oil. Studies by Santos *et al.* [18] achieved an increase in the yield of capsaicinoids from chili peppers by 77%. Thus, combining the ultrasound technique with SFE is a promising extraction route for obtaining medicinal herbal compounds.

Until the present moment, no study on a reliable route for high-efficiency extraction from C. *spicatus* leaves has been published. Given this, this work presents the following specific objectives: (i) evaluate the effects of ultrasonic pretreatment (UAE + SFE) in the SFE process to maximize the yield and chemical profile of C. *spicatus* leaves, using Central Composite Design (CCD) with Response Surface Methodology (RSM); (ii) verify the linolenic acid content obtained from UAE + SFE by Gas Chromatography coupled to Mass Spectrometry (GCMS); (iii) analyze the total phenolic content, flavonoid content, SEM, and antioxidant activity. Extraction data were compared with traditional UAE and SFE.

4.2 MATERIAL AND METHODS

4.2.1 Plant material

Leaves and stems of C. *spicatus* were obtained from Comercial Charoma (Piraquara, PR – Brazil). The leaves were manually separated from the stems and dried

in an oven with forced air circulation (CE 220/2016, Cienlab, Campinas, SP, Brazil) at 35 °C for 24 h. Then, the leaves were ground in a coffee grinder (MDR302, Cadence, Balneário Piçarras, SC, Brazil). The moisture content of the leaves was determined using method 925.10, according to AOAC [19]. The moisture of the dried material (6.59 ± 0.07%) was obtained using an oven at 103 ºC until constant weight. The dry material was separated to determine particle diameter using a standard sieve (45 mesh) (a bronzinox, São Paulo, SP, Brazil). The particles were characterized by particle size classification on a Tyler Standard sieve (A bronzinox, São Paulo, SP, Brazil). The choice of particle size of 355 μm (45 mesh) was determined by preliminary tests that demonstrated a shorter time for the arrival of the diffusional extraction phase. It is known that the larger the particle, the smaller the contact area between the solid and the solvent, consequently, the lower the mass transfer and extraction yield. However, using an ideal particle size is necessary, as very small particles can create preferential paths and impair extraction efficiency. According to [20], the recommended particle size range to guarantee the efficiency of the extraction process corresponds to 100 μm to 2 mm, corroborating the particle size used in this work. Furthermore, [21] indicates that to avoid the formation of preferential paths in the extraction bed, the ratio between the diameter of the extraction bed and the average diameter of the particles needs to be between 50 and 250. Thus, with a bed of extraction presenting a diameter of 50 mm, the ratio between bed diameter and average particle diameter employed in the present study was 140.85, indicating a probable absence of preferential paths in the bed used. The solid particles were sealed and stored in a domestic freezer at -18 ºC (BRM39, Brastemp, São Bernardo do Campo, SP, Brazil) until use.

4.2.2 Ultrasound-assisted extractions (UAE)

Ultrasound-assisted extractions (UAE) were performed according to the method adapted from Luque-García and Luque De Castro [22]. Briefly, about 1 g of sample was placed in contact with 30 mL of solvent and subjected to an ultrasonic probe (DES5000, Unique, São Paulo, SP, Brazil) for 5 min at 70 % power (maximum power – 500 W) and frequency of 20 kHz. Pulsed ultrasound (5 s on, 5 s off) was applied to prevent the solvent

from overheating. Extractions were carried out in duplicate using ethanol (EtOH). The conditions were based on preliminary testing.

4.2.3 Ultrasound pretreatment (UAE + SFE)

To obtain a homogeneous matrix for SFE, ultrasound pretreatment combined with supercritical CO_2 extraction was performed as described by Liu *et al.* [14]. According to the experimental process illustrated in Figure 11, three steps were carried out: in the first step, ultrasound-assisted extractions (UAE) were performed according to the method adapted from Luque-García and Luque De Castro [22], as described in section 4.2.2. After ultrasonic treatment, in the second stage, the phases were separated by a centrifuge for 5 min at 3,000 rpm. The leaf residue was dried at 40°C for 24 h. The supernatant with 2 g of hollow glass microspheres (VS5500, 3 M, Minnesota, USA) was evaporated to dryness by a rotary vacuum evaporator (RE100-Pro, Scilogex, USA). This resulted in microspheres coated with crude extract. Finally, in the third step, the dry residue and the microspheres coated with crude extract were sufficiently mixed. They were then placed in the SFE chamber for re-extraction. The leaf sample without ultrasonic exposure was used as a control.

Figure 11. Schematic diagram of ultrasound pretreatment of C. *spicatus* leafs.

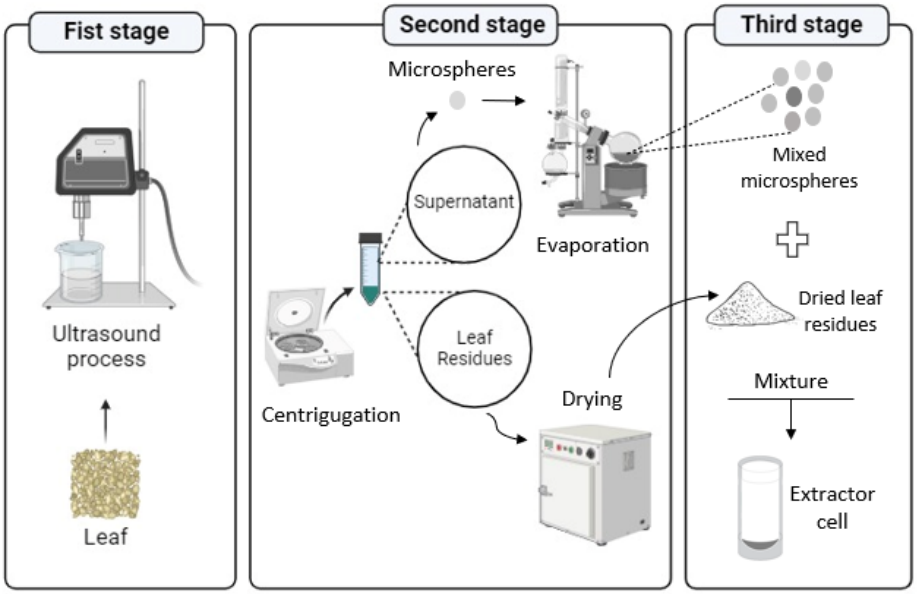

Source: Developed by the author.

4.2.4 Supercritical Fluid Extraction (SFE)

The high-pressure extraction process was performed in a chromatography and supercritical extraction unit (LC 2000, Jasco, Hachioji, Tokyo, Japan). The extraction conditions (pressure, temperature, volumetric flow of solvent, and cosolvent) were kept constant throughout the experimental period. The solvent (CO_2) sent from the cylinder passed through a cooling system with a temperature of -10 °C (FL-1201, Julabo, Seelbach, Baden-Württemberg, Germany). It was pressurized by a positive displacement HPLC pump (PU-2087/2087 Plus, Jasco, Hachioji, Tokyo, Japan) at a constant volumetric flow (mL min^{-1}). The volumetric flow of the cosolvent (EtOH) was defined as mass fractions about the mass of CO_2 used. It was also pumped by a positive displacement HPLC pump (PU-2087/2087 Plus, Jasco, Hachioji, Tokyo, Japan) and mixed with supercritical CO_2 before entering the extraction cell.

The mixture of dry residue and microspheres coated with crude extract (obtained in the third stage of session 2.3) was placed in the extraction column (127.5 mm long x 10 mm diameter and internal volume 10 cm^3), forming a fixed bed. All samples with the same extraction time of 120 min. The SFE condition adopted was determined by preliminary experiments by Laurintino [23]. Other process variables were fixed based on previous work by the same research group [24, 25, 26, 27]. The volumetric flow rate of CO_2 was kept constant at 3 mL min^{-1}. CO_2 was used as a solvent (99.99 %, White Martins, Florianópolis, SC, Brazil) and ethanol as a cosolvent (99.99 %, Metaquímica, Jaraguá do Sul, SC, Brazil). The collection of extracts was conducted in an offline collection system, or "trapping", whereby the solute precipitation occurs through depressurization of the solvent at atmospheric pressure [28]. The extract was filtered and stored in the domestic freezer at -18 ºC (BRM39, Brastemp, São Bernardo do Campo, SP, Brazil) until further analysis.

4.2.4.1 Response Surface Methodology (RSM)

A central composite design (CCD), consisting of 17 experiments and 5 central points, was used to evaluate compound extraction. All runs were duplicated, and the value presented in the results was the average. Statistical analysis was performed using all experimental values. The independent variables were defined by screening as follows: temperature (36–64 °C), pressure (8–20 MPa), and cosolvent (0-20 %w). The values of

these variables were based on preliminary tests, aiming to maximize the extraction of C. *spicatus* leaves.

In this study, RSM was applied to yield responses (X_0) to assess the significance of each factor studied and quantify and describe the impact of the combined effects of the independent variables on the dependent variables. Furthermore, the quadratic polynomial RSM model, described according to Equation 1, was adopted to evaluate the effect of the independent variables (pressure, temperature, and cosolvent) on the dependent variable, the overall yield.

$$A = \beta_0 + \beta_1 X_1 + \beta_2 X_2 + \beta_3 X_3 + \beta_{11} X_1^2 + \beta_{22} X_2^2 + \beta_{33} X_3^3 + \beta_{12} X_1 X_2 + \beta_{13} X_1 X_3 + \beta_{23} X_2 X_3 \quad (1)$$

Where A is the dependent variable; X_1, X_2 and X_3 are independent variables; β_0 is the intercept coefficient; β_1, β_2 and β_3 are linear effect coefficients; β_{11}, β_{22} and β_{33} are quadratic effect coefficients; and β_{12}, β_{13} and β_{23} are interaction effect coefficients.

The coefficient of determination symbolized as R^2 measures how well the regression equation models the actual data points, where the R^2 value is a number between 0 and 1, with values closer to 1 indicating more accurate models. This R^2 is not calculated directly from the predictive equation with all parameters but is based on comparing the observed values and the values predicted by the model [29, 30].

The factors and levels of correspondence for each independent variable are presented in Table 9.

Table 9. Independent variables and level coding for experimental design.

		Correspondence levels				
Variables	**Codification**	***-α***	***-1***	***0***	***+1***	***+α***
Pressure (MPa)	X_1	8	11	14	17	20
Temperature (°C)	X_2	36	40	50	60	64
Cosolvent (%w)	X_3	0	5	10	15	20

4.2.5 Extract characterization

For UAE, SFE, and UAE + SFE, the global yield (X_0) was calculated as the ratio between the mass of the extract and the mass of the dry solid used.

4.2.5.1 Chemical profile of *Costus spicatus* extracts

GC/MS analyses of the extracts were performed on an Agilent GC instrument (7890 A, Agilent, Santa Clara, CA, USA) coupled to an MS detector (5975 C MS, Agilent, Santa Clara, CA, USA). A fused silica capillary column (HP-5 ms, Agilent, Santa Clara, CA, USA) (30 m long × 250 µm internal diameter × 0.25 µm film thickness, composed of 5 % phenyl and 95 % methylpolysiloxane) was connected to a quadrupole detector operating in EI (electron impact ionization) mode at 70 eV. Helium was adopted as the carrier gas at a 0.8 mL min^{-1} flow rate. The input and interface (G6502B, Agilent, Santa Clara, CA, USA) have a temperature of 280 °C with a split ratio of 1:5. The injected sample volume was 1 µL. The oven temperature program consisted of maintaining the oven at 80 °C for 1 min, increasing it at a rate of 10 °C min^{-1} until it reached 190 °C and then reducing the heating rate to 5 °C min^{-1} until it reached 300 ºC and keep it there for 15 min. Compounds were identified by comparing their mass spectra with those provided by the National Institute of Standards and Technology [31]. The SFE extracts were diluted in EtOH (99.8 % Vetec, Duque de Caxias, RJ, Brazil) at an average concentration of 5.0 mg mL^{-1}.

4.2.5.2 Total phenolic content (TPC)

The total phenolic content (TPC) of C. *spicatus* leaf extracts was determined using the Folin-Ciocalteu method, according to Granato and Nunes [32], with modifications. Firstly, the UAE, SFE, and UAE + SFE extracts were solubilized in ethanol up to concentrations of 10 mg mL^{-1}. Briefly, 10 µL of sample solution, 600 µL of distilled water, and 50 µL of Folin-Ciocalteu reagent (Sigma-Aldrich, USA) were mixed. Then, 150 µL of 20% (w/v) Na_2CO_3 (LAFAN, 99%) and 190 µL of distilled water were added, shaken, and incubated for 2 h in the dark at room temperature. 300 µL of each sample was transferred to wells on a microplate. Finally, the absorbance of the samples was measured at 760 nm in a microplate reader (Tecan Infinite M200). Analyses were performed in triplicate, and the TPC value was calculated according to a standard curve prepared with gallic acid (Sigma Aldrich, > 98%) between 0.1 and 0.8 mg mL^{-1} (R^2 = 0.9994). The results are expressed in mg of Gallic Acid Equivalent per g of dry extract (mg of GAE g^{-1}). The results were expressed as mean values ± standard deviation. This activity was carried out in UAE and SFE combined with and without ultrasound

pretreatment under the same extraction conditions of 50 °C/14 MPa/10 %EtOH (the central point of experimental planning).

4.2.5.3 Total flavonoid content (TFC)

The total flavonoid content (TFC) of the extracts (1 mg mL^{-1} in ethanol) was determined by the aluminum chloride colorimetric method described by Chang *et al.* [33] with some modifications. The solution was prepared with 0.5 mL of the extract, 0.1 mL of a 10% $AlCl_3$ solution, and 1.5 mL of methanol (p.a.). The mixture was stirred and left to rest for 5 min. Then 0.1 mL of 1 mol L^{-1} potassium acetate and 2.8 mL of distilled water were added, and the reaction medium was stirred and left to rest for another 15 min at room temperature (25 °C). Absorbance was measured at 415 nm using a UV-Vis spectrophotometer (V-M5, Bel Engenharia, Piracicaba, SP, Brazil). Quercetin (HPLC grade, Sigma) was used to obtain the calibration curve (12.5 – 125 µg mL−1) using a UV-Vis spectrophotometer (V-M5, Bel Engenharia, Piracicaba, SP, Brazil), and the results are expressed in milligrams of quercetin (QE) equivalents per gram of extract (mg QE g^{-1}) through a linear regression equation (R^2 = 0.9992). This activity was carried out in UAE and SFE combined with and without ultrasound pretreatment under the same extraction conditions of 50 °C/14 MPa/10 %EtOH (the central point of experimental planning).

4.2.5.4 Antioxidant capacity

The in vitro antioxidant capacities of the extracts were determined through the DPPH and ABTS methods. This activity was carried out in UAE and SFE combined with and without ultrasound pretreatment under the same extraction conditions of 50 °C/14 MPa/10 %EtOH (the central point of experimental planning).

4.2.5.4.1 DPPH free radical scavenging activity (DPPH)

The antioxidant capacity of the extracts was measured by analyzing the free radical scavenging capacity using the 1,1-diphenyl-2-picrylhydrazyl (DPPH) radical based on Boroski *et al.* [34]. A 25 µL aliquot of the extract at a concentration of 0.05 g mL^{-1} was mixed with 2 mL of 0.091 mM DPPH in EtOH solution. The mixture was vigorously stirred, and after 30 min at room temperature, at 25 °C, the absorbance was measured at 517 nm with a spectrophotometer (V-M5, Bel Engenharia, Piracicaba, SP,

Brazil). The DPPH method's antioxidant potential was calculated from a linear regression of the absorbance at 517 nm and the Trolox equivalent antioxidant capacity variation between 0 and 2 Mm ($R^2 = 0.9992$). Results were expressed as μmol of Trolox equivalent (TE) per g of dry sample (μmol TE g^{-1} ± standard deviation).

4.2.5.4.2 $ABTS^+$ free radical scavenging activity

The ABTS assay [2,2'-azino-bis (3-ethylbenzothiazoline-6-sulfonic acid)] was performed according to Re *et al.* [35]. Briefly, ABTS was dissolved in water to a concentration of 7.0 mM and subjected to a reaction with potassium persulfate (2.45 mM) at room temperature (25 °C) to form the radical. The ABTS solution was diluted with ethanol to an absorbance of 0.70 ± 0.05 at 734 nm. Solutions were prepared with 30 μL of extract at a 0.001 g mL^{-1} concentration. 3 mL of ABTS solution was added to the test tubes, and after 6 min, the absorbance was read on a spectrophotometer (800XI, FEMTO, São Paulo, SP, Brazil) at a wavelength of 734 nm. The antioxidant capacity by the ABTS method was calculated from a linear regression of the absorbance at 734 nm and the variation of the Trolox equivalent antioxidant capacity between 0 and 2 mM ($R^2 = 0.9949$). Results were expressed as μmol of Trolox equivalent (TE) per g of dry sample (μmol TE g^{-1} ± standard deviation).

4.2.6 Determination of antibacterial and antifungal activity

4.2.6.1 Microorganisms and media

To determine antimicrobial activity, Gram-positive and Gram-negative bacteria, and fungi and yeast were used, including *Staphylococcus aureus* (ATCC 25923), *Bacillus subtilis* (ATCC 23858), *Escherichia coli* (ATCC 11775), *Enterococcus faecalis* (ATCC 19433), *Staphylococcus hominis* (amostra clínica), *Staphylococcus saprophyiticus* (ATCC 35552), *Klebsiella pneumoniae* (ATCC 13883), *Pseudomonas aeruginosa* (ATCC 27853), *Proteus mirabilis* (ATCC 25933), *Salmonella typhimurium* (ATCC 14028), *Aspergillus fumigatus* (ATCC 26934), *Epidermophyton floccosum* (C 114), *Microsporum canis* (C 112), *Microsporum gypseum* (C 115), *Rhisopus* sp. (CL 35), *Trichophyton mentagrophytes* (ATCC 9972), *Trichophyton rubrum* (C 137) e Candida albicans (ATCC 10231). These strains are standard reference of the American Type Culture Collection (ATCC) (Rockville, MD, USA), and clinical isolates were provided by the Centro de Referência de Micologia CEREMIC (C) of the Facultad de Ciencias

Bioquímicas y Farmacéuticas, Rosario, Argentina e Control Lab (CL), Rio de Janeiro, Brazil. Based on the GC/MS results, the UAE + SFE 3 and UAE + SFE 5 samples (which presented the highest and lowest linolenic acid content, respectively) and the SFE 3 and SFE 5 samples (without ultrasonic pretreatment) were tested for potential antimicrobial activity.

4.2.6.2 Determination of minimum inhibitory concentration (MIC)

The minimum inhibitory concentration (MIC) of each sample was determined using broth microdilution techniques, according to CLSI (2015), CLSI M38 (2017), and CLSI M27-A4 (2017) for bacteria, filamentous fungi, and yeast, respectively., with some modifications. MIC values were determined in Mueller-Hinton broth (Kasvi, Italy) for bacteria and 2% Sabouraud Dextrose broth (Kasvi, Italy) for fungi. Bacterial inocula were prepared to reach $5x10^4$ UFC/mL, for fungi at $1x10^4$ to $5x10^4$ conidia/mL, and for yeast between $5x10^2$ and $2.5x10^3$ UFC/mL. The bacteria microtiter plates were incubated at 35 ºC, the yeast at 30 ºC, and the filamentous plates at 25-30 ºC in a humid, dark chamber. The growth of microorganisms was recorded visually after 24 hours for bacteria, 48 hours for yeast, and according to the growth of control fungi for the other fungi (3 to 15 days), and the MIC was defined as the lowest concentration of extract or compound that shows no visible growth of microorganisms after incubation.

4.2.7 Scanning electron micrograph (SEM)

The samples' microstructure was analyzed using scanning electron microscopy (SEM) using a JEOL JSM-6390LV. The dried samples were fixed to the sample holder with aluminum tape and coated with a thin gold film to provide electrical conductivity. The evaluation of the microstructure was carried out under partial vacuum and electron beam conditions.

4.2.8 Statistical analysis

The assays were performed in duplicate. Data are expressed as mean ± standard deviation. To evaluate significant differences ($p < 0.05$) between the results obtained, the Tukey test was applied to the yield results of SFE extractions.

The response surface methodology (RSM) was applied to optimize the extraction yield, assess the significance of each factor employed, and quantify and describe the

impact of the combined effects of the independent variables on the dependent variable. The coefficient of determination R^2 was used to assess the stability of the regression model fit. All statistical analyses were evaluated using Statistica for Windows 7.0 software (Statsoft Inc., Tulsa, OK, USA).

4.3 RESULTS AND DISCUSSION

4.3.1 Global yield (X_0)

The effect of ultrasonic pretreatment on the yield of C. *spicatus* leaves was studied, as shown in Table 10. The yields were compared with those obtained from untreated leaves using traditional SFE and UAE. UAE used before SFE had a significant impact on C. *spicatus* leaf yield.

Table 10. Comparison of the yields of C.*spicatus* leaf extract obtained by ultrasound extraction (UAE) and supercritical CO_2 extraction (SFE) combined with and without ultrasound pretreatment (UAE + SFE).

Extraction method	**Solvent**	**Amplitude**	**Time(min)**	**X_0 (%)^2**
UAE	EtOH	70 %	5	$1{,}43^{K} \pm 0{,}13$
SFE/ Extraction condition	**Preteatment/ Solvent**	**Solvent/ cosolvent SFE**	**ρCO_2 (kg m^{-3})***	**X_0 (%)^2 Leaves**
50 °C/14 MPa/10 %	-	CO_2/ EtOH	672.17	$2.02^{I} \pm 0.01$
UAE + SFE/ Extraction condition	**Preteatment/ Solvent**	**Solvent/cosolvent SFE**	**ρCO_2 (kg m^{-3})***	**X_0 (%)^{1,2} Leaves**
1- 40 °C/11 MPa/5 %	UAE/ EtOH	CO_2/ EtOH	683.52	$1.95^{i,I,J} \pm 0.03$
2- 40 °C/11 MPa/15 %	UAE/ EtOH	CO_2/ EtOH	683.52	$4.18^{h,H} \pm 0.02$
3- 60 °C/11 MPa/5 %	UAE/ EtOH	CO_2/ EtOH	357.79	$1.98^{i,I} \pm 0.02$
4- 60 °C/11 MPa/15 %	UAE/ EtOH	CO_2/ EtOH	357.79	$4.22^{g,h,G,H} \pm 0.03$
5- 40 °C/17 MPa/5 %	UAE/ EtOH	CO_2/ EtOH	807.87	$5.22^{e,E} \pm 0.04$
6- 40 °C/17 MPa/15 %	UAE/ EtOH	CO_2/ EtOH	807.87	$5.44^{d,D} \pm 0.01$
7- 60 °C/17 MPa/5 %	UAE/ EtOH	CO_2/ EtOH	664.59	$5.28^{e,E,D} \pm 0.01$
8- 60 °C/17 MPa/15 %	UAE/ EtOH	CO_2/ EtOH	664.59	$5.93^{c,C} \pm 0.03$
9- 50 °C/8 MPa/10 %	UAE/ EtOH	CO_2/ EtOH	219.18	$1.74^{j,J} \pm 0.04$
10- 50 °C/20 MPa/10 %	UAE/ EtOH	CO_2/ EtOH	784.29	$6.56^{b,B} \pm 0.02$
11- 36 °C/14 MPa/10 %	UAE/ EtOH	CO_2/ EtOH	794.11	$4.46^{f,F} \pm 0.02$

12-	64 °C/14 MPa/10 %	UAE/ EtOH	CO_2/ EtOH	516.47	$4.47^{f,F} \pm 0.03$
13-	50 °C/14 MPa/0 %	UAE/ EtOH	CO_2	672.17	$1.01^{k,L} \pm 0.01$
14-	50 °C/14 MPa/20 %	UAE/ EtOH	CO_2/ EtOH	672.17	$6.97^{a,A} \pm 0.01$
15-	50 °C/14 MPa/10 %	UAE/ EtOH	CO_2/ EtOH	672.17	$4.47^{f,F} \pm 0.02$
16-	50 °C/14 MPa/10 %	UAE/ EtOH	CO_2/ EtOH	672.17	$4.42^{f,F,G} \pm 0.03$
17-	50 °C/14 MPa/10 %	UAE/ EtOH	CO_2/ EtOH	672.17	$4.34^{f,g,F,G,H} \pm 0.02$

* Density of CO_2 [18].
[1] Values from the same column with different lowercase letters represent a significant difference ($p < 0.05$) considering the experiment UAE+SFE technique.
[2] Values of the same column with different uppercase letters represent a significant difference ($p < 0.05$), considering all the experiments UAE, SFE and UAE + SFE techniques simultaneously.

UAE used before SFE had a significant impact on C. *spicatus* leaf yield. Compared to the yield gained by SFE from untreated leaves, the yield increased by up to 28% after the leaves were subjected to UAE. Thus, this UAE + SFE combination can be considered a highly efficient and environmentally friendly extraction procedure for C. *spicatus* leaves, justified by the different solute/solvent interactions that are involved in the individual extraction methods and that are intensified in the combination between them (UAE, SFE and UAE +SFE) [36]. These different mechanisms affect the performance of the methods in terms of process yield and chemical profile of the extract compounds (section 4.2.3), implying different values of TPC, TFC, DPPH, and ABTS (section 4.2.5.2 – 4.2.5.4). However, when UAE + SFE was applied in the condition without cosolvent (13- 50 °C/14 MPa/0 %), this combination of techniques did not significantly impact the yield, indicating the need to use the cosolvent to guarantee the efficiency of the combination.

Published results for UAE + SFE using other plant species also achieved satisfactory performance. Liu *et al.* [16] reported that the yield of cucurbitacin E from *Iberis amara* seeds was increased by 26.1% after introducing ultrasound into SFE. Studies carried out by De Souza *et al.* [37] achieved a yield increase of 12.54% by pre-treating grape seeds with ultrasound.

Global yield values for high-pressure extraction of C. *spicatus* with ultrasonic pretreatment were not found in the literature, making comparison impossible with the results presented in the present work. The highest overall yield of UAE + SFE was 6.97 ± 0.01% at 50 ºC/14 MPa/20%EtOH (ρCO_2 = 672.17 kg m^{-3}, test 14). The lowest overall yield was 1.01 ± 0.01% in the condition of 50 ºC/14 MPa/0 %EtOH (ρCO_2 = 672.17 kg m^{-3}, test 13). From these results, it can be concluded that adding polar cosolvent to the

CO_2 solvent increased the polarity of the extraction solvent at the molecular level, resulting in a higher overall extraction yield [38].

The overall extraction yield was evaluated using the response surface methodology, as shown in Figure 12.

Figure 12. Response surfaces for the global yield derived from UAE + SFE for leaves of C. *spicatus*. (a) Global yield response surface as a function of temperature and cosolvent concentration. (b) Global yield response surface as a function of pressure and cosolvent concentration. (c) Global yield response surface as a function of temperature and pressure.

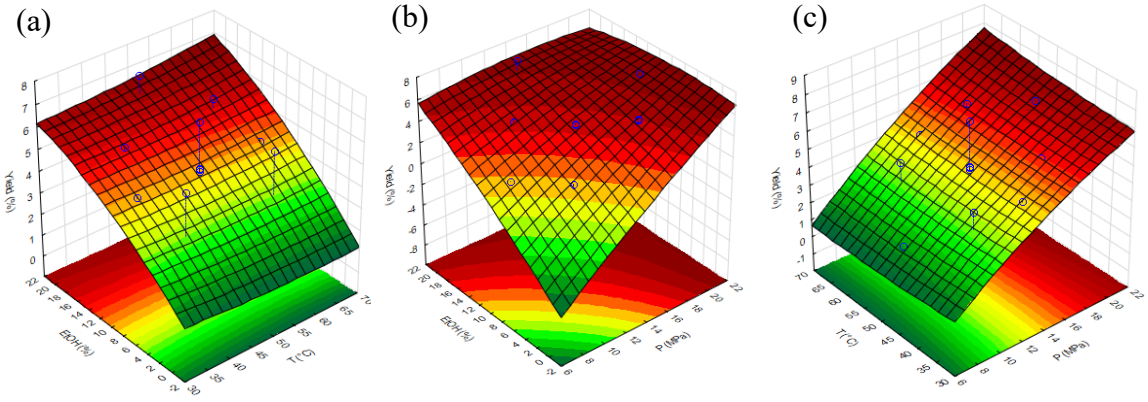

In Figure 12 a-c, increasing %EtOH and increasing pressure resulted in a higher yield. According to the ranges studied, yields increased when pressures above 16 MPa and more than 14% EtOH were applied. It was observed that the independent variable of the cosolvent (EtOH) affected the polarity of the EtOH/CO_2 system, allowing an increase in yield. Furthermore, increasing pressure with constant temperature (Figure 12-c) increased CO_2 density, improving the solubility power of the solute and providing a greater overall extraction yield [28]. This pressure effect is due to the decrease in the intermolecular distance between CO_2 molecules as the density increases, resulting in more intense and specific interactions between CO_2 and molecules of the active compound, favoring dissolution [39].

4.3.2 Effect of operating conditions

Table 11 presents the effects of independent variables on yield that were evaluated using the ANOVA response surface model's regression coefficients (RC).

Table 11. Regression coefficients (RC) of the adjusted model for global UAE + SFE yield.

Variables	Ultrasonic pretreatment in SFE (UAE + SFE)		
	RC	*p*-value	F_{calc}
X_1[1]	**1.1988**	**0.0002****	**5346.983**
X_1^2[2]	**-0.0643**	**0.0472***	**19.686**
X_2[1]	0.0532	0.1074^{ns}	7.842
X_2^2[2]	0.0309	0.3619^{ns}	1.373
X_3[1]	**1.0788**	**0.0002****	**4330.052**
X_3^2[2]	**-0.1043**	**0.0188***	**51.798**
$X_1 X_2$[3]	0.0600	0.1225^{ns}	6.698
$X_1 X_3$[4]	**-0.4500**	**0.0026****	**376.744**
$X_2 X_3$[5]	0.0550	0.1410^{ns}	5.628
R^2	0.9407		

$^{**}p < 0.01$ highly significant.
$^{*}0.01 < p < 0.05$ significant.
^{ns} $0.05 < p$ not significant.
[1] Linear term: X_1 = Pressure (MPa), X_2 = Temperature (°C) e X_3 = Cosolvent (%).
[2] Quadratic term: X_1 = Pressure (MPa), X_2 =Temperature (°C) e X_3 = Cosolvent (%).
[3] $X_1 X_2$ = Interaction term of pressure and temperature.
[4] $X_1 X_3$ = Interaction term of pressure and cosolvent.
[5] $X_2 X_3$ = Interaction term of temperature and cosolvent.

Considering the significance of the statistical analysis ($p < 0.05$), the linear terms of pressure and cosolvent returned positive effects on the overall yield. On the other hand, the quadratic term of the variable pressure and cosolvent and the interaction of pressure and cosolvent presented negative effects on the yield. The temperature did not significantly affect extraction yield (Table 11). The interaction of solvent density and solute vapor pressure limited the impact of temperature on yield. Therefore, predicting the effect of increasing temperature on a sample is quite complex. While the density of the solvent can increase with decreasing temperature, increasing its solvating power, the vapor pressure of the solute can decrease with temperature, reducing its solvating power. Thus, the extraction rate will depend on the factor that will interfere most strongly: the solubility in the supercritical fluid, which decreases as the temperature increases, or the volatility, which increases with the increase in temperature. Corroborating Joradon *et al.* [40], the authors also reported that the extraction yield of the *Hericium erinaceus* mushroom was not influenced by temperature when applied up to 60 ºC.

The pure error obtained in this analysis showed good repeatability and no statistical significance due to a lack of adjustment at the 5% level ($p > 0.05$). The performance model adjusted to experimental data as a function of the independent

variables pressure, temperature and % EtOH is represented by Equation 2, considering only the significant variables.

$$Yield(\%) = 4.40 + 1.19X_1^1 - 0.06X_1^2 + 1.07X_3^1 - 0.10X_3^2 - 0.45X_1X_3^4 \quad (2)$$

The coefficient of determination, R^2, for UAE + SFE indicates a good fit of the statistical model to the experimental data (R^2 = 94.07%). This value indicates that the model adequately represented the experimental data.

4.3.3 Scanning Electron Microscopy of C. *spicatus* leaves

The SEM analysis shows the sample's microstructure before and after being subjected to different extraction techniques (Figure 13). The leaves of C. *spicatus* that were not subjected to extractive mechanisms showed trichomes on the surface of the leaves, with compacted, intact, and smooth characteristics (Figure 13a). However, samples treated with UAE, SFE, and UAE + SCE revealed more irregular surfaces and damaged or removed trichomes (Figure 13b-d), highlighting the sample treated with UAE + SFE. Thus, this combination of techniques notably impacted tissue structures, where dense microcracks can be observed on the surface, heavily damaged and completely emptied of their contents (Figure 13-h). Such changes were not observed in samples submitted to traditional UAE and SFE.

Given these observations, ultrasound extraction acted with different independent or combined mechanisms, such as fragmentation, erosion, capillarity, detexturization, and sonoporation. A possible mechanism to justify the increase in extraction yield is related to the implosion of cavitation bubbles on the surface of the leaves, which can induce erosion of plant structures, expelling the extract out these structures more easily (Figure 13 d-h). Furthermore, the shear forces generated by the propagation of ultrasonic waves weakened the glandular envelopes of the trichomes, causing microfractures and accelerating mass transfer and the release of cellular contents [15,41]. These characteristics can intensify the porosity of the matrix and accelerate the permeation and diffusion of solvents in the solid matrix, resulting in greater extraction efficiency.

Figure 13. Scanning Electron Microscopy images of C. *spicatus* leaves (zoom 500 and 2000 times). (a-e). Untreated sheet. (b-f). Leaves treated with UAE (ultrasound extraction). (c-g). Leaves treated with SFE (supercritical CO_2 extraction). (d-h). Leaves treated with UAE + SFE (ultrasonic pretreatment in supercritical CO_2 extraction).

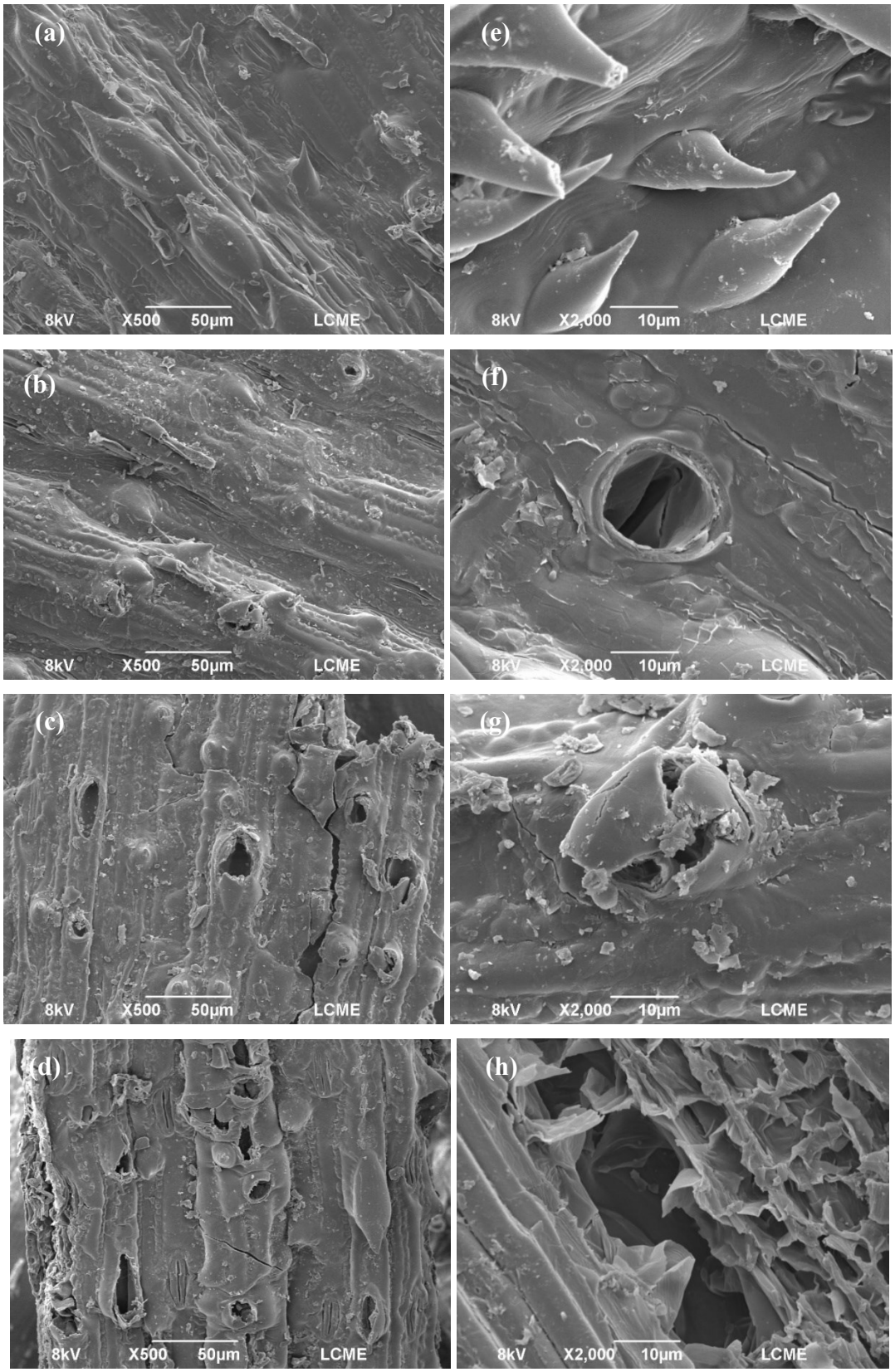

4.3.4 Chemical profile of C. *spicatus* extracts

The chemical composition of C. *spicatus* leaf extract obtained by ultrasound extraction (UAE) and supercritical CO_2 extraction (SFE) combined with and without ultrasound pretreatment (UAE + SFE) is shown in Table 12. The compounds varied in relative area depending on the technique, extraction condition, and solvent used.

Table 12. Chemical profile of C. *spicatus* leaf extract obtained by ultrasound extraction (UAE) and supercritical CO_2 extraction (SFE) combined with and without ultrasound pretreatment (UAE + SFE).

Compound	Molecular formula	Molecular weight ($gmol^{-1}$)	RT (min)	Relative area (%)																
				UAE	SFE	UAE + SFE*														
				EtOH	CO_2/EtOH	1	2	3	4	5	6	7	8	9	10	11	12	13	14	15
α-Terpineol	$C_{10}H_{18}O$	154.25	6,12	2.84	ND	ND	ND	ND	ND	ND	ND	ND	ND	ND	ND	ND	ND	ND	ND	ND
Lauric acid	$C_{12}H_{24}O_2$	200.31	10,71	1.12	ND	ND	ND	ND	ND	ND	ND	ND	ND	ND	ND	ND	ND	ND	ND	ND
Decanoic acid, ethyl ester	$C_{12}H_{24}O_2$	200.32	9.66	ND	ND	ND	ND	ND	ND	0.20	0.16	0.16	ND	ND	ND	0.42	ND	ND	0.12	ND
Dodecanoic acid	$C_{12}H_{24}O_2$	200.32	11.71	ND	ND	ND	0.30	0.13	0.16	0.51	0.68	0.54	0.31	0.14	0.22	ND	0.39	0.18	0.42	0.25
Cyclotrisiloxane, hexamethyl-	$C_6H_{18}O_3Si_3$	222.461	12.76	2.29	ND	1.02	0.73	0.84	0.77	ND	0.07	0.23	0.09	1.34	1.67	1.48	0.50	2.10	1.21	1.41
Tetradecanoic acid	$C_{14}H_{28}O_2$	228.37	14.13	2.49	ND	ND	0.23	ND	0.12	0.46	0.42	0.35	0.40	0.14	0.14	0.28	0.26	0.10	0.36	0.27
Pentadecanoic acid	$C_{15}H_{30}O_2$	242.40	15.48	3.45	ND	ND	0.12	ND	0.12	0.26	0.22	0.26	0.14	0.14	0.14	0.17	0.18	0.10	0.18	0.13
Palmitic acid	$C_{16}H_{32}O_2$	256.42	16.44	10.78	9.3	16.26	16.40	16.57	17.22	18.00	17.42	16.20	16.67	16.80	16.22	16.68	16.90	17.26	16.22	16.84
Heptadecanoic acid	$C_{17}H_{34}O_2$	270.45	18.40	1.32	ND	ND	0.21	0.16	0.19	0.33	0.26	0.26	ND	0.23	0.21	ND	0.23	0.19	ND	0.23
Phytol	$C_{20}H_{40}O$	296.53	18.71	2.97	4.62	0.91	1.37	0.68	1.42	1.63	1.32	1.30	1.72	1.59	1.42	1.74	1.28	1.32	1.09	2.38
Linoleic acid	$C_{18}H_{32}O_2$	280.45	19.08	3.71	3.61	5.18	3.87	ND	3.83	0.24	0.18	1.56	3.83	0.09	ND	3.94	1.82	ND	0.07	0.17
Linolenic acid	$C_{18}H_{30}O_2$	278.43	19.11	14.67	12.33	61.99	51.55	62.52	62.34	50.14	57.83	55.80	54.57	61.53	59.23	57.40	58.34	62.39	59.25	54.84
Octadecanoic acid	$C_{18}H_{36}O_2$	284.48	19.38	1.53	ND	1.65	1.16	4.16	ND	1.49	5.07	3.60	1.56	4.48	3.81	1.28	3.55	5.00	0.31	4.66
Ethyl 9,12,15-octadecatrienoate	$C_{20}H_{34}O_2$	306.48	20.12	ND	ND	ND	5.14	ND	ND	6.24	ND	ND	4.42	ND	ND	ND	ND	ND	ND	4.56
Eicosanoic acid	$C_{20}H_{40}O_2$	312.5	23.06	0.26	ND	0.69	1.03	0.78	0.91	1.52	1.64	1.53	1.38	1.18	1.01	1.40	1.44	0.83	1.59	1.31
Oleic Acid	$C_{18}H_{34}O_2$	282.46	24.54	ND	ND	ND	ND	ND	ND	0.05	ND	ND	ND	ND	ND	ND	ND	ND	ND	ND
Vitamin E	$C_{29}H_{50}O_2$	430.71	33.17	1.39	3.02	0.29	1.32	0.83	1.21	ND	ND	ND	ND	ND	1.04	ND	ND	1.15	ND	ND
Campesterol	$C_{28}H_{48}O$	400.68	34.16	1.67	2.63	ND	ND	ND	1.01	1.39	1.05	1.11	1.17	ND	ND	1.05	ND	0.95	1.21	1.10
Stigmasterol	$C_{29}H_{48}O$	412.69	35.64	5.11	7.19	2.25	3.25	2.51	2.87	3.80	3.01	3.04	3.34	2.87	2.71	2.80	3.30	2.49	4.04	3.17
γ-Sitosterol	$C_{29}H_{50}O$	414.70	36,51	2.35	10.10	2.50	ND	ND	ND	ND	3.01	ND	ND	ND	ND	ND	ND	ND	ND	ND
β-Sitosterol	$C_{29}H_{50}O$	414.71	36.52	ND	ND	ND	3.80	3.20	ND	4.09	ND	3.33	3.84	3.88	3.25	3.46	3.97	ND	3.53	3.56
β-Amyrin	$C_{30}H_{50}O$	426.72	37.13	1.71	ND	ND	ND	ND	ND	0.73	0.38	0.50	ND	ND	ND	ND	0.58	ND	0.60	ND

α-Amyrin	$C_{30}H_{50}O$	426.72	37.90	ND	ND	ND	ND	ND	ND	ND	ND	ND	ND	ND	ND	ND	ND	ND	0.50	ND
Friedelin	$C_{30}H_{50}O$	426.72	40.54	2.32	18.80	ND	2.73	2.76	2.48	1.93	2.34	2.81	2.10	2.81	2.38	2.60	3.28	2.17	3.42	2.60
TR	-	-	-	38.04	28.40	7.27	6.78	4.85	5.35	6.99	4.93	7.43	4.44	2.78	6.55	5.29	3.97	3.77	5.86	2.51

RT: Retention time. ND: Not detected. TR: Trace compound.
*Extraction condition: 1- 40 °C/11 MPa/5 %EtOH; 2- 40 °C/17 MPa/5 %EtOH; 3- 60 °C/11 MPa/5 %EtOH; 4- 60 °C/17 MPa/5 %EtOH; 5- 40 °C/11 MPa/15 %EtOH; 6- 40 °C/17 MPa/15 %EtOH; 7- 60 °C/11 MPa/15 %EtOH; 8- 60 °C/17 MPa/15 %EtOH; 9- 50 °C/8 MPa/10 %EtOH; 10- 50 °C/20 MPa/10 %EtOH; 11- 36 °C/14 MPa/10 %EtOH; 12- 64 °C/14 MPa/10 %EtOH; 13- 50 °C/14 MPa/0 %EtOH; 14- 50 °C/14 MPa/20 %EtOH; 15- 50 °C/14 MPa/10 %EtOH.

Among the conditions applied to UAE + SFE, the C. *spicatus* extract showed the highest content of linolenic acid (62.52%) in the condition of 60 °C/11 MPa/5 %EtOH (test 3), lower than the UAE -EtOH (14.26%) and SFE (12.33%) extracts, as shown in Table 12. The use of the UAE technique before SFE significantly influenced the selectivity of this fatty acid. This implies that UAE, combined with SFE, is the most efficient method in extracting linolenic acid compared to traditional methods. In this way, the application of pretreatment was justified by accelerating extraction and achieving more efficient exploitation of the material due to the breakdown of cell walls and a decrease in the internal resistance of the material, considerably increasing the availability of the target components in the solvent [42].

Linolenic acid (18:3 ω-3) is an essential fatty acid, as the human body cannot synthesize it, but it can be acquired through diet or supplements [43]. Therefore, its intake in the diet or as a pharmacological nutrient can reduce symptoms of inflammation caused by viral infectious diseases, such as COVID-19, caused by the coronavirus 2 (SARS-CoV-2) strain, recently emerged at the end of 2019 [44]. Furthermore, this fatty acid has multiple benefits, such as reducing the development of cancer and cardiovascular diseases [45].

Although the UAE + SFE combination presents itself as the most efficient method for fatty acid extraction, the SFE technique without the UAE pretreatment favored the solubilization of the Friedelin triterpene, giving a content equivalent to 18.8% under the condition of 50 °C/14 MPa/10 %EtOH. Thus, it appears that the yield of fatty acids was influenced by the solubility of the solutes in the solvents used, corroborating with Li *et al.* [46].

Therefore, the present results demonstrate that combining processes is an interesting tool for obtaining fractions rich in lipids, mainly linolenic acid. This may result from physical changes in the structure of the raw material during the first extraction stage (UAE), benefiting the recovery of target compounds in the following stage (SFE).

4.3.5 Phenolic and flavonoid content wich the antioxidant activity

Regarding the results obtained for the Total Phenolic Content (TPC) of C. *spicatus* leaf extracts, it is possible to observe a significant difference between the TPC values for all conditions evaluated (Table 13). The SFE technique presented the lowest value, with 52.67 ± 1.21 mg GAE g^{-1}. Commonly, oily extracts obtained by nonpolar

solvents, such as CO_2, have low TPC values, mainly due to the high polarity of these compounds [47].

Phenolic compounds are common secondary metabolites of plants, directly related to many beneficial health effects, such anti-inflammatory, anticancer, anti-aging, antibacterial, and antiviral activities [48]. Furthermore, they are the main class of natural antioxidants [49]. The antioxidants react through different mechanisms, where different methodologies can confer your antioxidant potential [50]. In the present work, the potential of C. *spicatus* leaf extracts was observed by the DPPH and ABTS assays, as shown in Table 13.

Table 13. The total phenolic and flavonoid contents and antioxidant capacities (DPPH and ABTS) of C. *spicatus* leaf extracts were obtained with ultrasound (UAE), supercritical CO_2 extraction (SFE), and ultrasound pretreatment in supercritical CO_2 extraction (UAE + SFE).

Extraction technique	TPC (mg GAE g^{-1})	TFC (mg GAE g^{-1})	DPPH (µmol TE g^{-1})	ABTS (µmol TE g^{-1})
UAE	$102,57^{a} \pm 0,34$	$201,23^{a} \pm 1,81$	$50,26^{a} \pm 2,81$	$2051,7^{a} \pm 3,13$
SFE[1]	$52,67^{c} \pm 1,21$	$64,20^{c} \pm 1,36$	$52,86^{a} \pm 0,21$	$364,40^{c} \pm 3,01$
UAE+SFE[1]	$67,13^{b} \pm 2,14$	$129,36^{b} \pm 2,26$	$6,56^{b} \pm 1,41$	$1188,14^{b} \pm 2,28$

Abbreviations: TPC, total phenolic contente; TFC, total flavonoid content; DPPH, 1,1-diphenyl-2-picrylhydrazyl; ABTS, 2,2′-azinobis (3-ethylbenzothiazoline-6-sulphonic acid); UAE, ultrasound extraction; SFE, supercritical CO_2 extraction; UAE + SFE, Ultrasonic pretreatment in supercritical CO_2 extraction.

The same letters in the same column indicate no significant difference at a level of 5%.

[1] Extraction condition: 50 °C/14 MPa/10 %EtOH

From the methods studied, it is possible to observe that TPC values increased in the following sequence: SFE (52.67 mg GAE g^{-1}) < UAE + SFE (67.13 mg GAE g^{-1}) < UAE (102.57 mg GAE g^{-1}). Notably, the TPC value obtained by applying the ultrasonic technique was higher than that observed by the single-stage supercritical extraction and the combined process (Table 13). In research carried out by other authors, an increase in phenolic content was also observed when using EtOH as a solvent in the extraction [25,51]. This observation reinforces the idea that applying polar solvents to the raw material favors the extraction of more polar substances, such as phenolic compounds.

Interestingly, Total Flavonoid Content (TFC) was higher than Total Phenolic Content (TPC), expressed in mg GAE g^{-1}. This result can be attributed to the chemical

composition of the extract obtained from C. *spicatus* leaves, where a profile richer in flavonoids than in phenolic acids was found. With a significant difference, at the 5% significance level, the effects of ultrasound combined with SFE increased the recovery of flavonoid compounds (129.36 mg GAE g^{-1}) when compared with the effects of the SFE method alone (64.20 mg GAE g^{-1}). Thus proving the high efficiency of the UAE + SFE combination.

When comparing the methods used to determine antioxidant activities, a clear pattern emerges. The results obtained by ABTS consistently outshine those of DPPH in all extraction techniques evaluated (UAE, SFE, and UAE+SFE). In both DPPH and ABTS, the activity determination is based on the direct capture of organic radicals by antioxidant compounds.

In general, positive correlations between antioxidant activity and phenolic compounds have been observed [52, 53]. The results suggest that the highest values of 50.26 ± 2.81 μmol TE g^{-1} and 2051.7 ± 3.13 μmol TE g^{-1} obtained for DPPH and ABTS, respectively, are from the extracts with the highest total phenolic content. It isn't easy to attribute antioxidant activity to just one compound in a naturally complex mixture, such as extracts. Additionally, the best antioxidant capacity by ABTS was found for UAE, probably because the components responsible for the antioxidant characteristics detected by the ABTS method were present in higher concentrations. More tests are needed to identify the compounds responsible for the antioxidant activity of C. *spicatus* leaf extracts.

It's worth noting that the ABTS method consistently outperforms the DPPH method (ABTS > DPPH), a trend observed in other studies as well [54, 55]. This higher value of the ABTS method can be justified by the reaction of the ABTS radical with hydrophilic and lipophilic antioxidants present in the sample [56]. Furthermore, the disparity in results can be attributed to the distinct reaction mechanisms, oxidizing species, and reaction conditions of both methods [57].

Data on the antioxidant activity of C. *spicatus* leaf extracts involving the UAE, SFE, and UAE+SFE techniques have yet to be published in the literature. Therefore, the results presented in the present work are pioneering and were discussed qualitatively.

4.3.6 Antimicrobial activity

The antimicrobial activity of extracts obtained under SFE and UAE + SFE conditions was evaluated using Gram-positive and Gram-negative bacteria, filamentous fungi, and yeast. The antibacterial and antifungal activities were analyzed using the minimum inhibitory concentration (MIC) of C. *spicatus*. The extracts that showed antimicrobial activity up to 2000 μg mL^{-1} are presented in Table 14. The results provided in the present work provide pioneering data concerning the UAE + SFE dynamics and selective character.

Table 14. Minimal inhibitory concentration MIC (mg mL^{-1}) obtained for C. *spicatus* extracts for specific fungi and bacteria.

	Minimum Inhibitory Concentration (µg mL^{-1})										
	Extract						Extract				
Bacteria	SFE 3[1]	SFE 5[2]	UAE+ SFE 3[1]	UAE+ SFE 5[2]	Cip	**Fungi**	SFE 3[1]	SFE 5[2]	UAE+ SFE 3[1]	UAE+ SFE 5[2]	Ket
S. *aureus*	250	1000	250	250	0.25	A. fumigatus	>2000	>2000	>2000	>2000	7
B. *subtilis*	1000	1000	500	500	0.03	E. floccosum	2000	2000	2000	2000	6
E. *faecalis*	125	250	62.5	125	0.06	M. canis	2000	2000	1000	1000	8
S. hominis	250	500	250	500	0.5	M. gypseum	2000	2000	1000	1000	6
S. saprophyiticus	500	1000	500	500	1.2	R.sp.	>2000	>2000	>2000	>2000	15
E. *coli*	2000	2000	2000	>2000	0.03	T. mentagrophytes	>2000	>2000	2000	>2000	8
K. pneumoniae	>2000	>2000	>2000	>2000	0.03	T. rubrum	>2000	>2000	>2000	>2000	3
P. aeruginosa	>2000	>2000	>2000	>2000	0.5	C. *albicans*	2000	>2000	2000	2000	7
P. mirabilis	>2000	>2000	>2000	>2000	0.06						
S. typhimurium	>2000	>2000	>2000	>2000	0.06						

Abbreviations: SFE, supercritical CO_2 extraction; UAE + SFE, Ultrasonic pretreatment in supercritical CO_2 extraction; Cip, Ciprofloxacin; Ket, Ketoconazole;

[1]Extraction condition: 3 - 60 °C/11 MPa/5 %EtOH;

[2]Extraction condition: 5 - 40 °C/11 MPa/15 %EtOH.

Duarte *et al.* [58] proposed that plants with MIC values below 2000 μg mL^{-1} will be considered to have antimicrobial activity. MIC values up to 500 μg mL^{-1} were classified as compounds with strong activity, those with MIC from 600 to 1500 μg mL^{-1} were classified as compounds with moderate antimicrobial activity, and those with MIC above 1600 μg mL^{-1} were considered to have weak antimicrobial activity.

Based on this classification, the SFE 3 extract showed strong antibacterial activity against S. *aureus*, E. *faecalis*, S. *hominis*, and S. *saprophyiticus* (MIC: 125 – 500 μg mL^{-1}); moderate activity for B. *subtilis* (MIC: 1000 μg mL^{-1}); and weak activity for E. *coli* (MIC: 2000 μg mL^{-1}). The extract obtained under the conditions 40 °C/11 MPa/15 %EtOH, SFE 5, showed strong antibacterial activity against E. *faecalis* (MIC – 250 μg mL^{-1}) and S. *hominis* (MIC: 500 μg mL^{-1}); moderate activity for S. *aureus*, B. *subtilis* and S. *saprophyiticus* (MIC: 1000 μg mL^{-1}); and weak activity for E. *coli* (MIC: 2000 μg mL^{-1}). Therefore, the extracts showed better results for Gram-positive bacteria than for Gram-negative bacteria.

Regarding antifungal activity, it was possible to observe that the SFE 3 and SFE 5 extracts showed weak activity against E. *floccosum*, M. *canis*, and M. *gypseum*, with MIC values of 2000 μg mL^{-1}. Unlike SFE 5, the SFE 3 extract showed weak activity against the yeast C. *albicans*.

The UAE + SFE 3 extract showed strong antibacterial activity against S. *aureus*, B. *subtilis*, E. *faecalis*, S. *hominis*, and S. *saprophyiticus* (MIC: 62.5 – 500 μg mL^{-1}), and weak activity for E. *coli* (MIC: 2,000 μg mL^{-1}), K. *pneumoniae*, P. *aeruginosa*, P. *mirabilis*, S. *typhimurium* (MIC: > 2,000 μg mL^{-1}). The extract obtained under conditions 40 °C/11 MPa/15 %EtOH, UAE + SFE 5, also showed the same behavior as UAE+SFE 3, with strong antibacterial activity against S. *aureus*, B. *subtilis*, E. *faecalis*, S. *hominis*, and S. *saprophyiticus* (MIC: 125 – 500 μg mL^{-1}); and weak activity for E. *coli*, K. *pneumoniae*, P. *aeruginosa*, P. *mirabilis*, S. *typhimurium* (MIC: > 2,000 μg mL^{-1}). Therefore, the extracts showed better results for Gram-positive than Gram-negative bacteria.

Regarding antifungal activity, it was possible to observe that the UAE + SFE 3 and UAE + SFE 5 extracts showed moderate activity against M. *canis* and M. *gypseum*, with MIC values of 1000 μg mL^{-1}. The UAE+SFE 3 and UAE+SFE 5 extracts showed weak activity for the other fungi, with MIC values starting at 2000 μg mL^{-1}.

The best results for antifungal activity were obtained for the UAE + SFE extract with MIC values = 1000 μg mL^{-1} against dermatophytes (M. *canis*, M. *gypseum*). These

fungi provoke diseases caused by pathogenic keratinocyte fungi capable of invading the skin, hair, and nails, called dermatophytosis, in animals and humans [59].

Overall, the results demonstrated that the extract obtained by combining ultrasound and supercritical extraction showed superior antimicrobial activity against Gram-positive bacteria compared to traditional supercritical extraction. When analyzing the compounds found in the chemical profile of the extract determined by GC/MS and related to antimicrobial action, it was found that two of the main compounds present in the extract (linolenic acid and palmitic acid) have strong antimicrobial action. Studies have identified that palmitic acid may be responsible for the antimicrobial activity of some extracts [60]. The antibacterial activity of fatty acids is likely due to the ability of these compounds to disrupt bacterial cell membranes and cause cell lysis [61]. Furthermore, this biological activity can also be attributed to a synergistic effect between different components [62, 63]. This synergy behavior is commonly found in essential oils and other products of natural origin with complex compositions [62].

Only a few studies have reported antimicrobial activity for C. *spicatus* leaves; therefore, only a few studies are available for comparison with the present study. Despite this limitation, the same studies suggest that C. *spicatus* extract has antimicrobial activity. For example, Uliana *et al.* [64] evaluated that using C. *spicatus* leaf extract obtained by the maceration technique and acetone solvent showed antimicrobial activity against S. *aureus*, E. *coli*, and C. *albicans*.

Employing the same low-pressure methodology (maceration) but using ethanol as a solvent, Silva *et al.* [5] verified the antifungal efficacy of C. *spicatus* leaves against T. *mentagrophytes*, T. *rubrum*, M. *gypseum*, and E. *floccosum*, with the greatest activity being against M. *cani*. In this way, the difference between the results can be justified by the extraction methods, solvent used, microorganisms, or the plant's climatic and regional factors [65].

4.4 CONCLUSIONS

This study improved the process of obtaining bioactive compounds using ultrasonic pretreatment and supercritical CO_2 extraction from C. *spicatus* leaves. It is worth mentioning that the results presented are pioneering for this species studied. Applying UAE before SFE resulted in a higher extract yield than traditional UAE and SFE, where the best condition occurred in 50°C/14MPa/20%EtOH, with 6.97%.

SEM analysis revealed that the UAE + SFE treated sample had a notable impact on the tissue structures, with dense microcracks on the surface, which appeared to have been highly damaged and completely emptied of their contents. Such changes were not observed in samples submitted to traditional UAE and SFE.

The chemical profiles determined by GC/MS for UAE + SFE conditions showed an important diversity of compound classes. The ultrasonic pretreatment improved the selectivity of linolenic acid when the SFE technique was applied. Within the range of conditions studied, the optimal condition for the extraction of linolenic acid was 60 °C/11 MPa/5 % EtOH, with 62.52%.

The techniques studied presented different phenolic and flavonoid compounds, the content of which varied according to the following sequence: UAE > UAE + SFE > SFE. Although UAE had the highest content, the UAE + SFE combination showed better results due to the selectivity of the bioactives found. Regarding antioxidant activity, the extracts obtained from all techniques studied presented ABTS higher than DPPH.

The combination of ultrasound and supercritical extraction showed superior antimicrobial activity against Gram-positive bacteria compared to traditional supercritical extraction. Regarding antifungal activity, UAE + SFE extracts showed moderate activity against M. *canis* and M. *gypseum*, with MIC values of 1000 μg mL^{-1}.

These results reveal that extracts obtained from C. *spicatus* leaves from ultrasonic pretreatment at SFE presented several compounds of interest for developing natural products in the food, pharmaceutical, and cosmetic industries.

4.5 REFERENCES

[1] H. Lorenzi, F. J. A. Matos. Plantas Medicinais no Brasil: nativas e exóticas, editora Plantarum, Nova Odessa, São Paulo, (2002). ISBM 85-86714-28-3.

[2] U. P. De Albuquerque, J. Monteiro, M. Ramos, E. Amorim. Medicinal and magic plants from a public market in northeastern Brazil. Journal of Ethnopharmacology 110 (2007) 76–91. https://doi.org/10.1016/j.jep.2006.09.010.

[3] M. Coelho-Ferreira. Medicinal knowledge and plant utilization in an Amazonian coastal community of Marudá, Pará State (Brazil). Journal of Ethnopharmacology 126 (2009) 159-175. https://doi.org/10.1016/j.jep.2009.07.016.

[4] A.C. Keller, I. Vandebroek, Y. Liu, M.J. Balick, F. Kronenberg, E.J. Kennelly, A.M.B. Brillantes. *Costus spicatus* tea failed to improve diabetic progression in C57BLKS/J db/db mice, a model of type 2 diabetes mellitus. J. Ethnopharmacol 121 (2009) 248-254. https://doi.org/10.1016/j.jep.2008.10.025.

[5] D. N. Silva, M.J. Gonçalves, M.T. Amoral, M.T. Batista. Antifungal activity of a flavonoid-rich fraction from *Costus spicatus* leaves against dermatophytes. Planta Medica 74 (2008) 961-961. 10.1055/s-0028-1084088.

[6] L.J. Quintans Júnior, M.T. Santana, M.S. Melo, D.P. De Sousa, I.S. Santos, R.S. Siqueira, T.C. Lima, G.O. Silveira, A.R. Antoniolli, L.A.A. Ribeiro, M.R.V. Santos. Antinociceptive and anti-inflammatory effects of *Costus spicatus* in experimental animals. Pharm. Biol 48 (2010) 1097-1102. https://doi.org/10.3109/13880200903501822.

[7] United States Environmental Protection Agency, Green Chemistry., 2016. (Accessed 10 April, 2024), https://www.epa.gov/greenchemistry.

[8] T.C. Ho, A.T. Kiddane, F. Khan, Y.J. Cho, P.Jin- Seok, H.J. Lee, A.D. Kim, J.M. Kim, B.S. Chun. Pressurized liquid extraction of phenolics from Pseuderanthemum palatiferum (Nees) Radlk. leaves: Optimization, characterization, and biofunctional properties. Journal of Industrial and Engineering Chemistry 108 (2022) 418-428. https://doi.org/10.1016/j.jiec.2022.01.018.

[9] F. Chemat, M.A. Vian, A.S.F. Tixier, M. Nutrizio, A.R. Jambrak, P.E.S. Munekata, J.M. Lorenzo, F.J. Barba, A. Binello, G. Cravotto. A review of sustainable and intensified techniques for extraction of food and natural products. Green Chemistry 8 (2020). 10.1039/c9gc03878g.

[10] Y. C. Yang, M. C. Wei. A combined procedure of ultrasound-assisted and supercritical carbon dioxide for extraction and quantitation oleanolic and ursolic acids from Hedyotis corymbosa. Industrial Crops and Products 79 (2016) 7-17. https://doi.org/10.1016/j.indcrop.2015.10.038.

[11] N. Mezzomo, J. Martínez, M. Maraschin, S. R. S. Ferreira. Pink shrimp (P. brasiliensis and P. paulensis) residue: Supercritical fluid extraction of carotenoid

fraction. The Journal of Supercritical Fluids, 74, 22-33, 2013. https://doi.org/10.1016/j.supflu.2012.11.020.

[12] M.M.R. De Melo, A.J.D. Silvestre, C.M. Silva. Supercritical fluid extraction of vegetable matrices: Applications, trends and future perspectives of a convincing green technology. Journal of Supercritical Fluids, v. 92, p. 115-176, 2014. https://doi.org/10.1016/j.supflu.2014.04.007.

[13] K. S. Duba, L. Fiori. Supercritical CO_2 extraction of grape seed oil: Effect of process parameters on the extraction kinects. The Journal of Supercritical Fluids. 98, 33-43, 2015. https://doi.org/10.1016/j.supflu.2014.12.021.

[14] X. Liu, H. Ou, Z. Xiang, H. Gregersen. Ultrasound pretreatment combined with supercritical CO2 extraction of Iberis amara seed oil. Journal of Applied Research on Medicinal and Aromatic Plants, 18, 100265, 2020. https://doi.org/10.1016/j.jarmap.2020.100265.

[15] F. Chemat, N. Rombaut, A.G. Sicaire, A. Meullemiestre, A.F. Tixier, Vian, M.A. Ultrasound assisted extraction of food and natural products. Mechanisms, techniques, combinations, protocols and applications. A review. Ultrasonics Sonochemistry 34 (2017) 540–560. https://doi.org/10.1016/j.ultsonch.2016.06.035.

[16] X.Y. Liu, H. Ou, H. Gregersen. Ultrasound-assisted supercritical CO_2 extraction of cucurbitacin E from *Iberis amara* seeds. Industrial Crops and Products 145 (2020) 112193. https://doi.org/10.1016/j.indcrop.2020.112093.

[17] F.M. Barrales, C.A. Rezende, J. Martínez. Supercritical CO_2 extraction of passion fruit (*Passiflora edulis* sp.) seed oil assisted by ultrasound. J. Supercrit. Fluids 104 (2015) 183–192. https://doi.org/10.1016/j.supflu.2015.06.006.

[18] P. Santos, A.C. Aguiar, G.F. Barbero, C.A. Rezende, J. Martínez. Supercritical carbon dioxide extraction of capsaicinoids from malagueta pepper (*Capsicum frutescens* L.) assisted by ultrasound. Ultrasonics Sonochemistry 22 (2015) 78–88. https://doi.org/10.1016/j.ultsench.2014.05.001.

[19] AOAC Associação de químico analítico oficial, métodos oficiais de análise 18º, AOAC Internacional (2002).

[20] T. BelwaL, S.M. Ezzat, L. Rastrelli, I.D. Bhatt, M. Daglia, A. Baldi, H.P. Devkota, I.E. Orhan, J.K. Patra, G. Das, C. Anandharamakrishnan, L. Gomez-Gomez, S.F. Nabavi, S.M. Nabavi, A.G. Atanasov. A critical analysis of extraction techniques used for botanicals: Trends, priorities, industrial uses and optimization strategies. TrAC - Trends in Analytical Chemistry 100 (2018) 82–102.

[21] M.A.A. Meireles. Extraction of bioactive compounds from latin american plants. In. J.L. Martinez. Supercritical fluid extraction of nutraceuticals and bioactive compounds. Boca Raton, CRC Press (2008) 243-274.

[22] J.L. Luque-García, M.D Luque De Castro. Ultrassom: uma ferramenta poderosa para a lixiviação TrAC - Trends Anal. Química. 22 (2003) 41-47. 10.1016 / S0165-9936 (03)00102-X.

[23] T. K.S. Laurintino. Avaliação de compostos bioativos e potencial antioxidante da folha e caule da cana do brejo (*costus spicatus*) por diferentes métodos de extração. Dissertação (mestrado), Programa de pós-graduação em engenharia química, Florianópolis, 2020.

[24] T.N.S. Laurintino, D.P. Tramontin, J. Assreuy, A.B. Cruz, C.C.B. Cruz, A. Marangoni, M.A. Livia, A. Bolzan. Evaluation of the biological activity and chemical profile of supercritical and subcritical extracts of Bursera graveolens from northern Peru. J. Supercrit. Fluids 198 (2023) 105934. https://doi.org/10.1016/j.supflu.2023.105934.

[25] D.P. Tramontin, S.E. Cadena-Carrera, A.B. Cruz, C.C.B. Cruz, A. Bolzan, M.B. Quadri. Biological activity and chemical profile of Brazilian jackfruit seed extracts obtained by supercritical CO_2 and low pressure techniques. J. Supercrit. Fluids 152 (2019) 104551. https://doi.org/10.1016/j.supflu.2019.104551.

[26] J.J.S. Ciarlini, A. Marangoni, A. Bolzan. Selectivity of supercritical CO_2 extraction and atmospheric pressure techniques for the major volatile compounds of Eugenia involucrata leaves from Southern Brazil. Food and Bioproducts Processing 106 (2017) 29–34. https://doi.org/10.1016/j.fbp.2017.08.008.

[27] D.G. Citadin, C.A. Claumann, A.W. Zibetti, A. Marangoni, A. Bolzan, R.A.F. Machado. Supercritical fluid extraction of Drimys angustifolia Miers: Experimental data and identification of the dynamic behavior of extraction curves using neural networks

based on wavelets. J. Supercrit. Fluids 112 (2016) 81-88. https://doi.org/10.1016/j.supflu.2016.02.007.

[28] L.T. Taylor. Supercritical Fluid Extraction, WileyInterscience, New York, 1996. https://doi.org/10.1007/BF01242421.

[29] M.I. Rodrigues, A.F. Lemma. Planejamento de experimentos & otimização de processos. 3. ed. Campinas, SP: Editora Cárita, 2014.

[30] D. Zhang. A coefficient of determination for generalized linear models. The American statistician 71 (2017) 310-316. https://amstat.tandfonline.com/doi/abs/10.1080/00031305.2016.1256839.XUiHCstKicw

[31] NIST. Webbook, Instituto Nacional de Normas e Tecnologia - NIST (2018).

[32] D. Granato, D. S. Nunes. Análises químicas, propriedades funcionais e controle de qualidade de alimentos e bebidas: uma abordagem teórico prática. Rio de Janeiro: Elsevier Brasil, 2016.

[33] C.-C. Chang, M.-H. Yang, H.-M. Wen, J.-C. Chern. Estimation of total flavonoid content in propolis by two complementary colometric methods. Journal of Food and Drug Analysis, 10 (2002)178-182.

[34] M. Boroski, J. Visentainer, S. Cottica, D. Morais. Antioxidantes princípios e métodos analíticos, first ed., Appris, Curitiba, 2015.

[35] R. Re, N. Pellegrini, A. Proteggente, A. Pannala, M. Yang, C. Rice-Evans. Antioxidant activity applying an improved ATBS radical, free cadic, Biol. Med. 26 (1999) 1231–1237. http://dx.doi.org/10.1016/S0891-5849(98)00315-3.

[36] C. Guindani, R. Podest´a, J. M. Block, M. J. Rossi, N. Mezzomo, S. R. S. Ferreira. Valorization of chia (*Salvia hispanica*) seed cake by means of supercritical fluid extraction. The Journal of Supercritical Fluids, 112 (2016) 67–75. https://doi.org/ 10.1016/j.supflu.2016.02.010.

[37] R.D. De Souza, B.A.S. Machado, G.D. Barreto, I.L. Leal, J.P. Dos Anjos, M.A. Umsza-Guez. Effect of experimental parameters on the extraction of grape seed oil

obtained by low pressure and supercritical fluid extraction. Molecules 25 (2020) 1634. https://doi.org/10.3390/molecules25071634.

[38] E.K. Asep, S. Jinap, M.H.A. Jahurul, I.S.M. Zaidul, H. Singh. Effects of polar cosolvents on cocoa butter extraction using supercritical carbon dioxide. Innov. Food Sci. Emerg. Technol 20 (2013)152-160. https://doi.org/10.1016/j.ifset.2013.06.010.

[39] J. Yi, J. Yeo, F.E. Soetaredjo, S. Ismadji, J. Sunarso. Experimental measurement and correlation of phase equilibria of palmitic, stearic, oleic, linoleic, and linolenic acids in supercritical carbon dioxide. Journal of Industrial and Engineering Chemistry 97 (2021) 485-491. https://doi.org/10.1016/j.jiec.2021.03.002.

[40]P. Joradon, V. Rungsardthong, U. Ruktanonchai, K. Suttisintong, B. Thumthanaruk, S. Vatanyoopaisarn, D. Uttapap, A. C. Mendes. Extraction of bioactive compounds from Lion's Mane mushroom by-product using supercritical CO_2 extraction. The Journal of Supercritical Fluids 206 (2024) 106162. https://doi.org/10.1016/j.supflu.2023.106162.

[41] B. Khadhraoui, M. Turk, A.S. Fabiano-Tixier, E. Petitcolas, P. Robinet, R. Imbert, M. El Maâtaoui, F. Chemat. Histo-cytochemistry and scanning electron microscopy for studying spatial and temporal extraction of metabolites induced by ultrasound. Towards chain detexturation mechanism. Ultrasonics Sonochemistry, 42 (2018) 482-492. https://doi.org/10.1016/j.ultsonch.2017.11.029.

[42] V. Ummat, S.P. Sivagnanam, G. Rajauria, C. O'Donnell, B.K.Tiwari. Advances in pre-treatment techniques and green extraction technologies for bioactives from seaweeds. Trends Food Sci. Technol. 110 (2021) 90–106. https://doi.org/10.1016/j.tifs.2021.01.018.

[43] L. Baldino, M. Scognamiglio, E. Reverchon. Supercritical fluid technologies applied to the extraction of compounds of industrial interest from *Cannabis sativa* L. and to their pharmaceutical formulations: A review, J. Supercrit. Fluids 165 (2020) 104960. https://doi.org/10.1016/j.supflu.2020.104960.

[44] P. Weill, C. Plissonneau, P. Legrand, V. Rioux, R.Thibault. May omega-3 fatty acid dietary supplementation help reduce severe complications in Covid-19 patients? J. Biochi., 179 (2020)275-280. https://doi.org/10.1016/j.biochi.2020.09.003.

[45] N. Kaur, V. Chugh, A.K. Gupta. Essential fatty acids as functional components of foods-a review, J. Food Sci. Technol 51 (2014) 2289–2303. 10.1007/s13197-012-0677-0.

[46] Y. Li, F.G. Naghdi, S. Garg, T.C. Adarme-Vega, K.J. Thurecht, W.A. Ghafor, S. Tannock, P.M. Schenk. A comparative study: The impact of different lipid extraction methods on current microalgal lipid research. Microbial Cell Factories 13 (2014) 14. 10.1186/1475-2859-13-14.

[47] G. Brunner. Gas extraction: an introduction to fundamentals of supercritical fluids and the application to separation processes. (1a). Steinkopff, Darmstadt, 1994. 10.1007/978-3-662-07380-3.

[48] M. Rahman, S. Rahaman, R. Islam, F. Rahman, F.M.Mithi, T. Algahtani, *et al.* Role of Phenolic Compounds in Human Disease: Current Knowledge and Future Prospects. Molecules 27(1): 233 (2022). 10.3390/molecules27010233

[49] V. Cheynier. Phenolic compounds: From plants to foods, Phytochem. Rev. 11 (2012) 153–177. http://dx.doi.org/10.1007/s11101-012-9242-8.

[50] A.A.F. Zielinski, A. Alberti, E. Bona, D.G. Bortolini, L. Benvenutti, F. Bach, I.M. Demiate, A. Nogueira. A multivariate approach to differentiate yerba mate (*Ilex paraguariensis*) commercialized in the southern Brazil on the basis of phenolics, methylxanthines and in vitro antioxidant activity, Food Sci. Technol. 2061 (2020) 1–9. http://dx.doi.org/10.1590/fst.15919.

[51] W. Zzaman, Optimization of Antioxidant Extraction From Jackfruit (Artocarpus Heterophyllus Lam.) Seeds Using Response Surface Methodology, Faculty of Bioscience Engineering Academic Year 2011 – 2012, Optimization of antioxidant extraction from jackfruit Ghent University, 2012.

[52] V.M. Burin, N.E. Ferreira-lima, C.P. Panceri, M.T. Bordignonluiz. Bioactive compounds and antioxidant activity of Vitis vinifera and Vitis labrusca grapes: evaluation of different extraction methods, Microchem. J. 114 (2014) 155–163. https://doi.org/10.1016/j.microc.2013.12.014.

[53] D. Tagliazucchi, E. Verzelloni, D. Bertolini, A. Conte. In vitro bio-accessibility and antioxidant activity of grape polyphenols. Food Chem. 120 (2) (2010) 599–606, https://doi.org/10.1016/j.foodchem.2009.10.030.

[54] A.P.F. Machado, A.L.D. Pereira, G.F. Barbero, J. Martínes Recovery of anthocyanins from residues of Rubus fruticosus, Vaccinium myrtillus and Eugenia brasiliensis by ultrasound assisted extraction, pressurized liquid extraction and their combination. Food Chemistry 231 (2017) 1-10. https://doi.org/10.1016/j.foodchem.2017.03.060.

[55] W. Routray, V. Orsat, Y. Gariepy. Effect of different drying methods on the microwave extraction of phenolic components and antioxidant activity of highbush blueberry leaves. Drying Technology, 32(16) (2014) 1888–1904. 10.1080/07373937.2014.919002.

[56] S. Gorjanovic, D. Komes, F.T. Pastor, A. Bels, C. ak-Cvitanovic, L. Pezo, I. Hec, I. Hecimovic, D. Suznjevic. Antioxidant capacity of teas and herbal infusions: Polarographic assessment. J. Agric. Food Chem. 60 (2012) 9573–9580. http:// dx.doi.org/10.1021/jf302375t.

[57] A. Karadag, B. Ozcelik, S. Saner. Review of methods to determine antioxidant capacities, Food Anal. Methods 2 (2009) 41–60. https://doi.org/10.1007/s12161- 008-9067-7.

[58] M. C. T. Duarte, G. M. Figueira, A. Sartoratto, V. L. G. Rehder, C. Delarmelina. Anti-Candida activity of Brazilian medicinal plants. Journal of ethnopharmacology, 97 (2005), 305-311. https://doi.org/10.1016/j.jep.2004.11.016.

[59] J. Begum, N.A. Mir, M.C. Lingaraju, B. Buyamayum, K. Dev. Recent advances in the diagnosis of dermatophytosis. J. Basic Microbiol 60 (2020). https://doi. org/10.1002/jobm.201900675.

[60] J.A. Mendiola, Extracción de compuestos bioactivos de microalgas mediante fluidos supercríticos. Tesis Doctoral, Universidad Autónoma de Madrid, Espana, 2008.

[61] A. Hinton, K.D. Ingram. Use of oleic acid to reduce the population ofthe bacterial flora of poultry skin. Journal of Food Protection, 9 (2000) 1282–1286. 10.4315/0362-028x-63.9.1282.

[62] S. Burt. Essential oils: their antibacterial properties and potential applications in foods – a review. International J. Food Microbiology, 94 (2004) 223–253. https://doi.org/10.1016/j.ijfoodmicro.2004.03.022.

[63] P.P. Alvarez-Castellanos, C.D. Bishop, M.J. Pascual-Villalobos. Antifungal activity of the essential oils of flower heads of garland chrysanthemum (Chrysanthemum coronarium) against agricultural pathogens. Phytochemistry 57 (2001) 99–102. https://doi.org/10.1016/S0031-9422(00)00461-1.

[64] M. P. Uliana, A. G. Da Silva, M. Fronza, R. Scherer. In vitro antioxidant and antimicrobial activities of *Costus spicatus* swartz used in folk medicine for urinary tract infection in Brazil. Lat Am J Pharm, 34 (2015) 766-72.

[65] S. Mazzutti, S.R.S. Ferreira, C.A.S. Riehl, A. Smania, F.A. Smania, J. Martínez. Supercritical fluid extraction of *Agaricus brasiliensis*: antioxidant and antimicrobial activities. J Supercrit Fluids 70 (2012) 48–56. https://doi.org/10.1016/j.supflu.2012.06.010.

CHAPTER V - EVALUATION OF BIOLOGICAL ACTIVITY, PHYSICOCHEMICAL AND MORPHOLOGICAL CHARACTERISTICS OF LOW AND HIGH PRESSURE EXTRACTS OF *COSTUS SPICATUS* LEAVES.

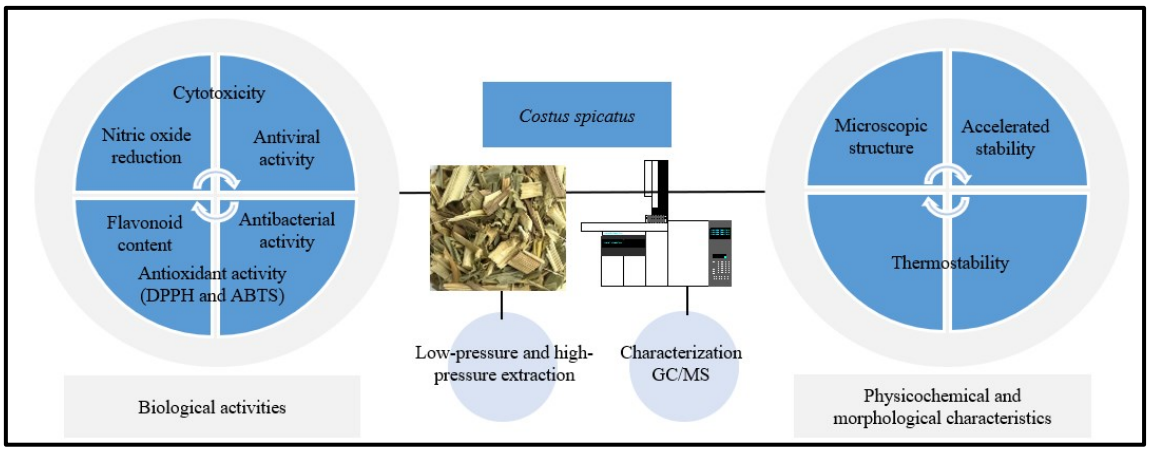

ABSTRACT

Costus spicatus, from the Costaceae family, has valuable nutritional, pharmacological, and medicinal properties. This study evaluated the biological activities, physicochemical and morphological characteristics of *C. spicatus* leaves using low-pressure techniques (LPE) such as maceration (MAC), ultrasound (UAE), and Soxhlet (SOX) and high-pressure techniques such as supercritical fluid extraction (SFE) and the UAE+SFE combination. The results showed that LPE and UAE+SFE did not reduce cell viability to 100 μg mL^{-1}, with a significant reduction only at 300 μg mL^{-1} and higher for SFE. UAE+SFE inhibited nitric oxide by more than 90% at 30 to 300 μg mL^{-1} concentrations. LPE with EtOH showed high levels of flavonoids (150.38–1328.73 mg GAE g^{-1}), and UAE+SFE improved the recovery of these compounds compared to SFE alone. Antioxidant activity was superior with ABTS, and all extracts showed antibacterial activity against B. cereus. UAE+SFE was also the most effective against HSV-1. Confocal microscopy confirmed autofluorescence, and UAE+SFE showed higher efficiency in lipid droplet extraction. Furthermore, the UAE+SFE extract showed thermal stability according to TG and DTG analyses. All samples showed high physical stability. This study characterizes the properties of *C. spicatus* leaves and supports their application in food, pharmaceutical, and industry.

Keywords

Costus spicatus; Supercritical extraction; Bioactive compounds; Biological activities; Cytotoxicity; Antimicrobial

5.1 INTRODUCTION

Costus spicatus (Jacq.) Sw. is a plant found in humid coastal forests and belongs to the Costaceae family. It is popularly known as “cana do brejo”, “cana de macaco”, or “cana do mato” [1]. In Brazil, this plant material is native to regions of the Atlantic Forest and Amazon [2]. *Costus* is the most important genus commercially, with 125 to 175 species distributed in tropical regions of all continents, mainly in the Americas [3].

The literature highlights several biological activities of *Costus spicatus*, such as analgesic, antioxidant, antimicrobial, antifungal, and nephroprotective, attributed to triterpenes, sterols, flavonoids, saponins, alkaloids, and tannins present in the plant oil [4, 5]. Ethnopharmacological studies show that its leaves are used in infusions and decoctions to treat kidney pain, back pain, urinary problems, hepatitis, kidney stones, and other urinary afflictions [6, 7].

Based on their potential pharmacological benefits, several extraction techniques can be explored to obtain bioactive compounds for analytical and industrial purposes. Conventional techniques, such as maceration (MAC) and Soxhlet (SOX), offer advantages such as convenience and low cost. However, these techniques have disadvantages such as high consumption of organic solvents, low efficiency, and low selectivity for analytes. These limitations can be overcome by unconventional extraction methods, such as ultrasonic extraction (UAE) and supercritical fluid extraction (SFE) [8].

Supercritical technology can be used with various fluids, especially CO_2, since it is non-toxic, non-flammable, and easily removed from the extracted materials. To increase the solvation power of this solvent, a small amount of ethanol is necessary to increase the solubility of the extractable compounds [9]. However, SFE requires hermetic autoclaves, which results in high operating costs and slow mass transfer [10]. To improve performance, SFE can be expanded and combined with other techniques. Ultrasound, for example, has shown great potential in intensifying the extraction process, making the combination with SFE a promising route to obtain medicinal phytotherapeutic compounds.

Based on the above, the compounds from *Costus spicatus* leaves have the potential to develop new products, but in-depth studies are lacking. The present work seeks to apply low-pressure (MAC, UAE, SOX) and high-pressure (SFE and UAE+SFE) extraction techniques to evaluate the biological properties of the extracts, including cytotoxicity, nitric oxide reduction, flavonoid content, antioxidant activity (DPPH and

ABTS), antibacterial and antiviral activity against HSV-1. Physicochemical and morphological characteristics such as microscopic structure, accelerated stability, and thermostability (TGA) will also be analyzed.

5.2 MATERIAL AND METHODS

5.2.1 Raw material and sample preparation

C. spicatus leaves and stems were obtained from Comercial Charoma (Piraquara, PR – Brazil). Leaves were manually separated from stems and dried in an oven with forced air circulation (CE 220/2016, Cienlab, Campinas, SP, Brazil) at 35 °C for 24 h. Leaves were then ground in a coffee grinder (MDR302, Cadence, Balneário Piçarras, SC, Brazil). The particles were characterized by particle size classification on a Tyler Standard Sieve (A bronzinox, São Paulo, SP, Brazil), using only a 45 mesh sieve (355 μm) as obtained by preliminary tests by Laurintino *et al.* [11]. To maintain the stability of the sample and prevent oxidation of compounds due to the action of heat and light, the sample was packaged and stored in a domestic freezer at -18 ºC (BRM39, Brastemp, São Bernardo do Campo, SP, Brazil) until extraction.

5.2.2 Extractions

5.2.2.1 Low-pressure Extraction (LPE)

Maceration extraction (MAC) was performed according to Mazzutti *et al.* [12], using a sample: solvent ratio of 1:4 w/v for 168 h with daily manual stirring at room temperature (25 °C).

Ultrasound-assisted extractions (UAE) were performed according to the method adapted from Luque-García and Luque De Castro [13]. About 1 g of sample was briefly placed in contact with 30 mL of solvent and subjected to an ultrasonic probe (DES5000, Unique, São Paulo, SP, Brazil) for 5 min at 70 % power (maximum power – 500 W) and frequency of 20 kHz.

Soxhlet extraction (SOX) was performed according to method 920.39 of AOAC Official Methods [14]. The procedure involved recycling 150 mL of solvent in 5 g of raw material in a Soxhlet apparatus. The system was heated to the solvent's boiling point, and reflux was maintained for 5 h. The low-pressure extraction (LPE) was performed using ethanol (EtOH) and hexane (HEX) as solvents.

5.2.2.2 Supercritical Fluid Extraction (SFE)

The high-pressure extraction process was performed in a supercritical chromatography and extraction unit (LC 2000, Jasco, Hachioji, Tokyo, Japan). The extraction conditions (pressure, temperature, volumetric flow rate of solvent, and cosolvent) were kept constant throughout the experimental period. The solvent (CO_2) sent from the cylinder passed through a cooling system with a temperature of -10 °C (FL-1201, Julabo, Seelbach, Baden-Württemberg, Germany). It was pressurized by a positive displacement HPLC pump (PU-2087/2087 Plus, Jasco, Hachioji, Tokyo, Japan) at a constant volumetric flow rate (mL min^{-1}). The volumetric flow rate of the cosolvent (EtOH) was expressed as mass fractions relative to the mass of CO_2 used. This cosolvent was pumped using a positive displacement HPLC pump (PU-2087/2087 Plus, Jasco, Hachioji, Tokyo, Japan) and mixed with supercritical CO_2 before being introduced into the extraction cell.

Due to the low apparent density of the raw material particle and the small volume of the extraction column, approximately 1.27 g of leaves were added to the extraction column (127.5 mm in length x 10 mm in diameter and internal volume of 10 cm^3), forming a fixed bed. All samples with the same extraction time of 120 min. The adopted SFE condition was determined by preliminary experiments by Laurintino *et al.* [11], where conditions 1- 50 ºC/14 MPa/0 %EtOH, 2- 50 ºC/14 MPa/20 %EtOH, 3- 50 ºC/8 MPa/10 %EtOH, 4- 50 ºC/20 MPa/10 %EtOH, 5- 36 ºC/14 MPa/10 %EtOH, 6- 64 ºC/14 MPa/10 %EtOH, 7- 40 ºC/11 MPa/5 %EtOH, 8- 50 ºC/14 MPa/10 %EtOH, 9- 60 ºC/17 MPa/15 %EtOH, 10- 60 ºC/11 MPa/5 %EtOH.

The volumetric flow rate of CO_2 was kept constant at 3 mL min^{-1}. CO_2 was used as a solvent (99.99%, White Martins, Florianópolis, SC, Brazil) and ethanol as cosolvent (99.99%, Metaquímica, Jaraguá do Sul, SC, Brazil). The extracts were collected using an offline collection system, or "trapping," where solute precipitation occurs by depressurizing the solvent at atmospheric pressure [15]. The extract was filtered and stored in a domestic freezer at -18 ºC (BRM39, Brastemp, São Bernardo do Campo, SP, Brazil) until further analysis.

5.2.2.3 Ultrasound pretreatment (UAE + SFE)

The UAE+SFE extraction was performed as described by Laurintino *et al.* [11]. Three steps were performed: in the first step, ultrasound-assisted extractions (UAE) were

performed according to the adapted method of Luque-García and Luque De Castro [13], as described in section 2.2.1. After ultrasonic treatment, the phases were separated by a centrifuge for 5 min at 3.000 rpm in the second step. The leaf residue was dried at 40 °C for 24 h. The supernatant with 2 g of hollow glass microspheres (VS5500, 3 M, Minnesota, USA) was evaporated to dryness by a vacuum rotary evaporator (RE100-Pro, Scilogex, USA). This resulted in microspheres coated with crude extract. Finally, the dried residue and microspheres coated with crude extract were sufficiently mixed in the third step. They were then placed in the SFE chamber for re-extraction.

The conditions evaluated were: 1- 50 ºC/14 MPa/0 %EtOH, 2- 50 ºC/14 MPa/20 %EtOH, 3- 50 ºC/8 MPa/10 %EtOH, 4- 50 ºC/20 MPa/10 %EtOH, 5- 36 ºC/14 MPa/10 %EtOH, 6- 64 ºC/14 MPa/10 %EtOH, 7- 40 ºC/11 MPa/5 %EtOH, 8- 50 ºC/14 MPa/10 %EtOH , 9- 60 ºC/17 MPa/15 %EtOH, 10- 60 ºC/11 MPa/5 %EtOH.

5.2.3 Post-processing of extracts

A rotary evaporator (R-100, BUCHI, Flawil, St. Gallen, Switzerland) was used for LPE, SFE, and UAE+SFE to separate the solvent at the end of extractions.

5.2.4 Cell viability

5.2.4.1 Cell culture

A L929 cell line (mouse fibroblast) was purchased from Rio de Janeiro Cell Bank (BCRJ, Rio de Janeiro, RJ, Brazil) and maintained in Dulbecco's Minimal Essential Media (DMEM) supplemented with 10 % Fetal Bovine Serum (FBS), 100 μg mL^{-1} streptomycin, 100 IU mL^{-1} penicillin and 10 mM HEPES buffer at 37 °C in a 5 % CO_2 atmosphere. Cells were seeded in 96-well plates at a density of 1×10^5 cells per well, and when confluency was achieved, the extracts were added at concentrations of 30, 100, and 300 μg mL^{-1} culture medium. The following extracts were evaluated with these cells by the MTT method: MAC-EtOH, MAC-HEX, UAE-EtOH, UAE-HEX, SOX-EtOH, SOX-HEX, SFE 1, SFE 2, SFE 3, SFE 4, SFE 5, SFE 6, UAE+SFE 1, UAE+SFE 2, UAE+SFE 3, UAE+SFE 4, UAE+SFE 5, and UAE+SFE 6. Only 6 samples of SFE and UAE+SFE were evaluated, considering the conditions of higher and lower pressure, temperature, and cosolvent concentration Laurintino *et al.* [11].

5.2.4.2 Cell viability assay

This assay was performed according to the methodology proposed by Van de Loosdrecht *et al.* [16]. After 24 h of contact between extracts and cells, the MTT reagent ([3-(4,5-dimethylthiazol-zyl) − 2,5-diphenyl tetrazolium bromide]) was added to a final concentration of 0.5 mg mL^{-1} of culture medium, and incubated for 1 h at 37 °C and 5 % CO_2 atmosphere. The medium was removed, and the cell monolayer was solubilized in DMSO (dimethylsulfoxide). Absorbance was measured at a wavelength of 540 nm (Infinity M-200, Tecan, Männedorf, Zurich, Switzerland). The absorbance of control cells was considered 100 % viability, and the optical density from the other groups was calculated as a percentage of viability. No harmful effect of DMSO was observed at the maximal final concentration of 1 %.

5.2.5 Nitric oxide inhibitory activity

5.2.5.1 Cell cultures and treatment

The murine macrophage cell line J774 was purchased from the Rio de Janeiro Cell Bank (BCRJ, Rio de Janeiro, RJ, Brazil) and cultured in Dulbeco's Minimum Essential Medium (MEMD) supplemented with 10% Fetal Bovine Serum (FBS), 100 μg L^{-1} streptomycin and 100 IU mL^{-1} penicillin under 5% CO_2 at 37 °C. Macrophages were subjected to cell viability assay and NO production inhibition to obtain an anti-inflammatory potential index. Extracts were added to the plate wells at 30, 100, and 300 μg mL^{-1} of culture medium. The following extracts were evaluated with the macrophages: MAC-EtOH, UAE-EtOH, SOX-EtOH, SFE 7, SFE 8, SFE 9, UAE+SFE 7, UAE+SFE 8, UAE+SFE 9. Only three conditions of SFE and UAE+SFE were evaluated, considering the lower, upper, and central limits of Laurintino *et al.* [11].

J774 cells were seeded in 96-well plates at 5 × 105 cells/well and incubated for 12 h at 37 °C, 5% CO_2 to allow cell attachment. Cells were treated with 20 μg mL^{-1} extract prepared in FCS-free DMEM. After 1 h of treatment, cells were stimulated with 5 μg mL^{-1} lipopolysaccharide (LPS) for 24 h.

5.2.5.2 Griess assay

NO production was determined in the supernatants by measuring the formation of nitrite ion ($NO2^-$ - a stable metabolite of NO) [17]. Briefly, 100 μL of Griess reagent (equal parts of 1% sulfanilamide in 10% phosphoric acid in 0.1% naphthyl

ethylenediamine in water) was added to 50 µL of supernatant. After an incubation of 15 min, the absorbance was read at a wavelength of 540 nm (Infinity M-200, Tecan, Männedorf, Zurich, Switzerland) at room temperature. The amount of nitrite in the medium was calculated from the standard curve of sodium nitrite ($NaNO_2$).

5.2.6 Total flavonoid content (TFC)

The TFC in *C. spicatus* leaf extracts (1 mg mL^{-1} in ethanol) was determined by the method described by Chang *et al.* [18] with some modifications. Briefly, 0.5 mL of the extract was mixed with 0.1 mL of 10% $AlCl_3$ solution and 1.5 mL of methanol (pa). The mixture was shaken and left to stand for 5 min. Then, 0.1 mL of 1 mol L^{-1} potassium acetate and 2.8 mL of distilled water were added. After shaking, the mixture was kept at room temperature (25 °C) for another 15 min. Subsequently, the absorbance was measured at 415 nm using a UV-vis spectrophotometer (V-M5, Bel Engenharia, Piracicaba, SP, Brazil). A standard curve (12.5–125 µg mL^{-1}) was established using quercetin (HPLC grade, Sigma) to quantify the flavonoid content. The results were expressed as milligrams of quercetin equivalents (QE) per gram of extract (mg QE g^{-1}) based on a linear regression equation ($R^2 = 0.9992$). This activity was performed in MAC-EtOH, MAC-HEX, UAE-EtOH, UAE-HEX, SOX-EtOH, SOX-HEX, SFE 3, SFE 4, UAE+SFE 3, UAE+SFE 4. Only two conditions of SFE and UAE+SFE were evaluated, considering the lower and higher pressure limits: 50 ºC/8 MPa/10 %EtOH and 50 ºC/20 MPa/10 %EtOH, respectively [11].

5.2.7 Antioxidant capacity

The in vitro antioxidant capacity of the extracts was determined by DPPH and ABTS methods. This activity was performed in MAC-EtOH, MAC-HEX, UAE-EtOH, UAE-HEX, SOX-EtOH, SOX-HEX, SFE 3, SFE 4, UAE+SFE 3, UAE+SFE 4. Only two conditions of SFE and UAE+SFE were evaluated, considering the lowest and highest pressure limits: 50 ºC/8 MPa/10 %EtOH and 50 ºC/20 MPa/10 %EtOH, respectively [11].
5.2.7.1 DPPH free radical scavenging activity (DPPH)

The DPPH (1,1-diphenyl-2-picrylhydrazyl) radical scavenging activity of the extracts was determined according to the method described by Boroski *et al.* [19]. A 25 µL aliquot of the extract at a concentration of 0.05 g mL^{-1} was mixed with 2 mL of 0.091 mM DPPH in EtOH solution. The mixture was shaken and allowed to stand for 30 min at

25 °C under dark conditions. The absorbance was measured at 517 nm with a spectrophotometer (V-M5, Bel Engenharia, Piracicaba, SP, Brazil). The antioxidant potential was calculated from a linear regression and the variation of the equivalent antioxidant capacity of Trolox between 0 and 2 Mm (R^2 = 0.9992). The results were expressed as μmol of Trolox equivalent (TE) per g of dry sample (μmol TE g^{-1} ± standard deviation).

5.2.7.2 ABTS+ free radical scavenging activity

The radical scavenging activity of the extracts was evaluated spectrophotometrically by the ABTS [2,2′-azino-bis (3-ethylbenzothiazoline-6-sulfonic acid)] assay following a method detailed by Re *et al.* [20]. ABTS was generated by the reaction of 7 mM ABTS aqueous solution with 2.4 mM potassium persulfate at room temperature (25 °C). This solution was diluted in ethanol to give an absorbance at 734 nm of 0.70 ± 0.05. Trolox was used as the reference standard. The solutions were prepared with 30 μL of extract at a 0.001 g mL^{-1} concentration and 3 mL of ABTS solution. After 6 min, the absorbance was read on a spectrophotometer (800XI, FEMTO, São Paulo, SP, Brazil) at a wavelength of 734 nm. The antioxidant capacity value was calculated from a linear regression of the absorbance at 734 nm and the Trolox equivalent antioxidant capacity variation between 0 and 2 mM (R^2 = 0.9949). The results were expressed as μmol of Trolox equivalent (TE) per g of dry sample (μmol TE g^{-1} ± standard deviation).

5.2.8 Determination of antibacterial activity

5.2.8.1 Microorganisms and media

Antimicrobial activity screening was performed using the agar well diffusion method [21]. Two representative strains of Gram-negative microorganisms (*Escherichia coli* ATCC 25922 and *Pseudomonas aeruginosa* ATCC 27853) and two representative strains of Gram-positive microorganisms (*Staphylococcus aureus* ATCC 25923 and *Bacillus cereus* ATCC 10876) were used to investigate the activity. These are standard reference strains of the American Type Culture Collection (ATCC) (Rockville, MD, USA). The following extracts were evaluated: MAC-EtOH, UAE-EtOH, SOX-EtOH, SFE 10 and UAE+SFE 10. Only one condition of SFE and UAE+SFE was evaluated, considering the best condition in obtaining linolenic acid (60 ºC/11 MPa/5% EtOH) [11].

Initially, the rotary evaporated extracts were resuspended with 3 mL of dimethyl sulfoxide (Sigma-Aldrich®) and sterilized with a 0.22 μm diameter filter membrane. The concentration obtained was calculated through the dry mass in mg of each extract for 1 mL of solvent. Briefly, standardized inocula on the McFarland scale 0.5 (equivalent to a bacterial cell concentration of 108 CFU mL^{-1}) were confluently inoculated with the aid of a sterile swab in Petri dishes containing Mueller-Hintor agar culture medium (Kasvi®) at a thickness of 4.0 ± 0.5 mm. Wells of 6 mm diameter were made, and 50 μL of each extract was pipetted inside. Afterward, the plates were incubated at 37 ºC for 24 h. A 10 mcg Imipenem antimicrobial disk was used as a positive control, and as a negative control, 50 μL of sterile 0.85% saline was pipetted.

After the incubation period, the reading was taken through the formation of inhibition halos around the wells. The halos' diameter was measured and expressed in millimeters (mm).

5.2.9 Viability of VERO cells and antiviral activity against HSV-1 virus

5.2.9.1 Cytotoxicity Assay

The cytotoxic screening was conducted using Vero cells (ATCC CCL-81), an immortalized culture from fibroblasts derived from African green monkey kidneys. The cell culture was grown in Minimal Essential Medium (MEM) supplemented with 10% fetal bovine serum (FBS; Gibco, Grand Island, NY) and maintained at 37 °C and 5% CO_2 in a humidified atmosphere. The cytotoxicity of the compounds was evaluated by the colorimetric assay of sulforhodamine B (SRB) [22]. The assay consists of an in vitro method that measures total protein mass related to cell viability. Briefly, Vero cells were seeded (2.5 × 104 cells per well in 96-well plates), and after 24 h of incubation, the cells were exposed to different concentrations of the extracts. After 48 h of incubation at 37 °C and 5% CO_2, 10% trichloroacetic acid (TCA) was added to each well to fix the cells. After 1 h, the TCA solution was removed, and SRB was added. After 30 min, the plates were washed with a watery 1% acetic acid solution to remove unbound SRB. Afterward, 100 μL of a 10 mM Tris-Base [tris(hydroxymethyl) aminomethane] solution (pH 10,5, Trizma®, Sigma-Aldrich) was added to each well. The absorbance reading was performed using a microplate spectrophotometer (Spectra MD2, Molecular Devices, Sunnyvale, CA, EUA) at 510 nm. Using statistical software, the results are expressed as CC50 values, the concentrations that inhibit 50% of cell viability. The CC50 values

represent the average of three independent experiments. The following extracts were evaluated in the best condition to obtain linolenic acid (60 ºC/11 MPa/5% EtOH): SFE 10 and UAE+SFE 10 [11].

5.2.9.2 Antiviral Assay

The plaque number reduction assay was performed to determine the potential antiviral effect of the extracts [23]. Vero cells were seeded in 24-well plates at 2.5 × 105 cells per well. After forming a confluent cell monolayer, the cells were infected with approximately 100 plaque-forming units (PFU) of HSV-1 for 1 h, the necessary time to allow viral adsorption and penetration, at 37 ˚C. After the infection period, the cells were overlaid with MEM containing 1.5% carboxymethylcellulose (CMC; Sigma-Aldrich, St. Louis, MO, USA) in the presence or absence of the extracts, in different concentrations, and incubated for 48 h, at 37 °C and 5% CO_2. Then, cells were fixed and stained with naphthol blue-black (Sigma-Aldrich) to visualize and quantify viral plaques using a stereomicroscope. Acyclovir was used as a positive control for HSV-1 infection. Using linear regression analysis, the concentration of each extract that inhibited viral replication was estimated to be 50% (IC50). With CC50 and IC50 values, it was possible to estimate each sample's selectivity index (SI). All experiments were performed in independent triplicates.

5.2.10 Confocal laser scanning microscopy

The oil distribution in the leaves of *C. spicatus*, obtained in nature and after extractions by UAE-EtOH, SFE 10, and UAE+SFE 10, was investigated using a confocal laser scanning microscope (Leica TCS SPC5/DMI 6000, GER). The SFE and UAE+SFE extracts were evaluated under the best conditions for obtaining linolenic acid (60 °C/11 MPa/5% EtOH) [11]. The samples were cut with stainless steel blades, placed on glass slides, and stained with Nile red at 5 μg mL^{-1} (soluble in PBS, pH 7.4). Images were obtained with a 40× objective, using excitation wavelengths of 514 nm and emission wavelengths of 590 nm for Nile red. To verify the autofluorescence of the untreated leaf, 405 nm for excitation and 430 nm for emission were used. Confocal fluorescence images were acquired and processed using image analysis software (Leica TCS SPC5/DMI 6000, GER).

5.2.11 Accelerated stability analysis

The accelerated stability of the extracts (MAC-EtOH, UAE-EtOH, SOX-EtOH, SFE 10, and UAE+SFE 10) was performed in the LUMiSizer® equipment (LUMiSizer-651, Berlin, Germany). The SFE and UAE+SFE extracts were evaluated in the best condition to obtain linolenic acid (60 °C/11 MPa/5% EtOH) [11]. The intensity of the transmitted light was measured as a function of time and position along the length of the sample in a cuvette during centrifugation. For this analysis, the extracts were placed in rectangular polycarbonate cuvettes and centrifuged at 4,000 rpm for 5 hours (equivalent to 6 months of shelf life) at 25 °C. The samples were analyzed in duplicates and diluted to a concentration of 0.017 g mL^{-1}. The results were expressed as an instability index as a time (s) function. Values closer to zero indicate no phase separation (greater formulation stability), while values closer to 1 indicate phase separation or unstable formulations.

5.2.12 Thermogravimetric analysis (TGA and DTG)

The samples were inserted into a closed circular alumina crucible and subjected to a heating rate of 10 °C/min^{-1}, in the reading range of 30 to 800 °C in an inert nitrogen gas atmosphere with a flow of 20 mL/min^{-1} in the JUPITER equipment, model STA 449 F3.

5.2.13 Statistical analysis

The Tukey test was applied to extractions to evaluate significant differences ($p < 0.05$) between the results obtained. All statistical analyses were evaluated using Statistica for Windows 7.0 software (Statsoft Inc., Tulsa, OK, USA).

5.3 RESULTS AND DISCUSSION

5.3.1 Cell viability

Figure 14 shows the cytotoxicity tests performed on extracts obtained by LPE, SFE, and UAE+SFE techniques against the mouse fibroblast cell line (L929) using colorimetric MTT assay. LPE extracts with HEX, such as MAC-HEX, UAE-HEX, and SOX-HEX, as well as UAE-EtOH and UAE+SFE (2, 4, 6), were not toxic to L929 cells at all extract concentrations analyzed (30, 100, and 300 µg mL^{-1}). Similarly, LPE (HEX and EtOH), SFE (3 to 6), and UAE+SFE (1 to 6) at concentrations of 30 and 100 µg mL^{-1} of extract were not toxic to these cells.

Figure 14. Cytotoxicity of *C. spicatus* extracts determined by colorimetric MTT in L929 cells. All treatments were tested at 30, 100, and 300 µg mL^{-1}.

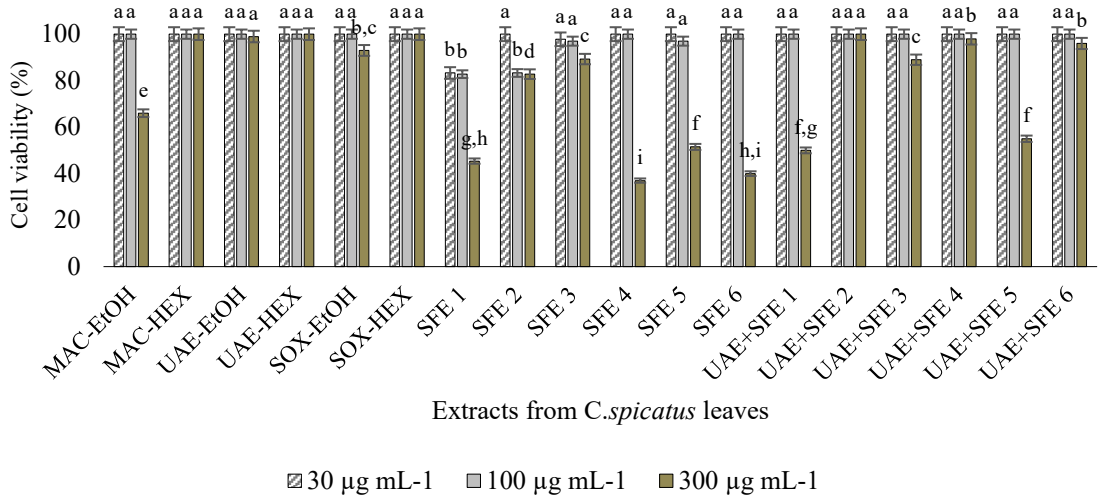

Abbreviations: MAC, maceration extraction; UAE, ultrasound extraction; SOX, Soxhlet extraction; SFE, supercritical CO_2 extraction; UAE + SFE, Ultrasonic pretreatment in supercritical CO_2 extraction; EtOH, solvent ethanol; HEX, solvent hexane;

a-i Different letters indicate significant differences between treatments $p < 0.05$ considering concentrations separately; Extraction condition: 1- 50 ºC/14 MPa/0 %EtOH, 2 - 50 ºC/14 MPa/20 %EtOH, 3 - 50 ºC/8 MPa/10 %EtOH, 4 - 50 ºC/20 MPa/10 %EtOH, 5 - 36 ºC/14 MPa/10 %EtOH, 6 - 64 ºC/14 MPa/10 %EtOH.

The Tukey test was used to verify the presence of significant differences ($p < 0.05$) between the assays analyzed. The cell viability results, at concentrations of 30 and 100 µg mL^{-1}, did not show significant differences in all LPE and UAE+SFE conditions examined. However, some extracts caused a reduction in cell viability at the highest concentration tested, resulting in a statistical difference. This was more evident in the extracts SFE 1 (~55% reduction in cell viability), SFE 4 (~63% reduction), and SFE 6 (~60%), suggesting a dose-dependent phenomenon [24].

No cell viability results were found in the literature for *C. spicatus* in L929 cells. However, several studies indicate that *C. spicatus* extracts demonstrated efficacy in different treatments. Moreno *et al.* [25] investigated the diuretic and nephroprotective effects of *C. spicatus* in Wistar rats and evaluated its antilithiasis activity through in vitro crystallization. In the review by Caamal-Fuentes *et al.* [26], the authors highlighted that compounds isolated from *C. spicatus* had curative potential for renal cancer. Azhagumadhavan *et al.* [27] showed that the macerated preparation of *C. spicatus* (rhizome extract) prevented renal lesions in Wistar rats with streptozotocin-induced diabetes, as evidenced by histopathological examinations.

The results of this study show that the extracts obtained by LPE and UAE+SFE did not cause a reduction in cell viability up to a concentration of 100 μg mL^{-1}. In some LPE and UAE+SFE conditions, cell viability decreased only at the highest concentration tested. In SFE conditions, the reduction was even more pronounced, suggesting that the cells showed greater tolerance to the extracts obtained under low-pressure conditions and those subjected to ultrasonic pretreatment before SFE.

When simultaneously comparing the results of the conditions with and without ultrasonic pretreatment, it was found that the concentration of 30 μg mL^{-1} in SFE is statistically similar to that of UAE+SFE in all conditions analyzed, except in SFE condition 1. The samples extracted at 100 μg mL^{-1} under SFE conditions (3 to 6) showed statistical similarity with all UAE+SFE samples, while the concentration of 300 μg mL^{-1} presented significant differences in most samples. These variations can be attributed to the composition of the extracts since different extraction methods can release distinct compounds.

The data obtained in the present study are quite relevant, as they evaluate the cytotoxic activity of *C. spicatus* extracts obtained by LPE, SFE, and UAE+SFE, suggesting possible promising applications. However, more detailed studies are needed to elucidate the mechanisms of action of these extracts.

5.3.2 Nitric oxide (NO) inhibitory activity

A total of 9 plant extracts were analyzed for their inhibitory effect on NO release in J774 cells (Figure 15). The extracts were classified as showing strong, moderate, or weak activity based on NO inhibition: more than 90% for strong activity, between 50% and 89% for moderate activity, and less than 50% for weak activity, respectively [28].

Furthermore, the viability of J774 cells, assessed by the MTT method, was greater than 85%, indicating that the decrease in NO production was not a result of cell death [29].

Figure 15. Evaluation of NO inhibition through the application of *C. spicatus* leaf extracts. All treatments were tested at 30, 100 and 300 µg mL^{-1}.

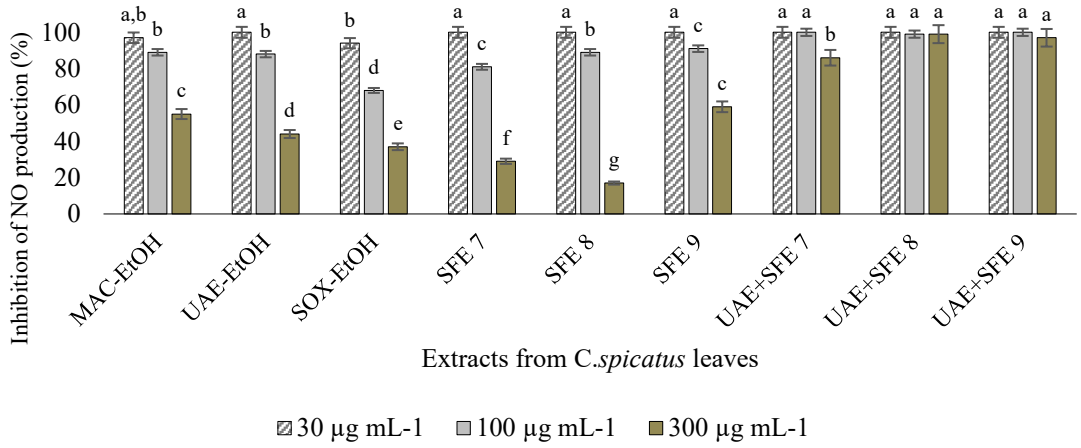

Abbreviations: MAC, maceration extraction; UAE, ultrasound extraction; SOX, Soxhlet extraction; SFE, supercritical CO_2 extraction; UAE + SFE, Ultrasonic pretreatment in supercritical CO_2 extraction; EtOH, solvent ethanol;
a-g Different letters indicate significant differences between treatments $p < 0.05$ considering concentrations separately;
*Extraction condition: 7- 40 ºC/11 MPa/5 %EtOH, 8 - 50 ºC/14 MPa/10 %EtOH, 9 - 60 ºC/17 MPa/15 %EtOH.

The results revealed that the extracts obtained at 30 µg mL^{-1}, for all conditions evaluated, presented greater NO inhibitory activity (lower NO production) than those concentrations of 100 and 300 µg mL^{-1} (Figure 15). Therefore, the concentration of 30 µg mL^{-1} suggests an extract rich in compounds with potent anti-inflammatory properties.

The results showed that five plant extracts had moderate inhibitory activity (68–89%), and four exhibited strong activity (91–100%) on NO production at 100 µg mL^{-1}. The UAE+SFE 8 and UAE+SFE 9 extracts strongly inhibited (97–99%) NO secretion at 300 µg mL^{-1} without cytotoxic effect. Among those that moderately reduced NO at 300 µg mL^{-1}, UAE+SFE 7 had the highest NO inhibition with 86%, without cytotoxicity. At this same concentration (300 µg mL^{-1}), UAE-EtOH, SOX-EtOH, SFE 7 and SFE 8 showed weak NO inhibition (17–44%). Thus, the best conditions to extract an extract with strong anti-inflammatory activity and no cytotoxic effect were UAE+SFE at 50 ºC/14 MPa/10 %EtOH and 60 ºC/17 MPa/15 %EtOH. To the author's knowledge, there are no previous reports on the anti-inflammatory activity of the plant in question.

5.3.3 Flavonoid content wich the antioxidant activity

The results obtained for the TFC of *C. spicatus* leaves are presented in Table 15. Comparing all the evaluated techniques, LPE with the EtOH solvent presented the highest values, ranging from 150.38-1328.73 mg GAE g^{-1}. This richness in flavonoids confers the plant many biological properties, such as antioxidant, antimicrobial, anti-inflammatory, antiviral, and anticarcinogenic activity [30, 31, 32]. Specifically for *C. spicatus* leaves, a previous study has already reported that, in the case of supercritical extractions, combining UAE with SFE increases the recovery of flavonoid compounds compared to the SFE method alone [11].

Table 15. The total flavonoid content and antioxidant capacities (DPPH and ABTS) of C. spicatus leaf extracts were obtained with maceration (MAC), ultrasound (UAE), Soxhlet (SOX), supercritical CO_2 extraction (SFE), and ultrasound pretreatment in supercritical CO_2 extraction (UAE + SFE).

Extraction technique	TFC (mg GAE g^{-1})	DPPH (μmol TE g^{-1})	ABTS (μmol TE g^{-1})
MAC-EtOH	$150.38^{c} \pm 0.90$	$29.56^{g} \pm 0.71$	$912.68^{c} \pm 2.05$
MAC-HEX	$83.68^{f} \pm 1.81$	$56.36^{b} \pm 1.27$	$264.85^{g} \pm 0.32$
UAE-EtOH	$201.2^{b} \pm 1.81$	$50.26^{c,d} \pm 2.81$	$2051.7^{a} \pm 3.13$
UAE-HEX	$62.92^{g} \pm 0.45$	$64.66^{a} \pm 0.21$	$202.63^{h} \pm 3.02$
SOX-EtOH	$1328.73^{a} \pm 3.20$	$13.86^{h} \pm 0.49$	$48.60^{j} \pm 1.80$
SOX-HEX	$71.55^{g} \pm 0.90$	$61.36^{a,b} \pm 0.71$	$110.68^{i} \pm 1.81$
SFE 3	$65.80^{g} \pm 1.81$	$60.16^{a,b} \pm 0.42$	$340.85^{f} \pm 1.16$
SFE 4	$91.99^{e,f} \pm 0.54$	$43.90^{d,e} \pm 0.07$	$1016.35^{b} \pm 1.69$
UAE+SFE 3	$96.72^{d,e} \pm 1.45$	$38.16^{e,f} \pm 0.99$	$894.5^{d} \pm 1.43$
UAE+SFE 4	$106.04^{d} \pm 2.71$	$32.56^{f,g} \pm 1.02$	$630.40^{e} \pm 1.66$

Abbreviations: TFC, total flavonoid content; DPPH, 1,1-diphenyl-2-picrylhydrazyl; ABTS, 2,2′-azinobis (3-ethylbenzothiazoline-6-sulphonic acid); MAC, maceration extraction; UAE, ultrasound extraction; SOX, Soxhlet extraction; SFE, supercritical CO_2 extraction; UAE + SFE, Ultrasonic pretreatment in supercritical CO_2 extraction; EtOH, solvent ethanol; HEX, solvent hexane.

The same letters in the same column indicate no significant difference at a level of 5 %.

* Extraction condition: 3- 50 ºC/8 MPa/10 %EtOH; 4- 50 ºC/20 MPa/10 %EtOH

When comparing the methods used to determine the antioxidant activity of the extracts, it was found that the results obtained by ABTS surpassed those of DPPH in all extraction techniques evaluated (MAC, UAE, SOX, SFE, and UAE+SFE). The highest DPPH value was observed when applying UAE-HEX, with 64.66 ± 0.21 μmol TE g^{-1}, statistically similar to SOX-HEX and SFE3 (61.36 ± 0.71 μmol TE g^{-1} and 60.16 ± 0.42 μmol TE g^{-1}, respectively). These results suggest that the presence of the nonpolar solvent

in the extraction process increased the extraction of antioxidant compounds by the DPPH method.

Interestingly, DPPH values did not show the same trend observed in the ABTS assay. Instead, the UAE-EtOH extract, analyzed by the ABTS assay, demonstrated the highest antioxidant activity ($p < 0.05$), with 2051.7 ± 3.13 µmol TE g^{-1}. At the same time, the lowest value was found in the SOX-HEX extract, with 48.60 ± 1.80 µmol TE g^{-1}. This suggests that, in the composition of the plant matrix used, there is a predominance of hydrophilic and lipophilic compounds, whose solubility in the chosen solvent facilitated their extraction [33].

With a significant difference of 5%, the UAE+SFE 3 combination at the lowest pressure (50 ºC/8 MPa/10 % EtOH) increased the antioxidant activity by the ABTS method 2.6-fold (894.5 ± 1.43 µmol TE g^{-1}) compared to SFE 3 alone (340.85 ± 1.16 µmol TE g^{-1}), demonstrating the high efficiency of the UAE + SFE combination under this condition. However, at the highest pressure (50 ºC/20 MPa/10 % EtOH), SFE 4 (1016.35 ± 1.69 µmol TE g^{-1}) showed an antioxidant activity approximately 1.6 times higher than the UAE+SFE 4 combination (630.40 ± 1.66 µmol TE g^{-1}). This difference suggests that the variation in pressure influences the extraction of antioxidant components detected by the ABTS method. This result corroborates with Miao *et al.* [34], who obtained the optimal condition for the extraction of flavonoids from *Ginkgo biloba* leaves at 20 MPa, 40 ºC and CO_2 flow rate of 10 g min^{-1} with ethanol flow rate of 6 ml min^{-1}. Further tests are needed to identify the compounds responsible for the antioxidant activity in *C. spicatus* leaf extracts.

5.3.4 Antibacterial activity

Although *C. spicatus* leaf extracts have been associated with many beneficial biological activities, their antimicrobial potential remains largely unexplored. As such, we evaluated the antimicrobial activity of the extracts against Gram-positive and Gram-negative bacteria (Table 16).

Table 16. Diameter of inhibition halos formed by different extraction conditions from *C. spicatus* leaves.

Sample	Concentration mg mL^{-1}	Diameter of the inhibition zone (mm)			
		Gram-positive bactéria		Gram-negative bacteria	
		B. cereus	S. aureus	E. coli	P. aeruginosa
MAC-EtOH	40	10	no	no	no
UAE-EtOH	40	10	no	no	no
SOX-EtOH	40	10	no	no	no
SFE*	40	10	no	no	no
SFE*	80	10	no	no	no
UAE+SFE*	40	11	no	no	no
UAE+SFE*	363	19	11	no	no
Positive control	-	35	24	14	30
Negative control	-	No	no	no	no

Abbreviations: MAC, maceration extraction; UAE, ultrasound extraction; SOX, Soxhlet extraction; SFE, supercritical CO_2 extraction; UAE + SFE, Ultrasonic pretreatment in supercritical CO_2 extraction; EtOH, solvent ethanol; no: not observed.

* Extraction condition: 10- 60 ºC/11 MPa/5 %EtOH.

All extracts showed antibacterial activity against B. *cereus* at all concentrations tested. For S. *aureus*, only the UAE+SFE extract at the highest concentration (363 mg mL^{-1}) showed an antimicrobial effect. Other authors attribute the antibacterial action of essential oils to lipophilic compounds, such as monoterpenes and sesquiterpenes, which cause damage to the cell membrane, affect homeostasis and the balance of pH and inorganic ions within the microbial cell, resulting in cell death [35, 36].

In contrast, Gram-negative bacteria (E. *coli* and P. *aeruginosa*) were more resistant to all samples tested, not forming an inhibition zone using the agar well diffusion method (Table 16). This may be related to the thick layer of lipopolysaccharides (LPS) that covers the surface of these bacteria, which is negatively charged and has nonpolar structures immune to polar compounds, thus hindering their chemical interaction and effect [21].

In section 5.3.3, on flavonoid content and antioxidant activity, it was demonstrated that the UAE+SFE combination presented a higher flavonoid content than SFE alone. This suggests that the higher antibacterial activity of the UAE+SFE combination may be associated with the presence of several plant phenolic compounds, including flavonoids [37]. Furthermore, this biological activity may be attributed to a synergistic effect between the components [38].

Our results indicate that *C. spicatus* leaf extract can potentially combat Gram-positive bacteria, especially S. *aureus*. This corroborates previous studies that reported

similar effects with extracts from the same species [11, 39]. However, further studies are needed to investigate how the chemical composition of *C. spicatus* leaves influences the antimicrobial activity and the inhibition mechanism, as this aspect has not yet been explored.

5.3.5 Cytotoxicity and antiviral activity against HSV-1.

As part of our research, *C. spicatus* leaf extracts obtained by SFE and UAE+SFE were tested for antiviral activity against *Herpes simplex virus 1* (HSV-1). The results of the cytotoxicity and antiviral activity evaluation of the tested extracts are presented in Table 17. The CC_{50} indicated that both extracts showed low cytotoxicity, although the UAE+SFE extract was more cytotoxic than the SFE.

Table 17. Cytotoxicity on Vero cells and antiviral activity against HSV-1 in *C. spicatus* extracts.

	Cytotoxicity on Vero cells		**Antiviral activity against HSV-1**		
Extract	**CC_{50} µg mL^{-1}**	**CI 95 % µg mL^{-1}**	**IC_{50} µg mL^{-1}**	**CI 95 % µg mL^{-1}**	**SI**
UAE+SFE[1]	370.6 ±	308.7 – 444.9	142.3 ±	119.2 – 169.8	2.6
SFE[1]	418.7	365.4 – 479.6	174.7	161.0 – 189.5	2.4

Abbreviations: CC_{50}: 50% cytotoxic concentration (µM); CI 95%: 95% confidence interval; IC_{50}: 50% inhibitory concentration (µM); SI: Selectivity index (SI = CC_{50}/IC_{50}); SFE, supercritical CO_2 extraction; UAE+SFE, Ultrasonic pretreatment in supercritical CO_2 extraction.

[1] Extraction condition: 60 ºC/11 MPa/5 %EtOH.

In Table 17, the UAE+SFE extract showed the most promising antiviral activity against HSV-1, with an IC_{50} value of 142.3 µg mL^{-1}, while the SFE extract showed lower activity (IC_{50} value of 174.7 µg mL^{-1}). These results indicate that the antiviral activity depends on the extraction technique and the compounds present. Data from the literature have showed that HSV is sensitive to fatty acids, such as linolenic acid [40], terpenes [41], and flavonoids [42], which are the main constituents of the UAE+SFE extract, possibly associated with the observed antiviral activity, although other compounds may also contribute.

The UAE+SFE extract, with a selectivity index (SI) of 2.6, showed the most significant anti-HSV1 activity, followed by the SFE extract, which had an SI of 2.4. There are no reports in the current literature on the antiviral activity of C. *spicatus* leaf extracts. Zhou *et al.* [42] found that *Cinnamomi ramulus* twig extracts, obtained by SFE and ethanoic acid, exhibited antiviral activities against HSV-1, with SI of 1.63 and 0.48,

respectively. Santoyo *et al.* [43] observed that hexane extracts of the microalgae *Haematococcus pluvialis* and *Dunaliella salina* had the lowest SI values, with 3.57 and 2.88, respectively.

Therefore, the activity of *C. spicatus* leaf extracts against HSV-1 was evaluated, and the SFE and UAE+SFE extracts could be considered inhibitors of HSV-1 viral replication. This activity is important because HSV affects both adults and children, and no cure or vaccine is available. In addition, there is an urgent need to develop new treatments due to the emergence of resistant strains to acyclovir, the drug currently used to reduce the time of infection and the pain produced by HSV [44].

5.3.6 Confocal microscopy

The extracts analyzed by confocal microscopy are shown in Figure 16. Untreated and unstained leaves exhibited autofluorescence with excitation at 405 nm (Figure 16a), indicating the presence of secondary metabolites, such as flavonoids, chlorophyll, phenolic acids, and others [45]. Autofluorescence occurs when electromagnetic radiation at specific wavelengths excites endogenous molecules (extracellular matrix and cellular components). This property can be used to monitor the extraction of certain compounds since factors such as pH, polarity, temperature, and solvent concentration can impact the intensity of these compounds [46].

Figure 16. Confocal laser scanning microscopy images. (a) Untreated sheet without Nile Red dye. (b) Leaves treated with UAE. (c) Leaves treated with SFE*. (d) Leaves treated with UAE+SFE*.

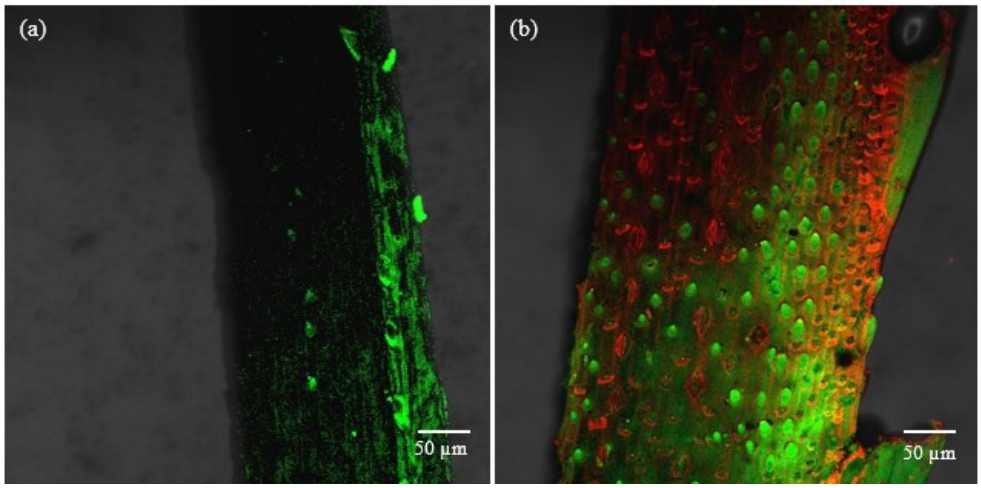

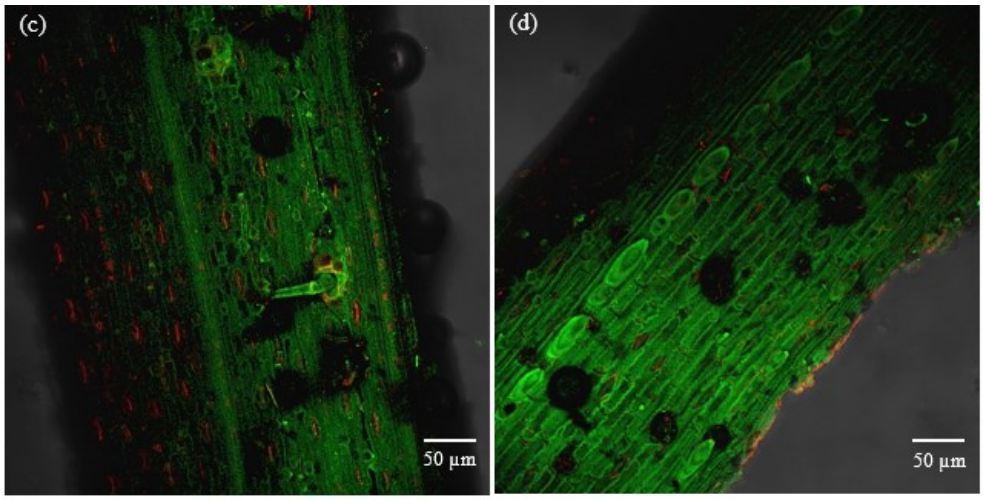

Abbreviations: UAE, ultrasound extraction; SFE, supercritical CO_2 extraction; UAE + SFE, Ultrasonic pretreatment in supercritical CO_2 extraction;

* Extraction condition: 10- 60 ºC/11 MPa/5 %EtOH.

In Figure 16b–d, the fluorescence of the extracts followed an increasing order: UAE > SFE > UAE+SFE. This indicates that the residue obtained with UAE exhibited a more prominent red emission, suggesting that many lipids were not extracted and may still be present. However, the UAE+SFE combination showed lower fluorescence, indicating a lower amount of residual compounds and a more efficient extraction under this condition. The remaining trace of oil may be difficult to obtain since it is probably linked to the matrix by chemical bonds [47].

Therefore, the image obtained by confocal microscopy confirmed that the leaves of *C. spicatus* exhibited autofluorescence. In addition, the distribution of lipid droplets in the extracts obtained in the different methods was possible, and it was verified that the UAE+SFE combination presented the greatest efficiency among the extraction processes evaluated.

5.3.7 Accelerated stability analysis

The accelerated stability study of the extracts was carried out on the LUMiSizer® equipment, which evaluates the stability of the samples based on sedimentation using centrifugal force [48]. This index is crucial in pharmaceutical and cosmetic formulations since greater instability can compromise the efficacy and safety of the product [49]. As illustrated in Figure 17, the instability indexes of the extracts were low, ranging from 0.05 to 0.16. After the standard test was carried out at 2493 RPM for

approximately 5 hours (equivalent to 6 months of shelf life), no noticeable phase separation was observed, indicating that the samples presented high stability.

Figure 17. Instability index of C. *spicatus* leaf extracts.

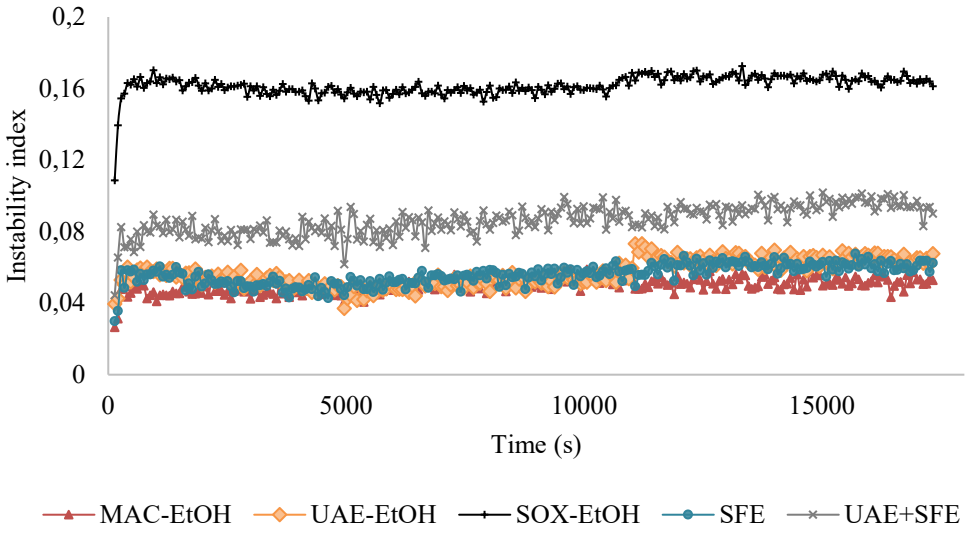

Abbreviations: MAC, maceration extraction; UAE, ultrasound extraction; SOX, Soxhlet extraction; SFE, supercritical CO_2 extraction; UAE + SFE, Ultrasonic pretreatment in supercritical CO_2 extraction; EtOH, solvent etanol;
* Extraction condition: 10- 60 ºC/11 MPa/5 %EtOH.

As shown in Figure 17, there are two main reasons for the high stability observed: first, the samples consisted of a solution of molecules rather than dispersed products such as suspensions and emulsions [50], which contain manometric particles. Second, the equipment is limited since the LUMiSizer® is not capable of measuring sizes as small as a molecule. This equipment is designed to analyze solid particles with sizes ranging from 20 nm to 100 µm.

Therefore, according to the instability index from 0 to 1, with 1 being the value indicating the greatest instability. All samples were stable in the accelerated stability study, suggesting high physical stability. The difference between the instability indices may be related to differences in the total oil content [48].

5.3.8 Thermogravimetric analysis (TGA and DTG)

Thermogravimetric analyses (TGA and DTG) were performed to evaluate the thermal stability of the extracts obtained through the UAE+SFE combination. The thermal behavior of the samples was plotted in Figure 18, where the weight loss (TG) curves together with derived thermogravimetric evolution (DTG) profiles, as a function of the reaction temperature at a heating rate of 10 °C/min can be observed.

Figure 18. Thermogravimetric analysis of *C. spicatus* extracts.

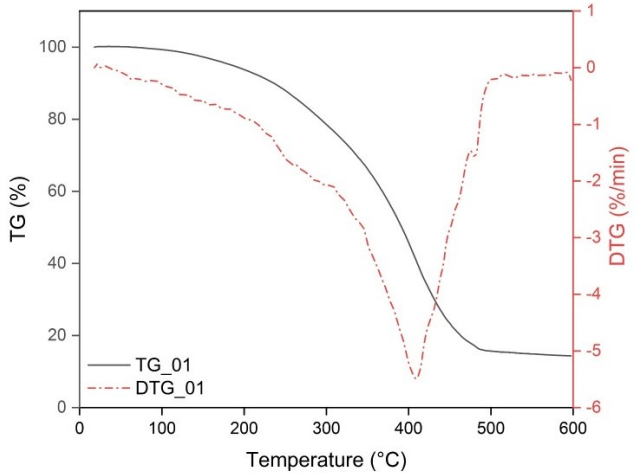

Abbreviations: DSC_01, Ultrasonic pretreatment in supercritical CO_2 extraction; EtOH, solvent ethanol; * Extraction condition: 10- 60 ºC/11 MPa/5 %EtOH.

As Figure 18 shows, the thermogram curves initially showed a slight variation in weight. Then, a more pronounced weight loss occurred, with the curve indicating that this change began around 250°C and continued until approximately 480°C, at which point the maximum degradation rate was reached. After this, in the final phase, slower reductions in weight loss were recorded, where there was almost no additional conversion. This result corroborates the data obtained by Sodeifian *et al.* [51], where the authors studied the extraction omega-3 with supercritical fluid from Dracocephalum kotschyi seed oil and found similar behavior.

5.4 CONCLUSIONS

Therefore, the investigated extraction techniques, including MAC, UAE, SOX, and SFE, revealed that UAE+SFE is particularly effective, not only preserving cell viability up to 100 μg mL^{-1} but also inhibiting nitric oxide by more than 90% and showing high antioxidant and antiviral activity. LPE with EtOH produced high levels of flavonoids, while the UAE+SFE combination improved the recovery of these compounds compared to SFE. All extracts exhibited antibacterial activity against B. *cereus* and physical stability of the extracts. UAE+SFE excelled in the extraction of lipid droplets and showed thermal stability according to TG and DTG analyses. This study provides a solid basis for future applications of *C. spicatus* in food, pharmaceuticals, and industry, evidencing its potential value as a multifunctional natural resource.

5.5 REFERENCES

[1] A.P.R. Bitencourt, S.S.M.S. Almeida. Estudo fitoquímico, toxicológico e microbiológico das folhas de *Costus spicatus* Jacq. Biota Amazônia 4 (2014) 75-79. http://dx.doi.org/10.18561/2179-5746/biotaamazonia.v4n4p75-79.

[2] H. Lorenzi, F.J.A. Matos. Plantas Medicinais no Brasil: nativas e exóticas, 3th ed. Nova Odessa, São Paulo, 2022.

[3] D.W.M. Stevenson, J.W. Stevenson. Costaceae (*Costus* Family). In Flowering Plants of The Neotropics. (Smith N, Mori SA, Henderson A, Stevenson DWM, Heald SV. eds.). Princeton University Press, Princeton (2004) 429-431. ISBN: 0691116946.

[4] L.J. Quintans Júnior, M.T. Santana, M.S. Melo, D.P. de Sousa, I.S. Santos, R.S. Siqueira, T.C. Lima, G.O. Silveira, A.R. Antoniolli, L.A.A. Ribeiro, M.R.V. Santos. Antinociceptive and anti-inflammatory effects of *Costus spicatus* in experimental animals. Pharm. Biol 48 (2010) 1097-1102. https://doi.org/10.3109/13880200903501822.

[5] K.G.T. Moreno, A.G. Junior, A.C. Santos, R.A.C. Palozi, L.P. Guarnier, A.A.M. Marques, P.V.M. Romão, B.R. Lorençone, N.S. Cassemiro, D.B. Silva, C.A.S. Tirloni, M.E. Barros. Nephroprotective and antilithiatic activities of *Costus spicatus* (Jacq.) Sw.: Ethnopharmacological investigation of a species from the Dourados region, Mato Grosso do Sul State, Brazil. Journal of Ethnopharmacology 266 (2021) 113409. https://doi.org/10.1016/j.jep.2020.113409.

[6] U. P. De Albuquerque, J. Monteiro, M. Ramos, E. Amorim. Medicinal and magic plants from a public market in northeastern Brazil. Journal of Ethnopharmacology 110 (2007) 76–91. https://doi.org/10.1016/j.jep.2006.09.010.

[7] M. Coelho-Ferreira. Medicinal knowledge and plant utilization in an Amazonian coastal community of Marudá, Pará State (Brazil). Journal of Ethnopharmacology 126 (2009) 159-175. https://doi.org/10.1016/j.jep.2009.07.016.

[8] S. O. Essien, B. Young, S. Baroutian. Recent advances in subcritical water and supercritical carbon dioxide extraction of bioactive compounds from plant materials.

Trends in Food Science & Technology 97 (2020) 156–169. https://doi.org/10.1016/j.tifs.2020.01.014

[9] E.K. Asep, S. Jinap, M.H.A. Jahurul, I.S.M. Zaidul, H. Singh. Effects of polar cosolvents on cocoa butter extraction using supercritical carbon dioxide. Innov. Food Sci. Emerg. Technol 20 (2013) 152-160. https://doi.org/10.1016/j.ifset.2013.06.010.

[10] Y.C. Yang, M.C. Wei. Development and characterization of a green procedure for apigenin extraction from Scutellaria barbata D. Don. Food Chemistry, 252 (2018) 381–389. https://doi.org/10.1016/j.foodchem.2017.12.086

[11] T.K.S. Laurintino, T.N.S. Laurintino, D.P. Tramontin, A.B. Cruz, D.W. Paiva, A. Bolzan, M.B. Quadri. Ultrasound pretreatment combined with supercritical CO_2 extraction of *Costus spicatus* leaf extract. J. Supercrit. Fluids (2024) 106372. https://doi.org/10.1016/j.supflu.2024.106372.

[12] S. Mazzutti, S.R.S. Ferreira, C.A.S. Riehl, A. Smania, F.A. Smania, J. Martınez. Supercritical fluid extraction of *Agaricus brasiliensis*: antioxidant and antimicrobial activities. J Supercrit Fluids 70 (2012) 48–56. https://doi.org/10.1016/j.supflu.2012.06.010.

[13] J.L. Luque-García, M.D. Luque De Castro. Ultrassom: uma ferramenta poderosa para a lixiviação. TrAC - Trends Anal. Química 22 (2003) 41-47. 10.1016 / S0165-9936 (03)00102-X.

[14] AOAC. Association of official analytical chemist, official methods of analysis, 18, a. AOAC International, Maryland, 2005.

[15] L.T. Taylor. Supercritical Fluid Extraction, Wiley Interscience, New York, 1996. https://doi.org/10.1007/BF01242421.

[16] A.A. Van De Loosdrecht, E. Nennie, G.J. Ossenkoppele, R.H.J. Beelen, M.M.A.C. Langenhuijsen. Cell mediated cytotoxicity against U 937 cells by human monocytes and macrophages in a modified colorimetric MTT assay. J. Immunol. Methods 141 (1991) 15–22. https://doi.org/10.1016/0022-1759(91)90205-T.

[17] M.B. Grisham, G.G. Johnson, J.R. Lancaster Jr. Quantitation of nitrate and nitrite in extracellular fluids. Methods Enzymology 268 (1996) 237–246.

[18] C.C. Chang, M.H. Yang, H.M. Wen, J.C. Chern, Estimation of total flavonoid content in propolis by two complementary colometric methods, J. Food Drug Anal 10 (2002) 178–182.

[19] M. Boroski, J. Visentainer, S. Cottica, D. Morais. Antioxidantes princípios e métodos analíticos, first ed., Appris, Curitiba, 2015.

[20] R. Re, N. Pellegrini, A. Proteggente, A. Pannala, M. Yang, C. Rice-Evans, Antioxidant activity applying an improved ATBS radical, free cadic, Biol. Med 26 (1999) 1231–1237. https://doi.org/10.1016/S0891-5849(98)00315-3.

[21] G.R. Martins, F.R.L. Amaral, F.L. Brum, R. Mohana-Borges, S.S.T. Moura, F.A. Ferreira, L.S. Sangenito, A.L.S Santos, N.G Figueiredo, A.S. Silva. Chemical characterization, antioxidant and antimicrobial activities of açaí seed (*Euterpe oleracea Mart*.) extracts containing A- and B-type procyanidins. Lwt 132 (2020) 109830. http://dx.doi.org/10.1016/j.lwt.2020.109830.

[22] V. Vichai, K. Kirtikara, B. Sulforhodamine. Colorimetric Assay for Cytotoxicity Screening. Nat. Protoc. 2006; 1:1112–1116. 10.1038/nprot.2006.179.

[23] F.G. Burleson, T.M. Chambers, D.L. Wiedbrauk. Techniques for assessing antiviral agents. In: Burleson FG (editor). Virology a laboratory manual. California: Academic Press, 1992.

[24] H. Haryoto, P. Widowati. Cytotoxicity of methanol leaf extract of Artocarpus altilis, Artocarpus heterophyllus and Artocarpus camansi against MCF7 breast cancer cells. J Nutraceuticals Herb Med 1 (2018) 16–23.

[25] K.G.T. Moreno, A.G. Junior, A.C. Santos, R.A.C. Palozi, L.P. Guarnier, A.A.M. Marques, P.V.M. Romão, B.R. Lorençone, N.S. Cassemiro, D.B. Silva, C.A.S. Tirloni, M.E. Barros. Nephroprotective and antilithiatic activities of *Costus spicatus* (Jacq.) Sw.: Ethnopharmacological investigation of a species from the Dourados region, Mato Grosso do Sul State, Brazil. Journal of Ethnopharmacology 266 (2021) 113409. https://doi.org/10.1016/j.jep.2020.113409.

[26] E. Caamal-Fluentes, L.W. Torres-Tapia, P. Simá-Polanco, S. Peraza-Sánchez, R. Moo-Puc. Screening of plants used in Mayan traditional medicine to treat cancer-like symptoms. Journal of Ethnopharmacology 135 (2011) 719-724. https://doi.org/10.1016/j.jep.2011.04.004.

[27] S. Azhagumadhavan, S. Senthilkumar, S. Ganesan. Histopathological assessment of the kidney of STZ-induced diabetic rats treated with macerated Costus *Spicatus* Jacq. rhizome extract. Int. J. Pharm. Drug Anal 6 (2018) 203–209. http://ijpda.com; ISSN: 2348-8948.

[28] N. Tohar, J.A. Shilpi, Y. Sivasothy, S. Ahmad, K. Awang. Chemical constituents and nitric oxide inhibitory activity of supercritical carbon dioxide extracts from *Mitragyna speciosa* leaves. Arabian Journal of Chemistry 12 (2019) 350-359. https://doi.org/10.1016/j.arabjc.2016.09.005.

[29] T. Mosmann. Rapid colorimetric assay for cellular growth and survival: application to proliferation and cytotoxicity assays. J. Immunol. Methods 65 (1983) 55–63. http://dx.doi.org/10.1016/ 0022-1759(83)90303-4.

[30] Dias, M.C., Pinto, D., Silva, A.M.S., 2021. Plant flavonoids: chemical characteristics and biological activity. Molecules 26 (17). https://doi.org/10.3390/ molecules26175377.

[31] I.C. Marinas, E. Oprea, E.-I. Geana, C. Chifiriuc, V. Lazar, Antimicrobial and antioxidant activity of the vegetative and reproductive organs of Robinia pseudoacacia, J. Serb. Chem. Soc. 79 (2014) 1363–1378.

[32] W. Ren, Z. Qiao, H. Wang, L. Zhu, L. Zhang, Flavonoids: promising anticancer agents, Med. Res. Rev. 23 (4) (2003) 519–534, https://doi.org/10.1002/ med.10033.

[33] S. Gorjanovic, D. Komes, F.T. Pastor, A. Bels, C. ak-Cvitanovic, L. Pezo, I. Hec, I. Hecimovic, D. Suznjevic. Antioxidant capacity of teas and herbal infusions: Polarographic assessment. J. Agric. Food Chem. 60 (2012) 9573–9580. http:// dx. doi.org/10.1021/jf302375t.

[34] S.F. Miao, J.P. Yu, Z. Du, Y.X. Guan, S.J. Yao, Z.Q. Zhu. Supercritical fluid extraction and micronization of ginkgo flavonoids from Ginkgo biloba leaves, Ind. Eng. Chem. Res 49 (11) (2010) 5461–5466. https://doi.org/10.1021/ie902001x.

[35] S.M. Da Silveira, F.B. Luciano, N. Fronza, A. Cunha, G.N. Scheuermann, C.R.W. Vieira, Chemical composition and antibacterial activity of *Laurus nobilis* essential oil towards foodborne pathogens and its application in fresh Tuscan sausage stored at 7 ◦C, LWT - Food Sci. Technol 59 (2014) 86–93. http://dx. doi.org/10.1016/j.lwt.2014.05.032.

[36] M.M. Cowan. Plant Products as Antimicrobial Agents, 12 (1999) 564–582 https://www.ncbi.nlm.nih.gov/pmc/articles/PMC88925/pdf/cm000564.pdf

[37] L.A. Mitscher, Y.H. Park, D. Clark. Antimicrobial agents from higher plants. Antimicrobial isoflavanoids and related substances from Glycyrrhiza glabra L. var. typica. Journal of Natural Products 43 (1980) 259–269.

[38] S. Burt. Essential oils: their antibacterial properties and potential applications in foods – a review, Int. J. Food Microbiol 94 (2004) 223–253. https://doi.org/ 10.1016/j.ijfoodmicro.2004.03.022.

[39] M.P. Uliana, A.G. Da Silva, M. Fronza, R. Scherer, In vitro antioxidant and antimicrobial activities of Costus spicatus swartz used in folk medicine for urinary tract infection in Brazil, Lat. Am. J. Pharm 34 (2015) 766–772.

[40] S. Santoyo, L. Jaime, M. Plaza, M. Herrero, I. Rodriguez-Meizoso, E. Ibanez, G. Reglero, Antiviral compounds obtained from microalgae commonly used as carotenoid sources, J. Appl. Phycol 24 (2012) 731e741. https://doi.org/ 10.1007/s10811-011-9692-1.

[41] S. Santoyo, L. Jaime, M.R. García-Risco, A. Ruiz-Rodríguez, G. Reglero, Antiviral properties of supercritical CO_2 extracts from oregano and sage. Int. J. Food Prop 17 (2014) 1150e1161. https://doi.org/10.1080/ 10942912.2012.700539.

[42] J. Zhou, X. Yuan, L. Li, T. Zhang, B. Wang. Comparison of different methods for extraction of *Cinnamomi ramulus*: yield, chemical composition and in vitro antiviral activities, Nat. Prod. Res 31 (2017) 2909e2913. https://doi.org/ 10.1080/14786419.2017.1299724.

[43] S. Santoyo, L. Jaime, M. Plaza, M. Herrero, I. Rodriguez-Meizoso, E. Ibañez, G. Reglero. Antiviral compounds obtained from microalgae commonly used as carotenoid sources. J Appl Phycol 24 (2012) 731–741. 10.1007/s10811-011-9692-1.

[44] J. Treml, M. Gazdova, K. Smejkal, M. Sudomova, P. Kubatka, S.T.S. Hassan, Natural products-derived chemicals: breaking barriers to novel anti-HSV drug development, Viruses 12 (2020). https://doi.org/10.3390/v12020154.

[45] P. Talamond, J. L. Verdeil, G. Conejero. Secondary metabolite localization by autofluorescence in living plant cells. Molecules 20 (2015) 5024–5037. https://doi.org/10.3390/molecules20035024.

[46] J. I. García-Plazaola, B. Fernandez-Marín, S. O. Duke, A. Hernández, F. Lopez-Arbeloa, J. M. Becerril. Autofluorescence: Biological functions and technical applications. Plant Science (2015). Elsevier Ireland Ltd. https://doi.org/10.1016/j.plantsci.2015.03.010.

[47] A. Mustafa, C. Turner, Pressurized liquid extraction as a green approach in food and herbal plants extraction: a review, Anal. Chim. Acta 703 (2011) 8–18. https://doi.org/10.1016/j.aca.2011.07.018.

[48] D.S. Porto, B.C.B. Porto, J. Conte, D.F. Argenta, M.P. Balleste, G.A. Micke, A.M. Campos, K.S. Caumo, T. Caon. Development of ophthalmic nanoemulsions of β-caryophyllene for the treatment of *Acanthamoeba* keratitis. International Journal of Pharmaceutics 659 (2024) 124252.

[49] K. Huynh-Ba. Handbook of Stability Testing in Pharmaceutical Development - Regulations, Methodologies and Best Practices; Huynh-Ba, K., ed.; Springer: New York, chaps (2008) 2-3.

[50] M.T. Melo. Preparo, caracterização e aplicação em engenharia de tecidos de suportes de alginato/quitosana, associados a processos fotodinâmicos para fotobioestimulação. Tese (doutorado), Universidade de São Paulo, 2019.

[51] G. SodeifiaN, S.A. Sajadian, N.S. Ardestani. Supercritical fluid extraction of omega-3 from Dracocephalum kotschyi seed oil: Process optimization and oil properties. The Journal of Supercritical Fluids 119 (2017) 139-149. 10.1016/j.supflu.2016.08.019.

CHAPTER VI - MATHEMATICAL MODELING OF THE EXTRACTION OF BIOACTIVE COMPOUNDS FROM *COSTUS SPICATUS* WITH SUPERCRITICAL CO_2 AND ULTRASOUND

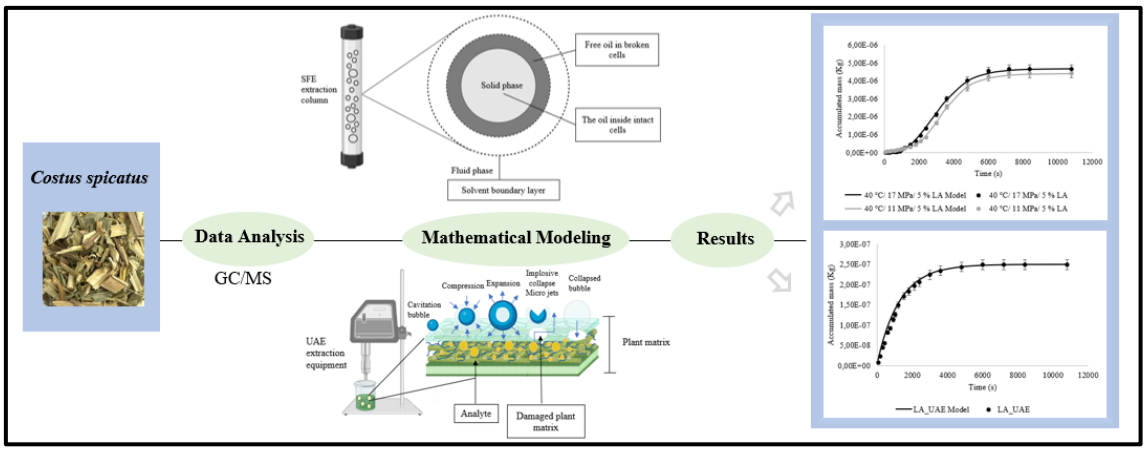

ABSTRACT

Mathematical modeling is essential to optimize the yield and selection of bioactive compounds from plant matrices. This study aims to model the extraction of bioactive compounds (linolenic acid, palmitic acid, and friedelin) from *Costus spicatus* leaves using supercritical extraction (SFE) and ultrasound-assisted extraction (UAE) to investigate the mass transfer aspects. Two models were developed in COMSOL Multiphysics® software: I-dynamic (SFE) and II-batch (UAE); to evaluate the effects of pressure (8-20MPa), temperature (36-64°C) and co-solvent concentration in SFE (0-20% EtOH) and to analyze the parameters that affect the extraction profile I and II of the compounds analyzed by GC/MS. The models used differential mass balances to analyze the mass flow between the fluid and the particles. The results indicate that the mass transfer coefficient and the diffusion coefficient increase with pressure, temperature, and ethanol concentration, and they also show improvements with the UAE treatment.

Keywords

Mathematical modeling; Plants; Leaves; Mass transfer; Bioactive compounds

6.1 INTRODUCTION

The extraction of bioactive compounds from plants can be done by several methods. Conventional methods, which pioneered the conceptual development of techniques such as Soxhlet, maceration, hydrodistillation, and steam distillation, have over time shown limitations, such as excessive use of organic solvents, time-consuming processes, and low efficiency [1, 2, 3]. These disadvantages have driven the development of more sustainable techniques, such as ultrasound-assisted extraction (UAE), microwave, pressurized liquid, and supercritical fluid (SFE) [2].

UAE produces high-frequency ultrasonic waves that can promote cavitation phenomena and increase energy and mass transfer in liquid media, thus causing the rupture of plant cell walls and promoting solvent penetration [4]. Other ultrasonic effects that facilitate mass transfer processes include the thermal effect [5], microagitation at the interface [6], and some structural effects, such as the 'sponge effect' and the generation of microchannels [7].

SFE is efficient and selective for obtaining high-purity extracts. Carbon dioxide (CO_2) is a widely used supercritical solvent because it has a relatively low critical temperature and pressure, preventing the degradation of thermolabile compounds. SFE is widely used in the extraction of plant matrices and can be performed at different scales and in different modes (static, dynamic, or combined) [8]. Due to its complexity, elucidating the mechanisms of transport phenomena using only experimental data is challenging. Therefore, mathematical modeling is used to unravel the phenomenological details and optimize resources and time [9, 10]. Several authors have developed empirical kinetic equations for SFE. Goto *et al.* [11] proposed a retractable core model for the extraction of ginger rhizomes, considering effective diffusivity and solubility. Sovová [12] used the broken and intact cell model, considering the accessibility of vegetable oil. Reverchon [13] adjusted the model based on particle shape, especially for large particles. Roy *et al.* [14] used the retractable core model, focusing on the contraction of the particle core as the solute diffuses into the plant matrix.

For UAE, models using artificial neural networks (ANN) and RSM (response surface methodology) were developed [15, 16]. These models are effective in simulation but lack physical meaning. In a more phenomenological approach, UAE is influenced by the diffusion coefficient and the dissolution rate of the compounds until they reach the equilibrium concentration in the solvent [17]. Toepfl *et al.* [18] used the electrochemical

potential to model the enhancement of mass transfer induced by applying pulsed electric fields. Milic *et al.* [19] reported a phenomenological kinetic model describing the UAE in two stages: washing and diffusion of the compounds, with sonication affecting only the first stage. Orphanides *et al.* [20] developed a model to predict the enhancement of polyphenol extraction in ethanol using the effect of ultrasonic irradiation on the chemical potential. Despite the various mass transfer models available, there is no data on the diffusion kinetics of *Costus spicatus* compounds with UAE and SFE.

Costus spicatus (Jacq.) Sw., of the Costaceae family, is a plant native to the Atlantic Forest and the Amazon. It is characterized by being a plant species with a long life cycle (perennial), rhizomatous (underground stems), cespitose, erect, and unbranched [21]. Although it is cultivated mainly for ornamental purposes, it is also widely used in folk medicine for the treatment of kidney pain, back pain, hepatitis, and kidney and urinary problems [22, 23, 24]. Studies on this plant have reported several biological activities, such as antiviral, analgesic, antioxidant, antimicrobial, antifungal, and nephroprotective, attributed to the presence of triterpenes, sterols, flavonoids, saponins, alkaloids, and tannins [25, 26].

Therefore, the main objective of the study was to model the extraction of bioactive compounds (linolenic acid, palmitic acid, and friedelin) from *C. spicatus* leaves identified by GC/MS, using two models: I - dynamic (SFE) and II - batch (UAE). For this, the COMSOL Multiphysics® software (COMSOL Inc., Stockholm, Uppland/Södermanland, Sweden) was used, allowing a detailed analysis of the mass transfer during extraction. In addition, the effects of pressure, temperature, and cosolvent concentration on the modeling (I) and the parameters that affect the extraction curve profile (I and II) could be evaluated.

6.2 MATERIAL AND METHODS

6.2.1 Sample preparation and characterization

Leaves and stems of *C. spicatus*, grown in the Piraquara-PR region, Brazil, were obtained from Comercial Charoma. The leaves were manually separated from the stems and dried in an oven with forced air circulation (CE 220/2016, Cienlab, Campinas, SP, Brazil) at 35 °C for 24 h. They were ground in a coffee grinder (MDR302, Cadence, Balneário Piçarras, SC, Brazil), and their moisture content was determined by method

925.10, according to AOAC [27]. The particles were classified by Tyler Standard sieves (A bronzinox, São Paulo, SP, Brazil).

The specific mass was determined by helium pycnometry (AccuPyc II 1340V1.05, Micromeritics, Norcross, GA, USA). The particle porosity was inferred by the difference between the bed specific mass and the cellulose specific mass. The samples were sealed and stored in a domestic freezer at -18 °C (BRM39, Brastemp, São Bernardo do Campo, SP, Brazil) until extractions were performed.

6.2.2 Supercritical Fluid Extraction (SFE)

The SFE procedure was performed as described by Laurintino *et al.* [28]. Approximately 1.37 g of sample was loaded into the extraction vessel. The pressure, temperature, and cosolvent concentration variables were based on preliminary tests, aiming to maximize the extraction of bioactive compounds.

The extraction conditions were established based on a three-factor, three-level central composite (CCD) design. The effects of pressure (8, 11, 14, 17, and 20 MPa), temperature (36, 40, 50, 60, and 64 °C), and cosolvent concentration (ethanol, 99.99%, Metaquímica, Jaraguá do Sul, SC, Brazil) (0, 5, 10, 15, and 20% w) on the yield of the compounds (linolenic acid “LA”, palmitic acid “PA,” and friedelin “FR”) were investigated. The 0 % w cosolvent condition did not show a measurable extraction yield, leaving a total of 14 extractions related to the other cases studied.

The volumetric flow rate of CO_2 (99.99%, White Martins, Florianópolis, SC, Brazil) was kept constant at 3 mL min^{-1}. Samples were collected to prepare the extraction curve at the following intervals: every 2 minutes (0 to 20 min), every 5 minutes (20 to 40 min), every 10 minutes (40 to 60 min), every 20 minutes (60 to 120 min) and, finally, every 40 minutes (120 to 180 min).

The apparent specific mass of the bed (ρ_b) was obtained from the ratio between the sample's mass and the extraction cell's volume (127.5 mm long x 10 mm diameter and internal volume 10 cm^3). The porosity of the bed (ε) was obtained from Equation 3, which is related to the specific mass of the particle (ρ_{pe}) and the bed (ρ_b).

$$\varepsilon = 1 - \frac{\rho_b}{\rho_{pe}} \tag{3}$$

Where ε is the porosity of the fixed bed, (ρ_b) is the specific mass of the bed (kg m^{-3}), and (ρ_{pe}) is the specific mass of the particle (kg m^{-3}).

6.2.3 Ultrasound-assisted extractions (UAE)

Ultrasound-assisted extractions (UAE) were performed according to the method adapted from Luque-García and Luque De Castro [29]. The extraction was carried out using an ultrasonic probe device (DES5000, Unique, São Paulo, SP, Brazil) at a power of 500 W, a frequency of 20 kHz, and a solid/solvent ratio of 1:30 (m/v). Independent essays were performed to prepare the extraction curve. When the desired extraction time was reached, the sample was removed for post-processing, and another batch was started under the same conditions until the next stipulated time, totaling 20 samples at the following time intervals: every 2 minutes (0 to 20 min) every 5 minutes (20 to 40 min), every 10 minutes (40 to 60 min), every 20 minutes (60 to 100 min), and finally, every 40 minutes (100 to 180 min). The extractions were performed in triplicate.

6.2.4 Conventional extraction in a water bath with manual agitation

Conventional extraction in a water bath was carried out with a solid/solvent ratio of 1:30 (m/v). Independent essays were performed to prepare the extraction curve. When the desired extraction time was reached, the sample was removed for post-processing, and another batch was started under the same conditions until the next stipulated time, totaling 20 samples at the following time intervals: every 2 minutes (from 0 to 20 minutes), every 5 minutes (from 20 to 40 minutes), every 10 minutes (from 40 to 60 minutes), every 20 minutes (from 60 to 100 minutes) and, finally, every 40 minutes (from 100 to 180 minutes). The extractions were performed at a controlled temperature of 25°C, with manual stirring every 30 minutes, and in triplicate.

6.2.5 Post processing of extracts

In the SFE, UAE, and conventional extraction in a water bath extracts, the solvent was removed with a vacuum rotary evaporator (R-100, BUCHI, Flawil, St. Gallen, Switzerland) at 40 °C. The extracts obtained were stored in a domestic freezer (BRM39, Brastemp, São Bernardo do Campo, SP, Brazil) at -18 °C until extract characterization analyses.

6.2.6 Extract characterization

6.2.6.1 Global yield of compounds

The calculation of the overall yield (Y_i) for each compound of interest in the extraction was determined according to Equation 4.

$$Y_i = \frac{m_i}{m_{sample}} \quad (4)$$

Where Y_i is the overall yield of the compounds of interest in the extracts (mg g^{-1}), m_i is the mass of each of the compounds of interest: linolenic acid "LA," palmitic acid "PA" and friedelin "FR" obtained in the extracts (mg), and m_{sample} is the mass of the sample on a dry basis (g).

6.2.6.2. Quantification of the compounds of interest by GC/MS

The procedure for determining the chemical profile of the extract was described by Laurintino *et al.* [28]. GC/MS analyses of the extracts were performed on an Agilent GC instrument (7890 A, Agilent, Santa Clara, CA, USA) coupled to an MS detector (5975 C MS, Agilent, Santa Clara, CA, USA). A fused silica capillary column (HP-5 ms, Agilent, Santa Clara, CA, USA) (30 m long × 250 µm internal diameter × 0.25 µm film thickness, composed of 5 % phenyl and 95 % methylpolysiloxane) was connected to a quadrupole detector operating in EI (electron impact ionization) mode at 70 eV. The oven temperature program consisted of maintaining the oven at 80 °C for 1 min, increasing it at a rate of 10 °C min^{-1} until it reached 190 °C and then reducing the heating rate to 5 °C min^{-1} until it reached 300 ºC and keep it there for 15 min. Compounds were identified by comparing their mass spectra with those provided by the National Institute of Standards and Technology [30]. Quantitative analysis was based on the internal standard method described by Sparkman *et al.* [31]. Bornyl acetate (Sigma-Aldrich Chemical Co., St. Louis, MO, USA) was used as an internal standard to quantify the peak areas of the chromatogram. Analyses were performed in triplicate.

6.2.7 Finite element method (FEM) model

The mathematical modeling and numerical simulation of the LA, PA, and FR compounds were performed using the COMSOL Multiphysics® software (COMSOL Inc., Stockholm, Uppland/Södermanland, Sweden). This software describes the transport

phenomena through conservation laws and respective differential equations using the finite element method for their resolution.

The proposed approach for SFE-FEM was based on the convection and diffusion model for dilute species, incorporating a convective resistance at the particle surface (film model) to describe the concentration coupling between the bed particles and the surrounding fluid. This model aims to represent the mass transfer in the column with the porous medium. On the other hand, the UAE-FEM model addressed the diffusion inside the plant particles, assuming ideal external mixing and adding a convective film resistance around the particles.

6.2.7.1 Hypotheses (SFE-FEM and UAE – FEM)

In the mathematical modeling of bioactive compounds extracted by SFE-FEM, the extraction cell has a one-dimensional geometry with a length of 0.1 m. In the UAE-FEM model, the particle has a circular geometry with a diameter of 0.427 mm. The assumptions made for elaborating the models are shown in Table 18.

Table 18. Assumptions adopted for SFE-FEM and UAE-FEM mathematical modeling.

	Finite element method (FEM) model		
Hypotheses	I - SFE-FEM	II - UAE-FEM	Reference
Thermal regime	Isothermal	Isothermal	[12, 33]
Coordinate system	1D plan (bed) 1D radial (particle)	1D radial (particle)	
Type of regime	Transient	Transient	
Chemical reaction	Without chemical reaction	Without chemical reaction	
Bed porosity	Uniform and constant	Uniform and constant	[12, 13]
Particle shape	Spherical	Spherical	[12, 13]
Coupled effects of mass transfer	Interparticles and Intraparticles	Interparticles and Intraparticles	[32, 33, 34]
Outer surface of particles	Convective resistance	Convective resistance	
Chemical species present in the extract	Not interact with each other.	Not interact with each other.	[32]

The following subsections present the equations considered in the mathematical modeling of the extraction process and the initial and boundary conditions used in solving the numerical simulation.

6.2.7.2 Mass transfer (Model I – SFE-FEM)

The proposed model is based on the transport theory of diluted species in a column filled with porous medium, assuming the system is pseudo-homogeneous and without chemical reaction. The differential balance in the bed (macroscale) is given by Equation 5:

$$\varepsilon_b \frac{\partial c_i}{\partial t} + u\frac{\partial c_i}{\partial x} + \frac{\partial}{\partial x}(-D_{b,i}\frac{\partial c_i}{\partial x}) = 0 \quad (5)$$

Where ε_b is the bed porosity, c_i is the interparticle concentration of species i (mg m^{-3}), t is the time (s), x is the axial coordinate, u is the velocity (m s^{-1}) and $D_{b,i}$ is the effective diffusion coefficient (m^2 s^{-1}).

Equations 6 to 8 govern transport within each pellet (microscale). According to the Millington and Quirk model [35], a correction factor was applied to consider tortuosity (Equation 7).

$$\varepsilon_{pe}\frac{\partial c_{pe,i}}{\partial t} + \frac{a}{r^2 r_{pe}^2}\frac{\partial}{\partial r}.(-r^2 D_{pe,i}\frac{\partial}{\partial r}c_{pe,i}) = 0 \quad (6)$$

$$D_{pe} = \frac{\varepsilon_{pe} D}{\tau} \quad (7)$$

$$\tau = \varepsilon^{-1/3} \quad (8)$$

Where ε_{pe} is the particle porosity, $c_{pe,i}$ is the intraparticle concentration of species i (mg m^{-3}) in the fluid volume within the micropores, r is the radial coordinate, r_{pe} is the particle radius, $D_{pe,i}$ is the effective diffusion coefficient in the particle (m^2 s^{-1}), r is the radial coordinate, r_{pe} is the particle radius, τ is the tortuosity, and D is the molecular diffusivity in the fluid (m^2 s^{-1}). The initial condition considered was that at t = 0, the concentration c_i (interparticle) is equal to 0 mg m^{-3}.

The mass balance in the particle is considered unidirectional according to the radial coordinate (r) (Equations 9 and 10).

$$4\pi N\left\{r^2 r_{pe}^2 \varepsilon_{pe}\frac{\partial c_{pe,i}}{\partial t} + \frac{\partial}{\partial r}\left(-r^2 D_{pe,i}\frac{\partial c_{pe,i}}{\partial r}\right) = 0\right\} \quad (9)$$

$$N = \frac{(1-\varepsilon_b)}{V_{pe}} \quad (10)$$

Where N is the number of particles per unit volume of the bed, r is the dimensionless radial coordinate that goes from 0 (center) to 1 (particle surface), and V_{pe} is the particle volume.

Equation 11 is solved by applying the boundary condition at the interface between the pellet surface and the fluid, where a convective resistance was introduced at the particle surface (film model). This resistance is expressed using a mass transfer coefficient described in Equation 11.

$$N_{i,inward} = \mathrm{h}_{D,i}(C_i - C_{pe,i}) \tag{11}$$

Where $N_{i,inward}$ is the molar flux from free fluid inside the particle pores (mol m^{-2} s^{-1}) and $\mathrm{h}_{D,i}$ is the mass transfer coefficient (m s^{-1}).

With the above-mentioned film resistance formulation, the interparticle-free fluid balance (Equation 5) needs to be adjusted to ensure flow continuity, as specified in Equation 12. Furthermore, a packed bed is assumed without considering the pores within the particles, as described in Equation 13.

$$\varepsilon_b \frac{\partial c_i}{\partial t} + u\frac{\partial c_i}{\partial x} + \frac{\partial}{\partial x}\left(-D_{b,i}\frac{\partial c_i}{\partial x}\right) = -N_{i,inward}S_b \tag{12}$$

$$S_b = \frac{3}{r_{pe}}(1-\varepsilon_b) \tag{13}$$

Where: Sb (m^2 m^{-3}) is the specific surface area exposed to the free fluid of the packed bed (not including the pores inside the particles), whose expression is valid for randomly packed spherical particles.

The mass transfer coefficient (Equation 11) can be calculated from the fluid properties and flow characteristics within the porous medium. For this calculation, the Sherwood number (Sh) was used, which is defined as the ratio of the convective mass transfer coefficient and the diffusive mass transfer coefficient, as specified in Equation 14.

$$\mathrm{Sh} = \frac{h\,L}{D} \tag{14}$$

Where: Sh is the Sherwood number, L is the characteristic length (m), and D is the diffusion coefficient in the fluid (m^2 s^{-1}).

6.2.7.2.1. Initial and boundary condition (Model I – SFE-FEM)

For the initial condition, $C_{in,i} = 0$ and C$C_{pe,i} = C_{pe0,i}$ were considered uniformly distributed throughout the sample packed in the column. The initial concentration of solute *i* by volume of voids in the particle ($C_{pe\_in,i}$) (mg m^{-3}) was obtained by GC/MS, calculated from the ratio of total mass extracted and volume of voids of the particles that are part of the sample.

At the column inlet (x = 0), a concentration condition of $C_{0,i} = 0$ was imposed, and at the outlet (x = L), a Danckwerts condition ($n \cdot D_i \nabla c_i = 0$). The CO_2 flow rate with ethanol varied between 0.0007897 and 0.0029107 m s^{-1}. Furthermore, $h_{D,i}$ was multiplied by a linear ramp function in order to increase its initial value with time, during the initial extraction phase, up to a pre-established limit.

6.2.7.2.2 Mathematical modeling strategy (Model I – SFE-FEM)

The phenomenological model for SFE-FEM extraction uses mass balance equations for the solute in the packaged bed (macroscale) and in the particles (microscale). Integrating these differential equations yields temporal concentration profiles for each phase. The extraction curve is calculated from the solute concentration in the fluid phase (macroscale) at the extractor outlet. In the model, as in the experiments, the solute extraction gradually increases over 10.800 seconds (180 minutes) with a continuous flow of CO_2 and solvent through the extraction column.

To determine the mass of the component remaining in the extraction column, the sum of the concentrations of component *i* is integrated in the interparticle fluid phase and within the particle pores for the entire column volume, for successive simulation times since the start of the operation, as described in Equation 15. The integration is done along the column represented by a line in the one-dimensional model.

$$n_i tot = \int_0^L \left(\varepsilon_b C_i + (1 - \varepsilon_b)\varepsilon_{pe}\bar{C}_{pe,i}\right) A\, dx \tag{15}$$

Where $n_i tot$ is the total mass in mg of *i* obtained from the integration of the column volume ($A\ L$), ε_b is the bed porosity, C_i is the concentration of i in the bed (mg m^{-3}), ε_{pe} is the particle porosity, $\bar{C}_{pe,i}$ is the average particle concentration (mg m^{-3}), *A* is the column cross-sectional area, and $A\ dx$ is the differential volume element (m^3).

The mass extracted as a function of time is obtained by the difference between the initial mass (mg) in the extraction column (initial condition) and the instantaneous residual mass obtained in the simulation.

6.2.7.3 Mass transfer (Model II – UAE-FEM)

This model considers the extraction of solute (i) from porous particles dispersed in a finite volume of ideally stirred solvent with increasing and uniform bulk concentration ($C_{bulk,}i$) throughout the process. The solute is assumed to be transported only by the diffusion mechanism from the saturated pores, where it is initially located, for the external solvent. Furthermore, the differential mass balance for particles with radial symmetry and one-dimensional in the *r* coordinate is considered. The Millington and Quirk model [35] was also used to correct the molecular diffusion coefficient due to the tortuosity effect. Equations (16), (17), and (18) establish the mass balance in the particles for the species studied.

$$\varepsilon_{pe}\frac{\partial c_{pe,i}}{\partial t}+\frac{1}{r^2}\frac{\partial}{\partial r}(-r^2 D_{pe,i}\frac{\partial c_{pe,i}}{\partial r})=0 \quad (16)$$

$$D_{pe,i}=\frac{\varepsilon_{pe}}{\tau}D \quad (17)$$

$$\tau = {\varepsilon_{pe}}^{-1/3} \quad (18)$$

6.2.7.3.1. Initial and boundary condition (Model II – UAE-FEM)

The initial concentration (em $t = 0$) of solute I by mass of sample ($C_{in,i}$) (mg kg^{-1}) was obtained from the GC/MS results of the solution at the end of the extraction. The initial solute concentration in the particles ($C_{pe0,i}$) is calculated from the ratio of concentration in the sample ($C_{in,i}$), density (ρ_{pe}), and porosity (ε_{pe}) of the particles, according to Equation 19.

$$C_{pe0,i}=\frac{C_{in,i}\,\rho_{pe}}{\varepsilon_{pe}} \quad (19)$$

The boundary conditions apply at the outer surface ($r = r_{pe}$) and center ($r = 0$) of the particles:

$$-D_{pe,i}\frac{\partial c_{pe,i}}{\partial r}=k_{c,i}\left(C_{bulk,i}-C_{pe,i}\right) \quad para \quad r=r_{pe} \quad (20)$$

Where: $k_{c,i}$ is the convective mass transfer coefficient (m s^{-1}), according to the film model.

$$\frac{\partial c_{pe,i}}{\partial r} = 0 \ \ para\ r = 0 \tag{21}$$

Which zeroes the diffusive flux at the center of the particle due to the adopted radial symmetry.

6.2.7.3.2. Mathematical modeling strategy (Model II – UAE-FEM)

The UAE-FEM model describes the transport of solutes in a porous particle that is saturated with a liquid (solvent). The reduction in the extraction rate of the plant compound, which is observed after the initial period, may be caused by a change in the phase equilibrium. Thus, once the free compound is exhausted, the equilibrium concentration in the fluid phase becomes dependent on the concentration in the solid phase [36].

To determine the mass of the remaining component in the sample's set of *N* particles, the concentration of component *i* is integrated for each simulation time, as described in Equation 22. The integration is done along the radius, considering a pseudo-homogeneous medium with radial symmetry.

$$n_i tot = N \int_0^{r_{pe}} \varepsilon_{pe} 4\pi r^2 C_{pe}(r) dr \tag{22}$$

$$N = \frac{Mass_{tot}}{\left(\rho_{pe} \frac{4}{3} \pi r_{pe}^3\right)} \tag{23}$$

Where $n_i tot$ is the total number of moles of *i* obtained from integration over the particle volume (mol), $Mass_{tot}$ is the total mass of the sample (kg), ε_{pe} is the porosity of the particles, $C_{pe,i}$ is the concentration in the particles (mg m^{-3}), ρ_{pe} is the specific mass of the particles (kg m^{-3}), d is the particle diameter and *dr* is the differential increment in the *r* coordinate (m).

The extracted mass is calculated as the difference between the initial number of moles in the set of *N* particles (initial condition) and the instantaneous residual value obtained in the simulation.

6.2.7.4 Model parameters

The experimental data related to the extraction of *C. spicatus* leaves obtained by SFE and UAE are used for model validation. In the present work, two models (I - dynamic and II - batch) were performed, and their equations were solved by COMSOL Multiphysics® (COMSOL Inc., Stockholm, Uppland/Södermanland, Sweden). After solving the model equations, the results were validated with the experimental data using the fitting parameters $D_{F,i}$, $D_{pe,i}$, and h_D for model I and $D_{F,i}$ and $K_{D,i}$ for model II.

6.2.7.5 Mesh study for numerical simulation

Four simulations were performed to define the appropriate mesh, comparing different numbers of elements (50, 100, 500, and 1000) while keeping the other parameters constant. The choice of the mesh was based on the one that produced a solution consistent with the experimental data, with fast processing and numerical stability. This study used experimental data for linolenic acid in the SFE-FEM model (50 °C/8 MPa/10 % EtOH) and UAE-FEM.

6.2.8 Statistical analysis

To evaluate significant differences ($p < 0.05$) between the Y_i, results, the Tukey test was applied to the extraction yields of SFE, UAE, and conventional extraction in a water bath. The mean and standard deviation of triplicate experiments represented the dynamic extraction curves. The performance of the mass transfer models for the FEM of *C. spicatus* leaves was evaluated by the correlation coefficient (R^2). All statistical analyses were performed using Statistica for Windows 7.0 software (Statsoft Inc., Tulsa, OK, USA).

6.3 RESULTS AND DISCUSSION

6.3.1 Characterization of particles and properties fluid

The supercritical extraction essays tested different P, T, and % cosolvent conditions, which resulted in different CO_2 properties. The moisture content of the particles in all essays was kept constant. Table 19 shows the values for the characterization of the particles and the properties of supercritical CO_2.

Table 19. Characterization of particles and fluid properties.

	Characterization of particles					
Simulation	**ε**	**ε_{pe}**	**ρ_b** kg m^{-3}	**ρ_{pe}** kg m^{-3}	**r_{pe}** mm	**Moisture content %**
SFE-FEM	0.89±0.02	0.15±0.05	139±0.05	1239.4±0.0022	0.214±0.02	6.65± 0.03
	$Mass_{tot}$ g	**V_{sol}** mL	**ε_{pe}**	**ρ_{pe}** kg m^{-3}	**r_{pe}** mm	**Moisture content %**
UAE-FEM	1	30	0.15±0.05	1239.4±0.0022	0.214±0.02	6.65±0.03
	Fluid Properties – SFE					
	P MPa	T °C	Cosolvent %w	ρl * kg m^{-3}	μ* Pa s	u * m s^{-1}
	11	40	5	683.52	5.42 10^{-5}	9.33 10^{-4}
	17	40	5	807.87	7.33 10^{-5}	7.90 10^{-4}
	11	60	5	357.79	2.68 10^{-5}	1.78 10^{-3}
	17	60	5	664.59	5.27 10^{-5}	9.60 10^{-4}
	11	40	15	683.53	5.42 10^{-5}	9.33 10^{-4}
	17	40	15	807.87	7.33 10^{-5}	7.90 10^{-4}
	11	60	15	357.79	2.68 10^{-5}	1.78 10^{-3}
	17	60	15	664.59	5.27 10^{-5}	9.60 10^{-4}
	8	50	10	219.18	2.03 10^{-5}	2.91 10^{-3}
	20	50	10	784.29	6.95 10^{-5}	8.13 10^{-4}
	14	36	10	794.11	7.07 10^{-4}	8.03 10^{-4}
	14	64	10	516.47	3.79 10^{-5}	1.24 10^{-3}
	14	50	20	672.17	5.32 10^{-5}	9.49 10^{-4}
	14	50	10	672.17	5.32 10^{-5}	9.49 10^{-4}

ε: bed porosity; ε_{pe}: particle porosity; ρ_b: bed specific mass (kg m^{-3}); ρ_{pe}: particle specific mass (kg m^{-3}); r_{pe}: radius of the particle (mm); $Mass_{tot}$: massa total; $V_{sol:}$ volume da solução; P: Pressure (MPa); T: Temperature (◦C); Cosolvente: EtOH (%w); ρl: fluid specific mass (kg m^{-3}); μ: dynamic viscosity of the mixture (Pa s); u: velocity (m s^{-1}).

* Nist [18].

6.3.2 Yield of component extraction

The results will be presented according to the extraction conditions (Table 20). The compounds selected for the simulation are those that showed a higher mass proportion in relation to the extract, since a predominant compound was not identified. It was decided that the simulation should be performed with individual compounds.

Table 20. Yield and mass percentage by extraction component.

Sample	Extraction conditions[1]	Compound	Y_i^2 mg g^{-1}	Y_i^2 %
1	40 °C/11 MPa/5 %	LA	$0{,}319^{b,c,d} \pm 0.005$	$14{,}47^{d} \pm 0.03$
		PA	$0{,}225^{p} \pm 0.002$	$9{,}68^{q} \pm 0.02$
		FR	$0{,}273^{g,h,i,j,k} \pm 0.003$	$13{,}01^{j} \pm 0.02$
2	40 °C/11 MPa/15 %	LA	$0{,}339^{a,b,c} \pm 0.009$	$16{,}29^{c} \pm 0.02$

		PA	$0,266^{g,h,i,j,k,l,m} \pm 0.002$	$13,33^{h,i} \pm 0.03$
		FR	$0,286^{g,h,i} \pm 0.006$	$13,66^{f,g} \pm 0.05$
3	60 °C/11 MPa/5 %	LA	$0,342^{a,b,c} \pm 0.003$	$17,08^{b} \pm 0.06$
		PA	$0,256^{j,k,l,m,n,o} \pm 0.002$	$12,40^{l} \pm 0.02$
		FR	$0,273^{g,h,i,j,k} \pm 0.004$	$13,01^{j} \pm 0.01$
4	60 °C/11 MPa/15 %	LA	$0,288^{f,g,h} \pm 0.001$	$13,80^{e,f} \pm 0.04$
		PA	$0,246^{k,l,m,n,o,p} \pm 0.005$	$11,47^{m} \pm 0.02$
		FR	$0,284^{g,h,i,j} \pm 0.006$	$13,64^{f,g} \pm 0.03$
5	40 °C/17 MPa/5 %	LA	$0,338^{a,b,c} \pm 0.009$	$16,28^{c} \pm 0.03$
		PA	$0,227^{o,p} \pm 0.003$	$9,86^{q} \pm 0.07$
		FR	$0,274^{g,h,i,j,k} \pm 0.006$	$13,02^{j} \pm 0.08$
6	40 °C/17 MPa/15 %	LA	$0,347^{a,b} \pm 0.009$	$17,13^{b} \pm 0.01$
		PA	$0,267^{g,h,i,j,k,l} \pm 0.002$	$12,39^{l} \pm 0.02$
		FR	$0,318^{b,c,d,e} \pm 0.005$	$14,46^{d} \pm 0.02$
7	60 °C/17 MPa/5 %	LA	$0,345^{a,b,c} \pm 0.001$	$17,11^{b} \pm 0.09$
		PA	$0,257^{i,j,k,l,m,n} \pm 0.008$	$12,73^{k} \pm 0.01$
		FR	$0,277^{g,h,i,j} \pm 0.006$	$13,47^{g,h} \pm 0.01$
8	60 °C/17 MPa/15 %	LA	$0,290^{d,e,f,g} \pm 0.003$	$13,82^{e} \pm 0.04$
		PA	$0,257^{i,j,k,l,m,n} \pm 0.002$	$12,73^{k} \pm 0.03$
		FR	$0,316^{c,d,e,f} \pm 0.001$	$14,44^{d} \pm 0.01$
9	50 °C/8 MPa/10 %	LA	$0,285^{g,h,i,j} \pm 0.004$	$13,65^{f,g} \pm 0.02$
		PA	$0,235^{n,o,p} \pm 0.008$	$10,7^{o} \pm 0.01$
		FR	$0,280^{g,h,i,j} \pm 0.005$	$13,58^{f,g} \pm 0.02$
10	50 °C/20 MPa/10 %	LA	$0,289^{e,f,g,h} \pm 0.009$	$13,81^{e,f} \pm 0.03$
		PA	$0,268^{g,h,i,j,k,l} \pm 0.002$	$12,42^{l} \pm 0.05$
		FR	$0,341^{a,b,c} \pm 0.003$	$17,06^{b} \pm 0.08$
11	36 °C/14 MPa/10 %	LA	$0,260^{h,i,j,k,l,m,n} \pm 0.009$	$13,14^{i,j} \pm 0.02$
		PA	$0,237^{m,n,o,p} \pm 0.001$	$10,97^{n} \pm 0.01$
		FR	$0,319 \pm 0.004$	$14,47^{d} \pm 0.03$
12	64 °C/14 MPa/10 %	LA	$0,273^{g,h,i,j,k} \pm 0.007$	$13,01^{j} \pm 0.02$
		PA	$0,256^{j,k,l,m,n,o} \pm 0.003$	$12,40^{l} \pm 0.05$
		FR	$0,333^{a,b,c} \pm 0.001$	$16,21^{c} \pm 0.04$
13	50 °C/14 MPa/20 %	LA	$0,269^{g,h,i,j,k,l} \pm 0.002$	$12,43^{l} \pm 0.06$
		PA	$0,241^{l,m,n,o,p} \pm 0.001$	$11,17^{n} \pm 0.03$
		FR	$0,350^{a} \pm 0.001$	$18,02^{a} \pm 0.01$
14	50 °C/14 MPa/10 %	LA	$0,266^{g,h,i,j,k,l,m} \pm 0.003$	$13,33^{h,i} \pm 0.02$
		PA	$0,231^{n,o,p} \pm 0.003$	$10,29^{p} \pm 0.04$
		FR	$0,333^{a,b,c} \pm 0.008$	$16,21^{c} \pm 0.07$

Sample	**Extraction conditions**	**Compound**	**Y_i^2 mg g^{-1}**	**Y_i^2 %**
1	Ultrasonic extraction	LA	$0.249^{a} \pm 0.019$	$12.67^{a} \pm 0.15$
		PA	$0.212^{a} \pm 0.017$	$9.42^{b} \pm 0.18$
		FR	$0.194^{a} \pm 0.010$	$8.32^{c} \pm 0.010$

2	Conventional extraction *in a water bath*	LA	$0.082^{b} \pm 0.022$	$4.21^{d} \pm 0.19$
		PA	$0.064^{b} \pm 0.014$	$3.12^{e} \pm 0.20$
		FR	$0.062^{b} \pm 0.014$	$2.70^{e} \pm 0.013$

Y_i: Yield of component per g of feed; Y_i%: Mass percentage of the component in the total extract obtained after 180 min of extraction;
[1] Extraction conditions: T: Temperature (◦C); P: Pressure (MPa); Cosolvent: EtOH (%w);
[2] Values in the same column with different lowercase letters represent significant differences ($p < 0.05$) considering the experiment of the SFE and UAE techniques separately.

In Table 20, the 40 °C/17 MPa/15 %EtOH condition was the most favorable for the extraction of LA (18:3 ω-3), achieving the best yield of 0.347 mg g^{-1} compared to the other conditions. Furthermore, the combination of 40 °C/15 %EtOH also favored the PA (18:2 ω-6) compound extraction, with a yield of 0.266 mg g^{-1}, although under a lower pressure of 11 MPa. This suggests that, among the conditions evaluated, 40 °C/15 %EtOH is the most efficient extraction of the two main fatty acids (LA and PA) from *C. spicatus* leaves. These fatty acids have multiple benefits, such as antimicrobial activity and reduced risk of inflammation, cancer, and cardiovascular diseases [37].

Although the extracts had a similar chemical composition, FR achieved the maximum yield of 0.266 mg g^{-1} under 50 °C/14 MPa/20% EtOH. In this condition, adding the polar cosolvent to CO_2 increased the polarity of the extraction solvent, resulting in a higher yield. This compound is a pentacyclic triterpene formed by three isoprene units present in different plant genera, such as *Azima*, *Vismia*, and *Maytenus*, highlighting that this compound has promising bioactive properties, including protective action against gastric lesions, antioxidant activity, and analgesic, antipyretic, anti-inflammatory, antimicrobial and antitumor effects [38-41].

6.3.3 Finite element method (FEM) method

6.3.3.1 Mesh study for numerical simulation

The experimental data set related to linolenic acid (50 °C/ 8 MPa/10 % EtOH) was used in the study of the mesh for numerical simulation. The simulations were performed with four meshes: mesh 1, containing 1000 elements, with 22,022 degrees of freedom and a simulation time of 31 s; mesh 2, containing 500 elements, with 11,022 degrees of freedom and simulation time of 21 s; mesh 3 containing 100 elements, with 2,222 degrees of freedom and simulation time of 12 s; mesh 4 containing 50 elements, with 1122 degrees of freedom and simulation time of 9 s. The mesh that best represented

the experimental data with the lowest computational cost was mesh 3, and all analyses related to mathematical modeling were obtained from this mesh.

6.3.3.2 Model fit to experimental data (Model I – SFE-FEM)

The extraction yields obtained were compared with the model results (Figure 19). Table 21 presents the values referring to the adjustment parameters, coefficient of determination, and dimensionless constants for each condition and compound studied.

Figure 19. Model I fitted to the experimental data of the extracted mass of the compounds as a function of time. Columns: Same compound studied, left side (linolenic acid), center (palmitic acid) and right side (friedelin); Rows: Same extraction condition*.

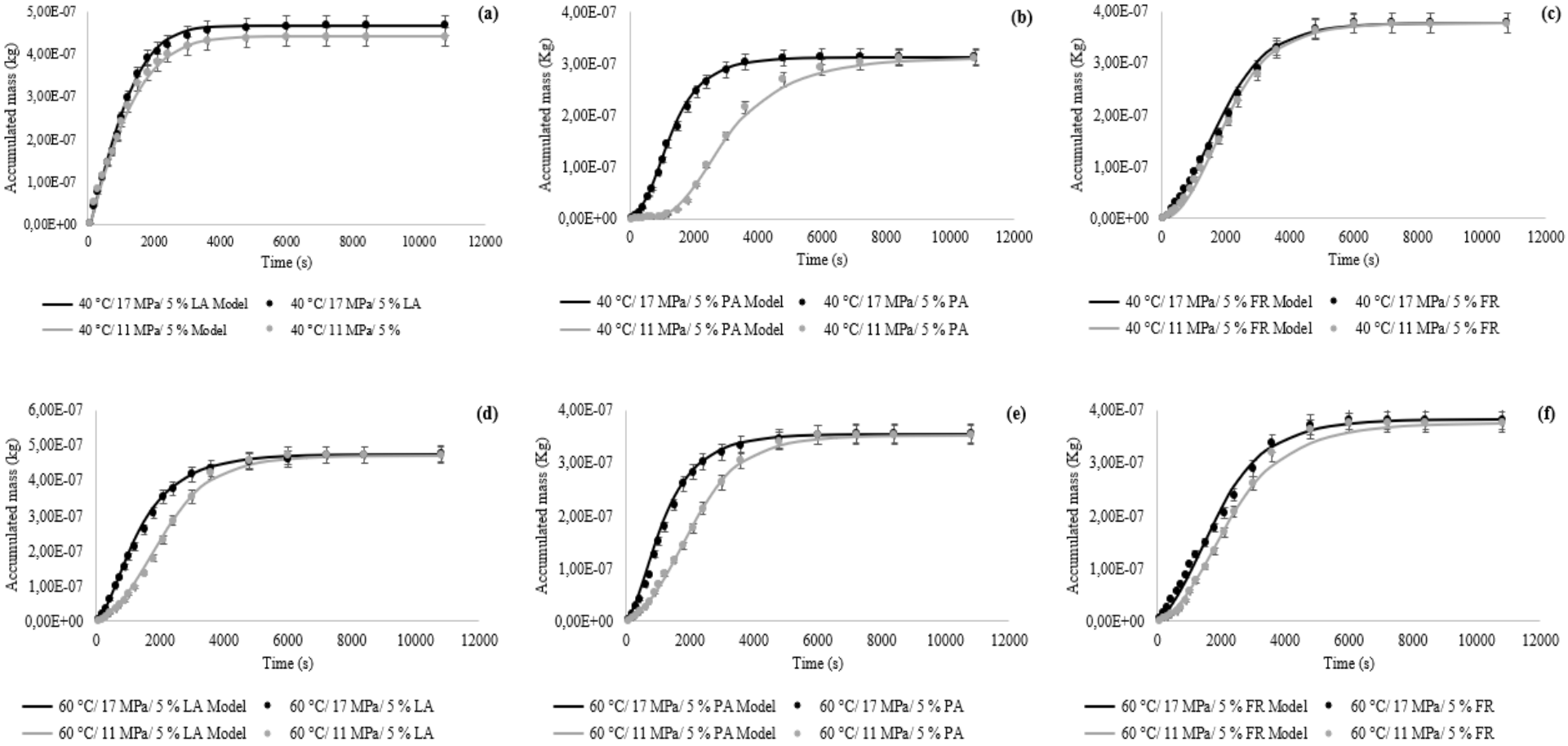

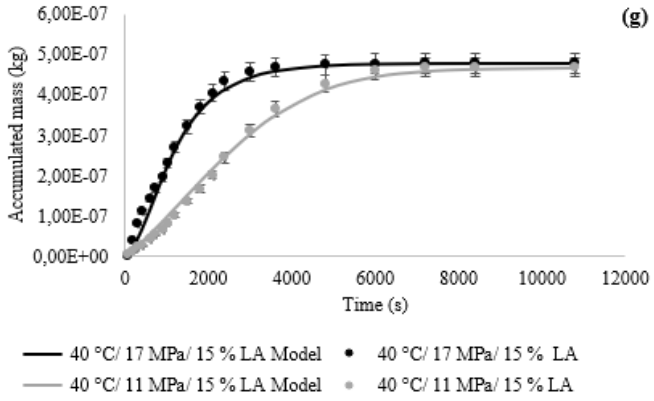
(g)
6,00E-07
5,00E-07
4,00E-07
3,00E-07
2,00E-07
1,00E-07
0,00E+00
Accumulated mass (kg)
0
2000
4000
6000
8000
10000
12000
Time (s)
40 °C/ 17 MPa/ 15 % LA Model
40 °C/ 17 MPa/ 15 % LA
40 °C/ 11 MPa/ 15 % LA Model
40 °C/ 11 MPa/ 15 % LA

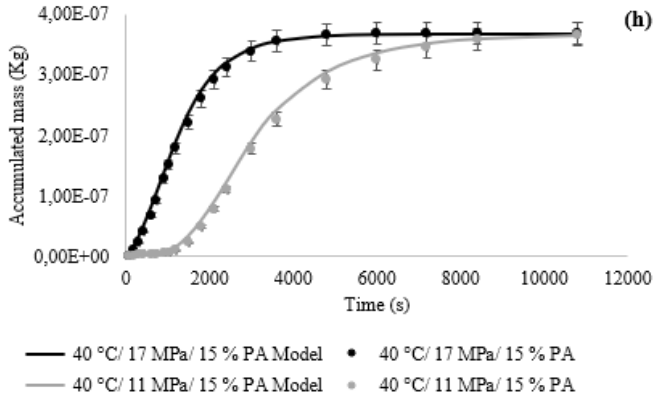
(h)
4,00E-07
3,00E-07
2,00E-07
1,00E-07
0,00E+00
Accumulated mass (Kg)
0
2000
4000
6000
8000
10000
12000
Time (s)
40 °C/ 17 MPa/ 15 % PA Model
40 °C/ 17 MPa/ 15 % PA
40 °C/ 11 MPa/ 15 % PA Model
40 °C/ 11 MPa/ 15 % PA

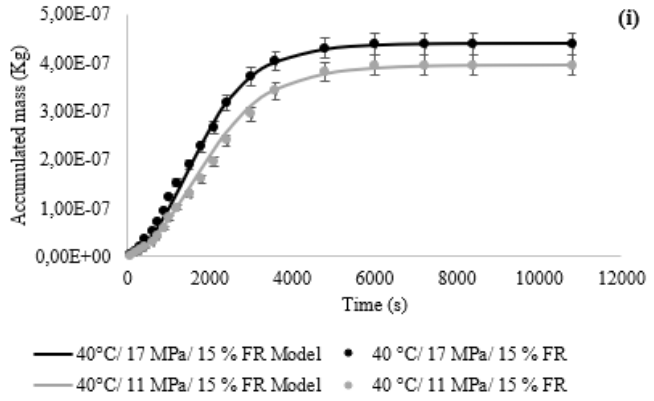
(i)
5,00E-07
4,00E-07
3,00E-07
2,00E-07
1,00E-07
0,00E+00
Accumulated mass (Kg)
0
2000
4000
6000
8000
10000
12000
Time (s)
40°C/ 17 MPa/ 15 % FR Model
40 °C/ 17 MPa/ 15 % FR
40°C/ 11 MPa/ 15 % FR Model
40 °C/ 11 MPa/ 15 % FR

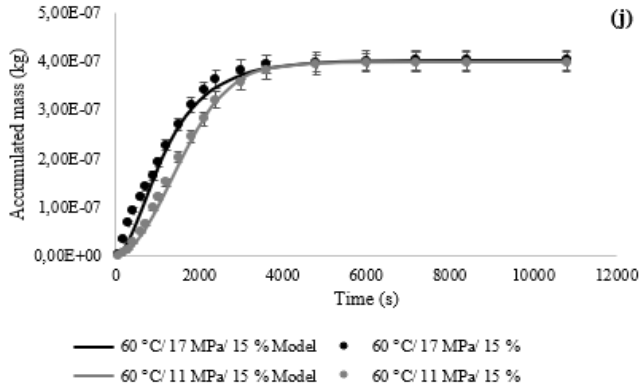
(j)
5,00E-07
4,00E-07
3,00E-07
2,00E-07
1,00E-07
0,00E+00
Accumulated mass (kg)
0
2000
4000
6000
8000
10000
12000
Time (s)
60 °C/ 17 MPa/ 15 % Model
60 °C/ 17 MPa/ 15 %
60 °C/ 11 MPa/ 15 % Model
60 °C/ 11 MPa/ 15 %

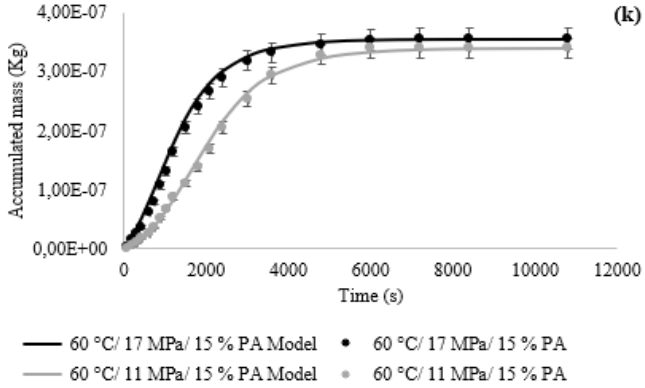
(k)
4,00E-07
3,00E-07
2,00E-07
1,00E-07
0,00E+00
Accumulated mass (Kg)
0
2000
4000
6000
8000
10000
12000
Time (s)
60 °C/ 17 MPa/ 15 % PA Model
60 °C/ 17 MPa/ 15 % PA
60 °C/ 11 MPa/ 15 % PA Model
60 °C/ 11 MPa/ 15 % PA

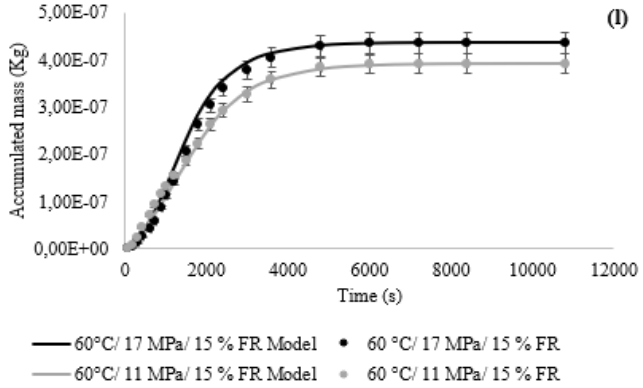
(l)
5,00E-07
4,00E-07
3,00E-07
2,00E-07
1,00E-07
0,00E+00
Accumulated mass (Kg)
0
2000
4000
6000
8000
10000
12000
Time (s)
60°C/ 17 MPa/ 15 % FR Model
60 °C/ 17 MPa/ 15 % FR
60°C/ 11 MPa/ 15 % FR Model
60 °C/ 11 MPa/ 15 % FR

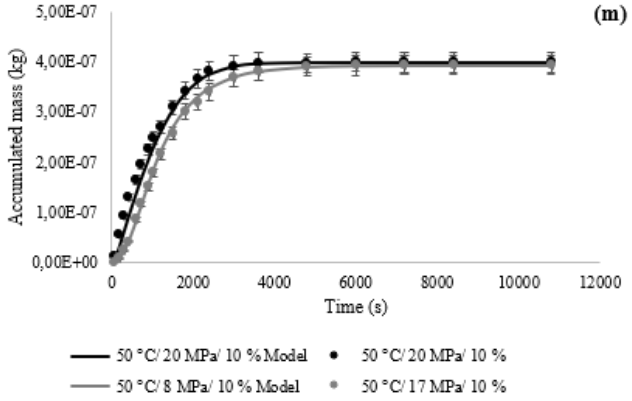
(m)
Accumulated mass (kg)
Time (s)
50 °C/ 20 MPa/ 10 % Model
50 °C/ 20 MPa/ 10 %
50 °C/ 8 MPa/ 10 % Model
50 °C/ 17 MPa/ 10 %

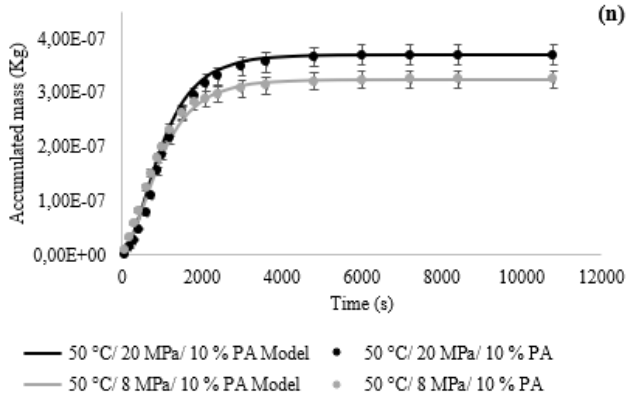
(n)
Accumulated mass (Kg)
Time (s)
50 °C/ 20 MPa/ 10 % PA Model
50 °C/ 20 MPa/ 10 % PA
50 °C/ 8 MPa/ 10 % PA Model
50 °C/ 8 MPa/ 10 % PA

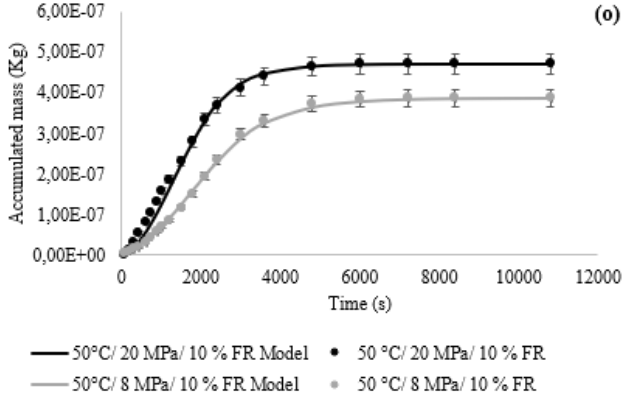
(o)
Accumulated mass (Kg)
Time (s)
50°C/ 20 MPa/ 10 % FR Model
50 °C/ 20 MPa/ 10 % FR
50°C/ 8 MPa/ 10 % FR Model
50 °C/ 8 MPa/ 10 % FR

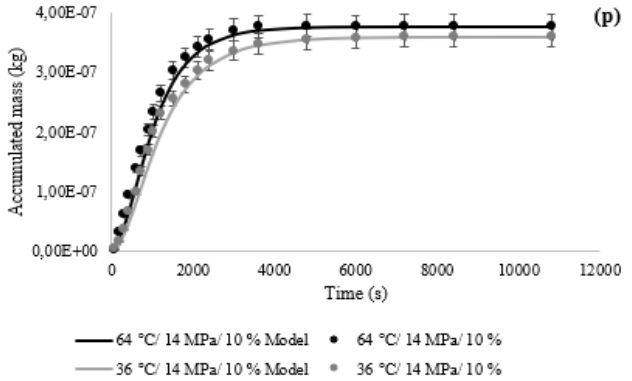
(p)
Accumulated mass (kg)
Time (s)
64 °C/ 14 MPa/ 10 % Model
64 °C/ 14 MPa/ 10 %
36 °C/ 14 MPa/ 10 % Model
36 °C/ 14 MPa/ 10 %

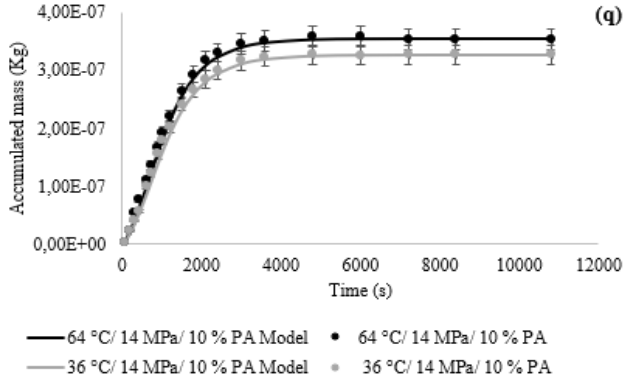
(q)
Accumulated mass (Kg)
Time (s)
64 °C/ 14 MPa/ 10 % PA Model
64 °C/ 14 MPa/ 10 % PA
36 °C/ 14 MPa/ 10 % PA Model
36 °C/ 14 MPa/ 10 % PA

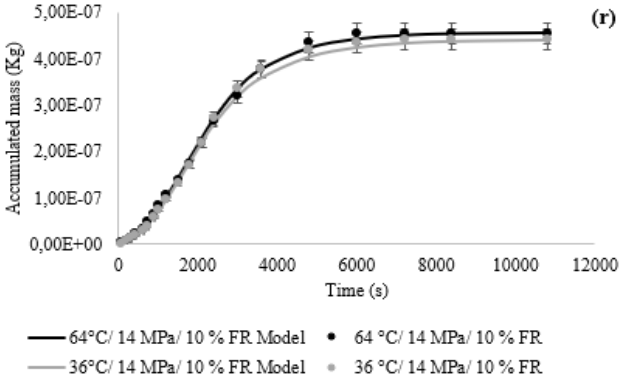
(r)
Accumulated mass (Kg)
Time (s)
64°C/ 14 MPa/ 10 % FR Model
64 °C/ 14 MPa/ 10 % FR
36°C/ 14 MPa/ 10 % FR Model
36 °C/ 14 MPa/ 10 % FR

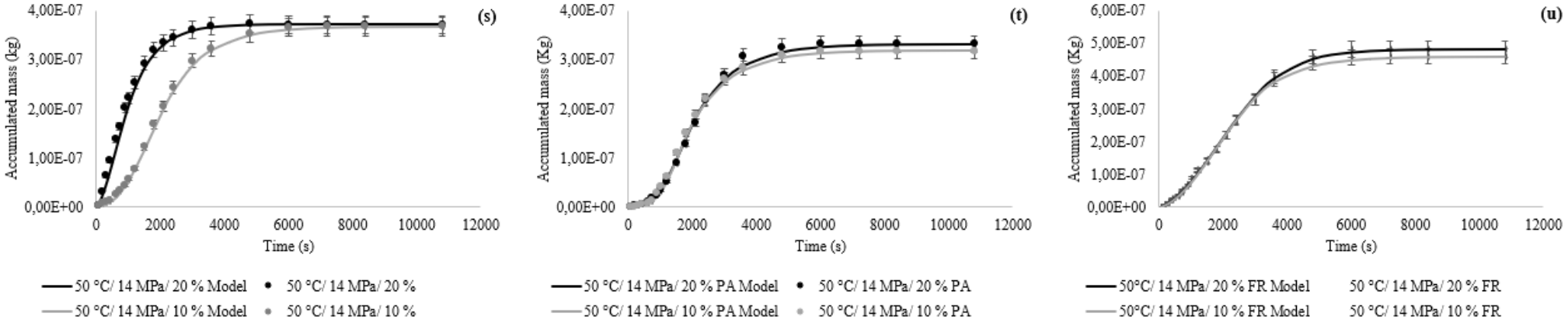

* Extraction conditions: (a), (b), (c) - 40 °C/11 MPa/5 %EtOH and 40 °C/17 MPa/5 %EtOH; (d), (e), (f) - 60 °C/11 MPa/5 %EtOH and 60 °C/17 MPa/5 %EtOH; (g), (h), (i) - 40 °C/11 MPa/15 %EtOH and 40 °C/17 MPa/15 %EtOH; (j), (k), (l) - 60 °C/11 MPa/15 %EtOH and 60 °C/17 MPa/15 %EtOH; (m), (n), (o) - 50 °C/8 MPa/10 %EtOH and 50 °C/20 MPa/10 %EtOH; (p), (q), (r) - 36 °C/14 MPa/10 %EtOH and 64 °C/14 MPa/10 %EtOH; (s), (t), (u) - 50 °C/14 MPa/20 %EtOH and 14- 50 °C/14 MPa/10 %EtOH.

Table 21. Kinetic parameters of model I (SFE-FEM).

Sample	Extraction conditions[1]	Compound	$D_{F,i}$	$D_{pe,i}$	$h_{D,i}$		Ramp					
			$m^2\ s^{-1}$	$m^2\ s^{-1}$	$m\ s^{-1}$	R^2	Location	Slope	Cutoff	Baseline	Size start	Size Cutoff
			x 10^{-9}	x 10^{-11}	x 10^{-4}							
1	40 °C/11 MPa/5 %	LA	5.35	1.85	0.95	0.995	0	0.005	1	0.25	5	22
		PA	5.52	1.69	0.72	0.998	12	0.029	1	0.01	5	22
		FR	5.28	1.98	1.07	0.997	0	0.021	1	0.01	10	2
2	40 °C/11 MPa/15 %	LA	5.33	1.93	1.03	0.997	0	0.023	1	0.25	5	22
		PA	5.30	1.96	1.05	0.998	10.5	0.024	1	0.007	5	22
		FR	5.14	2.09	1.15	0.996	0	0.024	1	0.09	12	2
3	60 °C/11 MPa/5 %	LA	5.33	1.93	1.03	0.998	0.02	0.022	1	0.25	10	2
		PA	5.30	1.96	1.05	0.998	0.02	0.022	1	0.25	5	22
		FR	5.24	2.02	1.09	0.997	1	0.023	1	0.1	0	2
4	60 °C/11 MPa/15 %	LA	5.35	1.85	0.95	0.996	0.02	0.009	1	0.25	12	2
		PA	5.49	1.71	0.75	0.997	1	0.023	1	0.09	5	22
		FR	5.27	1.99	1.08	0.997	1	0.019	1	0.2	12	2
5	40 °C/17 MPa/5 %	LA	5.30	1.96	1.05	0.996	0	0.009	1	0.25	5	22
		PA	5.05	2.18	1.22	0.998	0.02	0.055	1	0.25	5	22
		FR	5.20	2.04	1.10	0.996	0	0.023	1	0.15	10	2
6	40 °C/17 MPa/15 %	LA	4.11	2.82	1.82	0.996	0	0.055	1	0.25	5	22
		PA	4.94	2.29	1.30	0.998	0.02	0.033	1	0.25	5	22
		FR	4.90	2.33	1.35	0.998	1	0.025	1	0.1	12	2
7	60 °C/17 MPa/5 %	LA	3.93	3.00	3.50	0.998	5	0.055	1	0.15	10	2
		PA	4.81	2.42	1.45	0.998	0.02	0.033	1	0.25	5	22
		FR	5.17	2.07	1.13	0.995	1	0.023	1	0.2	0	2
8	60 °C/17 MPa/15 %	LA	4.97	2.26	1.28	0.998	1	0.043	1	0.05	12	2

		PA	5.01	2.22	1.25	0.997	0.02	0.029	1	0.25	5	22
		FR	5.04	2.19	1.23	0.997	1	0.022	1	0.09	12	2
9	50 °C/8 MPa/10 %	LA	4.76	2.47	1.50	0.998	0	0.010	1	0.02	5	20
		PA	4.24	2.69	1.63	0.996	0.02	0.054	1	0.25	5	22
		FR	5.30	1.96	1.05	0.998	1	0.019	1	0.09	12	2
10	50 °C/20 MPa/10 %	LA	3.93	3.00	3.50	0.997	0	0.073	1	0.25	5	20
		PA	4.20	2.73	1.65	0.995	0.02	0.055	1	0.25	5	22
		FR	4.43	2.50	1.52	0.997	1	0.025	1	0.09	12	2
11	36 °C/14 MPa/10 %	LA	4.94	2.29	1.30	0.994	0.02	0.053	1	0.25	5	22
		PA	4.41	2.52	1.55	0.997	0.02	0.038	1	0.25	5	25
		FR	5.42	1.78	0.85	0.998	1	0.025	1	0.1	12	2
12	64 °C/14 MPa/10 %	LA	4.25	2.68	1.62	0.996	0.02	0.055	1	0.25	5	22
		PA	4.29	2.64	1.60	0.998	0.02	0.040	1	0.25	5	25
		FR	5.38	1.82	0.92	0.998	1	0.026	1	0.1	12	2
13	50 °C/14 MPa/20 %	LA	4.24	2.69	1.63	0.998	0.02	0.055	1	0.25	10	20
		PA	5.30	1.96	1.05	0.998	10	0.049	1	0.07	14	2
		FR	5.12	2.11	1.16	0.998	1	0.019	1	0.09	12	2
14	50 °C/14 MPa/10 %	LA	5.27	1.99	1.08	0.996	5	0.030	1	0.07	10	20
		PA	5.33	1.93	1.03	0.998	10	0.045	1	0.04	14	2
		FR	5.33	1.93	1.03	0.998	1	0.015	1	0.09	12	2

$D_{F,i}$: Fluid diffusion coeficiente; $D_{pe,i}$: Diffusion coefficient; $h_{D,i}$: Mass transfer coefficient; R^2: Determination coeficiente; Ramp: Is a linear increase with a user-defined;
[1] Extraction condition: T: Temperature (◦C); P: Pressure (MPa); Cosolvent: EtOH (%w).

In Figure 19, all extraction curves presented behavior compatible with that described by Silva *et al.* [42], except for the conditions in Figure 19-b, h and t. The linear phase was located in the region between 0 and 2000 s, where convection was the main mass transfer mechanism. Between 2000 and 4000 s, the combined effect of convection and diffusion began, resulting in a decrease in the extraction rate. From 4000 s (the plateau of the curve), diffusion acted as the dominant mechanism, resulting in mass transfer and negligible increments in the extract yield. Consequently, the time to reach the diffusive phase in the LA, PA, and FR compounds was similar.

For the conditions in Figure 19b, h and t, the dynamic curve indicated a slow initial stage, until approximately 12 to 20 minutes, little or no extract was obtained. This behavior may be related to the specific mass of CO_2 and, consequently, to its solvation power, which determines the solute/solvent interaction [43]. Furthermore, the characteristics of the oil's location in the cavities of the cell wall of the leaves may have delayed the solubilization of the compounds. This initial stage was incorporated into the mathematical model by applying the *Ramp* function as a correction factor to the mass transfer coefficient (h_D) considered on the surface of the particles, which allowed better adjustment of the extraction simulation to the experimental results.

The kinetic model used to describe the SFE extraction proved to be effective in representing the mass transfer behavior, presenting high R^2 values (> 0.99) (Table 21). The analysis indicated that the extraction occurred in two distinct stages: fast and slow. This behavior can be explained by the presence of two types of oils in the particles: the oil released from the cells broken during grinding and the oil not released from the intact cells [44]. During the fast extraction stage, the released oil that was on the surface of the particles was extracted. During this period, the extraction was limited by the solubility of the oil in the solvent and the resistance to mass transfer predominated in the solvent (fluid) phase. In the slow extraction stage, the oil not released from the intact cells was extracted, and the extraction was controlled by the diffusion of the oil within the particles, with the resistance to mass transfer predominating in the solid phase [45]. Therefore, the estimated mass transfer coefficient at the pellet-fluid phase interface increased with temperature, pressure, and cosolvent content.

6.3.3.2.1 Effect of pressure

As expected, the extraction rate of SFE from *C. spicatus* leaves increased largely with pressure. Thus, a large part of the extraction process is controlled by this

thermodynamic parameter, as suggested by the experimental data. The effect of extraction pressure can be explained by taking into account the large increase (e.g., from 683.52 to 807.87 Kg m^{-3} CO_2 for 40 °C/11 MPa and 60 °C/11 MPa, respectively) in the solubility of the extract constituents (mainly of linolenic acid) with pressure. Therefore, increasing the pressure while keeping the temperature and cosolvent concentration constant resulted in an increase in the solvent power, which is closely related to the variation in solvent density, providing a higher extraction yield. Similar behavior was also observed in the literature [46, 47, 48, 49].

The duration of the fast extraction rate period was pressure-dependent (Figure 19a-o). For example, at 40 °C/15%EtOH for LA, increasing the pressure from 11 MPa to 17 MPa decreased the duration of the fast extraction period from 3600 to 1800 s, and the h_D increased from $1.03x10^{-4}$ m s^{-1} to $1.82x10^{-4}$ m s^{-1} (this was due to the increased solubility of the *C. spicatus* extract in SC- CO_2). Furthermore, the increase in the *Slope* parameter from 0.023 to 0.055, with the pressure varying from 11 MPa to 17 MPa, indicates an increase in the extraction rate, causing a shift in the curve to shorter times. Therefore, in the different process conditions analyzed, the mass transfer coefficient was higher at higher pressures, possibly due to the rupture of the cell walls under high pressure. This behavior was also observed by [50, 51].

When the extraction pressure increased from 11 - 17 MPa to LA (40 °C/15%EtOH), the $D_{pe,i}$ coefficient increased ($1.93\text{-}2.82x10^{-11}$ m^2 s) and the $D_{F,i}$ coefficient decreased ($5.33\text{-}4.11\times10^{-9}$ m^2 s^{-1}) (Table 21). Stamenic *et al.* [52] reported that exposing a plant matrix to supercritical CO_2 would cause significant swelling of the herbaceous matrix. This swelling provides faster diffusion through the plant matrix during dynamic extraction, which leads to an increase in the diffusion coefficient. Therefore, the increase in h_D and D_{pe} coefficient with increasing pressure explains the increase in extraction yield and rate.

6.3.3.2.2. Effect of temperature

The effect of temperature was studied for experiments performed at 36 and 64 °C, maintaining the same pressure conditions of 14 MPa and cosolvent content of 10% EtOH. Studies in the literature show an increase in the solubility of the extract with the extraction temperature [53, 54]. Typical extraction curves are presented in Figure 19p-r.

The extract obtained from C. *spicatus* leaves contained mainly the oil released for the solvents LA and PA under 36 and 64 °C (14 MPa/10% EtOH). Considering the

extract recovered in 1800 s of extraction for LA and PA, almost all the initial amount (approximately 77–85%) was recovered during the fast extraction period. In contrast, only about 38% of the extract was released for the compound FR, while the rest presented the unreleased extract. The fast extraction observed for the compounds LA and PA can be confirmed by the Slope parameter, which presented higher values, ranging from 0.038–0.055, compared to FR, with values between 0.025–0.026.

These results were also reflected in the mass transfer coefficient of the film, where the h_D value for LA and PA (at 36 °C/14 MPa/10% EtOH) was approximately 1.5 times higher than that for the FR compound (Table 21). This is because h_D is related to the transport resistance due to the film, i.e., the higher its value, the lower the transport resistance, and consequently, the extraction of the compound occurs faster. This is consistent with the results reported for extracting black pepper essential oil [55], chamomile essential oil, and oleoresin [56].

Temperature presented impact on the diffusion coefficients of the compounds, indicating that the increase in temperature had a promoting effect on the diffusion of LA, PA, and FR molecules. Thus, the Brownian motion intensified with the increase in temperature, which caused the diffusion coefficient of the molecules of the compounds in carbon dioxide to increase with the increase in temperature [57].

As can be seen in Figure 19, the yield of the compounds increased with pressure, temperature, and cosolvent concentration. However, the behavior of the system at 11 and 17 MPa (for 15% EtOH) at 60 °C was not as expected for LA, PA, and FR. Therefore, it can be suggested that between 40 and 60 °C, the retrogradation phenomenon occurs, which is related to the opposing effects of the solute vapor pressure and the solvent solvation power [58, 59]. This behavior is common in extraction with supercritical fluids and the most frequent temperature conditions are between 40 and 60 °C, as reported in the supercritical CO_2 extraction of *Senecio brasiliensis* [60] and *Santalum album* [61].

6.3.3.2.3 Effect of cosolvent

The extraction yield increased with increasing cosolvent concentration (Figure 19s-u). This behavior may be a consequence of the greater solubilization of polar compounds in the EtOH/ CO_2 mixture [62], which leads to an increase in the driving force [51]. For LA (Figure 19s), the duration of the fast extraction period decreased from 3000 to 1500 **min** as the ethanol addition increased from 10 to 20 % EtOH. In this condition, the Ramp initial point (location) starts at a value lower than 0.02, with a slope of 0.055

and a baseline of 0.25, which represents the constant value of the correction factor before the start of the ramp. However, for the PA and FR compounds, little difference was observed in the linear phase in the two conditions analyzed (10 – 20% EtOH).

The mass transfer coefficient, h_D, increased with the addition of ethanol (Table 21) due to increased extract diffusivity in SC- CO_2 [51], indicating reduced resistance to mass transfer in the fluid phase. Increased oil yield with ethanol in SC- CO_2 was reported for pistachio [63] and sesame oil extractions [64].

When the cosolvent addition was increased from 10 to 20% EtOH (50 °C/14 MPa) for LA, PA and FR, the D_{pe} coefficient also increased to 1.99-2.69x10^{-4} m^2 s^{-1}, 1.93-1.96x10^{-4} m^2 s^{-1} and 1.93-2.11x10^{-4} m^2 s^{-1}, respectively. A larger amount of cosolvent favors mass transfer, and the extraction solute yield increases [65, 66].

6.3.3.3. Model fit to experimental data (Model II – UAE-FEM)

Figure 20 compares the extraction yields obtained with the model results. Table 22 presents the values referring to the adjustment parameters and coefficient of determination for the condition with and without ultrasound.

Figure 20. Model II fitted to the experimental data of the extracted mass of the compounds as a function of time. Columns: Same compound studied, left side (linolenic acid), center (palmitic acid) and right side (friedelin); Rows: Same extraction condition*.

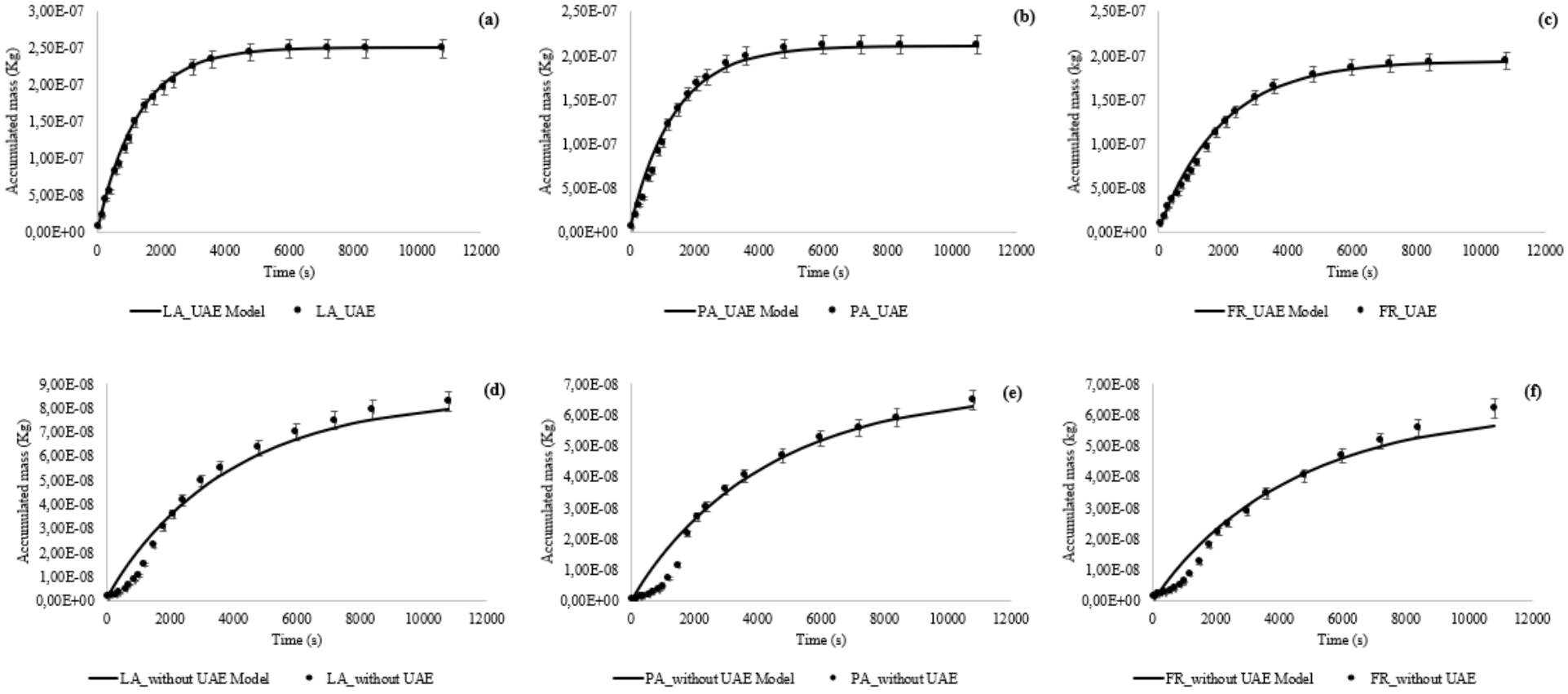

* Extraction conditions: (a), (b), (c) - UAE; (d), (e), (f) - Without ultrasonic treatment.

Table 22. Kinetic parameters of model II (UAE-FEM).

Sample	Extraction conditions	Compound	$D_{F,i}$ $m^2\ s^{-1}$	$K_{D,i}$ $m\ s^{-1}$	R^2
			x 10^{-11}	x 10^{-9}	
1	Ultrasonic extraction	LA	2.43	9.93	0.997
		PA	2.20	9.21	0.996
		FR	1.92	6.24	0.995
2	Without ultrasonic treatment	LA	0.80	3.30	0.986
		PA	0.71	3.05	0.976
		FR	0.62	2.05	0.981

$D_{F,i}$: Fluid diffusion coefficient; $K_{D,i}$: Mass transfer coefficient; R^2: Determination coefficient.

In Figure 20a-c, an increase in the extraction yield is observed for all studied compounds when ultrasonic treatment was applied, compared to extraction without ultrasound (Figure 20d-f). This increase can be attributed to the disruption of cellular structures caused by ultrasound, which increases the accessibility of the solvent to the internal structure of the plant matrix and promotes an increase in intraparticle diffusivity [67]. Other works, such as Vidovic *et al.* [4] and Liu *et al.* [68], have demonstrated that the mechanical effects of ultrasound can accelerate both internal and external diffusion, resulting in greater mass transfer.

In Table 22, the application of ultrasound resulted in a higher superior of three-fold increase in the values of $k_{D,i}$ and $D_{F,i}$, especially for the LA compound 9.93×10^{-9} m s^{-1} and 2.43×10^{-11} m^2 s^{-1}, respectively). This occurs because ultrasound produces cavitation, where asymmetric cavitation bubbles burst on the surface of the cell wall and form microjets in the plant matrix to allow the entry of the solvent, thus accelerating the diffusion rate [69]. This phenomenon may explain the expressive increase in the values of $k_{D,i}$ and $D_{F,i}$ in the samples treated with UAE.

6.3.3.4 Comparison between model I and II

The fluid phase's mass transfer and diffusion coefficients were compared between models I – UAE-FEM and II – UAE-FEM. Although they are different systems, both present the same mass transfer principle. It was observed that the resistance was lower, and the diffusion coefficient was higher in the SFE (Table 21) compared to the UAE (Table 22). These results suggest that the effect of cavitation was not as expressive

as the diffusivity power of the supercritical fluid, which has excellent transport properties in plant tissue [52, 57].

6.4 CONCLUSIONS

The fitting parameters $D_{F,i}$, $D_{pe,i}$, and $h_{D,i}$ for model I – SFE-FEM and $D_{F,i}$ and K_D for model II – UAE-FEM represented the experimental data of extracting *C. spicatus* leaves well. In the models, two extraction periods were discerned: the fast one, in which the extract was released from the surface of the particles, and the slow one, which involved the extraction of the extract from the intact oil cells. Continuing the extraction in the slow extraction period was not beneficial since the amount of oil recovered was insignificant.

The experimental results show that for the model I – SFE-FEM, the yield increased with pressure (8-20 MPa), temperature (36-64°C), and co-solvent concentration (0-20% EtOH). However, the behavior of the system between 40 and 60 °C at 11 and 17 MPa (for 15% EtOH) occurred the retrogradation phenomenon. The procedure used to mathematically describe the system adjusted well to the experimental data. The increase in h_D and D_{pe} coefficient, as a function of pressure, temperature, and co-solvent concentration, explains the increase in yield and extraction rate.

For model II – UAE-FEM, an increase in the extraction yield was observed for all compounds studied with ultrasonic treatment, compared to extraction without ultrasound. Furthermore, the application of ultrasound resulted in a higher superior of three-fold increase in the values of $k_{D,i}$ and $D_{F,i}$, especially for the LA compound 9.93×10^{-9} m s^{-1} and 2.43×10^{-11} m^2 s^{-1}, respectively). This increase can be attributed to ultrasound's disruption of cellular structures. However, models I and II, supported by the experimental results, evidence that the effect of cavitation produced by ultrasound was not as expressive as the extraction power observed with the supercritical fluid. Thus, the modeling attests that the SFE-FEM operation is quantitatively more efficient for obtaining the bioactive compounds of LA, PA, and FR.

6.5 REFERENCES

[1] A. Cabeza, F. Sobrón, J. García-Serna, M.J. Cocero. Simulation of the supercritical CO_2 extraction from natural matrices in packed bed columns: User-friendly simulator tool using Excel. J. Supercrit. Fluids 116 (2016) 198–208.

[2] P.A. Uwineza, A. Waśkiewicz. Recent Advances in Supercritical Fluid Extraction of Natural Bioactive Compounds from Natural Plant Materials. Molecules 25 (2020) 3847.

[3] B. Pavlić, L. Pezo, B. Marić, L.P. Tukuljac, Z. Zeković, M.B. Solarov, *et al.* Supercritical fluid extraction of raspberry seed oil: Experiments and modelling. J. Supercrit. Fluids 157 (2020)104687.

[4] S. Vidovic, Z. Zekovic, B. Marosanovic, J.V. Todorovic. Influence of pre-treatments on yield, chemical composition and antioxidant activity of Satureja montana extracts obtained by supercritical carbon dioxide. The jornal of supercritical fluids 95 (2014) 468-473.

[5] T. Mason, J. Lorimer, Applied Sonochemistry: Uses of Power Ultrasound in, Chemistry (2002).

[6] J.A. Carcel, J. Benedito, C. Rossello, A. Mulet, Influence of ultrasound intensity on mass transfer in apple immersed in a sucrose solution, Journal of Food Engineering 78 (2007) 472–479.

[7] H.S. Muralidhara, D. Ensminger, A. Putnam, Acoustic dewatering and drying (low and high frequency): State of the art review. Drying Technology 3 (1985) 529–566.

[8] T. Clifford, Fundamentals of Supercritical Fluids, Oxford University Press, New York, 1999.

[9] A. Bamafi, S.K. Wee, A.N.T. Tiong, Z.Y. Kong, A. Sptoro, J. Sunarso. Modeling of supercritical fluid extraction bed: A critical review. Chemical Engineering Research and Design 193 (2023) 685-712. https://doi.org/10.1016/j.cherd.2023.04.001.

[10] V. Abrahamsson, N. Andersson, B. Nilsson, C. Turner. Method development in inverse modeling applied to supercritical fluid extraction of lipids. J. Supercrit. Fluids 111 (2016) 14–27.

[11] M. Goto, B.C. Roy, T. Hirose, Shrinking-core leaching model for supercritical fluid extraction. J. Supercrit. Fluids 9 (1996) 128–133.

[12] H. Sovova, Rate of the vegetable oil extraction with supercritical CO_2 - I. Modelling of extraction curves, Chem. Eng. Sci. 49 (1994) 409–414. https://doi.org/10.1016/ 0009-2509(94)87012-8.

[13] E. Reverchon, Mathematical modeling of supercritical extraction of sage oil, Am. Inst. Chem. Eng. J. 42 (1996) 1765–1771, https://doi.org/10.1002/ aic.690420627.

[14] B.C. Roy, M. Goto, T. Hirose, Extraction of ginger oil with supercritical carbon dioxide: experiments and modeling, Ind. Eng. Chem. Res. 35 (1996) 607–612, https://doi.org/10.1021/ie950357p.

[15] J. Wang, H. Zhao, X. Xue, Y. Han, X. Wang, Z. Sheng. Application of ionic liquid ultrasound-assisted extraction (IL-UAE) of lycopene from guava (*Psidium guajava* L.) by response surface methodology and artificial neural network-genetic algorithm. Ultrasonics Sonochemistry 106 (2024) 106877. https://doi.org/10.1016/j.ultsonch.2024.106877.

[16] L. Wen, L. Lin, L. You, B. Yang, G. Jiang, M. Zhao. Ultrasound-assited extraction and structural identification of polysaccharides from Isodon lophanthoides var. gerardianus (Bentham) H. Hara. Carbohydrate Polymers 85(2011) 541-547. https://doi.org/10.1016/j.carbpol.2011.03.003.

[17] E.R. Soto, C.M. Galanakis, M. Brncic, V. Orlien, F.J. Trujillo, R. Mawson, K. Knoerzer, B.K. Tiwri, F.J. Barba. Clean recovery of antioxidant compounds from plant foods, by-products and algae assisted by ultrasounds processing. Modeling approaches to optimize processing conditions. Trends in Food Science & Technology 42 (2015) 134-149.

[18] S. Toepfl, V. Heinz, D. Knorr. High intensity pulsed electric fields applied for food preservation. Chemical Engineering and Processing: Process Intensification 46 (2007) 537-546. https://doi.org/10.1016/j.cep.2006.07.011.

[19] P. S. Milic, K. M. Rajkovic, O. S. Stamenkovic, V. B. Veljkovic. Kinetic modeling and optimization of maceration and ultrasound-extraction of resinoid from the aerial parts of white lady's bedstraw (Galium mollugo L.). Ultrasonics Sonochemistry, 20 (2013) 525-534. https://doi.org/10.1016/j.ultsonch.2012.07.017.

[20] A. Orphanides, V. Goulas, V. Gekas. Introducing the concept of sono-chemical potential: a phenomenological model for ultrasound assisted extraction. Journal of Food Engineering, 120 (2014) 191-196. https://doi.org/10.1016/j.jfoodeng.2013.07.031.

[21] H. Lorenzi, F. J. A. Matos. Plantas Medicinais no Brasil: nativas e exóticas, editora Plantarum, Nova Odessa, São Paulo, (2002). ISBM 85-86714-28-3.

[22] U. P. De Albuquerque, J. Monteiro, M. Ramos, E. Amorim. Medicinal and magic plants from a public market in northeastern Brazil. Journal of Ethnopharmacology 110 (2007) 76–91. https://doi.org/10.1016/j.jep.2006.09.010.

[23] M. Coelho-Ferreira. Medicinal knowledge and plant utilization in an Amazonian coastal community of Marudá, Pará State (Brazil). Journal of Ethnopharmacology 126 (2009) 159-175. https://doi.org/10.1016/j.jep.2009.07.016.

[24] A.C. Keller, I. Vandebroek, Y. Liu, M.J. Balick, F. Kronenberg, E.J. Kennelly, A.M.B. Brillantes. *Costus spicatus* tea failed to improve diabetic progression in C57BLKS/J db/db mice, a model of type 2 diabetes mellitus. J. Ethnopharmacol 121 (2009) 248-254. https://doi.org/10.1016/j.jep.2008.10.025.

[25] D. N. Silva, M.J. Gonçalves, M.T. Amoral, M.T. Batista. Antifungal activity of a flavonoid-rich fraction from *Costus spicatus* leaves against dermatophytes. Planta Medica 74 (2008) 961-961. 10.1055/s-0028-1084088.

[26] L.J. Quintans Júnior, M.T. Santana, M.S. Melo, D.P. De Sousa, I.S. Santos, R.S. Siqueira, T.C. Lima, G.O. Silveira, A.R. Antoniolli, L.A.A. Ribeiro, M.R.V. Santos. Antinociceptive and anti-inflammatory effects of *Costus spicatus* in experimental animals. Pharm. Biol 48 (2010) 1097-1102. https://doi.org/10.3109/13880200903501822.

[27] AOAC Associação de químico analítico oficial, métodos oficiais de análise 18º, AOAC Internacional (2002).

[28] T.K.S. Laurintino, T.N.S. Laurintino, D.P. Tramontin, A.B. Cruz, D.W. Paiva, A. Bolzan, M.B. Quadri. Ultrasound pretreatment combined with supercritical CO_2 extraction of *Costus spicatus* leaf extract. J. Supercrit. Fluids (2024) 106372. https://doi.org/10.1016/j.supflu.2024.106372.

[29] J.L. Luque-García, M.D Luque De Castro. Ultrassom: uma ferramenta poderosa para a lixiviação TrAC - Trends Anal. Química. 22 (2003) 41-47. 10.1016 / S0165- 9936 (03)00102-X.

[30] NIST. Webbook, Instituto Nacional de Normas e Tecnologia - NIST (2018).

[31] D.O. Sparkman, Z.E. Penton, F.G. Kitson, Gas Chromatography and Mass Spectrometry: a Practical Guide, second ed., Academic Press, Cambridge, 2011 https://doi.org/10.1016/C2009-0-17039-3.

[32] E. Reverchon, G. Donsi, L.S. Osséo, Modeling of supercritical fluid extraction from herbaceous matrices, Ind. Eng. Chem. Res. 32 (1993) 2721–2726. https://doi.org/ 10.1021/ie00023a039.

[33] M. Goto, M. Sato, T. Hirose, Extraction of peppermint oil by supercritical carbon dioxide, J. Chem. Eng. Jpn. 26 (1993) 401–407. https://doi.org/10.1252/ jcej.26.401.

[34] J. Martínez, A.R. Monteiro, P.T.V. Rosa, M.O.M. Marques, A.A. Meireles, Multicomponent model to describe extraction of ginger oleoresin with supercritical carbon dioxide, Ind. Eng. Chem. Res. 42 (2003) 1057–1063. https://doi.org/ 10.1021/ie020694f.

[35] R.J. Millington, J. Quirk, Permeability of porous solids, Trans. Faraday Soc. 57 (1961) 1200–1207.

[36] M. Perrut, J.Y. Clavier, M. Poletto, E. Reverchon. Mathematical modelling of sunflower seed extraction by supercritical CO_2. Industrial and Engineering Chemistry Research 36 (1997) 430–435.

[37] N. Kaur, V. Chugh, A.K. Gupta. Essential fatty acids as functional components of foods-a review. J. Food Sci. Technol 51 (2014) 2289–2303. 10.1007/s13197-012-0677-0.

[38] D.M. Ferro, S. Mazzutti, L. Vitali, C.M.O. Muller, S.R.S. Ferreira. Integrated extraction approach to increase the recovery of antioxidant compounds from *Sida rhombifolia* leaves. J. Supercrit. Fluids 149 (2019) 10-19. https://doi.org/10.1016/j.supflu.2019.03.013.

[39] S.F. Andrade, E. Comunello, V.F. Noldin, F.D. Monache, V. C. Filho, R. Niero. Antiulcerogenic activity of fractions and 3,15-dioxo-21α-hydroxy friedelane isolated from *maytenus robusta* (celastraceae). Arch Pharm Res 31 (2008) 41-46. https://doi.org/10.1007/s12272-008-1118-5.

[40] C. Sunil, V. Duraipandiyan, S. Ignacimuthu, N.A. Al-Dhabi. Antioxidant, free radical scavenging and liver protective effects of friedelin isolated from Azima tetracantha Lam. Leaves Food Chem. 139 (2013) 860-865.

https://doi.org/10.1016/j.foodchem.2012.12.041.

[41] F.C. Silva, L.P. Duarte, S.A.Vieira filho, F.C. Silva, L.P. Duarte, S.A.Vieira Filho. Celastráceas: fontes de triterpenos pentacíclicos com potencial atividade biológica. Revista virtual química 6 (2014) 1205- 1220. 10.5935/1984-6835.20140079.

[42] R.P.F.F. da Silva, T.A.P. Rocha-Santos, A.C. Duarte, Supercritical fluid extraction of bioactive compounds. Trends Anal. Chem. 76 (2016) 40–51. https://doi.org/ 10.1016/j.trac.2015.11.013.

[43] G. Brunner. Gas Extraction: an Introduction to Fundamentals of Supercritical Fluids and the Application to Separation Processes, second ed., Springer-Verlag, Berlin, 1994.

[44] C. Marrone, M. Poletto, E. Reverchon, A. Stassi. Almond oil extraction by supercritical CO_2: Experiment and modeling. Chemical Engineering Science, 53(21) (1998) 3711–3718.

[45] H. Sovová, A.A. Galushko, R.P. Stateva, K, Rochová, M. Sajfrtová, M. Bártlová. Supercritical fluid extraction of minor components of vegetable oils: β-Sitosterol. Jounal of Food Engineering 101 (2010) 201-209. https://doi.org/10.1016/j.jfoodeng.2010.07.002.

[46] U. Salgın, B.Z. Uysal, A. C¸ alımlı. Supercritical fluid extraction of jojoba oil. JAOCS 81 (2004) 293–296.

[47] B. Bozan, F. Temelli, Extraction of poppy seed oil using supercritical CO_2. J. Food Sci. 68 (2003) 422–426.

[48] M.N. Hassan, N.N.A. Rahman, M.H. Ibrahim, A.K.M. Omar, Simple fractionation through the supercritical carbon dioxide extraction of palm kernal oil. Sep. Purif. Technol. 19 (2000) 113–120.

[49] T.C. Confortin, I. Todero, N.I. Canabarro, L. Luft, G.A. Ugalde, J.R.C. Neto, M. A. Mazutti, G.L. Zabot, M.V. Tres, Supercritical CO_2 extraction of compounds from different aerial parts of Senecio brasiliensis: mathematical modeling and effects of

parameters on extract quality. J. Supercrit. Fluids 153 (2019) 104589. https://doi.org/10.1016/j.supflu.2019.104589.

[50] S.G. Özkal, U. Salgin, M.E. Yener. Supercritical carbon dioxide extraction of hazelnut oil. Journal of Food Engineering 69 (2005) 217-223. https://doi.org/10.1016/j.jfoodeng.2004.07.020

[51] S.G. Özkal, M.E. Yener. L. Bayindirli. Mass transfer modeling of apricot kernel oil extraction with supercritical carbon dioxide. J. Supercrit. Fluids 35 (2005) 119-127. https://doi.org/10.1016/j.supflu.2004.12.011

[52] M. Stamenic, I. Zizovic, R. Eggers, P. Jaeger, H. Heinrich, E. Roj, J. Ivanovic, D. Skala. Swelling of plant material in supercritical carbon dioxide. J. Supercrit. Fluids 52 (2010) 125–133. https://doi.org/10.1016/j.supflu.2009.12.004.

[53] J.W. Goodrum, M.K. Kilgo, C.R. Santtera, Oil seed solubility and extraction modeling, in: J.W. King, G.R. List (Eds.). Supercritical Fluid Technology in Oil and Lipid Chemistry. AOCS Press, Illinois, (1996) 101.

[54] T. Klein, S. Schultz. Measurement and model prediction of vapor-liquid equilibrium of mixtures of rapeseed oil and supercritical CO_2. Ind. Eng. Chem. Res. 26 (1989) 1073–1081.

[55] S.R.S. Ferreire, M.A.A. Meireles. Modeling the supercritical fluid extraction of black pepper (*Piper nigrum* L.) essential oil. J. Food Eng. 54 (2002) 263–269. https://doi.org/10.1016/S0260-8774(01)00212-6.

[56] N.P. Povh, M.O.M. Marques, M.A.A. Meireles, Supercritical CO_2 extraction of essential oil and oleoresin from chamomile (*Chamomilla recutita* [L.] Rauschert). J. Supercritical Fluids 21 (2001) 245–256. https://doi.org/10.1016/S0896-8446(01)00096-1.

[57] S. Wang, M. Xu, T. Peng, C. Zhang, T. Li, I. Hussain, J. Wang, B. Tan, Nat. Commun. 10 (2019) 676.

[58] T.N.S. Laurintino, D.P. Tramontin, J. Assreuy, A.B. Cruz, C.C.B. Cruz, A. Marangoni, M.A. Livia, A. Bolzan. Evaluation of the biological activity and chemical profile of supercritical and subcritical extracts of Bursera graveolens from northern Peru. J. Supercrit. Fluids 198 (2023) 105934. https://doi.org/10.1016/j.supflu.2023.105934.

[59] L.T. Taylor. Supercritical Fluid Extraction. WileyInterscience, New York, 1996.

[60] T.C. Confortin, I. Todero, N.I. Canabarro, L. Luft, G.A. Ugalde, J.R.C. Neto, M. A. Mazutti, G.L. Zabot, M.V. Tres. Supercritical CO_2 extraction of compounds from different aerial parts of *Senecio brasiliensis:* mathematical modeling and effects of parameters on extract quality. J. Supercrit. Fluids 153 (2019) 104589. https://doi.org/10.1016/j.supflu.2019.104589.

[61] B. Marongiu, A. Piras, S. Porcedda, E. Tuveri. Extraction of *Santalum album* and *Boswellia carterii Birdw*. volatile oil by supercritical carbon dioxide: influence of some process parameters, Flavour Fragr. J. 21 (2006) 718–724. https://doi.org/10.1002/ffj.1718.

[62] P. Benelli, C.A.S. Riehl, A. Smania, E.F.A. Smânia, S.R.S. Ferreira. Bioactive extracts of orange (*Citrus sinensis* L. Osbeck) pomace obtained by SFE and low pressure techniques: mathematical modeling and extract composition. J. Supercrit. Fluids 55 (2010) 132–141. https://doi.org/10.1016/j.supflu.2010.08.015.

[63] T.K. Palazoglu, M.O. Balaban. Supercritical CO_2 extraction of roasted pistachio nuts, Trans. ASAE 41 (1998) 679–684.

[64] A.Z. Odabas¸ı, M.O. Balaban, Supercritical CO_2 extraction of sesame oil from raw seeds. J. Food Sci. Technol.: Mysore 39 (2002) 496–501.

[65] A. Bogdanovic, V. Tadic, M. Stamenic, S. Petrovic, D. Skala, Supercritical carbon dioxide extraction of *Trigonella foenum-graecum* L. seeds: process optimization using response surface methodology. J. Supercrit. Fluids 107 (2016) 44–50. https://doi.org/10.1016/j.supflu.2015.08.003.

[66] A. Daraee, S.M. Ghoreishi, A. Hedayati, Supercritical CO_2 extraction of chlorogenic acid from sunflower (*Helianthus annuus*) seed kernels: modeling and optimization by response surface methodology. J. Supercrit. Fluids 144 (2019) 19–27. https://doi.org/10.1016/j.supflu.2018.10.001.

[67] A.C. Soria, M. Villamiel. Effect of ultrasound on the technological properties and bioactivity of food: a review. Trends in Food Science & Technology 21 (2010) 323-331.

[68] X. Liu, H. Ou, Z. Xiang, H. Gregersen. Ultrasound pretreatment combined with supercritical CO_2 extraction of *Iberis amara* seed oil. Journal of Applied Research on Medicinal and Aromatic Plants 18 (2020) 100265.

[69] J.A. Carcel, J. Benedito, J. Bon, A. Mulet. High intensity ultrasound effects on meat brining. Meat Science 76 (2007) 611–619.

CHAPTER VII - FINAL CONSIDERATIONS AND FUTURE STUDIES

In this study, an improved process using ultrasonic pretreatment combined with supercritical CO_2 extraction was successfully developed, obtaining bioactive compounds, mainly linolenic acid, from the leaves of *C. spicatus*.

The results indicated that the extraction techniques and the choice of solvent directly impacted the yields and metabolite content, reflecting on the biological activities and physicochemical characteristics. The extract obtained with the ethanol: water mixture yielded 7.25%, 18.74%, 9.29%, and 10.12% for the MAC, SOX, UAE, and UAE+SFE techniques, respectively. In the analysis of the ultrasound tests, it was observed that using the macrotip with 70% amplitude and a time of 5 minutes in the ethanol: water solvent increased the extract yield. However, under the same conditions, ethanol resulted in the extraction of a greater quantity of compounds of commercial interest.

The combination of UAE+SFE resulted in a higher extract yield than traditional techniques, reaching 6.97% under 50°C/14MPa/20% EtOH conditions. SEM analysis showed dense microcracks in the UAE+SFE-treated sample, evidencing the impact on tissue structures. UAE+SFE increased the selectivity of linolenic acid to 62.52% at 60°C/11MPa/5% EtOH. The extracts presented different phenolic and flavonoid compounds in the UAE > UAE + SFE > SFE order. Regarding antioxidant activity, the extracts obtained superior results in the ABTS assay compared to DPPH. Furthermore, UAE+SFE demonstrated superior antibacterial activity against Gram-positive bacteria and showed moderate activity against *M. canis* and *M. gypseum*, with a MIC of 1000 μg mL^{-1} for antifungal activity.

Among the extraction techniques investigated (MAC, UAE, SOX, UAE, and UAE+SFE), the UAE+SFE combination proved to be especially effective, preserving cell viability at concentrations up to 100 μg mL^{-1}, inhibiting nitric oxide by more than 90% and presenting high antioxidant and antiviral activity. LPE extraction with ethanol (EtOH) generated high levels of flavonoids, while the UAE+SFE combination improved the recovery of these compounds compared to SFE. All extracts demonstrated antibacterial activity against *B. cereus* and presented physical stability. The UAE+SFE technique stood out in the extraction of lipid droplets and showed thermal stability, as evidenced in the TG and DTG analyses.

The fitting parameters $D_{F,i}$, $D_{pe,i}$, and $h_{D,i}$ for model I – SFE-FEM, $D_{F,i}$ and $K_{D,i}$ for model II – UAE-FEM represented the experimental data well. The results showed

that, for model I, the yield, $D_{pe,i}$, and $h_{D,i}$, increased with pressure (8-20 MPa), temperature (36-64 °C), and co-solvent concentration (0-20% EtOH). However, between 40 and 60 °C at 11 and 17 MPa (with 15% EtOH), the retrogradation phenomenon was observed. In model II, an increase in the yield, $D_{F,i}$, and $K_{D,i}$ was noted with ultrasonic treatment, compared to extraction without ultrasound, due to the rupture of the cellular structures. However, the results indicate that the effect of ultrasound cavitation was not as expressive as the extraction power of the supercritical fluid. Thus, the modeling confirms that the SFE-FEM operation is quantitatively more efficient in obtaining bioactive compounds from LA, PA, and FR.

This study establishes a solid foundation for future applications of *C. spicatus* in the food, pharmaceutical, and cosmetic industries, highlighting its potential as a multifunctional natural resource. Thus, the combination of UAE+SFE can be considered an efficient and environmentally friendly alternative for obtaining high-quality extracts. This combination of techniques results in an extract rich in linolenic acid, which can contribute to human health by preventing infectious diseases such as COVID-19.

Future work on GAS encapsulation and in vivo release can be carried out to verify the reproducibility and bioavailability of bioactive compounds, confirming their benefits for human health. In addition, mathematical modeling of release profiles can include adequate representations of the release mechanisms involved in the process.